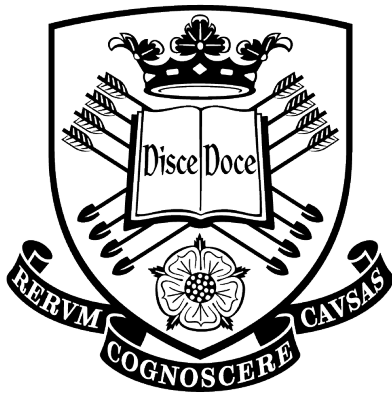


*Novel Insights into the Interaction Between GPRC6A and
Receptor Activity Modifying Proteins.*



The
University
Of
Sheffield.

By Ewan R. Lilley

Registration No: 170240280

Submitted: January 2021

Supervisors: Dr. Gareth Richards & Prof. Timothy Skerry

Thesis Abstract.

Novel Insights into the Interaction Between GPRC6A and Receptor Activity Modifying Proteins.

The G protein-coupled receptor GPRC6A is a nutrient receptor, promiscuously activated by L-amino acids in mouse and human. However, published data is conflicting about the ability of the receptor to respond to other ligands, such as testosterone, its analogues, and the bone-derived osteocalcin, where there are species differences. Reports have shown that whilst the murine receptor is successfully expressed at the cell membrane, the human GPRC6A (hGPRC6A) remains intracellularly retained. Receptor activity-modifying proteins (RAMPs) are small accessory proteins known to influence surface trafficking and ligand affinity when complexed with a GPCR. We hypothesised that hGPRC6A interacts with RAMPs thereby aiding in its forward trafficking and signalling capabilities. Here we show that association of the hGPRC6A receptor with RAMP1, allows the receptor to traffic to the cell surface and respond to additional ligands to which it is insensitive to in the absence of RAMP1. Specifically, we demonstrate using FRET and ELISA that transfection of hGPRC6A-expressing cells with RAMP1 (but neither RAMP2, nor RAMP3) changes the location of the GPRC6A within cells, so that there is cell surface localisation. This leads to the activation of intracellular calcium mobilisation by testosterone [pEC_{50} 6.63 \pm 0.28] and DHEA [pEC_{50} 6.61 \pm 0.34], as well as the L-amino acids L-Orn [pEC_{50} 6.23 \pm 0.35], L-Arg [pEC_{50} 6.01 \pm 0.33], L-Lys [pEC_{50} 6.52 \pm 0.38], although not osteocalcin. In order to determine the functional significance of these findings, we have explored the role of hGPRC6A and RAMP1 in prostate cancer cells *in vitro* and *in vivo*. It is already known that knockout of GPRC6A reduces PC-3 xenograft tumour growth in mice and that SNPs in GPRC6A reduces disease severity in men, while GPRC6A knockout in PC-3 cells also reduces tumour growth. We show that the absence of RAMP1 in hGPRC6A-expressing PC-3 prostate cancer cells reduces viability by 41% ($p < 0.0001$), colony formation 89% ($p < 0.0001$) and other markers of tumorigenesis, and the effects of GPRC6A agonists and antagonists is blunted in those cells, compared with GPRC6A/RAMP1-expressing cells. Taken together, our data are consistent with a requirement for RAMP1 for full functionality of GPRC6A in humans, and displays distinctly different profile in mice. Additionally, our data may provide a novel target for research into treatments for hormone refractory prostate cancer.

Acknowledgments.

I would first like to thank my supervisors Dr. Gareth Richards and Prof. Timothy Skerry. Both have provided excellent support and mentorship throughout the PhD; I know I would not have got this far without your guidance and encouragement. Tim has never let me forget the importance of the wider scope of my research. The lab meeting grilling's, although daunting and terrifying at times has enabled me to become a better scientist and critical thinker; something that I have brought into my life outside the lab. I cannot thank my mentor and friend Gareth enough, for encouraging me and getting me through even at the deepest lows of the project. Your knowledge and wisdom has always provided me answers to some of the works hardest challenges. Second, I'd like to thank Dr. Aditya Desai and Zhu Lan for providing the very building blocks for my research. For without their work on the CaSR, GPRC6A and RAMPs this project wouldn't even have begun. Furthermore, I'd also like to offer my gratitude to Dr. Jess Warrington for her work generating the RAMP KO PC-3 cell line that really elevated my work to the next level and broadened my research career horizons. Thank you, Dr. Paris Avgoustou for perusing my thesis, offering valuable guidance and being the dearest friend throughout. Dr. Karan Shah, Anokhee Parik & Joe Holmes, without you I would not possess an ounce of confidence and your council helped me through the toughest of times. Dr. Ameera Jailani & Kamilla Bigos, you two know how important you are to me and were my rock during this; without your love, I would not have come close to completing this work. Finally, I'd like to just thank everyone in the department for creating such a welcoming working environment and affable atmosphere.

Table of Contents

| | |
|---|-----------|
| Thesis Abstract | 2 |
| Acknowledgments | 3 |
| 1 Chapter 1: General Introduction | 13 |
| 1.1 Introduction | 14 |
| 1.1.1 G Protein-Coupled Receptors..... | 14 |
| 1.1.2 GPCR Activation..... | 15 |
| 1.2 G Protein-mediated Signal Transduction Pathways | 17 |
| 1.2.1 Phosphatidylinositol Signalling Pathway $G\alpha_q$ /PLC/IP3..... | 19 |
| 1.2.2 Cyclic AMP Signalling Pathway $G\alpha_s$ /AC/cAMP/PKA..... | 20 |
| 1.2.3 $G\alpha_i$ /AC/cAMP/PK Signalling..... | 21 |
| 1.2.4 Arrestin-Mediated Signalling..... | 22 |
| 1.2.5 MAPK/ERK Signalling Pathway..... | 23 |
| 1.3 GPRC6A Expression Profile | 23 |
| 1.4 GPRC6A Structure-Function Relationship | 25 |
| 1.4.1 Receptor Structure..... | 25 |
| 1.4.2 Cell Surface Trafficking..... | 29 |
| 1.4.3 Receptor Dimerization..... | 30 |
| 1.4.4 Desensitization & Internalisation..... | 31 |
| 1.5 GPRC6A Ligand Controversies | 32 |
| 1.5.1 L-Amino Acids..... | 32 |
| 1.5.2 Osteocalcin..... | 33 |
| 1.5.3 Testosterone..... | 35 |
| 1.6 Role of GPRC6A in Physiology & Pathophysiology | 36 |
| 1.6.1 Bone Metabolism..... | 36 |
| 1.6.2 Energy & Glucose Homeostasis..... | 37 |
| 1.6.3 Gastrointestinal Nutrient Receptor..... | 39 |
| 1.6.4 Inflammation..... | 39 |
| 1.6.5 Male Fertility..... | 40 |
| 1.6.6 Prostate Cancer..... | 41 |
| 1.7 RAMPs and Interaction with GPCRs | 42 |
| 1.7.1 Receptor-Activity-Modifying Proteins..... | 42 |
| 1.7.2 RAMP Structure-Function Relationship..... | 43 |
| 1.7.3 Evidence for the interaction of RAMPs and Calcium Sensing Receptor..... | 43 |
| 1.7.4 GPRC6A & RAMP1..... | 44 |
| 1.8 Hypothesis & Objectives | 46 |
| 1.8.1 Aims..... | 46 |
| 2 Chapter 2: GPRC6A & RAMP1: Interaction & Trafficking | 47 |
| 2.1 GPRC6A & RAMP1 Interaction Introduction | 48 |
| 2.1.1 GPRC6A Recombinant Expression..... | 49 |
| 2.1.2 GPCR-RAMP Interaction..... | 50 |
| 2.1.3 Receptor Cell Surface Expression..... | 55 |

| | | |
|------------|--|------------|
| 2.1.4 | Research Aims | 60 |
| 2.1.5 | Research Hypothesis..... | 60 |
| 2.2 | Methods & Materials..... | 61 |
| 2.2.1 | Cell Culture..... | 61 |
| 2.2.2 | CHO-K1 Characterisation. | 62 |
| 2.2.3 | Plasmid Constructs. | 66 |
| 2.2.4 | Generation of GPRC6A-Cit & RAMP-Cer CHO-K1 Cell Lines..... | 68 |
| 2.2.5 | Subcloning GPRC6A-myc construct. | 70 |
| 2.2.6 | Validation of GPRC6A-myc Protein Expression. | 75 |
| 2.2.7 | GPRC6A and RAMP1 Cell Surface Expression..... | 78 |
| 2.3 | Results..... | 82 |
| 2.3.1 | Native CHO GPRC6A and CHO RAMP1 Expression Characterisation..... | 82 |
| 2.3.2 | Cell Membrane FRET-based Analysis of GPRC6A and RAMPs..... | 83 |
| 2.3.3 | GPRC6A-myc Subcloning Validation. | 85 |
| 2.3.4 | RAMP1 Cell Surface Expression..... | 86 |
| 2.3.5 | GPRC6A-myc Cell Surface Expression. | 88 |
| 2.3.6 | Cell Surface Expression of GPRC6A-myc and RAMPs by ELISA..... | 90 |
| 2.3.7 | Cell Surface Expression of GPRC6A and RAMPs-Flag by ELISA..... | 90 |
| 2.4 | Discussion..... | 92 |
| 2.4.1 | FRET Analysis of GPRC6A and RAMP Interaction. | 92 |
| 2.4.2 | Validation of GPRC6A-myc Subcloning. | 96 |
| 2.4.3 | GPRC6A Cell Surface Expression by Flow Cytometric Analysis. | 98 |
| 2.4.4 | GPRC6A Cell Surface Expression by Whole-Cell Surface ELISA. | 100 |
| 2.4.5 | Alternative Methodologies. | 101 |
| 3 | Chapter 3: GPRC6A Intracellular Signalling. | 103 |
| 3.1 | GPRC6A Signalling Introduction..... | 104 |
| 3.1.1 | GPCR Signalling-Transduction Mechanism. | 104 |
| 3.1.2 | Promiscuous G-protein coupling..... | 107 |
| 3.1.3 | GPRC6A & PLC/DAG/IP ₂ Pathway Activation..... | 108 |
| 3.1.4 | GPRC6A & G α_s /AC/cAMP Signalling Pathway. | 109 |
| 3.1.5 | Role of RAMPs in GPCR Signalling. | 110 |
| 3.1.6 | GPRC6A Ligand Controversies..... | 112 |
| 3.1.7 | Research Aims. | 113 |
| 3.1.8 | Research Hypothesis..... | 113 |
| 3.2 | Materials and Methods. | 114 |
| 3.2.1 | Intracellular G α_q /PLC/IP ₃ Signalling. | 114 |
| 3.2.2 | Intracellular G α_s /AC/cAMP/PKA Signalling. | 117 |
| 3.2.3 | Data & Statistical Analysis..... | 119 |
| 3.3 | Results..... | 120 |
| 3.3.1 | RAMP1 Influence on hGPRC6A-mediated Calcium Mobilisation. | 120 |
| 3.3.2 | RAMP1 Influence on hGPRC6A-mediated cAMP Accumulation..... | 125 |
| 3.4 | Discussion..... | 129 |
| 3.4.1 | G α_q Signalling & Ca ²⁺ Mobilisation..... | 129 |
| 3.4.2 | FLIPR Calcium 6 Assay Format..... | 132 |

| | | |
|------------|--|------------|
| 3.4.3 | G α_s Signalling & cAMP Accumulation. | 133 |
| 3.4.4 | G Protein Signalling & ERK1/2 activation..... | 135 |
| 3.4.5 | Further Biochemical Analysis. | 136 |
| 4 | Chapter 4: GPRC6A & RAMP1 Role in Prostate Cancer..... | 138 |
| 4.1 | GPRC6A & RAMP1 Role in Prostate Cancer Introduction..... | 139 |
| 4.1.1 | Prostate Cancer. | 139 |
| 4.1.2 | GPRC6A & RAMP1 in Prostate Cancer. | 145 |
| 4.1.3 | Prostate Cancer Cell lines..... | 146 |
| 4.1.4 | Generation of RAMP1 ^{-/-} PC-3 Cell line. | 149 |
| 4.1.5 | Research Aims. | 155 |
| 4.1.6 | Research Hypothesis..... | 155 |
| 4.2 | Materials & Methods..... | 156 |
| 4.2.1 | PC-3 Cell Culturing. | 156 |
| 4.2.2 | Calcium 6 FLIPR Kit Assay..... | 156 |
| 4.2.3 | PC-3 Cell Viability Assay. | 156 |
| 4.2.4 | Statistical Analysis. | 157 |
| 4.3 | Results..... | 158 |
| 4.3.1 | Calcium Signalling in PC-3 Cell line. | 158 |
| 4.3.2 | NPS-2143 Effect on PC-3 Cells Viability..... | 160 |
| 4.4 | Discussion..... | 162 |
| 4.4.1 | hGPRC6A-mediated Testosterone Signalling in Wild Type PC-3 Cells. | 162 |
| 4.4.2 | GPRC6A on PC-3 Cell Viability. | 164 |
| 5 | Chapter 5: General Discussion..... | 166 |
| 5.1 | General Discussion. | 167 |
| 5.1.1 | GPRC6A Cell Surface Trafficking. | 168 |
| 5.1.2 | CHO-K1 GPRC6A/RAMP1 Overexpression System. | 171 |
| 5.1.3 | GPRC6A Downstream Signalling Profile..... | 172 |
| 5.1.4 | GPRC6A & RAMP1 in Prostate Cancer | 175 |
| 5.1.5 | Conclusions. | 176 |
| 6 | References..... | 178 |
| 7 | Appendix..... | 227 |

Contents of Figures.

Chapter 1

| | |
|--|----|
| Figure 1.1 Ligand Stimulation & Signalling at GPCRs;..... | 22 |
| Figure 1.2 Comparison of Human & Mouse <i>Gprc6a</i> ;..... | 24 |
| Figure 1.3 (A) Proposed 3D general structure of GPRC6A constructed from X-ray crystallography studies of mGlu ₁ , mGlu ₃ , and β_2 -adrenergic Class C GPCRs. | 27 |
| Figure 1.4; Receptor Activity-Modifying Proteins; | 43 |

Chapter 2

| | |
|--|----|
| Figure 2.1 Principles of Forster Resonance Energy Transfer;..... | 53 |
| Figure 2.2 FRET analysis of GPRC6A and RAMP1 interaction;). | 54 |
| Figure 2.3 (A) Illustration of Flow Cytometry staining;..... | 56 |
| Figure 2.4 GPRC6A constructs;..... | 67 |
| Figure 2.5 RAMP1 constructs; | 68 |
| Figure 2.6 BCA Protein Assay Stand Curve;..... | 77 |
| Figure 2.7 Endpoint PCR analysis of CHO GPRC6A and CHO RAMP1 endogenous expression;..... | 82 |
| Figure 2.8 Sanger sequence for endogenous CHO-K1 GPRC6A and RAMP1; | 83 |
| Figure 2.9 Citrine, Cerulean and FRET Imaging of FAC sorted CHO-K1 cell lines; | 84 |
| Figure 2.10 Endpoint PCR analysis and Sanger Sequencing of GPRC6A-myc constructs;..... | 86 |
| Figure 2.11 Flow Cytometry RAMP1-Flag Staining; | 87 |
| Figure 2.12 Flow Cytometry GPRC6A-myc Staining;..... | 89 |
| Figure 2.13 GPRC6A-myc Cell Surface Expression;..... | 90 |
| Figure 2.14 RAMP1-Flag Cell Surface Expression; | 91 |

Chapter 3

| | |
|--|-----|
| Figure 3.1 Mechanistic Model of GPCR Activation;..... | 106 |
| Figure 3.2 LANCE cAMP Assay Principle; | 117 |
| Figure 3.3 ATP Dose Response & Example ATP Traces of Intracellular Calcium Release; | 119 |
| Figure 3.4 Intracellular Calcium mobilisation induced by L-amino acids;..... | 121 |
| Figure 3.5 Calcium mobilisation induced by bone/hormone ligands on GPRC6A+RAMP1 expressing CHO-K1 cells; | 123 |

Figure 3.6; **(A)** Calcium mobilisation following UBO-QIC Gq inhibitor **(B)** NPS-2143 antagonist dose response curve; 125

Figure 3.7 Intracellular cAMP accumulation induced by L-amino acids; 126

Figure 3.8 Intracellular cAMP Accumulation induced by bone/hormone ligands; 127

Figure 3.9 Adenylyl cyclase inhibition induced by L-Orn and DJ V-159; 128

Chapter 4

Figure 4.1; **(A)** Amplified PC-3 DNA samples by endpoint PCR targeting RAMP1..... 149

Figure 4.2 Deletion of RAMP1 reduces the tumorigenic capability of PC3 cells in vitro; 152

Figure 4.3 Deletion of RAMP1 leads to reduction of subcutaneous xenograft tumour growth; 153

Figure 4.4 Calcium mobilisation stimulation on PC3 RAMP1 KO cells;..... 159

Figure 4.5 Treatment of NPS-2143 dose response on PC-3 cell line; 160

Figure 4.6 NPS-2143 Treatment PC-3 Cell Viability Assay;..... 161

Chapter 5

Figure 5.1 Proposed model for human GPRC6A/RAMP1 trafficking and signalling;..... 171

Appendix

Figure Ap.1 G418 antibiotic concentration kill curve; 228

Figure Ap. 2 Optimisation of GPRC6A-YFP transfection method; 229

Figure Ap.3 Fluorescence-assisted cell sort of GPRC6A-Cit and RAMP1-Cer populations;..... 230

Figure Ap.4 CHO-K1 LANCE cAMP kit assay cell number optimisation; 231

Figure Ap.5 Intracellular cAMP accumulation induced by testosterone metabolic derivatives;..... 232

Contents of Tables.

Chapter 1

| | |
|---|----|
| Table 1.1 G protein subtypes; | 19 |
| Table 1.2 GPRC6A Expression profile; | 25 |
| Table 1.3 EC ₅₀ values (μM) for L-amino acids on GPRC6A from mouse, rat, and human studies | 33 |

Chapter 2

| | |
|--|----|
| Table 2.1 ReliaPrep Cell Miniprep System; | 63 |
| Table 2.2 High capacity RNA-to-cDNA kit; <i>List of reagents for cDNA synthesis.</i> | 64 |
| Table 2.3 CHO-K1 GPRC6A and RAMP1 Primer design; | 65 |
| Table 2.4 GoTaq® PCR Mastermix reagents; | 65 |
| Table 2.5 GPRC6A-myc Sequencing primer design; | 75 |
| Table 2.6 Bicinchoninic acid (BCA) protein assay; | 76 |

Chapter 3

| | |
|--|-----|
| Table 3.1 Flexstation 3 plate reader parameters; | 116 |
|--|-----|

Chapter 4

| | |
|--|-----|
| Table 4.1 Current Anti-Androgen Therapies; | 144 |
|--|-----|

List of Abbreviations.

7TM – seven-pass transmembrane
AC – adenylyl cyclase
ATP – adenosine triphosphate
AR – androgen receptor
BCA – bicinchoninic acid
BMD – bone mineral density
BSA – bovine serum albumin
Ca²⁺ – calcium ions
cAMP – cyclic adenosine monophosphate
CaSR – calcium sensing receptor
Cer - Cerulean
CFP – cyan fluorescence protein
CGRP – calcitonin gene-related peptide (CLR+RAMP1)
Cit – Citrine
CLR – calcitonin receptor-like receptor
CRD – cysteine-rich domain
CTR – calcitonin receptor
DAG – diacylglycerol
ELISA – enzyme-linked immunosorbent assay
ER – endoplasmic reticulum
ERK – extracellular signal-regulated kinase
FACS – fluorescence-assisted cell sorting
FRET – fluorescence resonance energy transfer
FSK - forskolin
GABA_B – γ-aminobutyric acid receptor B
GDP – guanosine diphosphate
GTP – guanosine triphosphate
GPCR – G protein-coupled receptor
GPRC6A – G protein-coupled receptor, class C, group 6, member A
hGPRC6A – human GPRC6A

GWAS – genome-wide association study
HRP – horseradish peroxidase
mGPRC6A – mouse GPRC6A
HBSS – Hank’s buffer saline solution
ICL – intracellular loop
IP₃ – inositol 1, 4, 5-triphosphate
L-Ala – L-alanine
L-Arg – L-arginine
L-Lys – L-lysine
L-Orn – L-ornithine
MAPK – mitogen-activated protein kinases
Mg²⁺ – magnesium ions
mGlu – metabotropic glutamate receptor
Ocn - osteocalcin
PBS – phosphate-buffered saline
PCR – polymerase chain reaction
PKA – protein kinase A
PKC – protein kinase C
PLC – phospholipase C
PTX – pertussis toxin
RAMP – receptor activity-modifying protein
RT – reverse transcriptase
RT+VE – RT positive control (reaction conducted in the presence of RT)
RT-VE – RT negative control (reaction conducted in the absence of RT)
SDS – sodium dodecyl sulphate
SNP – single nucleotide polymorphism
T1R – taste 1 receptor
VFT – venus flytrap
WT – wild type
YFP – yellow fluorescence protein
KO – knock out
siRNA – small interference ribonucleic acid

Chapter 1: General Introduction.

1.1 Introduction.

The G protein-coupled receptor, class C, group 6, member A (GPC6A) is a novel G protein-coupled receptor (GPCR) belonging to the class C GPCRs; including the metabotropic glutamate (mGlu) receptors, the γ -aminobutyric acid receptor B (GABA_B), the calcium-sensing receptor (CaSR), as well as three taste receptors (T1R), pheromone receptors (abundant in rodents but not humans) and a group of orphan receptors (i.e. GPR156, GPR158, GPR179, and GPR5A-D) (Alexander et al., 2013; Armstrong et al., 2020). GPCR classification is based predominately upon similarities in their sequence homology in the transmembrane region and to a lesser extent the types of ligands they can therefore sense (Basith et al., 2018). Currently GPC6A falls into this family based on its similarities in sequence homology and types of ligands. The majority of research investigating GPC6A's physiological role has been based on the phenotypic observations from three GPC6A knockout (KO) mice models (Pi et al., 2015; Wellendorph et al., 2009; Jorgensen, et al. 2017). However, data from the different KO models have failed to produce concordant data, making the delineation of GPC6A's physiological profile increasingly challenging. Current pharmacological data is agreed that GPC6A is activated by L-type amino acids and high levels of divalent cations (Ca²⁺ and Mg²⁺); with such ligands reported to predominately initiate intracellular calcium mobilisation and inositol 1, 4, 5-triphosphate (IP₃) accumulation (Pi, Nishimoto and Quarles, 2017; Rueda, P. et al. 2016). However, pharmacological studies on GPC6A's responses to hormones osteocalcin (Ocn) and testosterone remain inconsistent (Pi et al., 2017). Here we sought to conduct a fundamental pharmacological study aiming to elucidate what ligands GPC6A is responsive to and begin preliminary investigations into GPC6A's physiological role.

1.1.1 G Protein-Coupled Receptors.

GPCRs represent the largest family of mammalian membrane-associated protein receptors (approximately 800 GPCRs in the human genome) (Leach & Gregory, 2017). These cell surface receptors play a pivotal part in transducing a variety of external stimuli to initiate intracellular signalling cascade reactions. GPCRs share common architecture, consisting of seven helical transmembrane domains (7TM) connected by alternating intracellular (ICL) and extracellular loops, an intracellular C-terminus and an extracellular N-terminus (Jacobson, 2016). GPCRs are currently categorised into six major classes; A through F, grouped on the basis of their

amino acid sequence homology, structural features and similarities in physiological ligands they sense (G. M. Hu *et al.*, 2017).

Due to their involvement in a wide variety of physiological processes and cell surface accessibility, GPCRs are the single largest class of drug targets. Approximately 35% of all pharmaceutical drugs approved by the FDA target a GPCR, with currently 320 new therapeutic agents in clinical trials (Hauser *et al.*, 2017; Sriram & Insel, 2018). Research has now identified several novel characteristics within GPCRs; including hetero- and homo-dimerization, and the recruitment of necessary accessory proteins, to potentially target in new drug development strategies (Rask-andersen *et al.*, 2014; Santos *et al.*, 2016). These characteristics could provide exploitative avenues to modulate the receptors actions, targeting interventions of specific cellular processes and minimising potential side effects (Hauser *et al.*, 2017; Jacobsen *et al.*, 2017). Therefore, mapping GPCRs expression and possessing a detailed knowledge of their functional mechanisms is increasingly valuable to the development of novel pharmaceuticals.

1.1.2 GPCR Activation.

GPCRs transduce extracellular stimuli through heterotrimeric G proteins associated at the intracellular side of the plasma membrane. Activation of G protein signalling can initiate a variety of intracellular signalling cascades (Weis & Kobilka, 2018). G proteins associate at the C-terminus of the GPCR and exist in a heterotrimeric complex, comprising three subunits; α , β , and γ . Subunits β and γ possess high affinity for one another and are often treated as a single unit (Syrovatkina *et al.*, 2016). In the unstimulated state, the $G\alpha$ subunit directly binds a single guanosine-diphosphate (GDP) molecule in complex with the peripheral β and γ subunits. Ligand binding to a GPCR triggers a conformation change within the GPCR structure allowing for transduction of the external stimuli to form a high affinity agonist-GPCR complex. Subsequent G protein activation allows for the displacement of the GDP molecule with a guanosine-triphosphate (GTP) molecule at the $G\alpha$ subunit, followed by the dissociation of the $\beta\gamma$ heterodimer (Neumann, Khawaja and Müller-ladner, 2014). Release of $G\alpha$ subunit enables activation of membrane-associated effector proteins to begin downstream signalling cascade reactions. G proteins remain in the active state whilst GTP is bound; however, hydrolysis of GTP to GDP initiates the re-assembly of the α , β , and γ subunits into the inactive

heterotrimeric state and commences re-association with the GPCR (Figure 1.1) (Neumann *et al.*, 2014; Syrovatkina *et al.*, 2016).

Additionally, role of the $\beta\gamma$ heterodimer also plays an important signalling role. Initially thought to act as the negative regulator of the $G\alpha$ subunit, allowing reassembly with the receptor for subsequent signalling. In the inactive state, GDP bound $G\alpha$ is tightly associated to the $\beta\gamma$ subunit, reducing the rate of which GDP is released thus acting as an inhibitor. Upon agonist binding, active $G\alpha$ releases GDP and now binds free GTP as described above. Here, the $\beta\gamma$ subunit plays a chief role in promoting nucleotide exchange (Gurevich & Gurevich, 2019). Research has proposed a mechanism for nucleotide exchange. Crystal structures of GPCRs in active and inactive conformations reveal shifts in receptor conformations in order to sufficiently activate G protein signaling. Most notably, TM6 and TM7 outward movements.

$G\alpha$ is thought to dissociate from the cognate $\beta\gamma$ subunit allowing access to the effector binding interfaces and enabling subsequent downstream signalling (Smrcka, 2008). Crystal structures of GPCRs in active and inactive conformations revealed important conformational changes for receptor mediated nucleotide exchange. $G\alpha$ subunits has been shown that the nucleotide binding site is buried at the interface between the two domains, the ras-homology domain (RHD) and the alpha-helical domain (AHD). This suggests a receptor-mediated rearrangement of these domains to enable nucleotide entry or exit (reviewed by Mahoney, & Sunahara, 2016). While RHD and AHD separation within $G\alpha$ is necessary for GDP release, opening the inter-domain interface is insufficient to stimulate nucleotide exchange. Rather, an activated receptor promotes GDP release by allosterically disrupting the nucleotide-binding site via interactions with the $G\alpha$ N- and C-termini (Devree, *et al.* 2016). Crystal structures of bound nucleotide is coordinated by interactions between the purine base with the $\beta 5$ - $\alpha 4$ and $\beta 6$ - $\alpha 5$ loops, as well as interactions between the nucleotide phosphates and the P-loop of the $G\alpha$ RHD (Kaya, *et al.* 2014; Pachov *et al.* 2016). These regions of $G\alpha$ are directly linked to receptor-interacting elements. The $\alpha 5$ helix (carboxy-terminus) of the G protein engages an activated GPCR by embedding into the site opened by the outward movement of TM6. Similarly, the P-loop is tied to the $G\alpha$ N-terminal helix via the $\beta 1$ strand, and several lines of evidence suggest that interaction of the receptor with the $G\alpha$ N-terminus

contributes to GDP release (reviewed by Duc, Kim, Chung 2017; Mahoney and Sunahara, 2016; Weis & Kobilka, 2018).

Gβγ subunits have also been shown to exhibit a role in the recruitment of GPCR signalling proteins (e.g GPCR kinases and arrestins) in order to regulate the sensitivity of GPCRs and prevent further signalling (Gurevich & Gurevich, 2019). In addition to desensitising GPCR signalling, research has now shown Gβγ subunits can modulate numerous effector proteins involved in GPCR signalling including ion channels (Logothetis *et al.*, 1987), phospholipase C (PLC) proteins (Philip *et al.*, 2010; Poon *et al.*, 2009; Jing Zhang *et al.*, 1996), adenylyl cyclase (AC) isoforms (Sunahara & Taussig, 2002; Taussig *et al.*, 1994), voltage gated calcium channels (Geib *et al.*, 2002; Gray *et al.*, 2007; Zamponi *et al.*, 1997), and mitogen-activated protein kinases (MAPK) (Kotecha *et al.*, 2002; L. M. Luttrell *et al.*, 1999). This field has become an intriguing new aspect of GPCR research and has been reviewed extensively by (Dupré *et al.*, 2009), (Khan *et al.*, 2013), and (Mahoney & Sunahara, 2016); however, is not main focus of this work.

The mechanism by which GPCRs become activated is based on a dynamic conformation equilibrium between the inactive and active biophysical states (Gardella & Vilardaga, 2015). Research suggests that ligand binding produces a subsequent shift in the receptors that favours the active conformation in order to transduce the extracellular stimuli (Routledge *et al.*, 2017).

1.2 G Protein-mediated Signal Transduction Pathways.

Following signal transduction and G protein activation, G proteins trigger intracellular signalling cascade through the activation of secondary messengers. Secondary messengers coordinate a cascade of enzymes which ultimately lead to an increase in protein phosphorylation and a biological response. Activation of G protein signalling can initiate the production of a wide range of different secondary messenger molecules including; cyclic adenosine monophosphate (cAMP), diacylglycerol (DAG), and IP₃. Three main G protein signalling pathways have been categorised based on the respective secondary messenger and signalling cascades (Figure 1.1) (Cabrera-vera *et al.*, 2003). The most well studied pathways mediated by G proteins act through the G protein subtypes, Gα_s, Gα_q, and Gα_i. These

pathways sequentially coordinate the activation/inactivation of the downstream effector proteins; AC and PLC, respectively (Jiang and Bajpayee, 2009). Activation of a distinct pathway is predominantly ligand-dependant; however, GPCRs has been shown to display preferential coupling to specific pathways depending on tissue types co-factors and/or external environmental influences (M. Jiang & Bajpayee, 2009) (Figure 1.1).

It is assumed that Gas subunit C-terminus interact with a cognate receptor and is a primary determinant for g-protein selectivity. Okashah et al., (2019) showed using BRET-based interaction methods that upon stimulation all receptors couple with $G\alpha_i$ to some extent and $G\alpha_s$ receptors all coupling somewhat to $G\alpha_q$. However, $G\alpha_i$ receptor such as the muscarinic 3 receptor appeared to be much more specific. Crystallography studies have attempted to elucidate the mechanisms which underpin G protein selectivity; however, these efforts have failed to deduce the precise coupling. This is likely due to these structure are GDP-released final state of GPCR-G protein complexes. Whereas, recent data has suggested a step-wise conformational change occurs whereby early-stage conformations differing from current crystallography models (Du et al., 2019; X. Liu et al., 2019; J. Wang et al., 2020). Interestingly, recent research revealed the existence of a “selectivity amino acid barcode” on each G protein that is recognised by distinct regions on the GPCR; as well as sequence-based coupling specificity features, inside and outside the transmembrane domain. Although universally conserved positions in the barcode allow the receptors to bind and activate G proteins in a similar manner, different receptors recognise the unique positions of the G-protein barcode through distinct residues (Flock et al., 2017; Inoue et al., 2019). This data was also mirrored recently by Seo et al., (2021) demonstrating GPCRs and G proteins have a common conserved and coevolved residues narrowing down the region known as G-Red.

Table 1.1 G protein subtypes; G pathways proteins and their interacting effector proteins, respective biological functions.

| G-protein | Subtype (s) | Protein Effector(s) | Physiological Function(s) |
|-----------------|---|--|--|
| G _s | G α_s ; G α_{olf} | <ul style="list-style-type: none"> Stimulates adenylyl cyclase activity | <ul style="list-style-type: none"> Myocardial hypertrophy, decrease in amino acid uptake, inhibition of synthesis of glycogen, oestrogen and progesterone synthesis, aldosterone and cortisol synthesis , reabsorption of calcium from bone, fluid secretion, inhibition of platelet aggregation and secretion |
| G _q | G α_q ; G α_{11} , G α_{14} ; G α_{15} | <ul style="list-style-type: none"> Activates phospholipase C p63RhoGEF | <ul style="list-style-type: none"> Myocardial hypertrophy, platelet activation, hormone release in anterior pituitary, synaptic transmission at Purkinje cell synapses |
| G _i | G α_{i1} ; G α_{i2} ; G α_{i3} ; G α_{oA} ; G α_{oB} ; G α_z ; G α_{t1} ; G α_{t2} ; G α_g | <ul style="list-style-type: none"> Inhibits adenylyl cyclase activity. Increases activity of cGMP-Phosphodiesterase E | <ul style="list-style-type: none"> Vision, taste, cardiac activation (contractility), regulation of cardiac L-type Ca²⁺ channels, hepatic autophagy, lipid metabolism, regulation of immune cells, renal function, platelet activation, |
| G ₁₂ | G α_{12} , G α_{13} | <ul style="list-style-type: none"> Regulates Ras homology guanine nucleotide exchange factors. Activates phospholipase D | <ul style="list-style-type: none"> Platelet activation, smooth muscle contraction, leukocyte migration, neuronal axon guidance |

1.2.1 Phosphatidylinositol Signalling Pathway G α_q /PLC/IP₃.

GPRC6A is reported to predominantly couple to the G α_q signalling pathway (Jacobsen et al., 2013; P Wellendorph et al., 2005). Activation of the G α_q protein allows the α -subunit to laterally diffuse through the plasma membrane and subsequently activate membrane-associated PLC to hydrolyse phosphatidylinositol 4, 5-biphosphate to secondary messengers; IP₃ and DAG. IP₃ can now migrate towards the endoplasmic reticulum (ER) where it binds its corresponding receptor to facilitate the mobilisation of intracellular calcium (Ca²⁺) stores (Shukla *et al.*, 2014). Concurrently, DAG elicits the activation of cytosolic protein kinase C (PKC) thus enabling the consequent phosphorylation of several cascade-associated proteins that results in the activation of transcription factors, enabling the modulation of gene expression (Figure 1.1) (Putney & Tomita, 2013).

It is agreed that PLC is that canonical target effector protein for the $G\alpha_q$ pathway, however, studies have now identified other direct effectors proteins activated by $G\alpha_q$. Studies have shown the p63RhoGEF to bind $G\alpha_q$ facilitating Rho activation by converting Rho-GDP to Rho-GTP. The canonical mechanism for this pathways activation involves the activation of the $G\alpha_{12/13}$ family and p115RhoGEF. However, this has been shown to be cell type and/or receptor-dependant with certain tissues preferentially activating the $G\alpha_q$ pathway (Aittaleb *et al.*, 2010).

A number of well validated $G\alpha_q$ inhibitors have been identified. These include; the cyclic peptide YM-254890 isolated from *Chromobacterium spp.* (Takasaki *et al.*, 2004), and UBO-QIC (also known as FR900359) isolated from *Ardisia crenata* (Schrage *et al.*, 2015). YM-254890 is reported to bind at hinge region connecting two domains of the $G\alpha_q$ protein; α -helical domain and the Ras-like domain. GDP and GTP bind at the interface between these two domains (Wall *et al.*, 1995). Binding of YM-254890 at the hinge stops the two domains from separating, thus preventing GDP/GTP binding at the concealed nucleotide binding site, resulting in G protein inhibition (Dror *et al.*, 2015; Rasmussen *et al.*, 2011). UBO-QIC is thought to act in a similar fashion due its structural similarities to YM-254890. However, biochemical investigation has reported UBO-QIC to possess a higher specificity for $G\alpha_q$ and bind via a slower reversible mechanism that demonstrates a longer duration of action (Charpentier *et al.*, 2016; Schrage *et al.*, 2015).

1.2.2 Cyclic AMP Signalling Pathway $G\alpha_s$ /AC/cAMP/PKA.

As well as its $G\alpha_q$ coupling capabilities; GPRC6A has also been shown to couple to the $G\alpha_s$ signalling pathway (Pi *et al.*, 2015, 2016; Pi & Quarles, 2012b). Activation of $G\alpha_s$ proteins initiates AC activity, increasing adenosine triphosphate (ATP) hydrolysis and cAMP production. cAMP's subsequent accumulation act as the secondary messenger necessary for downstream cascade reactions to occur; resulting in protein kinase A (PKA) activation. Increases in PKA activity allow for transcription factor activation and subsequent modulation of target gene expression (Figure 1.1) (Ali *et al.*, 2008; Rueda *et al.*, 2016). Several modulators have been identified to activate the nine AC isoforms, all can be activated by $G\alpha_s$. The $G\alpha_s$ family consists of two $G\alpha_s$ splice variant isoforms; $G\alpha_s$ short and $G\alpha_s$ long, and $G\alpha_{olf}$ (Table

1.1). Due to its involvement in major biological processes $G\alpha_s$ has been widely studied. The $G\alpha_s$ family members action can be inhibited by Suramin and related small molecules; however, their action exhibit low specificity and low membrane permeability thus have little use for targeting $G\alpha_s$ *in vivo* (Hohenegger *et al.*, 1998).

1.2.3 $G\alpha_i$ /AC/cAMP/PK Signalling.

The primary function of $G\alpha_i$ subunits is to act as a negative regulator of $G\alpha_s$ signalling through the inhibition of AC activity. This results in a decrease in cAMP production which prevents the activation of protein kinases. The $G\alpha_i$ family consists of $G\alpha_o$, $G\alpha_{i1}$, $G\alpha_{i2}$, $G\alpha_{i3}$, $G\alpha_z$ and $G\alpha_t$ (Table 1.1) (Hepler & Gilman, 1992). All $G\alpha_i$ isoforms have been shown to inhibit AC with biochemical assays revealing no isoform-specific functions (Sunahara *et al.*, 1996). Pertussis toxin (PTX) produced by *Bordetella pertussis* catalyses α subunit ADP-ribosylation of the $G\alpha_i$ protein, thereby inhibiting G proteins from interacting with their cognate receptor. This ADP-ribosylation locks the α subunit into an inactive GDP-bound state, preventing the inhibition of AC (Burns, 1988; Mangmool & Kurose, 2011; Pittman, 1979). Excluding $G\alpha_z$, all of the $G\alpha_i$ family members are inhibited by PTX through ADP-ribose modification of a unique cysteine residue at the C-terminus. This modification is thought to inhibit interaction with GPCRs by steric occlusion (Campbell & Smrcka, 2018). With numerous GPCRs being reported to couple through this pathway, $G\alpha_i$ is thought to be the most widely distributed signalling system. In receptor pharmacology, this $G\alpha_i$ inhibitory action has been can be exploited to investigate GPCRs $G\alpha_i$ modulation provoking an enhanced cAMP accumulation (Burns, 1988; Katada & Ui, 1982; Tamura *et al.*, 1982). Few reports have shown whether GPRC6A couples to the $G\alpha_i$ pathway with different groups unable to replicate the others findings (Jacobsen *et al.*, 2013; Pi & Quarles, 2012b).

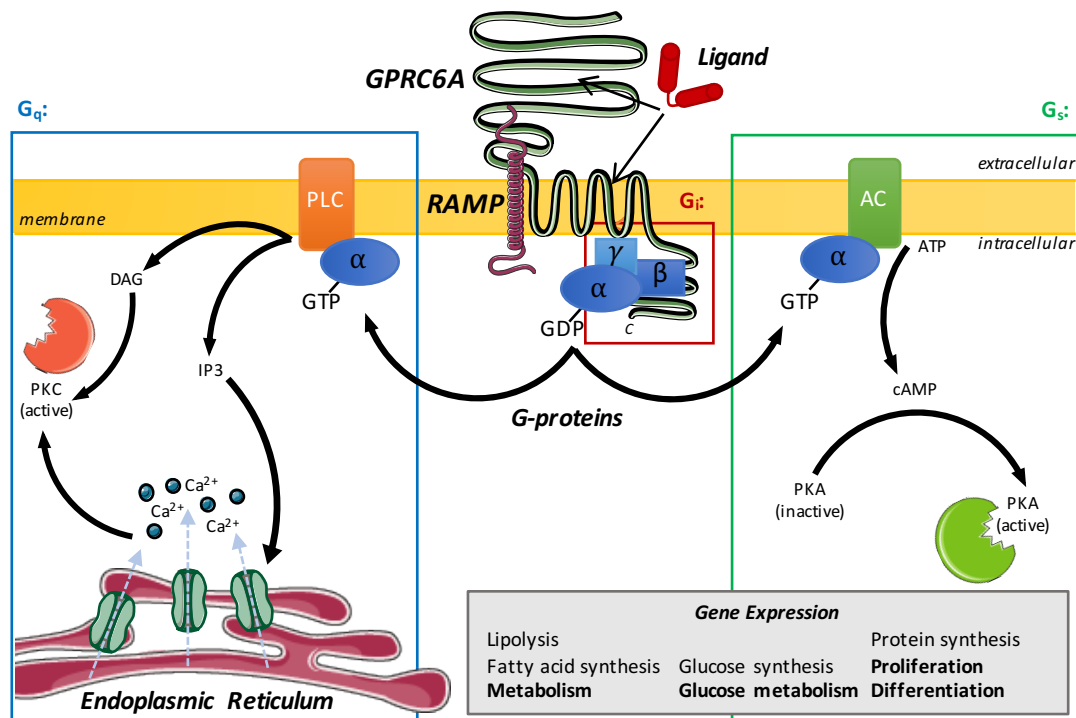


Figure 1.1 Ligand Stimulation & Signalling at GPCRs; GPCRs mediate the action of multiple specific ligands. Upon stimulation GPCR facilitates G α binding GTP (active state) and dissociates from $\beta\gamma$ -subunits. GPCRs couple to a multitude of signalling cascades, principally the G α s/cAMP/PKA pathway, the G α q/PLC/PKC pathway, and G α i pathways. Signal is transduced intracellular through a series of cascade reaction that ultimately result in the activation of transcription factors that will modulate cellular gene expression; influencing the overall biological response (adapted from with permissions from Nature Reviews Copyright 2016, Gardella & Vilardaga, 2015).

1.2.4 Arrestin-Mediated Signalling.

The first identified role of arrestins was the prevention of re-coupling of a phosphorylated GPCR to its cognate G proteins by successfully out-competing G protein complex (Wilden *et al.*, 1986). Recent data show both to engage at same interhelical cavity located at the cytoplasmic side of the receptor to block binding of the other (Carpenter *et al.*, 2016; Y. L. Liang *et al.*, 2017; Y. Zhang *et al.*, 2017; Zhou *et al.*, 2017). In the active phosphorylated state, G proteins readily dissociate from the GPCRs, thus arresting effaceable out compete G proteins. Binding of the arrestins promote the recruitment of clathrin, adaptor protein-2 and other proteins responsible for receptor internalisation (Goodman *et al.*, 1996; Laporte *et al.*, 1999). In addition to receptor desensitisation, arrestins have also been shown to serve as signalling transducers (reviewed by (Peterson & Luttrell, 2017). Arrestin signalling has been shown to initiate Src-dependent MAPK and extracellular signal-regulated kinase (ERK) 1/2 activation (L. M. Luttrell *et al.*, 1999; 2001). However, whether these events are entirely

arresting-dependent still remains an area of dispute and need further study. This rapidly developing field of GPCR research has been extensively reviewed by Gurevich & Gurevich, 2019.

1.2.5 MAPK/ERK Signalling Pathway.

Multiple reports have shown GPRC6A to activate ERK1/2 phosphorylation in response to a number of ligands (Pi *et al.*, 2012, 2016; Ye *et al.*, 2019). The ERK pathway is one of the four MAPK signalling pathways. The activation of ERK cascade is responsible for cell proliferation and differentiation, migration, apoptosis and survival. Aberrant signalling of this pathway is often linked to the development of many cancers. It has been well demonstrated that GPCRs may couple to the ERK signalling cascade (Eisingdrelo, 2013). GPCRs can activate the ERK phosphorylation through $G\alpha$ subtypes (Table 1.1) and $G\beta\gamma$ signalling through Ras, Rap, phospho-kinases, tyrosine kinases (i.e. Src) or arrestins (Ahn *et al.*, 2004; Leroy *et al.*, 2007; H. Wei *et al.*, 2003). As described in sections 1.3.1 and 1.3.2, PKA and PKC are important components in G-proteins mediated signalling. Researchers have demonstrated that treatment with the PKA inhibitor H89 and PKC inhibitor GF1090203X prevents G-protein-dependent ERK1/2 phosphorylation (Gesty-Palmer *et al.*, 2006; Mochizuki *et al.*, 1999).

1.3 GPRC6A Expression Profile.

Analysis of the Ensembl human genome database reports mouse and human *Gprc6a* comprises six exons with alternative splice variants that produces three functional receptor isoforms (Figure 1.2) (Law *et al.*, 2016). The most abundant of these is the human orthologue isoform 1, consisting of 926 amino acids, sharing approximately 34% sequence homology with the CaSR, 28% with the T1R1 and 24% with the mGluR1. The human and mouse homologs share an 80% sequence homology, with a key distinction between the two being the human variant is not successfully expressed at the cell surface in a recombinant system (Kuang *et al.*, 2005; P Wellendorph *et al.*, 2005; Petrine Wellendorph *et al.*, 2007; Petrine Wellendorph & Bräuner-Osborne, 2004). The reason for this intracellular retention motif is thought to be the result of an insertion/deletion variant in the third intracellular loop (ICL-3) (S. Jørgensen *et al.*, 2017). The short variant is only found in humans and least prevalent amongst the African (60%). The long variant observed in European and Asian populations is partially linked to a

premature stop codon producing a truncated non-functional form of the receptor (S. Jørgensen *et al.*, 2017; Ye *et al.*, 2017).

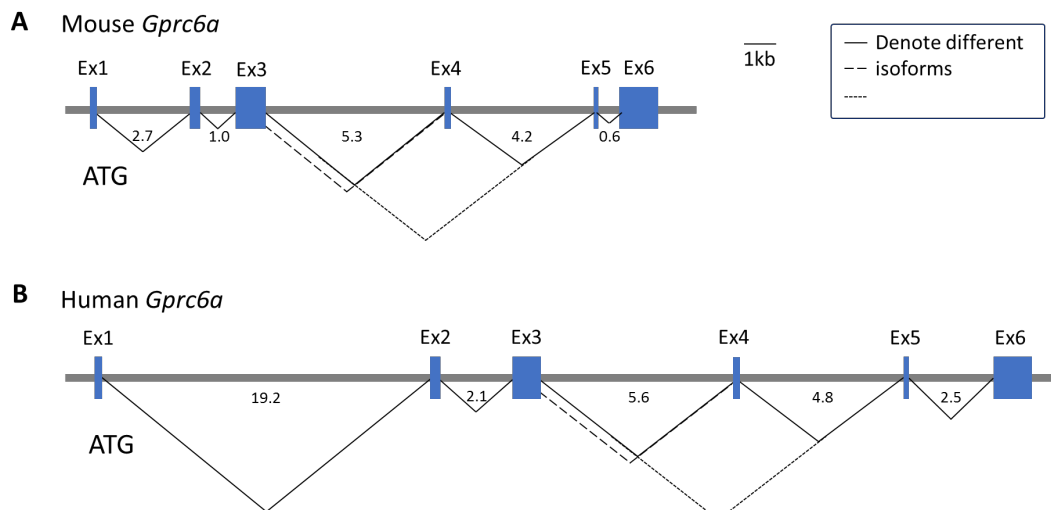


Figure 1.2 Comparison of Human & Mouse *Gprc6a*; Organisation of exons 1-6 (blue boxes) and introns (grey horizontal line); splicing at putative splice sites gives three isoforms of GPRC6A (Clemmensen *et al.*, 2014; Kuang *et al.*, 2005; Petrine Wellendorph & Bräuner-Osborne, 2004).

The expression pattern of a given receptor can often give indications to the physiological function of the receptor. The majority of data concerning GPRC6A's tissue expression profile and distribution has stemmed primarily from quantitative polymerase chain reaction analysis and *in situ* hybridisation. Quantification of GPRC6A transcripts in mouse, rat and human systems has reveal GPRC6A to be present in many tissues (see Table 1.2) although at relatively low levels (Bystrova *et al.*, 2010; Kuang *et al.*, 2005; Pi *et al.*, 2005; Regard *et al.*, 2007; Petrine Wellendorph *et al.*, 2007; Petrine Wellendorph & Bräuner-Osborne, 2004). Successfully translated GPRC6A receptor has been identified in thymus, bone, embryonic, lung, liver, heart, kidney, skeletal muscle, testis, pancreas, adipose and brain tissue (Clemmensen *et al.*, 2014). Multiple studies have reported GPRC6A mRNA to be expressed in islet of Langerhans β -cells suggesting the receptors regulatory role in insulin secretion and glucose metabolism (Pi *et al.*, 2008; Regard *et al.*, 2007; Petrine Wellendorph & Bräuner-Osborne, 2004). However, this was challenged by Luo *et al.*, (2010) stating that GPRC6A was prominently expressed in pancreatic exocrine tissues and not specifically the islets of Langerhans. Later studies confirmed of the receptors expression within the islet of Langerhans, with subsequent studies also identifying GPRC6A expression in intestinal L cells: STC-1 and GLUTag cells prompting

questions over its deeper role in energy metabolism (Oya *et al.*, 2013; Smajilovic *et al.*, 2013). Interestingly, GPRC6A transcripts has been also shown to be endogenously expressed and drastically upregulated in PC-3, 22Rv1, and LNCaP, human prostate carcinoma cell lines (Oya *et al.*, 2013a; Smajilovic *et al.*, 2013). This data sparked further investigation into GPRC6A role in prostate cancer progression discussed in chapter 4.

Table 1.2 GPRC6A Expression profile; GPRC6A receptor tissue expression pattern in mouse, rat, & human tissues (Copyright 2016 with permissions form the British Journal of Pharmacology, (Clemmensen *et al.*, 2014).

| Species | Tissues/Cell line | References |
|---------|--|--|
| Human | Brain Lung Liver Skeletal muscles Spleen Testis Heart Kidney Leukocytes Monocytes Prostate Pancreas Ovary | Wellendorph & Brauner-Osborne, 2004; Pi & Quarles 2012; Rossol <i>et al.</i> 2012 |
| Rat | Kidney Brain Lung Liver Mesenteric artery Tongue | Wellendorph <i>et al.</i> 2007; Harno, <i>et al.</i> 2008 |
| Mouse | Kidney Brain Lung Liver Testis Pancreas Salivary gland Aorta Skeletal muscles Adipose tissue Stomach Bone marrow Thymus Intestine | Kuang, <i>et al.</i> 2005; Regard, <i>et al.</i> 2007; Wellendorph, <i>et al.</i> 2009; Bystrova, <i>et al.</i> 2010; Luo, <i>et al.</i> 2010; Pi, <i>et al.</i> 2010; 2011; 2012; Oury, <i>et al.</i> 2011; Oya, <i>et al.</i> 2011; Smajilovic, <i>et al.</i> 2013 |

1.4 GPRC6A Structure-Function Relationship.

1.4.1 Receptor Structure.

Class C GPCRs are characterised by two unique structural features: first, a large extended extracellular domain that is distal from the 7TM and contains the orthosteric sites; second,

they form constitutive dimers with unique activation modes compared to other classes of GPCR. Class C GPCRs are further divided into 7 subtypes comprising; the mGlu, GABA_B, CaSR, sweet and amino acid T1R2, T1R3, pheromone receptors, odorant receptors, and orphan receptors. GPRC6A is classified as a class C GPCR comprising a characteristic extended extracellular N-terminus that has been reported to form a bi-lobed structure separate from the transmembrane domain important in ligands recognition. These two domains are separated by a region of conserved cysteine residues important in receptor activation (Figure 1.3) (Chun et al., 2012).

X-ray crystallography studies of class C GPCRs mGlu, CaSR, T1R and GABA_BR combined with analysis of GPRC6A primary sequence revealed GPRC6A to possess substantial homology (34% sequence conservation) with the human CaSR and the goldfish 5.24 receptor (44% sequence conservation) (Chun et al., 2012; Pi et al., 2011; Pi & Quarles, 2012b; Wu et al., 2014). The multiple crystal structures of class C GPCRs published reveal a characteristic seven transmembrane (7TM) domain and an extended bi-lobular N-terminal extracellular domain termed the Venus flytrap (VFT) domain, both connected by a conserved cysteine rich domain (CRD), common architectural features shared across class C GPCRs (Figure 1.3) (Brauner-Osborne et al., 2007; Chun et al., 2012; Jacobsen et al., 2013; Kunishima et al., 2000; J. Park et al., 2019; Rondard et al., 2011a; Petrine Wellendorph & Bräuner-Osborne, 2004; Wu et al., 2014).

Through mutational analysis the VFT domain has been shown to bear similar homology to that of the bacterial periplasmic binding proteins (O'Hara *et al.*, 1993) containing an orthosteric binding pocket situated between two extracellular lobes and an adjacent "hinge" region (F. Zhang *et al.*, 2008). The region is thought to provide flexibility to the structure allowing the cleft to enclose around the ligand in either an "closed" or "open" conformation (Chun et al., 2012; Kunishima et al., 2000; Tsuchiya et al., 2002). The majority of our knowledge concerning the mechanisms of GPRC6A ligand binding has been based upon mGlu receptors serving as a model system; the activation mechanism is purported to be conserved with the GPRC6A receptor given that both have been shown to be stimulated by L-amino acid agonists (Wellendorph & Bräuner-Osborne, 2009).

It is proposed that agonist binding promotes a conformation “closing” in the VFT cleft and subsequent torsion between the functional interfaces of a receptor dimer (Jensen and Spalding, 2004). This change in conformation extends downwards towards the 7TM domain through the VFT-CRD interaction allowing the activation of the cytoplasmic portion of the receptor (A. A. Jensen & Spalding, 2004). Site-directed mutagenesis of the VFT regions proposed orthosteric binding pocket identified two highly conserved serine/threonine residues, common in facilitating ligand recognition in multiple class C GPCRs (Rondard *et al.*, 2006).

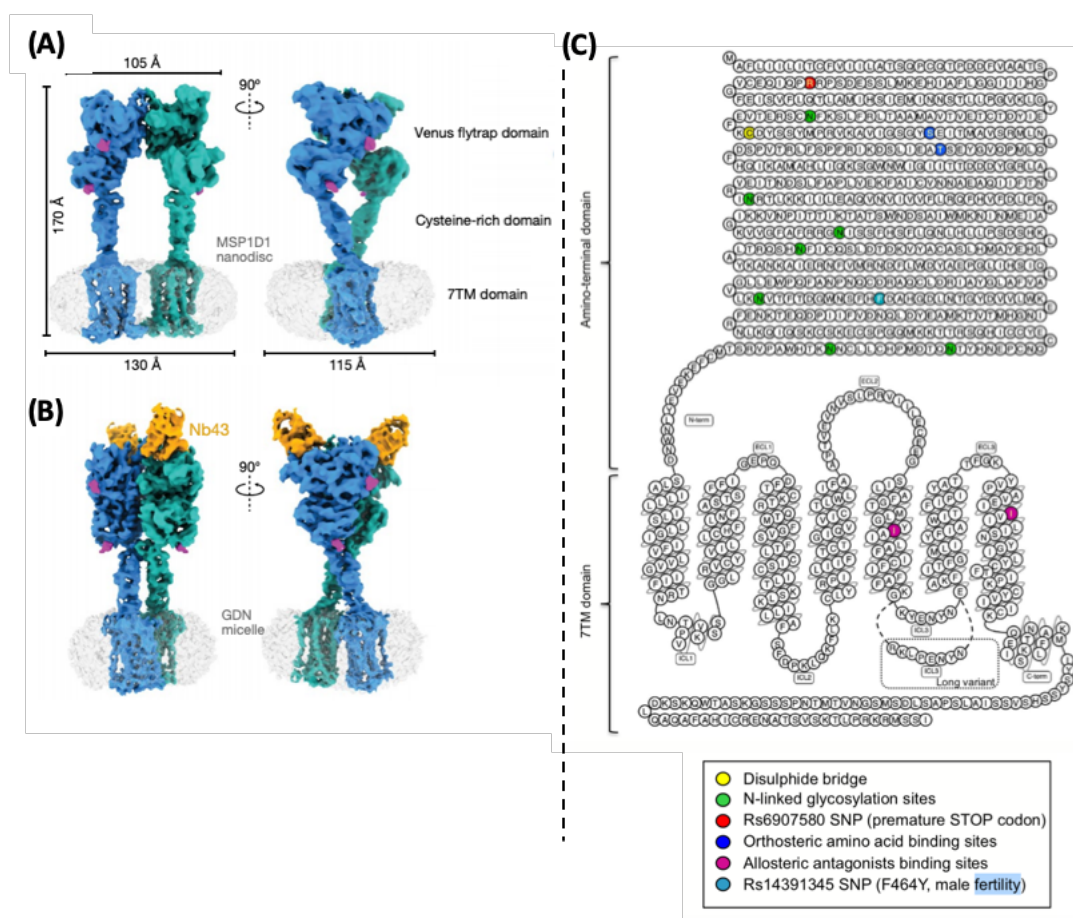


Figure 1.3 (A) Cryo-EM 3D model of full length class C mGlu5 receptor inactive (A) and active states (B). Positions in the VFT (red), CRD (yellow), CRD/7TM interface (purple) and 7TM domain (green) (Koehl *et al.*, 2019). (C) Snakeplot representation of structural features of human GPRC6A. The cysteine residue involved in homo-dimerization and the N-linked glycosylation sites are shown in yellow and green, respectively. Residues important for binding of an orthosteric ligand are shown in blue, while purple residues are involved in binding of allosteric antagonists. The long variant of the receptor (rs386705086) is indicated in the dashed area in the ICL3 region, and the premature STOP codon (rs6907580) that is partially linked to the long variant is shown in red. The SNP reported to be associated with male infertility (rs14391345) is shown in light blue. (adapted from with permissions from Nature Reviews Copyright 2016, Jorgensen & Brauner-Osborne 2019)

Further analysis of the receptor VFT domain suggests several possible sites for N-glycosylation. Western blot analysis has shown that treatment of GPRC6A using the amidase; peptide-N-glycosidase F leads to the loss of a heavier weight band revealing GPRC6A is glycosylated at its N-terminus (Wellendorph & Bräuner-Osborne, 2009; Petrine Wellendorph *et al.*, 2005a). More recent studies using site directed mutagenesis in conjunction with peptide-N-glycosidase F treatment found seven Asparagine (Asn) residues to possess N-glycans also identifying residues Asn86Q and Asn555Q impeding surface and total expression (Nørskov-Lauritsen *et al.*, 2015).

The CRD is known to be conserved across all class C GPCRs connecting the VFT and 7TM domains (excluding the GABA_{B1-2} receptors lacking a CRD region) (Brauner-Osborne *et al.*, 2007; Nørskov-Lauritsen *et al.*, 2015). CRD comprises approximately 80 amino acids containing nine conserved cysteine residues (Pin *et al.*, 2003). Further work has revealed the CRD to play an integral role in receptor activation of the mGlu₃, T1R and the CaSR (J. Hu *et al.*, 2000; P. Jiang *et al.*, 2004). The crystal structure of mGlu₃'s extracellular domain resolved by Muto *et al.*, (2007) revealed eight disulphide bond forming residues within the CRD region with a ninth forming a disulphide bridge between a cysteine residue situated within the VFT domain. The structural arrangement provides rigidity between the VFT and the CRD of the receptor (Figure 1.3). Furthermore, the disulphide link between these two domains is necessary for allosteric interaction between the VFT and 7TM domains. Mutagenesis of this site ablated agonist activation of the mGlu (Rondard *et al.*, 2006).

Recent work by Koehl *et al.*, (2019) has successfully generated cryo-EM structures for the class C GPCR mGlu5 dimers in both the active and inactive conformations. The models reveal the characteristic class C GPCR 7TM, CRD and VFT domains (Figure 1.3). Furthermore, the work demonstrated the activation mechanism for mGlu5 receptor. The active conformation of the mGlu5 is compacted with interactions occurring between subunit within the VFT, CRD and 7TM domains. The researched reports that agonist binding at the VFT domain causes a compaction of the subunit between the dimer interface, thus positioning the CRD into close proximity. Interactions between the CRD's and the second extracellular loops of the receptor enable the rigid-body repositioning of the 7TM domains, which come into contact to enable

signalling (Figure 1.3) (Koehl et al., 2019). This work is crucial in understanding how class C GPCRs function mechanistically, including the GPRC6A.

1.4.2 Cell Surface Trafficking.

Research focused towards recombinant human GPRC6A (hGPRC6A) receptor has proven to be more challenging as studies have shown the human isoform fail to be sufficiently expressed at the cell surface *in vitro*. Multiple supporting studies have demonstrated cell surface expression of rat, goldfish and mouse GPRC6A (mGPRC6A); however, hGPRC6A isoform appears to be retained and therefore fails to transduce to agonist stimuli (Kuang *et al.*, 2005; Wellendorph *et al.*, 2005; Christiansen *et al.*, 2007). A recent study by (Christiansen *et al.*, 2007; Kuang *et al.*, 2005; P Wellendorph *et al.*, 2005) sought to elucidate potential trafficking mechanisms by the creation of a chimeric receptor. The study found that substitution of the human 7TM region for the goldfish 7TM regained the receptors cell surface expression, suggesting that part of the human 7TM isoform inhibits forward trafficking. Furthermore, by site directed mutagenesis the researchers identified a change in the ICL-3 is associated with the receptors intracellular retention and impedes forward trafficking of the human ortholog. Interspecies analysis of the GPRC6A polypeptide sequence reveals a highly conserved “RKLP” sequence present in pre-human species; however, in humans a notable common polymorphism is observed at position 744 a region encoding the third intracellular loop substituting the “FAFKGRKLPENY” to a “FAFKGKYENY” amino acid sequence. The unique allele is indicative of the evolutionary changes that GPRC6A has undergone (Jørgensen *et al.*, 2017). The study identified replacement of the murine third intracellular short loop-KGKY for the human third intracellular long loop-KGRKLP variant results in minimal cell surface expression in HEK293 cells. The “KY” short form of the receptor is far more prevalent in humans with a genomic frequency ranging from 60% in the African population to 99% in the East Asian population (Jørgensen *et al.*, 2017). The longer, cell surface expressed variant has been shown to display higher prevalence in the African populations; whereas in the European and Asian population this variant is seen to be predominantly linked to a STOP codon at amino acids residue 57 leading to a truncated form of the protein (Figure 1.3) (Jørgensen *et al.*, 2017).

1.4.3 Receptor Dimerization.

It is widely accepted that receptor dimer formation is mandatory in class C GPCRs pharmacology, including; signal transduction, internalisation, and ontogeny. Many class C GPCRs have been shown to form higher order oligomers by covalent disulphide bridges at the lipophilic transmembrane domains (reviewed by Møller *et al.*, 2017). Research has shown that class C GPCRs; CaSR and mGlu forming homodimers (Bai *et al.*, 1998; Kunishima *et al.*, 2000; Romano *et al.*, 2001; Rondard *et al.*, 2011a; Tsuchiya *et al.*, 2002; Zaixiang Zhang *et al.*, 2001), while GABA_{B2} and T1R forms heterodimers in order to be successfully trafficked to the cell surface (Kaupmann *et al.*, 1997; Nelson *et al.*, 2001; Pagano *et al.*, 2001; Zhao *et al.*, 2003). Class C GPCRs form constitutive dimers at the VFT domain. mGlu₁ crystal structures reveal hydrophobic interactions between the VFT lobe 1 of each monomer which are stabilised by disulphide bond linkage (Ray *et al.*, 1999; Ray & Hauschild, 2000; Romano *et al.*, 2001; Tsuji *et al.*, 2000). This has also been demonstrated in the GABA_{B1} and GABA_{B2} heterodimer with lobe 1 mediating the subunit interaction (J. Liu *et al.*, 2004; Rondard *et al.*, 2008). Subsequent research utilising FRET-based methods has also shown mGlu₁₋₈ receptors ability to form heterodimers in HEK293 cells; however, this is yet to be demonstrated in an *in vivo* system (Doumazane *et al.*, 2011). It is important to note that class C hetero-dimerisation appears to follow receptors related within their phylogenetic tree. The CaSR is the closest homolog to GPRC6A with both receptors being widely expressed and having interrelating expression patterns (Rossol *et al.*, 2012; Wellendorph & Bräuner-Osborne, 2009). It could therefore be hypothesized that these receptors form heterodimers or alternatively, if expressed in the same system as distinct homodimers that work synergistically to facilitate intracellular signalling. While the murine receptor will successfully express at the cell surface the human receptor appears to remain intracellularly retained when expressed recombinantly (Kuang *et al.*, 2005). This species difference may be indicative of the necessity of a chaperone protein to enable forward trafficking of the receptor (Wellendorph *et al.*, 2005). This may be in the form of another receptor subtype, similar to the GABA_B receptor; or an accessory protein such as the receptor activity-modifying proteins (RAMPs) demonstrated to be fundamental components of many class B GPCRs (Morfis *et al.*, 2008).

Previously GPRC6A's ability to form dimers had only been demonstrated by bands of dimeric weight shown by Western Blot (Petrine Wellendorph *et al.*, 2007). However, recently mutagenic studies conducted by Nørskov-Lauritsen *et al.*, (2015) showed using time-resolved FRET-based analysis reported GPRC6A receptors formed homodimers through formation of disulphide linkage at a conserved extracellular cysteine 131 residue. Furthermore, agonist treatment increased the number of dimeric receptors and protected against the actions of reducing agents (Nørskov-Lauritsen *et al.*, 2015; Ward *et al.*, 1998). These findings suggest that agonist binding enhances dimer-stabilisation and the disulphide linkage aids in fine-tuning of the GPRC6A receptor conformation.

1.4.4 Desensitization & Internalisation.

Signal termination is another important aspect of GPCR signalling. The canonical model for GPCR signal termination reports intracellular kinases to phosphorylate the receptor's C-terminus, recruiting β -arrestins which in-turn uncouples the receptor-G-protein interaction, inhibiting further signalling (Reiter, *et al.* 2013). Internalised receptors then undergo endocytic compartmentalisation and sorting for degradation or recycling for further cell surface activation (Seachrist & Ferguson, 2003).

Three potential PKC phosphorylation sites have been identified in the C-terminus of GPRC6A and are believed to be involved in regulating receptor desensitization and internalization, and/or the interaction with crucial scaffolding proteins (Nørskov-Lauritsen *et al.*, 2015). Using antibody feeding assays in-tandem with time-resolved FRET revealed that the rat GPRC6A predominantly undergoes constitutive internalisation and co-localises with endosomal markers Rab5, Rab11 and to a lesser degree Rab7. These findings suggest that the GPRC6A receptor undergoes Rab11-dependant (long loop) recycling and therefore provides continual reserves of receptor at the cell surface, despite chronic exposure to agonists (Jacobsen *et al.*, 2017). A number of distinct trafficking pathways have been reported for several of the class C receptors (reviewed by Ferguson, 2001); the concept of non-canonical trafficking has become a reoccurring feature of nutrient-sensing class C GPCRs (Magalhaes *et al.*, 2012). This mechanism explains the large pool of class C receptor maintained at the cell surface despite prolonged exposure to agonists.

1.5 GPRC6A Ligand Controversies.

After first cloning the GPRC6A receptor, studies conducted by the groups led by Hampson and Brauner-Osborne quickly deorphanized the receptor as a promiscuous L-type amino acids receptor (Kuang et al., 2005; P Wellendorph et al., 2005). Later studies confirmed this, reporting $G\alpha_q$ coupled responses to L-amino acids (Faure et al., 2009; Pi et al., 2018; Rueda et al., 2016) and at physiologically relevant potencies in mice (Christiansen et al., 2007). Subsequent reports also observed divalent cations Ca^{2+} and Mg^{2+} acted either as positive allosteric modulators enhancing L-amino acid responses (Christiansen et al., 2007; Jacobsen et al., 2013; Kuang et al., 2005; Pi et al., 2005; P Wellendorph et al., 2005; Petrine Wellendorph & Bräuner-Osborne, 2004) similar characteristics observed in other class C GPCRs (Brauner-Osborne et al., 2007; Kuang et al., 2005). However, as further investigations continued into the GPRC6A, discrepancies began to emerge from different *in vitro* and *in vivo* models. Data collected from *in vivo* studies brought forth new ideas about GPRC6A's sensitivity to testosterone and Ocn. For the steroid hormone testosterone, certain studies firmly report testosterone acting through GPRC6A (Pi et al., 2015; Pi, Parrill, et al., 2010) whilst others have failed to replicate this (Jacobsen et al., 2013). Furthermore, groups also report Ocn as an GPRC6A agonist (Otani et al., 2015; Pi et al., 2005, 2011, 2016); whilst, other groups have failed to reproduce any activation (Jacobsen et al., 2013; Rueda et al., 2016). GPRC6A affinity for physiologically important ligands has made it an intriguing target for therapeutic intervention. However, due to the promiscuous array of suggested agonist and the lack of supportive pharmacological data it has made clarification of the receptors physiological role increasingly complicated.

1.5.1 L-Amino Acids.

Preliminary pharmacological studies of the hGPRC6A utilised a chimeric form of the receptor, comprising the extracellular portion of the hGPRC6A combined with the 7TM region of the goldfish 5.24-receptor. Using this approach researchers observed successful cell surface trafficking and comparable functionality in fluorometric calcium assays. Using the *Xenopus* oocyte system, GPRC6A exhibited dose-dependent responses upon L-amino acid stimulation with potent activation by L-ornithine (L-Orn), L-arginine (L-Arg), L-alanine (L-Ala), and L-lysine

(L-Lys) (micromolar range) (Table 1.3) (Kuang et al., 2005; P Wellendorph et al., 2005). Subsequent studies using alternate systems (i.e. HEK293 and CHO-K1) reported L-amino acid-induced GPRC6A activation, stating murine GPRC6A initiated intracellular calcium mobilisation and triggered endogenous Ca²⁺-dependant chloride channels coupled with IP₃ accumulation (Christiansen et al., 2007; Faure et al., 2009; Jacobsen et al., 2013; Pi et al., 2005; Rojas Bie Thomsen et al., 2012). In X-ray crystal studies, *in silico* docking of L-Arg indicated a tight fit within the orthosteric binding pocket of the VFT domain of the GPRC6A with minimal space for larger ligands (Minghua Wang et al., 2006). The findings supported previous observation reporting mutations S149A and/or S172A within the VFT orthosteric binding site ablated L-Lys and L-Arg agonistic activity (P Wellendorph et al., 2005).

Table 1.3 EC₅₀ values (μM) for L-amino acids on GPRC6A from mouse, rat, and human studies. Mouse and Rat data were determined using IP₃ accumulation in tsA cell co-expressing Gα_q(G66D). Human data was collected using chimeric receptor comprising human VFT/CRD domains and goldfish 5.24 7TM domain using Fluo-4 intracellular calcium assay. (Christiansen et al., 2007; P Wellendorph et al., 2005; Petrine Wellendorph et al., 2007)(Copyright 2016 with permissions from British Journal of Pharmacology, Clemmensen et al. 2014).

| L-amino acid | EC ₅₀ (μM) [% relative efficacy] | | | Concentration in Mouse Plasma [mean±SEM] (μM) |
|--------------|---|-------|-------|---|
| | Mouse | Human | Rat | |
| L-Orn | 63.6 | 112 | 264 | 86 |
| L-Lys | 135 | 169 | >1000 | 366 |
| L-Arg | 284 | 44.1 | >1000 | 137 |
| L-Cys | 356 | >1000 | >1000 | n/a |
| L-Ala | 486 | 173 | >1000 | 431 |

1.5.2 Osteocalcin.

Multiple studies have proposed the bone-derived peptide Ocn as a ligand for the GPRC6A. *In vitro* studies have reported the expression of GPRC6A to be essential to facilitate the effects of Ocn (Otani et al., 2015; Pi et al., 2005, 2011, 2016). Ocn is exclusively synthesised by osteoblasts, where it undergoes post-translational γ-carboxylation at three glutamate residues. In this carboxylated state, Ocn has a higher affinity to bind Ca²⁺, adopting an α-helical structure to bind to hydroxyapatite in bone ha (Hauschka & Carr, 1982; Hoang et al., 2003). During bone resorption Ocn becomes uncarboxylated losing its affinity for

hydroxyapatite and thus facilitating its release into circulation (Hauschka & Carr, 1982; Lacombe & Ferron, 2015). Multiple groups have reported that uncarboxylated Ocn's endocrine and metabolic actions are mediated through the activation of GPRC6A (Mera *et al.*, 2016; Oury *et al.*, 2011, 2013; Pi *et al.*, 2005, 2011, 2016).

GPRC6A has been shown to transduce Ocn using multiple *in vitro* models; reportedly coupling to Gα_q signalling pathways to facilitate anabolic effects in multiple tissues types (Hauschka & Carr, 1982; Oury *et al.*, 2013). Research published by Pi *et al.*, (2011) reported Ocn and Ocn-derived C-terminal hexapeptide directly stimulated GPRC6A PKD1 and ERK activation inducing increased insulin secretion from pancreatic β-cells. Furthermore, exon II GPRC6A^{-/-} significantly attenuated the observed ERK responses. Subsequent investigations into GPRC6A's sensitivity to Ocn revealed that heterologous cell lines gain Ocn sensing function when transfected with GPRC6A cDNA, whilst deletion of GPRC6A causes a loss on Ocn-induced signalling (Oury *et al.*, 2013; Pi *et al.*, 2016). Contrasting *in vitro* research by Jacobsen *et al.*, (2013) observed increases in intracellular calcium mobilisation and inositol phosphate turnover from L-amino acid stimuli but failed to see activation of GPRC6A from Ocn. Following this, supportive data observed only amino acid activation of the mGPRC6A, and were not able to reproduce the previously published data demonstrating the agonistic activity of Ocn or Ocn variants on GPRC6A, and posit that GPRC6A functionality is negligible in humans (Rueda *et al.*, 2016).

In vivo studies have attempted to make connections together with previous *in vitro* data with multiple groups arguing exon II GPRC6A^{-/-} mice exhibit identical phenotypes to that of the Ocn^{-/-} mouse model (Mera *et al.*, 2016; J. Wei *et al.*, 2014). However, a recent Ocn^{-/-} rat model challenges this conclusion where the mouse metabolic disturbances were not conserved in the rat model (Lambert *et al.*, 2016). The discrepancies here, pose the question as to whether Ocn's actions and/or GPRC6A's ligand sensitivity are conserved between species. One important point to note is the adiponectin receptors progestin and adipoQ are deleted as a consequence of generating the Ocn^{-/-} mice, and thus may cause non-specific metabolic disturbances. Therefore, it could be argued that alternate unknown Ocn receptors could be present (Ducy *et al.*, 1996; Lambert *et al.*, 2016). With the current data concerning GPRC6A's

sensitivity to Ocn it is difficult to draw any exact conclusions about the agonistic activity or the mechanisms of action further research is necessary before any consensus can be reached.

Interestingly, osteoblastic secretion of Ocn is reported to promote the biosynthesis of testosterone upon binding to GPRC6A in gonadal tissues (Wei *et al.*, 2014). The secretion of testosterone from the gonads has been established as an integral part of bone maturation and maintenance. In addition, androgens have been shown to prolong osteoblast lifespan, stimulate proliferation and differentiation, and aid in the maintenance of trabecular bone integrity (J. Wei *et al.*, 2014). A loss of function mutation in GPRC6A can lead to male sterility in humans and glucose intolerance, supporting GPRC6A importance in skeletal and gonadal cross talk (Oury *et al.*, 2013). The detailed subcellular pharmacology of this receptor and its importance in the testosterone-Ocn crosstalk currently remains unclear and thus warrants further study to elucidate this.

1.5.3 Testosterone.

Classically, testosterone is known to stimulate gene expression through nuclear androgen receptors (AR). For this to occur testosterone first must undergo conversion into 5-dihydrotestosterone so it binds with high affinity to the AR-transcription complex. However, emerging reports have suggested this process to not be essential for testosterone, hypothesising its important functions on alternate pathways distinct from AR-mediated gene transcription (Asuthkar *et al.*, 2015; Bhasin & Jasuja, 2009). Testosterone is known to facilitate fast-acting, transcription-independent effects through a GPCR, the identity of which remains to be elucidated. However, multiple groups have proposed the steroid hormone to be an endogenous GPRC6A ligand (Ko *et al.*, 2014; Pi *et al.*, 2015; Pi, Parrill, *et al.*, 2010; Ye *et al.*, 2017, 2019). Independent findings by Oury *et al.*, (2013) observed that overexpression the GPRC6A receptor in AR-deficient HEK293 cells led to rapid ERK1/2 signalling when stimulated with testosterone. In addition, GPRC6A small interference RNA (siRNA)-mediated knock down significantly attenuated testosterone-induced ERK1/2 phosphorylation compared to wild type (WT) control groups (Pi, Parrill, *et al.*, 2010). A follow up study identified target residues (Phe666 and Glu746) in the 7TM domains involved in testosterone binding by computational analysis. Subsequent site directed mutagenesis of these sites recorded significant losses in

testosterone-induced ERK1/2 phosphorylation in HEK293 cells. Results from this study strengthened previous work reporting exon II GPRC6A^{-/-} mice exhibited a reduction in β -cell insulin secretion when stimulated with testosterone (Oury *et al.*, 2011). Investigation into other models found the human prostate cancer cell-line PC-3 to be highly expressive of GPRC6A but lacking AR expression (Dreaden *et al.*, 2012; W. D. Tilley *et al.*, 1990). Repeating previous experiments revealed PC-3 cells to display substantial increases in ERK1/2 phosphorylation upon treatment with testosterone; however, negligible responses were observed in siRNA GPRC6A knockdown PC-3 cells (Pi *et al.*, 2015). Other studies provide supportive evidence reporting testosterone stimulation in skin keratinocytes provoked increased Duox1 activity and H₂O₂ production via IP₃ accumulation and calcium mobilisation. However, siRNA knock down of the GPRC6A receptor halted Duox1 activation thus preventing apoptosis induction (De Toni *et al.*, 2017; Oury *et al.*, 2011, 2013).

1.6 Role of GPRC6A in Physiology & Pathophysiology.

As previously stated the GPRC6A receptor is widely expressed and has been shown to be sensitive to range of ligands implicated in a variety of physiological processes. The majority of our knowledge on the physiology relevance of GPRC6A stems from knock out mouse studies. At present, three published KO models have been generated; exon II (Oury *et al.*, 2011; Petrine Wellendorph & Bräuner-Osborne, 2004), exon VI (Pi *et al.*, 2008) and full locus GPRC6A KO models (C. V. Jørgensen *et al.*, 2019; Kinsey-Jones *et al.*, 2015) (see Figure 1.2) . Collectively, this work has provided some insight into the phenotypic effects of GPRC6A in physiology; however, gaps in our understanding remain despite the availability of genetically modified animals. The need from strong supportive pharmacological data is required in order to correctly categorise this receptor physiological role; thus, providing a platform for future therapeutic research.

1.6.1 Bone Metabolism.

With expression studies showing GPRC6A to exhibit higher expression in bone tissues along with its broad amino acid and Ocn sensitivity many studies have attempted to identify whether this receptor has role regulating bone health (Pi *et al.*, 2008; Pi, Zhang, *et al.*, 2010; Pi & Quarles, 2012b). L-Arg is known to impact osteogenesis and osteoblastic differentiation,

and with reports mostly agreeing L-Arg as a putative ligand of GPRC6A, groups have hypothesised a regulatory role in mediating its effects. Research found that deletion of mGPRC6A exon II encoding a portion of the extracellular region of the receptor produced mice exhibiting lower bone mineral density (BMD) due to a decrease in bone mineralisation (Pi et al., 2008; Pi, Zhang, et al., 2010). These reports were later reinforced with subsequent investigation revealing *Gprc6a*^{-/-} mice exhibited a comparative osteopenia phenotype, and additional impaired osteoblast ability to sense amino acids and Ca²⁺ (S. Liu *et al.*, 2017). In contrast, targeting of exon VI of *Gprc6a* resulted in no changes in osteoblast function/numbers, bone microarchitecture, or BMD observed in the previously published research (Wellendorph & Bräuner-Osborne, 2009). Interestingly, analysis of the full locus GPRC6A KO mice (C. V. Jørgensen et al., 2019) revealed joint phenotypes, exhibiting reductions in serum osteocalcin levels (exon II) with no alterations to the bone microarchitecture (exon IV). Conclusion concerning GPRC6A's involvement in bone metabolism remain unclear. However, the data indicates that deletion of exon VI is related with a much subtler phenotype than that of exon II. Furthermore, the research also identified two single nucleotide polymorphisms (SNP) within the non-coding regions of the *Gprc6a* associated with lower spine BMD in an American cohort of 1,000 patients (Pi *et al.*, 2008; Pi, Zhang, *et al.*, 2010). However, this phenotype was unable to be fully replicated in mouse model, reporting reductions in serum Ocn levels but only minor alterations in long bone microstructure (C. V. Jørgensen et al., 2019; Petrine Wellendorph et al., 2009).

1.6.2 Energy & Glucose Homeostasis.

The majority of studies have focussed on the potential function of GPRC6A in regulating glucose metabolism. However, whether GPRC6A directly impacts on glucose homeostasis remains unclear. The lack of consensus stems again from the different knock out models used in order to study phenotypic changes (Pi et al., 2005; P Wellendorph et al., 2005). GPRC6A exon II KO mice displayed increases in adiposity, hepatic steatosis, hyperphagia, and fasting glucose levels; as well as, decreases in circulating insulin levels and insulin tolerance. Decreases in locomotion, glucose metabolic disruption and increases in levels of circulating leptin are all linked to the obesity phenotype (Pi *et al.*, 2008). In contrast, exon VI KO models exhibited no changes in body weight, nor on other indicators such as consumption of oxygen,

dietary intake. Furthermore, groups failed to support the increased body fat mass, insulin resistance, or glucose intolerance observed in the exon II model (Smajilovic *et al.*, 2013; Wellendorph & Bräuner-Osborne, 2009). These data are in accordance with phenotypes exhibited by full locus KO mice, reporting normal basal glucose levels, normal insulin sensitivity and body composition, and observed no detrimental effects on metabolic development (C. V. Jørgensen *et al.*, 2019; Kinsey-Jones *et al.*, 2015). Thus, suggesting the receptor is not integral to the regulation of energy consumption.

Research has shown that ablation of GPRC6A by the Flox/Cre methodology led to mice offspring exhibiting decreases in pancreatic weight, islet number and size, circulating insulin levels, and insulin expression; as well as reduced β -cell proliferation, all common phenotypes observed in glucose intolerance and insulin resistance (Pi *et al.*, 2008; Pi, Zhang, *et al.*, 2010). Conversely, Clemmensen *et al.*, (2013) using the same approach were unable to produce this phenotype and proposed that disruptions in glucose metabolism were identifiable when subjected to a high-fat diet; hypothesising that this phenotype may be secondary in coexistence and coexistent with adiposity and thus not directly linked to GPRC6A ablation.

Prior research has shown L-Arg; a GPRC6A agonist, is a potent insulin secretagogue and that dietary supplementation significantly aids in glucose metabolism *in vivo* (Newsholme & Krause, 2012; Pi *et al.*, 2012). Research conducted by Pi & Quarles, (2012) found islet β -cells isolated from their exon II GPRC6A KO mice, saw reductions in insulin levels and stimulation index in response to L-Arg. The work found decreases in basal serum insulin level in GPRC6A^{-/-} mice. Moreover, decreases in L-Arg-induced ERK1/2 and cAMP signalling were observed in GPRC6A^{-/-} mice. However, studies conducted using exon VI mice displayed L-Arg to potentially induce insulin secretion in both GPRC6A^{-/-} and WT cells *in vivo* and *ex vivo* (Smajilovic *et al.*, 2013). Without further study, it remains unclear as to whether GPRC6A has a direct role in L-Arg-induced insulin release.

Genetic cohort studies comparing the functional long ICL-3 GPRC6A and the non-functional short ICL-3/stop codon GPRC6A variant in a Danish population sample found that male carriers of the functional ICL-3 variant displayed increased insulin response to glucose tolerance tests compared to the short ICL-3 variant (S. Jørgensen *et al.*, 2017). Furthermore, a

separate study identified a common GPCR6A Pro91Ser genotype predisposing increased fasting insulin and HOMA-IR; however, this study failed to establish whether the patients involved were carriers of the either ICL-3 or stop codon genotypes (Di Nisio *et al.*, 2017).

1.6.3 Gastrointestinal Nutrient Receptor.

The majority of research is agreed upon GPCR6A's sensitivity to L-amino acids, combined with its expression in digestive system tissues, GPCR6A has been a suggested candidate to sense digested amino acids in the GI tract (D. Haid *et al.*, 2011; D. C. Haid *et al.*, 2012). Data has reported GPCR6A to mediate L-Orn-induced glucagon-like peptide-1 (GLP-1) release from GLUTag intestinal cells (Oya *et al.*, 2013b; Rueda *et al.*, 2016). Furthermore, studies have shown L-Arg stimulated peptide YY secretion in both WT and GPCR6A^{-/-} colonic L-cells; however, L-Arg-induced GLP-1 secretion was significantly attenuated in GPCR6A^{-/-} cells (Alamshah *et al.*, 2016). However, attempts to demonstrate this action *in vivo* have failed to show differences in GLP-1 secretion in both the exon VI and the full loci GPCR6A KO models. One explanation is that GPCR6A is not solely responsible for amino acid-induced GLP-1, with other receptors (i.e. T1R1-R3 and CaSR) working synergistically to sense L-Orn and L-Arg *in vivo* (Alamshah *et al.*, 2016; Clemmensen *et al.*, 2014; Wauson *et al.*, 2013; Wellendorph & Bräuner-Osborne, 2009).

1.6.4 Inflammation.

A smaller avenue of GPCR6A research has led to the receptors involvement in inflammation. As part of a genome-wide meta-analysis; GPCR6A was identified as a novel locus involved with concentrations of circulating C-reactive protein an established biomarker for systemic inflammation (Clemmensen *et al.*, 2013; Oya *et al.*, 2013a; Pi *et al.*, 2011; Pi & Quarles, 2012; Smajilovic *et al.*, 2013). Monocytes and macrophages harvested from GPCR6A exon VI mice reportedly expressed decreased calcium-induced secretions of pro-inflammatory cytokines IL-1 α , IL-1 β , and tumour necrosis factor. Subsequent studies reported supportive data, implicating GPCR6A in mediating Nlrp3 calcium-activated inflammasome responses in response to alum adjuvanticity *in vitro* and *in vivo* (Quandt *et al.*, 2015; Rossol *et al.*, 2012). The research into GPCR6A's proposed role in inflammatory response is relatively new, as

current reports remain speculative and the evidence is currently limited and needs further investigation.

1.6.5 Male Fertility.

With groups reporting GPRC6A's ability to sense testosterone it was proposed that hGPRC6A may participate in regulating male fertility and maturation. Global exon II GPRC6A^{-/-} mice studies observed significant reductions in male mice genito-anal distances, testicular size and weight, seminal vesicle weight, as well as lower levels of circulating testosterone and elevated oestradiol. Furthermore, the study reported KO-KO breeding resulted in litters of approximately half the size in comparison to heterozygous pairs (Pi *et al.*, 2008). Following these reports, research conducted by Oury *et al.*, (2011) showed GPRC6A expression in the Leydig cells of the testes and that osteocalcin promoted testosterone secretion. In addition, Leydig exon II deletion of GPRC6A caused matching feminisation phenotypes observed in the global exon II deletion. As previously mentioned, testosterone was reported to exhibit agonistic activity on GPRC6A in HEK-293 and in mice compared to GPRC6A^{-/-} cells and mice (Pi, Parrill, *et al.*, 2010). In addition, this study also reported that, when treated with testosterone saw castrated WT mice exhibit full recovery of seminal vesicles in size, weight and appearance compared to controls. Whereas, GPRC6A^{-/-} castrated mice exhibited negligible recovery to testosterone replacement regime. Combined genetic cohort studies, found two SNPs Phe464Tyr and Pro91Ser mutations associated with increased risk of infertility, oligozoospermia and cryptorchidism (De Toni *et al.*, 2017; Oury *et al.*, 2013). Conversely, none of the aforementioned phenotypic changes were observed in the exon VI KO models (*unpublished by Jorgensen*). Furthermore, in a genetic study conducted by S. Jørgensen *et al.*, (2017) in the Danish population observed no differences in testosterone levels or offspring numbers when comparing the short ICL-3 variant and carriers of the premature stop codon alleles. Taken together it could be argued that the exon VI KO model produces phenotypes more representative of humans than the exon II model; however, it must be noted that cohorts of east Asian and African populations are needed to support this.

1.6.6 Prostate Cancer.

Although controversy has made defining this receptor physiological function difficult; mounting supportive data has implicated GPRC6A in the physiology of male fertility and prostate cancer. In a genome-wide association study (GWAS) GPRC6A has been identified as one of five prostate cancer susceptibility loci in both the Asian and European population (Lindström *et al.*, 2012; Long *et al.*, 2012; Sullivan *et al.*, 2015; Takata *et al.*, 2010; Wang *et al.*, 2012). GPRC6A^{-/-} mice are observed to exhibit feminisation measured by the reductions in testicular and seminal vesicle size and weight in both global and Leydig cell KO models (De Toni *et al.*, 2017; Oury *et al.*, 2011; Pi, *et al.*, 2010). Subsequent research by Pi & Quarles, (2012a) observed significant increases in *Gprc6a* transcripts in prostate cancer cells; 22Rv-1, LNCaP, and PC-3 compared to levels in normal prostate cell types. In addition, researchers here crossbred *Gprc6a*^{-/-} mice with TRAMP (TRansgenic Adenocarcinoma Mouse Prostate) prostate cancer mice and found significant reductions in prostate cancer progression and improvements in survival. The TRAMP mice model has become widely used in prostate cancer research, as they closely imitate the disease pathogenesis (Greenberg *et al.*, 1995). TRAMP mice uniformly and spontaneously orthotopic prostate tumours following puberty following induced SV40 T antigen oncoprotein expression. The popularity of this model is that inducible TRAMP mice is androgen driven and regulated by development. This means TRAMP mice tumours transiently regress; mimicking androgen withdrawal (i.e. castration or anti-androgen therapies), but subsequently relapse, mirroring androgen-insensitive carcinomas commonly seen in humans (Hurwitz *et al.*, 2001). Additionally, treatment with siRNA targeting GPRC6A found significant reductions in migration and invasive capabilities in PC-3 cells. Furthermore, activity levels of the matrix metalloproteases which are commonly upregulated in metastatic progression, were decreased (Dehghan *et al.*, 2011). Generation of a novel GPRC6A exon III KO using the CRISPR/Cas technology, reported the attenuation of tumorigenesis in human prostate cancer xenograph mice; with reductions in proliferation, migration, and expression of genes involved for regulating testosterone biosynthesis (Ye *et al.*, 2017). Furthermore, follow on studies found hGPRC6A plays an integral role in mediating testosterone induced PC-3 cell proliferation and autophagy (Ye *et al.*, 2019). Similar trends have been reported with RAMP1's involvement in prostate cancer progression. We, and other groups have observed RAMP1 expression to be significantly upregulated in prostate cancer cell lines; and knock

down of RAMP1 drastically reduced tumour size, proliferative capabilities and tumorigenicity *in vitro* and *in vivo* (Logan *et al.*, 2013; Romanuik *et al.*, 2009; Warrington, 2018).

Taken together, we hypothesised that hGPC6A and RAMP1 play a combined role in prostate cancer and may in the future provide a novel therapeutic target where current androgen-insensitive interventions fail.

1.7 RAMPs and Interaction with GPCRs.

1.7.1 *Receptor-Activity-Modifying Proteins.*

Receptor activity-modifying protein (RAMPs) represent a small group of membrane-spanning accessory proteins that interact and alter a GPCR's phenotypic function. RAMPs have been identified to engender GPCR forwards trafficking activity, ligand affinity, and signalling coupling introducing a substantial functional diversity amongst GPCRs (Ko *et al.*, 2014). In humans, three isoforms have been identified to date; RAMP1, RAMP2 and RAMP3 (Ko *et al.*, 2014). RAMPs are structurally simplistic, comprising a single membrane-spanning domain, a short intracellular C-terminus and an extracellular N-terminus (Ko *et al.*, 2014). The first reports of RAMP1 identified it as a chaperone protein, enhancing the cell surface expression of the calcitonin-like receptor (CLR) to form a functional calcitonin gene-related peptide (CGRP) receptor (Routledge *et al.*, 2017). The research that followed returned the discovery of the two other RAMP isoforms and brought to light a novel paradigm of how classical GPCR functionality is perceived (Gingell *et al.*, 2016; Sexton *et al.*, 2009). The findings from these studies found that depending on which RAMP complexed with the CLR gave rise to three distinct functional receptors. The CLR receptor and RAMP1 complex forming a functional CGRP receptor; whilst complexing with RAMP2 and -3 result in two discrete adrenomedullin receptors, producing distinctly different signalling profiles and trafficking mechanisms (Figure 1.4).

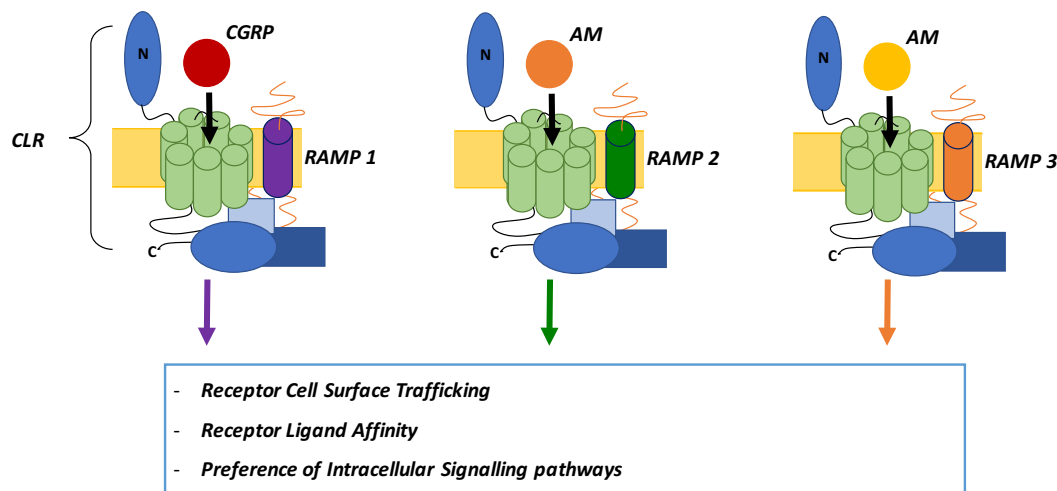


Figure 1.4; Receptor Activity-Modifying Proteins; Receptor complexes that are formed when CLR and RAMPs associate. CLR is the 7-TM protein in green. RAMP1 is shown in purple, RAMP2 in green, and RAMP3 in orange. When complexed with RAMP1; CLR forms the CGRP receptor whereas RAMP2 or RAMP3 with CLR form the AM₁ and AM₂ receptors, respectively.

1.7.2 RAMP Structure-Function Relationship.

RAMPs have been shown to be an integral part of GPCR activity and receptor phenotype. Mutations in RAMP1's N-terminus resulted in reduced responses to CGRP peptide, suggesting RAMP1 extracellular domain may be an integral participant in facilitating ligand affinity and binding. Furthermore, site directed mutagenesis of RAMP1 was found to significantly decrease CGRP binding and cell surface (Harikumar *et al.*, 2010; Hay & Pioszak, 2016; Simms *et al.*, 2009). Interestingly, RAMPs have been recently proposed to influence functional GPCR pathway coupling, posing as an essential component in preferential intracellular signalling bias (Mclatchie *et al.*, 1998). The research claims that certain GPCRs display a RAMP-dependent and ligand-dependant signalling bias among the $G\alpha_s$, $G\alpha_q$, and $G\alpha_i$ signalling pathways (Hay & Pioszak, 2016; Klein *et al.*, 2017; Mclatchie *et al.*, 1998).

1.7.3 Evidence for the interaction of RAMPs and Calcium Sensing Receptor.

The wealth of research has visibly demonstrated the considerable role RAMPs play in GPCR machinery and overall pharmacology; however, the large body of data exists on class B GPCRs making large strides in class B receptor characterisation. However, whether GPCR-RAMP interactions are a common and global feature in the human GPCR gene family is an open question and one with direct therapeutic implications (Simms *et al.*, 2009). The CaSR belongs to the class C GPCRs possessing significant homology with the human GPRC6A receptor

(~34%) and its research has aided in preliminary studies of GPR6CA. The CaSR plays a predominant role in regulating systemic Ca^{2+} homeostasis through its sensing of small changes in extracellular Ca^{2+} and modulating calciotropic hormones (Weston *et al.*, 2016). Gingell *et al.*, (2016) research sought to overview of the molecular determinants controlling CaSR; reporting that in COS-7 cells CaSR fails to be effectively expressed at the cell surface due to negligible levels of native RAMP1 and RAMP3 expression. However, HEK293 have been characterised to express sufficient levels of RAMP1 saw successful forward trafficking of CaSR to the membrane. In addition, co-expression of RAMP1 or RAMP3 found restorative action on CaSR trafficking in COS-7 cells extended the concept of RAMP escorting intermediates to class C GPCRs (Barbash *et al.*, 2017). Research by Bouschet *et al.*, (2012) and Desai *et al.*, (2014) reported immunoglobulin inactivation of RAMP1 resulted in a dose dependent decline in CaSR-mediated signalling in response to Cinacalcet in Thyroid carcinoma TT cells, suggesting a novel functional role for RAMP1 in regulation of CaSR signalling in addition to its known role in receptor trafficking. The collective research suggests that RAMP1 is necessary for CaSR cell surface trafficking and, in conjunction with its homology to GPRC6A a comparative system can be hypothesised.

1.7.4 GPRC6A & RAMP1.

While studies have shown functional mouse GPRC6A to be successfully expressed at the cell surface; human GPRC6A remains intracellularly retained (Jacobsen *et al.*, 2017b; Kuang *et al.*, 2005; Wellendorph *et al.*, 2005). Knowledge of RAMPs chaperone capabilities and the mechanistic profiles of homologous GPCRs; the concept of a GPRC6A/RAMP heterodimers may bridge the gap between discrepancies within the research field. Our preliminary findings by MSc student Zhu Lan and Dr. A. Desai have shown GPRC6A to interact with RAMP1, co-localising at the ER trafficking vesicles and at the cell surface, typical of a trafficking pathway suggesting RAMP1 necessity for human GPRC6A cell surface trafficking (discussed in detail in chapter 2). The combined concepts serve as the foundation for this research and current work aims to confirm a GPRC6A/RAMP1 trafficking heterodimer concept, investigate the effects on signalling and begin to provide perspective on its physiological relevance.

As previously stated, GPRC6A is widely expressed and seen in several tissues, such that results from this study could provide novel insight into a variety of disciplines; however, here the primary focus will be GPRC6A and RAMP1's implication in cancer. GWAS investigation cited *Gprc6a* SNP rs339331 as a prostate cancer susceptibility gene stating genetic predisposition is a higher contributing factor in prostate cancer than many other common human tumours (Lindström et al., 2012; Long et al., 2012; Sullivan et al., 2015; Takata et al., 2010; Meilin Wang et al., 2012). Characterisation studies have shown GPRC6A's expression to be elevated in Leydig cells and GPRC6A knockdown dampen the metastatic signalling and pro-invasive MMP activity, thus limiting the migration and invasive capabilities of prostate cancer cells (Ye et al., 2017). Furthermore, in comparison multiple studies have reported significant RAMP1 upregulation in differing tumour tissue, with prostate carcinoma being one of the highest type; however, its significant up-regulation is also reported in, meningioma's, human adrenal tumours and prostate carcinomas (A. J. Desai et al., 2014). The findings improve our understanding of the genetic basis of prostate carcinogenesis and provide insight into the genetic mosaic of prostate cancer susceptibility among different ethnic populations.

1.8 Hypothesis & Objectives.

Hypothesis: RAMP1 is a crucial requirement for successful forward trafficking of the hGPCR6A receptor and signal transduction.

1.8.1 Aims.

Objective 1: To generate and characterise a cell line that stably expresses hGPCR6A and RAMP1 in CHO-K1 cells.

Objective 2: To determine the degree of cell surface expression of hGPCR6A receptor in the presence of RAMP1 by Immunofluorescence-assisted flow cytometry and cell surface ELISA techniques.

Objective 3: To measure the extent of $G\alpha_q$ -activated intracellular calcium mobilisation when stimulated with various putative ligands by application of Ca^{2+} -sensitive fluorescence dye *in vitro* using the Calcium 6 FLIPR assay kit.

Objective 4: To measure the extent of $G\alpha_s$ -activated intracellular cAMP accumulation when stimulated with various putative ligands by using the LANCE cAMP detection assay kit.

Objective 5: To investigate the impact of RAMP knock out on GPCR6A intracellular signalling in PC-3 cells using the aforementioned biochemical assays.

Chapter 2: GPRC6A & RAMP1: Interaction & Trafficking.

2.1 GPRC6A & RAMP1 Interaction Introduction.

Research focused towards recombinant human GPRC6A receptor has proven to be more challenging as studies have shown that the human isoform fails to be sufficiently expressed at the cell surface *in vitro*. Multiple supporting studies have demonstrated cell surface expression of mouse, rat and goldfish GPRC6A; however, the human GPRC6A orthologue appears to be retained and therefore fails to transduce agonist stimuli (Ye *et al.*, 2017). A study by Wellendorph *et al.*, (2005) sought to elucidate potential trafficking mechanisms by the creation of a chimeric receptor. The study found that substitution of the human 7TM region for the 5.24 goldfish 7TM regained the receptors cell surface expression, suggesting that part of the human 7TM isoform inhibits forward trafficking. More recent work by Jørgensen *et al.*, (2017) generated a range of chimeric human/mouse receptors identifying a change in the ICL-3 was associated with the receptors intracellular retention and impedes forward trafficking of the human receptor. Furthermore, interspecies analysis of the GPRC6A polypeptide sequence revealed a highly conserved “RKLP” sequence present in pre-human species; however, in humans a notable common polymorphism is observed at position 744 a region encoding the ICL-3 changing the longer “FAFKGRKLPENY” to a shorter “FAFKGKYENY” amino acid sequence. The unique alleles are indicative of the evolutionary changes that GPRC6A has undergone and explains the difference in GPRC6A surface express between species. With this knowledge, the study identified replacement of the murine ICL-3 for the human short variant resulted in minimal cell surface expression in HEK-293 cells, whilst the longer variant displayed successful surface expression (Jørgensen *et al.*, 2017). The short loop is far more prevalent in humans (60% in African, 99% in East Asian); whilst the longer variant is often associated with a premature stop codon which results in truncated non-functional form of the receptor (C. V. Jørgensen & Bräuner-Osborne, 2020). GPCR ICL-3 is well known to be an essential region for scaffold/accessory protein interaction to facilitate surface trafficking (Lefkowitz, 2007). Due to the receptor’s wide spread tissue distribution combined with the more prevalent retained receptor allele, it could be argued that a requirement for a tissue specific chaperone proteins interacting with the ICL-3 of the hGPRC6A are crucial to enable successful surface trafficking.

2.1.1 GPRC6A Recombinant Expression.

The large extent of our knowledge concerning the GPRC6A receptor have come from studies carried out in CHO and HEK-293 cell lines (Jacobsen, *et al.*, 2013; Rueda *et al.*, 2016; Wellendorph *et al.*, 2005). These cell lines offer robust transfection systems combined with post-translational modification of complex recombinant proteins. CHO cells are epithelial cells derived from Chinese hamster ovum, often used in biological and medical research and commercially in the production of therapeutic proteins (Derouazi *et al.*, 2004; Puck, 1985; Wurm, 2004). They have found wide use in studies of genetics, toxicity screening, nutrition and gene expression, particularly to express recombinant proteins. CHO cells are the most commonly used mammalian hosts for industrial production; offering post-translational modification of recombinant exogenous proteins at high yields (Lai *et al.*, 2013; Wurm & Hacker, 2011).

In previous studies, Jacobsen *et al.* (2013) had generated a CHO cell line stably expressing mGPRC6A and hGPRC6A using the FlpIn/FRT technology. Here researcher saw successful surface expression of the mouse receptor in cell-surface staining enzyme-linked immunosorbent assay (ELISA). However, when stably expressing the hGPRC6A no surface expression was detected. The data was supportive of findings reported by Wellendorph *et al.*, (2004; 2005) and Rueda *et al.*, (2016) reporting that, in HEK-293 and COS-7 cells the hGPRC6A exhibited negligible cell surface expression. Due to this, investigation into the hGPRC6A pharmacological profile has been increasingly challenging. Therefore, the majority of trafficking and signalling data has been predominantly based upon the murine variant with hopes of drawing similarities between the two species (Christiansen *et al.*, 2007; Jacobsen *et al.*, 2013; Pi *et al.*, 2011; Rueda *et al.*, 2016).

Analysing the GPRC6A expression patterns in human, rat and mouse tissues has found widespread distribution; however, subsequent studies note not all tissues expressing GPRC6A are equally responsive when exposed to stimuli (see Table 1.2) (Clemmensen *et al.*, 2014). The receptors varied expression, combined with the importance of the ICL-3 region begin to suggest whether the presence of a tissue specific co-factor (i.e. RAMPs) is necessary for successful hGPRC6A function. It is important to note that all the aforementioned studies fail

to specify the relevance of this factor. HEK-293, COS-7 and CHO-K1 cells have previously been characterised to express negligible levels of RAMPs (A. J. Desai et al., 2014; Wootten et al., 2013) and thus may offer a possible explanation for the discrepancies within the literature.

The fundamentally important role of RAMPs in chaperoning GPCRs to the plasma membrane has been well demonstrated in class B GPCRs. The seminal study demonstrating this concept was reported by Mclatchie *et al.*, (1998), identifying RAMPs to positively modulate the translocation of the CLR to the cell surface. Over the past decade research has demonstrated that this phenomenon applies to an extensive range of GPCRs and is not limited to class B GPCRs only (Hay & Pioszak, 2016). The interactions between class C GPCRs and RAMPs have previously been shown by Bouschet *et al.*, (2005, 2008, 2012) and Desai *et al.*, (2014); where RAMP1 and RAMP3 protein complexes were formed with the CaSR and shown to successful forward trafficking to the plasma membrane in HEK-293 and COS-7 cell lines, respectively. As previously stated, GPRC6A shares 34% amino acid sequence identity with the CaSR (Wellendorph & Bräuner-Osborne, 2004) and thus could be hypothesised to exhibit similar interactions with RAMP proteins seen in other class C receptors.

2.1.2 GPCR-RAMP Interaction.

2.1.2.1 Class A GPCRs & RAMPs.

GPR30 is a novel oestrogen/oestradiol receptor belonging to the class A GPCR group, and have brought large amount of interesting due to its divergent from the classical nuclear oestrogen receptors (α and β) (Prossnitz & Maggiolini, 2009). Similar to that of GPRC6A, GPR30 has been subject to some controversy regarding its trafficking and subcellular localisation, as well as conflicting reports regarding its downstream signalling and even ligand binding specificity (Lenhart *et al.*, 2013). Early studies observed the majority of GPR30 to be expressed in intracellular membranes with little cell surface expression; similar to classical oestrogen receptors receptors (Filardo *et al.*, 2007; Otto *et al.*, 2008; Revankar *et al.*, 2007). However, more recent reports using bioluminescence resonance energy transfer titration studies, and co-immunoprecipitation, showed GPR30 and RAMP3 interaction that led to increased cell surface expression in HEK293 cells (Lenhart *et al.*, 2013). This concept was

further demonstrated *in vivo*, with marked phenotypic differences observed in the subcellular localisation of GPR30 in cardiac cells. RAMP3^{-/-} mice cardiac tissues displayed GPR30 cytosolic disorganisation and mislocalisation, whilst wild type mice exhibited health surface expression of the receptor. Moreover, deletion of RAMP3 *in vivo* resulted in significantly losses in GPR30's cardioprotective ability, citing significant reduction in cardiac hypertrophy and perivascular fibrosis. The novel data offers a potential explanation for the discrepancies in the field with current groups now positing previous cell lines used possessing poor/no endogenous expression of the relevant chaperone proteins i.e. RAMP3 (Bouschet *et al.*, 2012; Lenhart *et al.*, 2013).

2.1.2.2 Class B GPCRs & RAMPs.

Class B GPCRs have been the most well-researched group of GPCRs in relation to their interaction with RAMPs. The C-terminus of RAMPs has been demonstrated be been crucial to trafficking and signalling in the class B amylin receptors; interacting at sites contained within the intracellular connecting portions of the GPCR (Barwell, *et al.* 2010). Class B amylin receptor comprise the Calcitonin receptor (CTR) and a RAMP protein; depending on what RAMP is complexed with the CLR results in receptors with varying ligand affinity amylin receptor-1 (CTR+RAMP1) amylin receptor-2 (CTR+RAMP2), and amylin receptor-3 (CTR+RAMP3) (see Figure 1.4). In COS-7 cells, truncations of RAMP1-3 significantly decreased receptor surface expression, binding affinity and potency in cAMP accumulation when stimulated with amylin. However, when overexpressed alongside the G α_s subunits, this defect was ameliorated, suggesting RAMPs' involvement in direct coupling of the amylin receptor and G-proteins (Udawela, *et al.* 2006). This data was further extended with follow up studies reporting a marked increase in sensitivity amylin receptor-1 and amylin receptor-3 amylin-induced cAMP accumulation. Results demonstrated significantly weaker responses in amylin-induced calcium mobilisation and ERK activation, when compared to CTR when expressed alone in COS-7 and HEK-293 cells (Morfis *et al.*, 2008). This demonstrates a clear abilities for RAMPs to modulate CTR signalling (Christopoulos *et al.*, 2003; Wootten *et al.*, 2013).

2.1.2.3 Class C GPCRs & RAMPs.

Although this concept has been well-demonstrated in class A and B GPCRs, reports have now shown this mechanism is also crucial in class C GPCRs. Reports by Bouschet *et al.* (2005) and Desai *et al.* (2014) showed that RAMP1 and RAMP3 are key chaperones in the forwards trafficking the CaSR. When expressed alone, immunofluorescence imaging saw the CaSR to remain intracellularly retained in HEK293 or COS-7 cells. Neither of these cell lines endogenously express RAMP1; however, co-expression with RAMP1 or RAMP3; was sufficient to target CaSR to the plasma membrane. Furthermore, siRNA knock down of RAMP1 resulted in significant reductions in CaSR surface trafficking (Bouschet *et al.*, 2005). This data was later supported by Desai *et al.*, (2014) using FRET-based techniques in COS-7 cells. Co-expression of CaSR and RAMP1 or RAMP3, but not RAMP2 resulted in significant increases in surface co-localisation of the receptor.

2.1.2.4 FRET based Interaction & Stoichiometry.

Protein-protein interactions are often studied using a variety of techniques including immunofluorescent co-localisation, X-ray crystallography and co-immunoprecipitation. However, these methods are often limited by their sensitivity and the detergents used negatively affecting the natural protein interactions. Furthermore, these techniques often offer low resolution and therefore require vigorous mathematical corrections in order to provide reliable sensitivity (Hoppe *et al.*, 2002; Piston & Kremers, 2007; Van Rheenen *et al.*, 2004). However, novel FRET-based techniques offer a specific and highly sensitive methodology for measuring biological protein interaction.

The FRET system is reliant upon the transfer of energy from two fluorophore labels tagged to two proteins; characterised as the transport of electromagnetic energy transfer from one donor fluorophore in its excited state to an acceptor fluorophore through non-radiative coupling (Hoppe *et al.*, 2002; Ma *et al.*, 2014; Piston & Kremers, 2007; Van Rheenen *et al.*, 2004). The efficiency of this energy transfer is inversely proportional to the distance between the donor and acceptor, making FRET extremely sensitive to very small changes in distance

(Figure 2.1). The yellow fluorescence protein (YFP) and the cyan fluorescence protein (CFP) are a frequently used fluorophore pair when studying biological protein-protein interaction. Previous work conducted by a previous PhD student Dr. A. Desai (2012) utilised the Citrine (Cit) and Cerulean (Cer) tags - genetic variants of YFP and CFP - to tag to the intracellular C-terminus of the GPCR6A and RAMPs, respectively. Using these mutants offer much greater benefits over the eYFP and eCFP precursor tags. YFP and CFP were historically common fluorescent pair for detecting molecular interaction in living cells and biosensors (Jin Zhang et al., 2002). However, the YFP-to-CFP ratio generated by this pair only amounts to 10-30%; pushing the limits of modern digital microscopes often due to the noise is often over 10% of the signal at low intensity levels (Swedlow et al., 2002). eCFP is known to exhibit low fluorescence resulting in low signal-to-noise ratio (Rizzo et al., 2004). However, Cer is approximately 2.5-fold brighter than CFP, higher quantum yield and extinction coefficient, resistance to fluorophore dimerization and acid quenching (Heikal *et al.*, 2000; Markwardt *et al.*, 2011; Rizzo *et al.*, 2004; Shaner *et al.*, 2005).

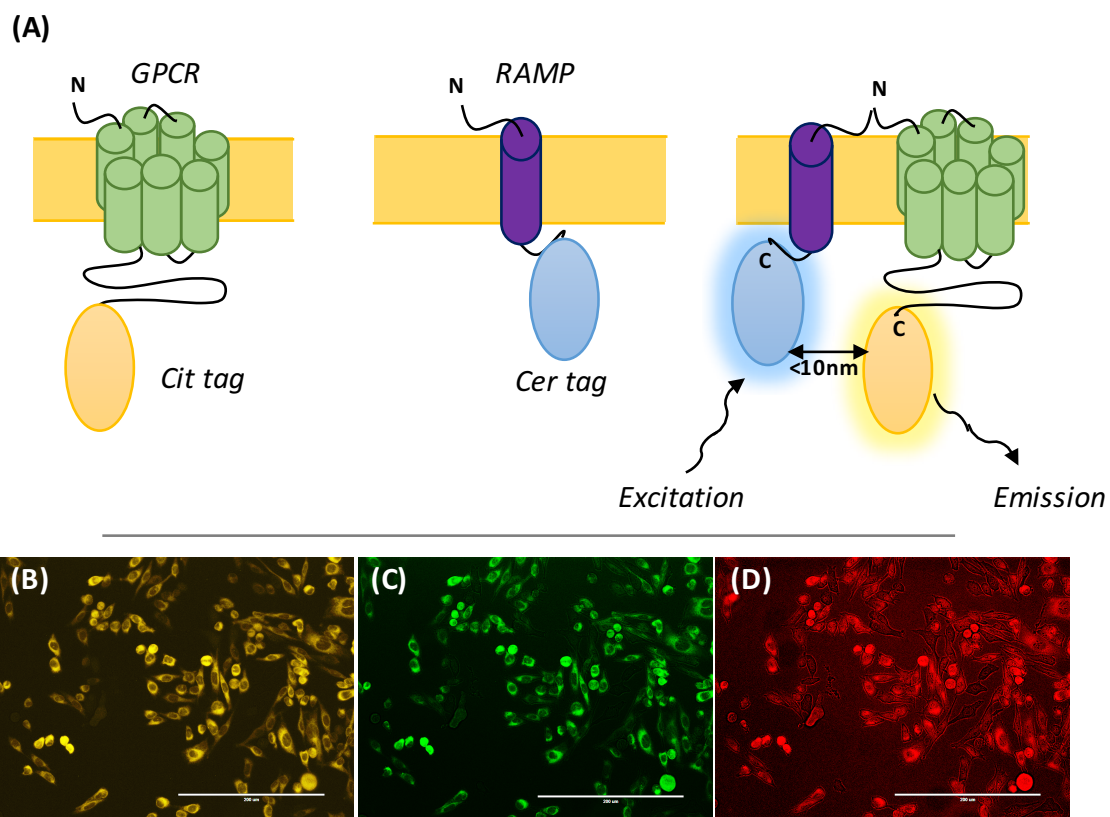


Figure 2.1 Principles of Förster Resonance Energy Transfer; (A) GPCR and RAMP are C-terminally tagged with Cit and Cer, respectively. If both proteins are not in close proximity (i.e. not interacting), the successful transfer of energy cannot occur. However, if both proteins are drawn close to one another through interaction, the distance between both fluorophores is now sufficient (<math><10\text{ nm}</math>) to allow the transfer of energy from the excited Cer to the Cit. The resultant emitted fluorescence is measured as the FRET. (B) GPCR-Cit expression (C) RAMP-Cer expression (D) GPCR-Cit + RAMP-Cer co-expression. Artificial colouring shown here are applied post imaging to demonstrate

2.1.2.5 FRET Imaging of GPRC6A & RAMP Interaction.

Previous work done by a previous MSc student Zhu Lan and Dr. A Desai utilised sensitised FRET to compare the efficiency of hGPRC6A and RAMPs interactions as well as semi-quantify the number of hGPRC6A/RAMP complexes at the cell membrane. Combinations of Cit *only* along with RAMP-Cer constructs were transfected in order to measure background levels of FRET. When transfected with GPRC6A-Cit *only*, the majority of receptors localised at the perinuclear region. However, when co-transfected with RAMP1-Cer or RAMP2-Cer areas of co-localisation FRET complexes were observed at the perinuclear halo, cytoplasm (Figure 2.2). Furthermore, when co-transfected with RAMP1-Cer FRET complexes are seen towards the cell membrane organised in small trafficking vesicles and at the plasma membrane (Figure 2.2). When co-expressed with RAMP2-Cer, FRET complexes were seen to only localise at the perinuclear region, failing to migrate to the cell surface; leaving GPRC6A-Cit to remain intracellularly retained. In the case of RAMP3-Cer, negligible FRET interaction was observed with no cell surface co-localisation being detectable. GPRC6A/RAMP1 complexes were significantly greater in intensity than that of the RAMP2/3 combinations $p < 0.0001$ (Figure 2.2).

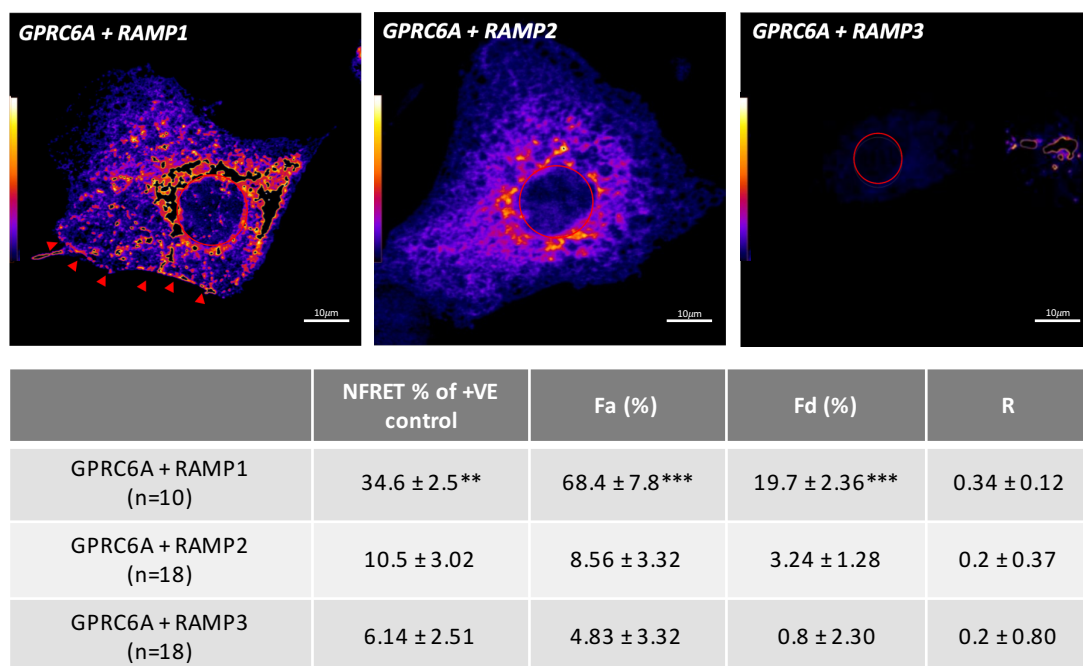


Figure 2.2 FRET analysis of GPRC6A and RAMP1 interaction gathered by MSc student Zhu Lan and Dr. A Desai; Regions of high FRET intensity (Yellow) is only seen when co-localisation of GPRC6A and RAMP1 occurs. RAMP1 is seen to co-localise with GPRC6A around the perinuclear halo and in trafficking vesicles; furthermore, GPRC6A and RAMP1 in FRET complexes are seen at the cell surface in significantly higher numbers than RAMP2 or RAMP3 combinations $p < 0.0001$. GPRC6A/RAMP2 are seen to co-localise; however, complexes are seen to be intracellularly retained around the perinuclear halo. Negligible

co-localisation is seen to occur between GPRC6A and RAMP3 (A. Desai, 2012). Normalised FRET (NFRET), Acceptor Fluorescence (Fa), Donor Fluorescence (Fd), Ratio (R).

2.1.3 Receptor Cell Surface Expression.

2.1.3.1 Cell surface Quantification Flow Cytometry.

In addition to protein-protein interaction, research aimed to investigate hGPRC6A forward trafficking and cell surface expression in CHO-K1 cells. One common methodology used to detect surface protein expression is flow cytometric methods and immunostaining. Flow cytometry is a well-established method for fast and accurate quantification of cellular protein levels and is a particularly appealing option for measuring cell surface antigens of intact cells. The principle on which this technique is based relies upon passing a suspension of cells through a fluidics system allowing the cells to be analysed individually in real time. With this configuration, each cell is passed uniformly through an excitation laser of specific wavelength and the resultant scattered light is captured by a series of photodetectors assessing; cell size, morphology and complexity, and fluorescence emission (Figure 2.3) (Nolan & Condello, 2013). Most modern flow cytometers contain a range of different lasers and photodetectors offering a number of excitation and emission wavelengths. This allows cells to be stained for many characteristics at once and the fluorescence from the different fluorophores distinguished by colour (Givan, 2010).

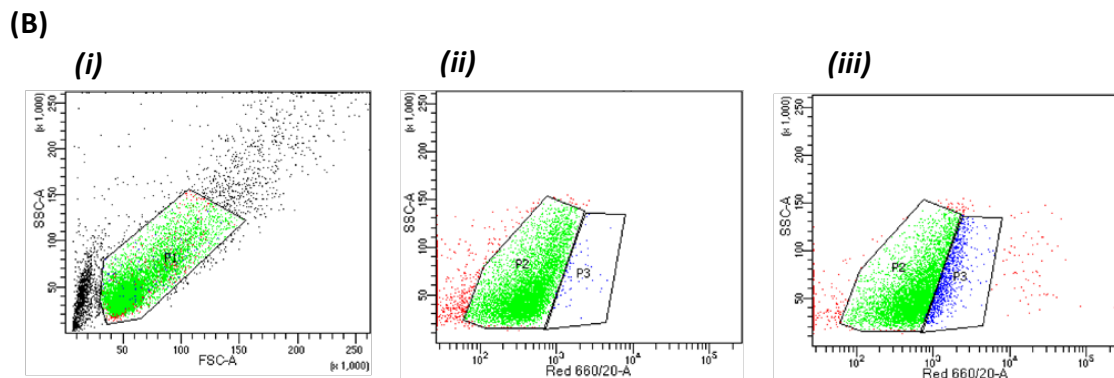
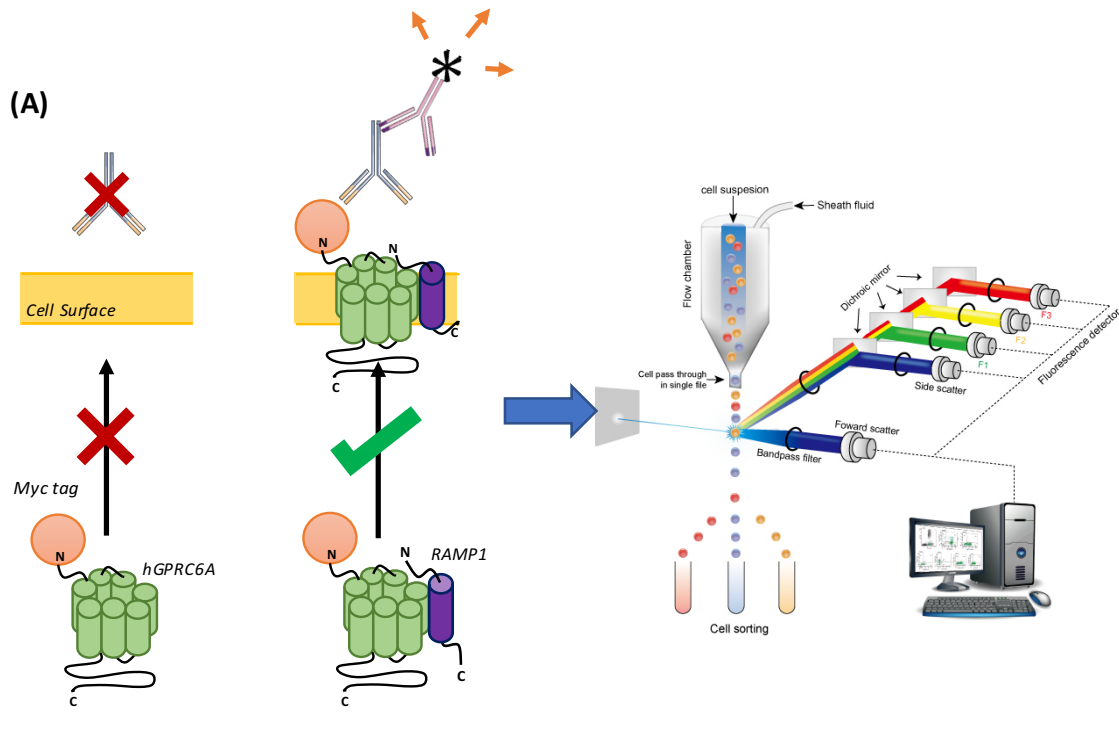


Figure 2.3 (A) Illustration of Flow Cytometry staining; Cell surface antibody staining is non-permeable thus only recognises cell surface proteins. If RAMP1 aids in surface trafficking of hGPCR6A positive staining will only be detected when both proteins are co-expressed. Samples will then be analysed by flow cytometry. **(B)** Flow cytometry gating; (i) FSC-A/SSC-A gating of live cells. (ii) Red 660/20-A/ SSC-A gating of negative and (iii) positive populations.

The most common approach to cell surface quantitative flow cytometry is through the use of fluorescently labelled antibodies. In order to optimise antibody-epitope binding considerations must be taken concerning; incubation temperature and duration as well as the pre-incubation with a FcR blocking serum to decrease non-specific binding of the antibody Fc portion (Anselmo *et al.*, 2014). Proteins known to be expressed at low levels may be masked by cell auto-fluorescence, in particular when expressed in highly auto-fluorescent cells, such as macrophages, polymorphonuclear neutrophils, and mesenchymal stem cells. Furthermore,

to minimize background signal antibodies conjugated with fluorophores with an emission wavelength red spectrum, such as PEcy-7, allophycocyanin, and Alexa-647, are recommended. Signal amplification may also be required to detect receptors with low expression levels, such as the GPRC6A receptor. One such strategy to increase the fluorophore : protein ratio is the use of biotin-conjugated primary antibodies followed by staining with a streptavidin-conjugated fluorophore (Givan, 2011). The major limitation of this staining approach – apart for the reliance on well-validated specific antibodies - is that samples must be handled with care (i.e. low centrifugation rate) to avoid the rupture of fluorophore-antibody complexes. Native receptors are often expressed at low levels, and the commercial availability of selective antibodies for any given GPCR is limited. Therefore, the creation of recombinant receptors by an insertion of epitope tags, fluorescent proteins, or small reporter enzymes, in conjunction with heterologous expression, is a common technique employed to facilitate surface measurement of GPCRs (Beerepoot *et al.*, 2013; Hislop & Von Zastrow, 2011). It is important to note that inserting an additional sequence or epitopes to receptors could potentially alter receptor function. With increasing understanding of the functional domains of GPCRs, the careful placement of an extracellular epitope generally does not alter receptor biology.

The insertion of epitopes, (e.g. Myc, Flag, HA) for which commercially available high-affinity antibodies are available, makes development of antibody-dependent surface expression assays possible for essentially any membrane protein (Bizzard, 2008). Although the use of antibodies against affinity tags is cheaper and the choice of secondary antibodies is much greater, they still require extended incubation and wash steps, decreasing suitability for high-throughput screens. Other approaches are available including fluorescent ligands and genetically encoded fluorescent proteins; however, these methods will not be discussed in detail here as they were not used in this project.

2.1.3.2 Fluorescence-Assisted Cell Sorting.

Once detected by flow cytometry, analysed cells undergo fluorescence-assisted cell sorting (FACS) whereby detected cells can then be sorted into respective populations based on the parameters discussed above. As cells are analysed on a uniform basis, cells that pass through the fluidics system can then be individually given a charge when passed through an electric field. This allows populations to then subsequently sorted by charge difference based on previous data gathered by flow cytometry (Figure 2.3). The charged droplets then fall through an electrostatic deflection system that diverts droplets into containers based upon their charge. Collected under sterile conditions, cells can be further cultured, manipulated, and studied (Adan *et al.*, 2017; Cossarizza *et al.*, 2017). The method therefore, offers an effective way of sorting a heterogeneous population into homogeneous stably expressing cell populations.

2.1.3.3 Whole-Cell Cell surface ELISA.

Flow cytometry detects fluorescence emitted from cell-bound fluorophores upon excitation as they pass in front of a light source (Nevins & Marchese, 2018). Whereas, an ELISA is a plate-based technique that employs an enzyme, like alkaline phosphatase, to detect an immobilized antigen after incubation with a substrate, yielding a measurable product (Engvall, 1980). Although radio ligand binding can be a powerful method to precisely and quantitatively measure receptor surface expression and endocytosis, there are numerous technical and logistic challenges associated with this method. Whole-cell ELISA provides a robust alternative to measure surface expression and agonist-induced GPCR internalization at least for N-terminally epitope tagged receptors expressed in heterologous cells (Ghosh *et al.*, 2017; Kumari *et al.*, 2016; Pandey *et al.*, 2019). The assay works in a similar manner as flow cytometry methods, utilising an epitope-specific primary antibody and a secondary antibody. However, a peroxidase enzyme-linked secondary antibody is used as the disclosing agent in place of a fluorescence secondary. This provides a colorimetric change when a substrate is applied to quantify the extent of positive staining. Similar to flow cytometry, certain caveats must be considered to ensure optimal antibody-epitope binding. Incubation temperature and

time as well as the pre-incubation with a FcR blocking serum are again an important factor to reduce non-specific binding.

One benefit that the whole-cell ELISA assay possess over flow cytometry methods is absence of any auto-fluorescence of background interference that can make detecting low expressing receptors difficult to quantify in flow cytometry. Some of the limitations still persists with this approach, again suffering a reliance on well-validated antibodies; however, as previously mentioned this issue can be resolved via the insertion of recognisable epitope tags. Thus, we adopted a similar strategy in both investigations, making use of our GPRC6A-myc tagged construct in order to look at RAMP1's effect on cell surface expression of the hGPRC6A. With the emergence of many GPCRs reliance upon RAMPs to facilitate effective surface trafficking; preliminary experiments sought to reproduce FRET data reported by previous PhD student Dr. Desai, and MSc student Zhu Lan (2012) generating a stable GPRC6A-Cit, RAMP1-Cer cell line. Furthermore, the work aimed to extend this data by studying the effect of RAMP1 on GPRC6A surface expression using multiple techniques to demonstrate this.

2.1.4 *Research Aims*

1. Generate a stable GPRC6A-Cit and RAMP1-Cer expressing CHO-K1 cell line.
2. Sub-cloning construct to produce functional Myc tagged hGPRC6A protein.
3. Quantify cell surface expression of GPRC6A and RAMP1 in CHO-K1 cells by Flow cytometric and ELISA immunostaining.

2.1.5 *Research Hypothesis.*

RAMP1 co-localises with hGPRC6A and subsequently increases its ability to successfully traffic to the cell surface.

2.2 Methods & Materials.

2.2.1 Cell Culture.

Chinese Hamster Ovum cells (CHO-K1, ATCC) were cultured in T-75 cm² flasks in F-12K Medium (Kaighn's Modification of Ham's F-12 Medium), containing, 1500 mg/L sodium bicarbonate, 10% Foetal Calf Serum (GIBCO, Paisley, UK), 2 mM L-glutamine, 1% of 10,000 units of penicillin and 10 mg/mL streptomycin (Sigma-Aldrich, St. Louis, Missouri, US), at 37°C in 5% CO₂ incubator.

2.2.1.1 Passaging of Cells.

CHO-K1 cells were washed twice with 1X Phosphate Buffered Saline (PBS, GIBCO, Paisley) prior to the addition of 1X TrypLE Express Enzyme Solution (GIBCO, Paisley) and incubated for approximately 10-15 minutes at 37°C until cells became fully detached from the flask. Enzyme detaching reagent was neutralised by the addition of equal volume of medium. Cells were subsequently centrifuged at 200 x *g* for 5 minutes and resuspended in warm F-12K media and added to a fresh flask at a ratio of 1:10 or 1:25 depending on their confluency. Cell lines were incubated at 37°C in 5% CO₂ with fresh media routinely changed twice a week. Cells were routinely passaged at 80-90% confluency.

2.2.1.2 Cell Counting.

Cells were detached and pelleted as previously described (section 2.2.1.1) and resuspended in 1 mL of medium. 20 µL of cell suspension was added to 20 µL Trypan Blue (GIBCO, Paisley) in a 200 µL Eppendorf microcentrifuge tube. 10 µL of cell-trypan mix was added to Countess™ Cell Counting Chamber Slides (Invitrogen, ThermoFisher Scientific) for counting. Cell number/mL was calculated using the formula below:

$$\text{Number of cells/mL} = \frac{\text{Desired number of cells} \times 1000}{\text{Average number of cells}}$$

2.2.1.3 Cell Cryopreservation and Thawing Procedure.

In order to store cells long term, cells were cryopreserved. Freezing media was prepared and stored at 4°C until use; freezing media comprised CHO-K1 F-12K Medium (Kaighn's Modification of Ham's F12 Medium) and RPMI complete medium with the addition of 10% dimethyl sulfoxide. Cells were washed and detached as previously described in section 2.2.3. Total cell number was determined using Trypan Blue and the Countess FL II Cell Counter (ThermoFisher) and subsequently resuspended in the appropriate volume of freezing media to give 1 million cells/mL. Suspension was then aliquoted into cryogenic storage vials and placed into Mr Frosty™ isopropanol chamber and stored overnight at -80°C. Frozen cells were then transferred to liquid nitrogen chambers.

When required frozen cell aliquots would be removed from storage and immediately placed into 37°C water bath. Cryovials were gently swirled for a few seconds to speed up process until 80% thawed. Vial was transferred to laminar flow hood and 1 mL of pre-warmed media was added to the vial. The suspension was now aspirated and transferred to a fresh 15 mL Falcon tube (Corning, UK) and spun at 200 x *g* for 5 minutes. Cells were then resuspended in fresh warm media and transferred to a new culture vessel.

2.2.2 CHO-K1 Characterisation.

Preliminary studies needed to ascertain whether CHO-K1 endogenously expressed GPRC6A and RAMP1 before proceeding with further experiments. CHO-K1 RNA was extracted using the Promega ReliaPrep RNA kit and converted to cDNA. Products were amplified by polymerase chain reaction (PCR) and PCR products were then separated by gel electrophoresis to determine correct molecular weight. Subsequently, products were sequenced by Sanger sequencing methods.

2.2.2.1 RNA Extraction.

CHO-K1 cells mRNA was extraction using Promega Reliaprep™ Cell Miniprep System. Cells were grown in T-75 culture flasks to 70% confluency as previously stated. Detached cells were

pelleted at 200 x g for 5 minutes; supernatant was discarded and cells pellet resuspended in 1mL of ice-cold PBS. Cell were then counted using the Countess II FL Automated Cell Counter (ThermoFisher) and resuspended in the appropriate volumes of BL and 1-thioglycerol (TG) buffer (Table 2.1). Subsequently, sample supernatant was discarded and cells were resuspended in 250 µL BL + TG Buffer containing 1-Thioglycerol, guanidine hydrochloride and guanidine thiocyanate lysing the cells and denaturing nucleoprotein complexes releasing RNA. Samples were stored at -20C. RNA was extracted using the ReliaPrep RNA Cell Miniprep System (Promega) following the manufacturers protocol provided. This included inactivation of endogenous ribonuclease (RNase) activity and the removal of contaminating DNA and proteins. Lysates were added to the proprietary RNA binding matrix columns and centrifuged at 14,000 x g for 1 minute. Subsequent flow-through was then discarded from the collection tube. 500 µL RNA wash buffer was then added to the column and then centrifuged again for 30 seconds. flow-through was discarded once again. Samples were treated with DNase I to ensure removal of genomic contaminants. Treatment was prepared by adding 3 µL 0.09 M MnCl₂, then 24 µL Yellow Core Buffer and finally 3 µL TURBO DNase I (Ambion) enzyme per sample. DNase treated samples were incubated for 15 minutes at room temperature. Columns were subsequently washed with 200 µL of Column wash and centrifuged again, discarding the collection tube flow-through. Columns were washed a further two times with 500 µL of RNA wash buffer. Finally, RNA extracts were eluted from the binding matrix column by the addition of 30 µL of nuclease-free water. Samples were quantified using the Nanodrop2000 (ThermoScientific, Waltham, Massachusetts, US). OD values at 260 nm were used to estimate DNA concentration in ng/mL, OD260/OD280 values in the range of 1.90-2.00 were considered to indicate good purity.

Table 2.1 ReliaPrep Cell Miniprep System; List of cell count ranges with the respective volumes of BL+TG Buffer and Isopropanol.

| Number of Cells | BL + TG Buffer | 100% Isopropanol |
|---|----------------|------------------|
| 1x10 ² to 5x10 ⁵ | 100µL | 35µL |
| >5x10 ⁵ to 2x10 ⁶ | 250µL | 85µL |
| >2x10 ⁶ to 5x10 ⁷ | 500µL | 170µL |

2.2.2.2 cDNA Synthesis.

RNA extractions subsequently underwent RNA to cDNA conversion using the High Capacity RNA-to-cDNA kit (Applied Biosystems). Reactions comprised at reverse transcriptase positive (containing reverse transcriptase RT+VE), RT negative control (not containing reverse transcriptase RT-VE) and a H₂O control reaction to ensure no genomic contamination and target specific amplification. 2 µg of RNA was quantified using the Nanodrop2000. Reagents were thawed on ice and mixed as per protocol provided (Table 2.2). Thermocycler reactions used the ThermoFisher Proflex Pro PCR system (Life Technologies) and program ran at 37°C for 60 minutes, 95°C for 5 minutes and subsequently held at 4°C. Synthesised cDNA samples were then stored at -20°C.

Table 2.2 High capacity RNA-to-cDNA kit; List of reagents for cDNA synthesis.

| Reagents | RT +ve | RT -ve | H ₂ O Control |
|--------------------------------|--------------------------------------|--------------------------------------|--------------------------------------|
| 2X RT buffer mix | 10µL | 10µL | 10µL |
| 20X Enzyme mix | 1.0µL | - | 10µL |
| RNA sample (1.0µg) | Up to 9.0µL | Up to 9.0µL | - |
| Nuclease free H ₂ O | Total reaction volume of 20µL | Total reaction volume of 20µL | Total reaction volume of 20µL |

2.2.2.3 Endpoint PCR.

Synthesised cDNA was amplified by endpoint PCR to establish endogenous GPRC6A and RAMP1 expression. The Primer3 web tool ELIXIR was used to design primers for each target. Forward and reverse primers were designed to specifically target gene exons to avoid intron splicing removing region of the target sequence (Table 2.3). Primer3 ELIXIR returned primer pairs for each target site. Primer selection criteria was based upon their length, guanosine-cytosine (GC) content, and melting point. Primers were chosen no longer than 20 nucleotides any longer as there is an increased risk of non-specific binding and hairpin formation. Primer pairs containing GC contents of 40 - 60% and similar melting points were preferable. G and C are able to form three hydrogen bonds; compared to adenosine and thymine who can only

form two. This enables stronger annealing of the primers to the target DNA site during PCR amplification.

Table 2.3 Primer design; Forward and reverse primer sequences for CHO Gprc6a and CHO Ramp1 with respective annealing temperatures and theoretical products sizes.

| Target site | Primer Sequence | Annealing Temperature (°C) | Product size (bp) |
|-------------|---|----------------------------|-------------------|
| CHO GPRC6A | Forward – 5'-CATGGCTGTCTCAAGGATGC-3' | 58.98 | 233 |
| | Reverse – 5'-CTGCAAAAGTGTTCAGGGCT-3' | 58.96 | |
| CHO RAMP1 | Forward – 5'-AGACTCTGTGGTGTGACTGG-3' | 58.96 | 216 |
| | Reverse – 5'-GCATGATGAAAGGGCAGAGG-3' | 58.97 | |

Each reaction sample was made in the GoTaq® Mastermix (Table 2.4). All reagents were thawed on ice and mixed using sterile pipette tips in PCR reaction tubes. All reactions were briefly centrifuged to remove the presence of any air bubbles. PCR amplification reactions were carried out using the ThermoFisher Proflex Pro PCR system and program ran for 35 cycles at 95°C for 3 minutes, 55°C for 1 minutes and 72°C for 1 minute; following this the samples were held at 4°C. Samples were stored long term at -20°C.

Table 2.4 GoTaq® PCR Mastermix reagents; List of reagents for endpoint PCR reaction.

| Mastermix Reagents | Volume (µL) |
|--------------------------------|--------------------------------------|
| 5X Green GoTaq® FlexiBuffer | 10 |
| MgCl ₂ | 1.5 |
| dNTPs | 1.0 |
| Forward Primer (10µM) | 5.0 |
| Reverse Primer (10µM) | 5.0 |
| DNA Polymerase | 0.25 |
| cDNA sample | 1.0 |
| Nuclease free H ₂ O | Total reaction volume to 50µL |

2.2.2.4 Gel Electrophoresis.

Samples were subsequently run along a 1.5% agarose gel to separate amplified products by molecular weight. 1.5 g of agarose (Fisher Scientific) was dissolved in 100 mL of tris-borate-EDTA (TBE) buffer (Scientific Laboratory Supplies) by heating for 120 seconds in a 750 W microwave. Solution was mixed by gently swirling and heated for a further 40 seconds to ensure agarose was fully dissolved. Ethidium bromide (Sigma-Aldrich) was added at a final concentration of 0.05 µg/mL to allow DNA identification under UV light. Agarose gel was allowed to cool to 50 – 60°C before the addition of ethidium bromide and the procedure was carried out wearing, lab coat, face mask and insulated gloves. Gels were cast in a 10 x 20cm tank, any bubbles were removed with pipette tip and a well comb was added before gel was allowed to set. The GoTaq Mastermix buffer density allowed for products to be loaded directly into agarose gel wells. Gel electrophoresis was carried out in a horizontal tank containing TBE buffer for 45 minutes at 200 V. Bands were imaged using ChemiDoc™ XRS+ Imaging system (Biorad, California, US) against HighRanger Plus 100 bp DNA Ladder (Norgen Biotek Corp., Canada, 2018).

2.2.3 Plasmid Constructs.

To be able to investigate different aspects of the GPRC6A receptor, several constructs were used in order to examine cell surface expression and downstream signalling. The different constructs are detailed in Figure 2.4 & 2.5 were kindly gifted from Dr. A. Desai and MSc student Zhu Lan. Construct 1a comprised a pcDNA3.1 vector (Invitrogen, UK) with human *Gprc6a* insert. Construct 1b, also a pcDNA3.1 vector contained human *gprc6a* insert with the addition of a C-terminal Cit tag; the system would allow for validating receptor expression FRET experiments and generating a stable cell line through FACS. Construct 1c utilised the pCMV ProLink II vector (Discover X, UK) with human *Gprc6a* insert with encoded N-terminal Myc-tag in order to assess cell surface expression, with a range of validated antibodies in flow cytometry and ELISA experiments.

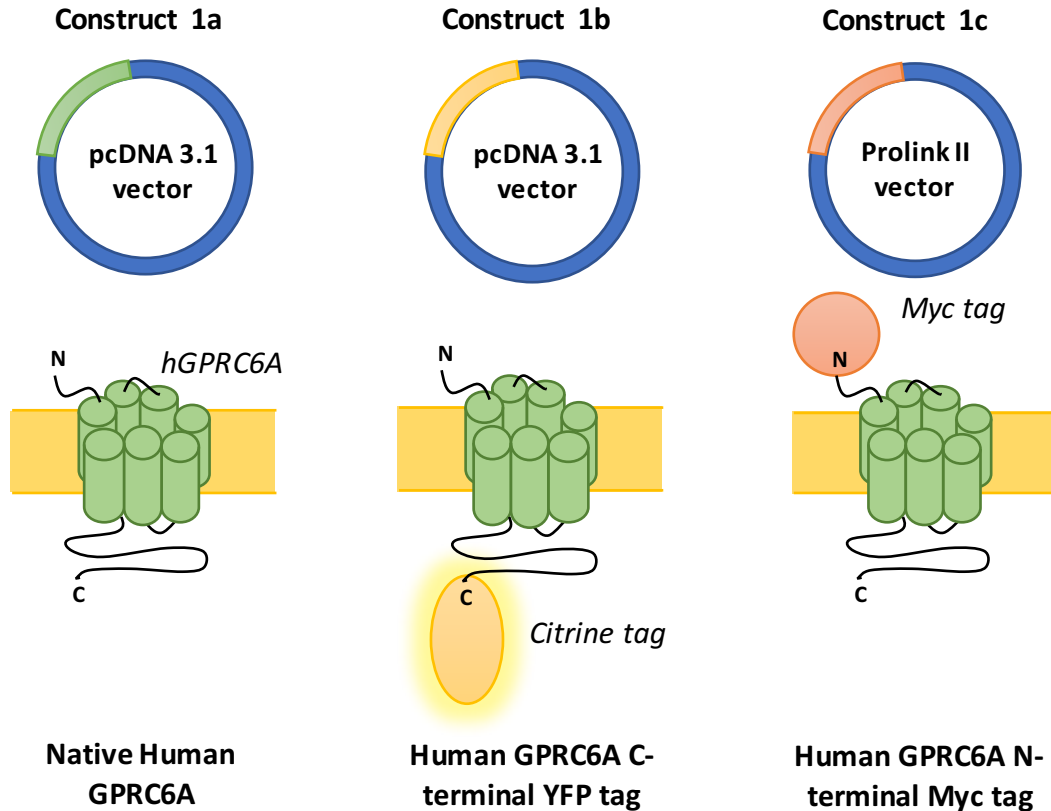


Figure 2.4 GPRC6A constructs; Construct 1a PKII vector containing native human GPRC6A. Construct 1b PKII vector containing human GPRC6A with intracellular citrine tag. Construct 1c PKII vector containing human GPRC6A with extracellular Myc tag. All constructs contained G418 resistance gene allowing for antibiotic selection.

Construct 2a comprised a pcDNA3.1 vector with human *RAMP1* insert. Construct 2b, also pcDNA3.1 vector contained human *RAMP1* insert with the addition of a C-terminal Cer tag; used in validate expression and provide the second component to enable FRET measurements of receptor-RAMP interaction. Construct 2c utilised the pcDNA3.1 vector with human *RAMP1* insert with encoded N-terminal Flag-tag in order to assess cell surface expression in flow cytometry and ELISA experiments. All plasmid constructs used contained G418 resistance gene allowing for antibiotic selection.

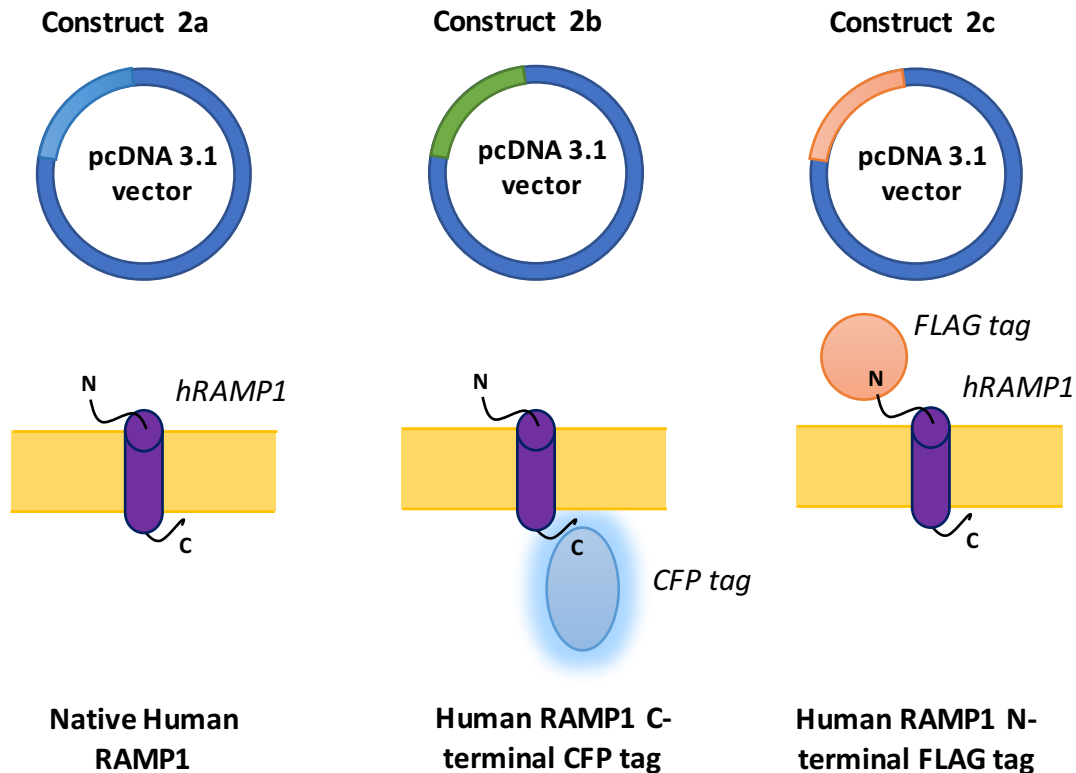


Figure 2.5 RAMP1 constructs; Construct 2a pcDNA3.1 vector containing native human RAMP1. Construct 2b pcDNA3.1 vector containing human RAMP1 with intracellular Cerulean tag. Construct 2c pcDNA3.1 containing human RAMP1 with extracellular Flag tag. All constructs contained G418 resistance gene allowing for antibiotic selection.

2.2.4 Generation of GPRC6A-Cit & RAMP-Cer CHO-K1 Cell Lines.

For high through-put screening high receptor expression is important to ensure adequate assay responses. GPRC6A is known to be expressed at relatively low levels in many tissues (C. Clemmensen *et al.*, 2014), thus selecting the correct expression system was essential to allow cell surface and biochemical investigation. In order to obtain sufficient signal output from biochemical assays previous signalling studies adopted the co-transfection of the permuted $G\alpha_{q(G66D)}$ protein alongside GPRC6A in order to boost subsequent assay signal output (Kuang *et al.*, 2005; Rueda *et al.*, 2016; Wellendorph *et al.*, 2005). However, this approach of overburdening cells with transfected DNA constructs can lead to an increased toxicity. This methodology also may produce responses that are not representable of native GPRC6A signalling.

Two main strategies can be adopted when generating cell lines expressing recombinant protein; transient or stable (Jayawickreme & Kost, 1997). Transient transfection offers rapid

expression of an exogenous plasmid at high levels over a short period, eventually ceasing as the foreign constructs are degraded by the host. Multiple transfections are often required when carrying out high throughput screening, which can lead to large variations in subsequent assays due to differences in transfection efficacy and expression levels (Chen *et al.*, 2007). Stably transfected cell lines offer consistent expression of the foreign gene of interest over a much long duration (Johnston & Johnston, 2002; Schroeder & Neagle, 1996). Both strategies can be employed in biochemical screening. Despite the target protein expression is lower compared to transient systems, stable expression systems are the much-preferred approach in biochemical assay due to the lower cost, ease of culture and reduced assay variation (Zhiyun Zhang *et al.*, 2012).

2.2.4.1 Lipofectamine 3000 Reagent

Using constructs 1b and 2b (Figure 2.4Figure 2.5), CHO-K1 cells were transfected using Lipofectamine 3000 reagent. Lipofectamine 3000 (Invitrogen, Carlsbad, California, US) was chosen to capitalise of its lower toxicity (T. Wang *et al.*, 2018) and greater efficiency compared to other transfection reagents PEIpro (PolyPlus Transfection, France) and Lipofectamine 2000 (Invitrogen, Carlsbad, California, US) (Figure Ap. 2). Cells were seeded 24 hours prior to give 70-90% confluency at time of transfection. DNA was diluted in to 5 µg along with P3000 reagent at a ratio of 2 µL : 1µg DNA to a final volume of 50 µL. Lipofectamine 3000 reagent was then diluted in following manufacturers suggested optimisation concentration to ensure optimal transfection efficiency. All tubes were then gently vortexed. 25 µL of diluted Lipofectamine 3000 reagent was then combined with 25 µL of diluted DNA solution. Tubes were then vortexed immediately and incubated at room temperature for 20 minutes. During this incubation cell plates were washed twice with PBS, and replaced with 1mL of Opti-MEM Reduced serum medium is then added. 50 µL of DNA/Lipofectamine 3000 mix was added dropwise to the respective wells. Plates are gently swirled for even distribution. Cells were then incubated at 37°C overnight. 24 hours post-transfection, cells were washed twice with PBS and fresh medium added.

2.2.4.2 *Fluorescence-assisted Cell Sorting.*

Successful expression of GPRC6A-Cit and RAMP1-Cer was verified by monitoring Cit and Cer fluorescence levels in cells post-transfection. Transfected populations were maintained in F12-K medium (Kaighn's Modification of Ham's F-12 medium), containing 2 mg/mL of G418 to ensure efficient selection of successfully transfected cells. Optimal G418 concentrations was determined by kill curve analysis (Figure Ap.1). Following 1 week of antibiotic treatment, cells were sorted based on their Cit and Cer fluorescence by FACS using lasers Violet 450/40-A and Blue 530/30-A (Figure Ap.3). This resulted four distinct populations; mock transfected negative control, GPRC6A-Cit *only*, RAMP1-Cer *only* and GPRC6A-Cit + RAMP1-Cer co-expressing CHO-K1 cells. Enriched populations were maintained in complete media containing 2 mg/mL G418 to ensure stable expression of GPRC6A-Cit and RAMP1-Cer. Following 1 week of selection, sorted populations underwent a further FACS enrichment and sorted populations were again maintained in complete media containing 2 mg/mL G418.

2.2.4.3 *GPRC6A & RAMP1 FRET Imaging in CHO-K1 Cells.*

Following the transfection and FACS, CHO-K1 cells populations enriched for GPR6CA-Cit, RAMP1-Cer and GPRC6A-Cit+RAMP1-Cer were seeded into 35 mm glass bottom imaging dishes (MatTek Life Sciences, Ashland, MA) at 50,000 cell/well in 2.5 mL of complete media. Subsequently, cell populations were imaged over the course of 1 week using the EVOS FL II fluorescence microscope tracking the levels of Cit, Cer and FRET intensities. Media was changed every 2 days (Perkin Elmer, US).

2.2.5 *Subcloning GPRC6A-myc construct.*

Constructs containing Cit and Cer fluorescent tagged were engineered previously by Dr. A. Desai (2012). However, these constructs did not allow for precise probing of the receptor/RAMP cell surface expression. Thus, we chose to engineer a novel construct incorporating the epitope tag –myc at the hGPRC6A N-terminal; enabling flow cytometric and

cell surface ELISA analysis using a variety of validated antibodies to investigate RAMP1's role in hGPCR6A forward trafficking.

2.2.5.1 DNA Restriction Digestion and Ligation.

GPCR6A-myc gene string (Invitrogen, UK) was engineered into pCMV Prolink II vector such that the myc tag was located at the extracellular N-terminus of the GPCR6A. The cloning sites SacI-GPCR6A-myc-HindIII were selected for engineering the constructs into the pCMV Prolink II vector (DiscoverX). To clone the purified GPCR6A-myc between SacI-HF and HindIII-HF restriction sites; 600 ng of GPCR6A-myc and 2 µg of pCMV Prolink II vector were separately digested using 20 units of SACI-HF and HindIII-HF restriction endonucleases (New England Biolabs) in 1X NEbuffer 2 (New England Biolabs) in nuclease-free water to give a final reaction volume of 50 µL. Reactions were then incubated at 37°C for 1 hour then heat inactivated at 65°C.

In an attempt to inhibit self-ligation of the SACI-HF and HindIII-HF restricted pCMV Prolink II vector; the vector underwent a dephosphorylation reaction using 5UI of Shrimp Alkaline phosphatase (New England Biolabs) in 1X Shrimp Alkaline phosphatase buffer (New England Biolabs) and nuclease free water. Reactions were incubated at 37°C for 1 hour and subsequently stopped at 65°C. DNA was quantified using Nanodrop2000 (ThermoScientific, Waltham, Massachusetts, US) at 260 nm. 100 ng of GPCR6A-myc insert was ligated into the dephosphorylated pCMV Prolink II vector using 2000 U of T4 DNA ligase enzyme (New England Biolabs) in 1X T4 DNA ligase reaction buffer (New England Biolabs) and nuclease-free water to give 60 µL final volume. Subsequently, reactions were then incubated at 4°C overnight.

2.2.5.2 Transformation of E. coli.

All vector constructs underwent transformation in *E. coli* for amplification and for glycerol stock production. 1 µL of plasmid DNA was added to 20 µL of competent *E. coli* cells (Invitrogen, Carlsbad, California, US), which were then thawed and incubated for 30 minutes at on ice. Cells were then heat shocked at 42°C for 30 seconds. 250 µL of super optimal broth

with catabolite suppression media was then added and incubated in orbital shaker for 60 minutes at 37°C set at 200 rpm. Cells were then spread onto kanamycin (50 µg/mL) or ampicillin (100 µg/mL) agar plates, respectively. Plates were then left to incubate at 37°C, overnight. If successful, single colonies were subsequently picked and dropped into broth containing the same concentration of antibiotics and incubated in orbital shaker overnight at 37°C set at 200 rpm. Samples were quantified using the Nanodrop2000 (ThermoScientific, US).

2.2.5.3 Preparation of Bacterial Glycerol Stocks.

For long term storage of successfully transformed colonies, 25% (v/v) glycerol was added to 1 mL of bacterial culture in a 2 mL cryotube (Falcon, Corning) and frozen in liquid nitrogen. Cryotubes were then kept at -80°C for future use.

2.2.5.4 Plasmid DNA Extraction Kits.

Plasmid isolation and extraction was performed at two scales; smaller scale using the PureLink Quick Plasmid DNA Miniprep Kit (Invitrogen), larger scale using the PureYield™ MaxiPrep DNA Extraction kit (Promega). Both kits work in a similar fashion; using sodium dodecyl sulfate (SDS) ionic detergent to lyse open bacterial cells releasing plasmid DNA. Cell suspensions are then centrifuged to separate cell debris and genetic material. The PureYield™ MaxiPrep DNA Extraction kit offers an additional endotoxin removal solution to remove bacterial endotoxins that might later interfere with DNA purity, transfection efficiency or expression. DNA preps are then pulled through a column containing a silica membrane; the PureLink Quick Plasmid DNA Miniprep Kit uses centrifugal force, whilst the PureYield™ MaxiPrep DNA Extraction kit uses a vacuum pump to force genetic material through the membrane. Plasmid DNA will bind to the positively charge silica gel. The column is then washed removing any remaining purities bound to the silica. Bound DNA is eluted by the addition of water or an elution buffer (usually Tris-EDTA). Outlined below is the PureLink Quick Plasmid DNA Miniprep Kit.

If colony growth was successful, single colonies were taken and grown in 5 mL of LB broth containing 50 µg/mL of Kanamycin at 37°C overnight in a shaking incubator set at 200 rpm. The following day, cells were subsequently pelleted by centrifugation for 5 minutes at 12,000 x *g* and resuspended in 250 µL Resuspension Buffer. To each sample, 250 µL of Lysis Buffer was added, mixed and incubated at room temperature for 5 minutes. 350 µL of Precipitate Buffer was subsequently added and samples were mixed immediately by vigorously shaking until mixture is homogenous. The lysates were then centrifuged at 12,000 x *g* at room temperature for 10 minutes. Lysate supernatants were then loaded into a spin columns contained in a 2 mL wash tube and centrifuged at 12,000 x *g* at room temperature for 1 minute. The flow-through was discarded and placed back into the Wash Tube. An additional wash was carried out by adding 500 µL of Wash Buffer 10 to the column and incubated for 1 minute. The column was then centrifuged at 12,000 x *g* for 1 minute. Column flow-through was discarded and returned to the Wash Tube. Subsequently, 700 µL of Wash Buffer 9 was added to the columns and centrifuged at 12,000 x *g* for 1 minute. This step was repeated, discarding the flow-through again before returning the column to a fresh Recovery Tube. To elute extracted DNA, 75 µL of preheated TE elution buffer was added to the centre of each binding column and incubated at room temperature for 1 minute. Finally, columns were centrifuged at 12,000 x *g* for 2 minutes and the flow-through was stored at -4°C. Extracts were quantified using the Nanodrop2000.

2.2.5.5 GPRC6A-myc Insertion Construct Validation.

Initially, the extracted colony DNA underwent restriction digestion to screen for the expression of the GPRC6A-myc insert. 1 µg of extracted DNA was treated with 10 U of restriction endonucleases SacI-HF and HindIII-HF for 1 hour at 37°C. The restricted DNA was then separated using gel electrophoresis on a 1.0% agarose and positive clones were identified under UV light (see section 2.2.2.4). The extracted DNA for each positive clone was then sent for Sanger sequencing using the ABI automated sequencer in the Genomic Core Facility, Medical School, University of Sheffield with the primers denoted in

Table 2.5.

Table 2.5 Sequencing primer design; Forward and reverse primer sequences for human Gprc6a with respective annealing temperatures and theoretical products sizes.

| Target site | Primer Sequence | Annealing Temperature (°C) | Product size (bp) |
|---------------|---|----------------------------|-------------------|
| GPRC6A Site 1 | Forward – 5'-GCCAATCCAGTTCCAACCAG-3' | 54.5 | 214 |
| | Reverse – 5'-GGCTGT CATAGGTCTGGGT-3' | 54.5 | |
| GPRC6A Site 2 | Forward – 5'-AGTCCTGGCTCAGCATAGTC-3' | 54.5 | 202 |
| | Reverse – 5'-ACTTGCTCCAGTGACAGT-3' | 52.3 | |

2.2.6 Validation of GPRC6A-myc Protein Expression.

CHO-K1 cells were transfected with Lipofectamine 3000 described in section 2.2.4.1. CHO-K1 underwent protein extraction and quantification by bicinchoninic acid (BCA) assay. CHO-K1 protein extractions were then probed for –myc by Western blot for successful GPRC6A-myc expression.

2.2.6.1 CHO-K1 Protein Extraction.

CHO-K1 cells were grown in T-75 cm² flasks to approximately 70% confluency and incubated on ice for 10 minutes. Subsequently, cells were washed twice with ice-cold PBS and 1 mL of 1% NP-40 lysis buffer (150 mM NaCl, 50 mM TrisBase, pH 8.0) containing 10 µL protease inhibitors; bestatin, aprotinin, and leupeptin inhibiting cysteine and serine proteases (Halt Protease Inhibitor Cocktail, Thermo Scientific). Phosphatase inhibitors contained sodium orthovanadate and sodium fluoride inhibiting, threonine, tyrosine and serine phosphatases. Cells were then incubated on ice for a further 5 minutes. Flasks were then scraped to detach cells and transferred to a sterile 2 mL Eppendorf tube. Samples were sonicated for 30 seconds at 60 Hz and then centrifuged at 14,000 x g at 4°C for 20 minutes. Supernatants were then removed and transferred to new 2 mL Eppendorf tubes and stored at -20°C.

2.2.6.2 *Bicinchoninic acid protein assay.*

Sample protein concentrations were quantified using the DC Protein Assay BCA assay kit (BioRad, Pierce). Protein samples are solubilized in detergent and quantified by a colorimetric reaction. The assay is reliant upon the reaction between alkaline copper tartare, Folin solution. The copper tartrate solution reacts with the solubilized proteins in the sample and then reduce the Folin reagent, losing up to 3 oxygen atoms. This reaction creates a number reduced species possessing a characteristic blue colour with an absorbance within 405 nm to 705 nm. 1.43 mg/mL bovine serum albumin Protein Assay Standard (BioRad) was used to make serial dilution range of 5 concentration in NP-40 lysis buffer to generate a standard curve assay (Table 2.6). 5µL of sample or standard was added a 96 well plate in triplicate. Samples of high concentration were assayed at a 1:10 and 1:100 dilution. 25 µL of working A/S reagent (prepared by adding 10 µL of reagent S to 500 µL of reagent A) to each well. Subsequently, 250 µL of Reagent B was added immediately to all wells and the plate incubated for 15-30 minutes at room temperature to allow colorimetric development. Optical Density (OD) values were measured using a spectrophotometer (Eppendorf) set at 562 nm. Plotting of the standard curve was conducted using the GraphPad Prism 7 software and unknown protein concentrations were interpolated from the standard curve linear equation (Figure 2.6).

Table 2.6 Protein standards for BCA assay standard curve.

| Protein Standard Concentration (mg/mL) | 0 | 0.286 | 0.572 | 0.858 | 1.144 | 1.43 |
|--|----|-------|-------|-------|-------|------|
| Stock Volume (µL) | 0 | 4 | 8 | 12 | 16 | 20 |
| NP-40 Lysis buffer (µL) | 20 | 16 | 12 | 8 | 4 | 0 |

Bicinchoninic acid protein assay Standard Curve

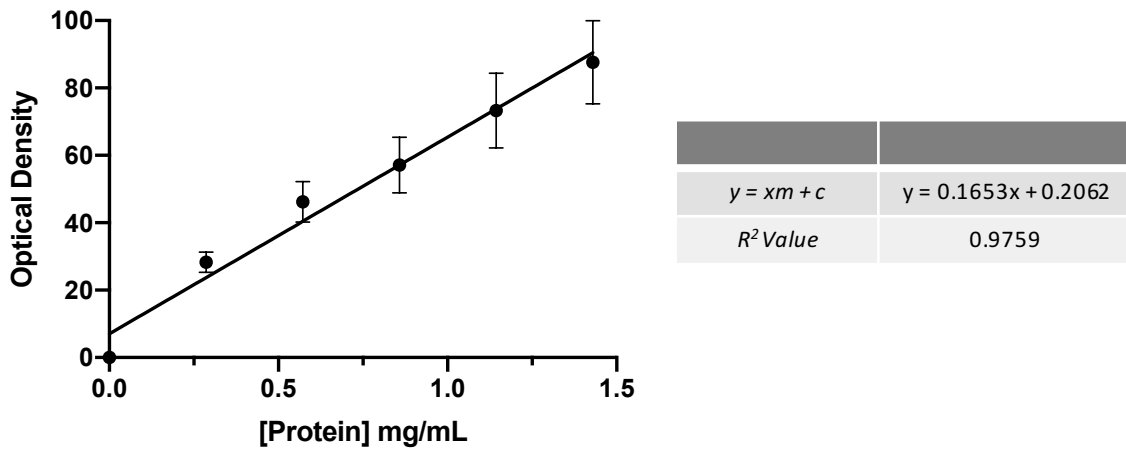


Figure 2.6 BCA Protein Assay Stand Curve; Plotted standard BSA protein standard to interpolate unknown sample protein concentrations; with respective $y = mx + c$ and R^2 values.

2.2.6.3 Western Blotting: Gel Electrophoresis & Transfer.

To check the successful expression of GPRC6A-myc construct following transfection in CHO-K1 cells, Western blotting analysis was chosen as an efficient means to validated successful expression of GPRC6A-myc at the protein level. Once the concentration of sample protein had been determined, samples were diluted in distilled water and Laemmli buffer (Biorad) (25% glycerol, 62.5 mM Tris-HCl, 2% SDS, 0.01% bromophenol blue, pH 6.8) mixed with 350 mM dithiothreitol (Fisher Scientific) to aid in disulphide band reduction and protein denaturation. Proteins were then denatured by incubation at 95°C for 10 minutes. Samples were then separated by molecular weight using gel electrophoresis method. 1-2% Mini-PROTEAN® TGX™ (Bio-Rad) Precast protein gels were used, running 10 µL of Precision Plus Protein™ Dual Colour Standards (Bio-Rad) alongside 50 µL of sample loaded in a Vertical Electrophoresis Cell (Bio-Rad) containing with 1X Tris/Glycine/SDS running buffer (Bio-Rad). Loaded samples were allowed to separate for 40-60 minutes at 150 V. Once separated, proteins are subsequently transferred to a Trans-Blot PVDF membrane (Bio-Rad) using the Trans-Blot® Turbo Rapid Transfer System (Bio-Rad) applying 25 V gradient perpendicular to the gels orientation for 7 minutes.

2.2.6.4 *Western blotting: Blocking & Probing.*

Proteins bound to this membrane were then probed for by immunostaining. Prior to staining membranes were folded into 50 mL Falcon tubes (Corning) and blocked with 3% milk in TBS-T (Tesco, UK) at room temperature for 1 hour on a tube roller. Membrane blocking reduces non-specific protein interactions prior to the primary antibody addition. The primary antibody goat anti-myc was then diluted 1:100 in blocking buffer and then incubated with the transfer membrane at 4°C overnight on a tube roller. The next day, membranes were washed thrice with 1X TBS-T (20 mM Tris Base, 0.1% Tween-20, Tween-20, 150 mM NaCl₂, pH 7.6) for 10 minutes on a tube roller. Subsequently, membranes were incubated with 1:1000 dilution rabbit anti-goat horse-radish peroxidase (HRP) conjugated secondary antibody (Dako) at room temperature for 1 hour on a tube roller. The blot was then washed thrice for 5 minutes in 1X TBS-T and then a further three times for 10 minutes in distilled water.

2.2.6.5 *Western blotting: Detection.*

Antibody probed membrane blots were detected by WestDura SuperSignal West Femto Maximum Sensitivity Substrate (ThermoScientific). 250 µL of Stable Peroxidase solution was mixed in equal volume Luminol/Enhancer solution. The conjugated peroxidase catalyses Luminol oxidation and releases prolonged chemiluminescence which can be visualized using a Gel Doc XR+ Gel Documentation System (Biorad).

2.2.7 *GPRC6A and RAMP1 Cell Surface Expression.*

To investigate the role of RAMP1 in successful forward trafficking of the hGPRC6A two methods were used; flow cytometry and whole-cell cell surface ELISA. Both techniques utilise tagged anti-myc and anti-flag antibodies stain for GPRC6A-myc and RAMP1-flag proteins to identify target protein cell surface expression. Due to the lower surface expression of the receptor, cells were transiently transfected to capitalise on spike in protein expression.

2.2.7.1 Flow Cytometry – RAMP1-Flag Cell Surface Expression Immunostaining Staining.

An alternative strategy used RAMP1-Flag constructs in order to identify RAMP1 expression enabling the use of well-validated Flag antibodies. CHO-K1 were transfected with Lipofectamine 3000 (see section 2.2.5.7) using Constructs 1a and 2c (Figures 2.4 & 2.5). Cells were counted as previously mentioned in section 2.2.1.2 and centrifuged at 1000 x g for 5 minutes at 4°C. Cells were then washed with 1 mL of Hank's buffered saline solution (HBSS) (containing 1 mM CaCl₃, 1 mM MgCl₃, pH 7.4), centrifuged and then resuspended in 100 µL of 4% paraformaldehyde. Cells were incubated for 30 minutes centrifuged and then resuspended in 100 µL of Fc block (10% chicken serum (Sigma-Aldrich, St. Louis, Missouri, US), in 3% bovine serum albumin (BSA) diluted in HBSS) and incubated for 30 minutes. Subsequently, cells were incubated for 60 minutes on ice in primary mouse anti-Flag (Trans Genic Inc, KO602-M) or Mouse isotype control IgG (ThermoFisher) at 1.88 µg/mL. All antibodies were diluted in 3% BSA in HBSS to prevent nonspecific antibody binding. Following a 60 minute incubation on ice, cells were washed twice with 3% BSA in HBSS, and secondary Chicken anti-mouse AlexaFluor647 IgG (Invitrogen) was added to appropriate reaction tubes at 1 µg/mL. Cells were incubated for another 60 minutes on ice and subsequently wash 3 times in 3% BSA in HBSS, before being resuspended in 300 µL of HBSS. Samples were then analysed immediately by flow cytometry LSR II (BD Bioscience).

2.2.7.2 Flow Cytometry – GPRC6A Cell Surface Expression Staining.

Flow cytometry was used to investigate cell surface RAMP1 was complexed with hGPRC6A. However, due to the lack of validated antibodies targeted at GPRC6A, transient transfection of Construct 1c and 2a (see Figures 2.4 & 2.5) utilising an extracellular myc tagged human GPRC6A receptor provided a choice of well researched antibodies to use from. Immunostaining procedure was carried out as previously stated (see section 2.2.7.1); however, antibody dilutions of the primary mouse anti-myc (Merck Millipore, Billerica, MA, USA; 9E10) and mouse isotype control (Sigma-Aldrich) were used at 1:50 dilution. The same secondary Chicken anti-mouse AlexaFluor647 IgG (Invitrogen) was used for detection at 1 µg/mL in 3% BSA in HBSS.

2.2.7.3 Flow Cytometry – Cell Populations.

Cell populations to be analysed were first gated on the basis of indices of forward and side scattering (FSC-A/SSC-A dot plot). Negative subpopulations were gated against the non-stained, isotype, and secondary alone controls (Figure 2.3B). A minimum of 100,000 events were gated. An interval gate was then established on the control histogram which was obtained from samples incubated in the absence of anti-RAMP1 antibodies, and subsequently, determined percent of positive events and mean fluorescence of cells carrying membrane-bound receptors. Immunofluorescent staining of live cells was performed using FACSBDS software on the BD LSRII (using laser – Red 633 nm to excite AlexaFluor647) (BD Biosciences, Oxford, UK). Histogram plots were analysed using the FlowJo analysis software (FlowJo LLC, Ashland, Oregon, US).

2.2.7.4 Immuno-linked ELISA - Cell Surface Expression Immunostaining Staining.

Cell surface expression was determined by ELISA and performed as previously described (Pandey *et al.*, 2019; Weston *et al.*, 2016). Cells were plated into a 24 well plates and transiently transfected with GPRC6CA-myc and RAMP1 for myc staining experiments and hGPRC6A and RAMP-Flag for flag staining experiments (see Figure 2.4Figure 2.5) as described in section 2.2.4.1 500 μ L of 4% paraformaldehyde in PBS was added directly to each well of a 24-well plate containing transfected cells and transfection media and incubated at room temperature with gentle shaking for 20 minutes at 500 rpm. The wells were aspirated and washed twice. All washing was performed with 500 μ L PBS for 10 minutes with gentle agitation. 500 μ L of 1% BSA in PBS was added to block non-specific antibody binding and incubated for 45 minutes at room temperature with gentle agitation at 500 rpm. Cell surface expression of receptor components was detected using mouse anti-Flag monoclonal antibody 1 μ g/mL (Trans Genic Inc, KO602-M), or anti-myc 1:2500 (Merck Millipore, Billerica, MA, USA; 9E10) to detect the tagged RAMP or receptors respectively. All antibodies were diluted in HBSS. 250 μ L of antibody dilution was added and incubated at room temperature for 30 minutes with gently agitation. Following incubation, cells are washed three times and re-blocked in 1% BSA in HBSS for a further 15 minutes. Subsequently, 250 μ L of goat anti-mouse HRP conjugate (Sigma-Aldrich) were used to detect the primary antibody at a 1:1000 dilution

and incubated for 30 minutes at room temperature with gently agitation. Thermo TMB Substrate (ThermoFisher) was used to reveal antibody staining; 100 μ L of substrate was added to all wells and incubated for 30 minutes with gently agitation. The reaction was stopped by adding 0.8 M H₂SO₄, mixing gently and absorbance was read at 450 nm on the Ensign Plate reader (Perkin Elmer, UK). Experiments were performed in triplicate and data shown are the mean \pm SEM of three to four independent experiments compared to GPRC6A *only* cells by non-parametric one-way ANOVA (Kruskal–Wallis test) followed by Dunn's multiple comparison test (Bailey & Hay, 2007).

2.3 Results.

2.3.1 Native CHO GPRC6A and CHO RAMP1 Expression Characterisation.

Characterization of CHO-K1 cells identified low expression levels of endogenous hamster GPRC6A and RAMP1. Bands were present in RT +VE reaction for CHO-GPRC6A and CHO-RAMP1 at the correct height for the theoretical product size (Figure 2.7). No bands were observed in RT -VE and H₂O control reactions negating nonspecific conversion and contamination respectively. Products from endpoint PCR were then Sanger sequenced to confirm target gene amplification. All sequenced targets were successfully sequenced and cross referenced using the NCBI database sequences using nucleotide Basic Local Alignment Search Tool (nBLAST) (Figure 2.8).

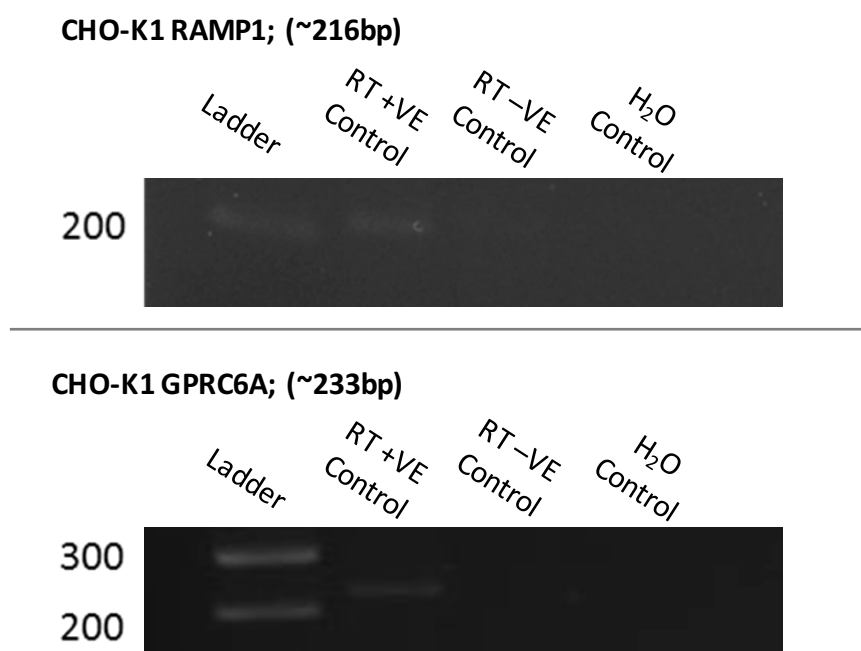


Figure 2.7 Endpoint PCR analysis of CHO GPRC6A and CHO RAMP1 endogenous expression; **(A)** Band present in RT+VE reaction at expected CHO RAMP1 band height (product size 216 bp). No bands present in RT -VE and H₂O control reactions assume no sample contamination. **(B)** Band present in RT+VE reaction at expected CHO GPRC6A band height (product size 233 bp). No bands present in RT -VE and H₂O control reactions assume no sample contamination.

Chinese Hamster RAMP1;

| Score | Expect | Identities | Gaps | Strand |
|---------------|--|--------------|-----------|------------|
| 248 bits(274) | 5e-62 | 154/168(92%) | 1/168(0%) | Plus/Minus |
| Query 18 | TCTGCN-GAGATGGGGCATTGCTGAAGTAGTGTGGTGGACAGCGATGAAGAATTNNNN | | | 76 |
| Sbjct 270 | TCTGCCAGAGATGGGGCATTGCTGAAGTAGTGTGGTGGACAGCGATGAAGAATTGTC | | | 211 |
| Query 77 | NNCTTCTGGNTTGGGCCAGAAACAGCCAATCTGTTTGGCCACNTGCTTGGTACAGTAGGT | | | 136 |
| Sbjct 210 | TACTTCTGGTTGGGCCAGAAACAGCCAATCTGTTTGGCCACATGCTTGGTACAGTAGGT | | | 151 |
| Query 137 | GAGCTCCCCGTAGCTCCCTATGGTCTTCCCCAGTCACANNANAGT | | | 184 |
| Sbjct 150 | GAGCTCCCCGTAGCTCCCTATGGTCTTCCCCAGTCACACCACAGAGT | | | 103 |

Chinese Hamster GPRC6A;

| Score | Expect | Identities | Gaps | Strand |
|---------------|---|---------------|-----------|------------|
| 307 bits(340) | 5e-80 | 170/170(100%) | 0/170(0%) | Plus/Minus |
| Query 9 | GTTGTTATGACACCAATCCAGTTCATCCAGATTGTTGAATCAGGTGGGCCATTGCTTTA | | | 68 |
| Sbjct 647 | GTTGTTATGACACCAATCCAGTTCATCCAGATTGTTGAATCAGGTGGGCCATTGCTTTA | | | 588 |
| Query 69 | GTTTGGTAGAAGTCACTGGGCACAGTTCGTAATAAATGAAGGAAAGCGGATTTTGTCACTC | | | 128 |
| Sbjct 587 | GTTTGGTAGAAGTCACTGGGCACAGTTCGTAATAAATGAAGGAAAGCGGATTTTGTCACTC | | | 528 |
| Query 129 | AGGATTTACAGCAGTGGATTCGTAACACCTGTGGCATGAGCTGTAAGTT | | | 178 |
| Sbjct 527 | AGGATTTACAGCAGTGGATTCGTAACACCTGTGGCATGAGCTGTAAGTT | | | 478 |

Figure 2.8 Sanger sequence for endogenous CHO-K1 GPRC6A and RAMP1; analysed using 4Peaks software; Sanger sequences for GPRC6A and RAMP1 aligned with NCBI XM_003510334.2 and XM_016979132.1 mRNA sequences with 92% and 100% identity match found, respectively.

2.3.2 Cell Membrane FRET-based Analysis of GPRC6A and RAMPs.

Fluorescent imaging of the FACS populations GPRC6A-Cit *only*, RAMP1-Cer *only*, and GPRC6A-Cit+RAMP1-Cer cells revealed comparable results to the previous FRET experiments carried out in COS-7 cells (A. Desai, 2012). pcDNA3.1 mock transfected CHO-K1 control cells, displayed no fluorescent signal in all Cit, Cer and FRET capture channels (Figure 2.9). CHO-K1 cells transfected with GPRC6A-Cit *only* displayed Cit [Ex 516 nm; Em 529 nm] fluorescence when excited at 516 nm filter; but no signal was recorded when excited for Cer [Ex 433 nm; Em 475 nm] or FRET signal [Ex 433 nm; Em 529 nm] (Figure 2.9). Cells transfected with RAMP1-Cer *only*, fluorescence signal was observed when excited for Cer but not for Cit or FRET (Figure 2.9). CHO-K1 cells transfected with both GPRC6A-Cit and RAMP1-Cer, fluorescent signal was recorded in both the Cit and Cer filter channels. In addition, fluorescence signal was seen in the FRET filter channel with co-localisation appearing diffuse throughout the cytosol (Figure 2.9). Phase imaging displayed all cells populations imaged showed no abnormalities in morphology or viability

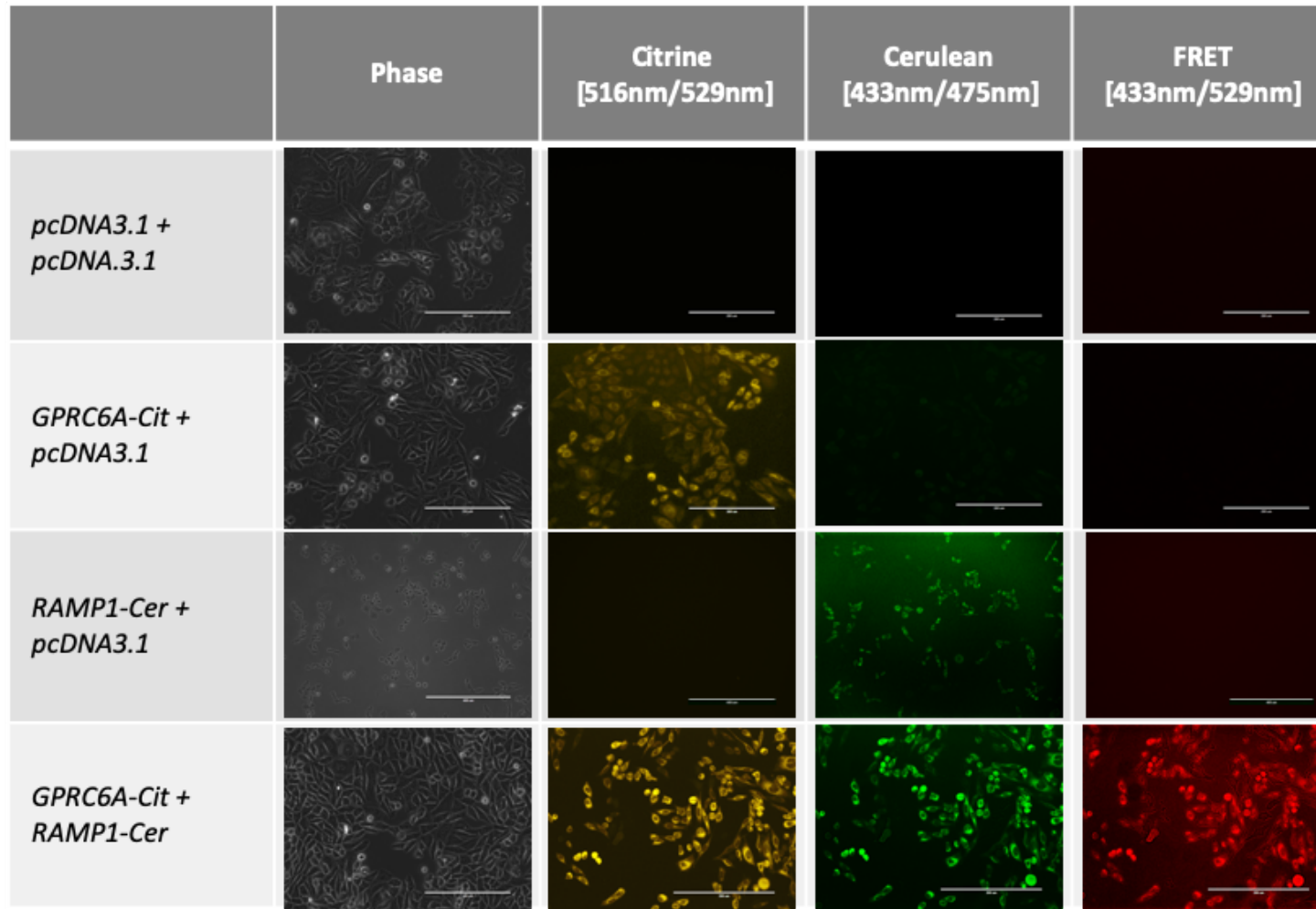
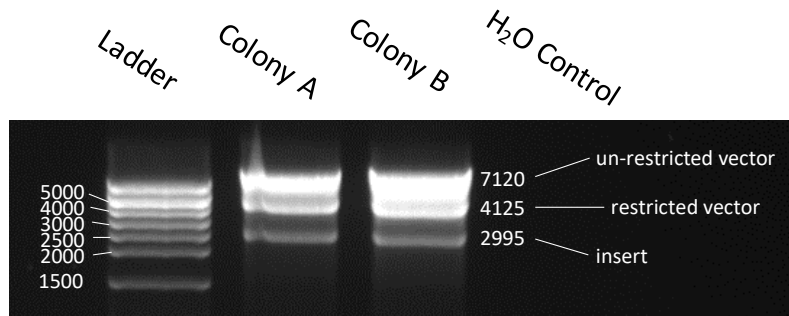


Figure 2.9 Citrine, Cerulean and FRET Imaging of FAC sorted CHO-K1 cell lines; Relative Citrine, Cerulean and FRET fluorescence signals CHO-K1 following two FACS sorts. *pcDNA3.1* mock transfection displayed no fluorescence in any of the channels. *GPRC6A-Cit+pcDNA3.1* see regions of high fluorescence intensity (yellow) when excited for citrine; however, no signal in cerulean or FRET channels. In *RAMP1-Cer+pcDNA3.1* see regions of high fluorescence intensity (green) when excited for cerulean; however, no signal in citrine or FRET channels. In *GPRC6A-Cit+RAMP1-Cer*, strong signal is seen in citrine and cerulean channels indicative of both proteins being expressed. Additionally, strong FRET signal (red) is observed in these cells, suggestive of protein-protein interaction in CHO-K1 cells, as previously seen in COS-7 cells (Figure 2.2). All images were taken at approximately 70% confluency and cells appeared healthy as detailed in phase images. Images are representative of 3 independent repeats.

2.3.3 *GPRC6A-myc Subcloning Validation.*

Successful insertion of GPRC6A-myc construct and recombinant expression was validated by using semi quantitative restriction digest endpoint PCR, Sanger sequencing, and Western blot analysis (Figure 2.10). Treatment of the re-ligated constructs with HindIII-HF and SacI-HF found observed bands of three molecular weights (Figure 2.10A) corresponding to the theoretical molecular weights of the restricted pCMV ProLink II vector and the GPRC6A-myc insert. A higher molecular weight band was also observed in the restriction digest gel, whose weight equated to the sum of both the pCMV ProLink II vector and insert. Sanger sequencing of the recombinant construct product returned the correct target and matched to NCBI database sequences using nBLAST (Figure 2.10B). Subsequent CHO-K1 cells transfected with construct 1c (Figure 2.4) saw positive staining for the –myc tag protein (~154.8 kDa [Receptor 104.8 kDa + Myc 50 kDa]) in Western blot analysis (Figure 2.10C). CHO-K1 WT and mock vector cells also saw no positive staining in comparison.

(A) GPRC6A-Myc construct restriction; (~2995bp)



(B) Myc Gene sequence;

| Score | Expect | Identities | Gaps | Strand | Frame |
|--------------|---------|--|-----------|-----------|-------|
| 167 bits(90) | 1e-38() | 96/100(96%) | 1/100(1%) | Plus/Plus | |
| Features: | | | | | |
| Query | 96 | GCCCATCACCTCTTCATGACCACTGCCTGCCAGGAGGCTAACTACGGTGCCCTCCTCCGG | | | 155 |
| Sbjct | 184 | GCCCATCACCTCTTCATGACCACTGCCTGCCAGGAGGCTAACTACGGTGCCCTCCTCCGG | | | 243 |
| Query | 156 | GAGCTCTGCCTCACCCAGTTCAGGTANN-ATGNAGGCCG | | | 194 |
| Sbjct | 244 | GAGCTCTGCCTCACCCAGTTCAGGTAGACATGGAGGCCG | | | 283 |

(C) Myc tag protein staining; (~154.8kDa)

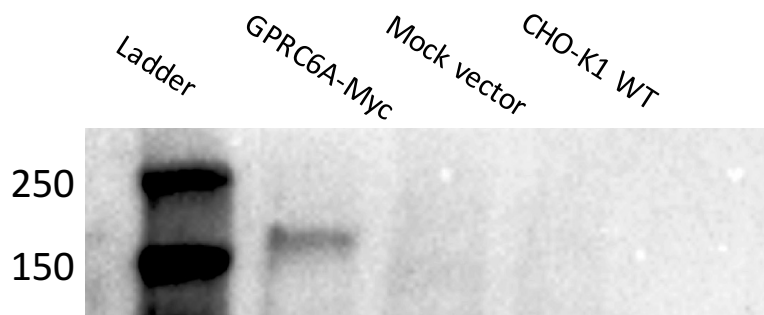


Figure 2.10 Endpoint PCR analysis and Sanger Sequencing of GPRC6A-myc constructs; **(A)** Gel presented shows two picked colonies containing re-ligated GPRC6A-myc construct. Extracted DNA from both colonies shows three distinct bands; unrestricted vector (~7120bp), restricted vector (~4125bp), and insert (~2995bp). H₂O control showed no contamination bands. **(B)** Sanger sequences for GPRC6A-myc construct aligned with NCBI XM_ mRNA sequences with 92% and 100% identity match found. **(C)** Subsequent Western blot analysis of these constructs revealed positive staining for -myc in CHO-K1 cells transfected GPRC6A-myc at the desired MW (~154.8kDa). No bands were present in mock vector or CHO-K1 WT control groups.

2.3.4 RAMP1 Cell Surface Expression.

Investigation of RAMP1 cell surface expression was performed by non-permeabilised flow cytometry, providing semi-quantitative measurement. Staining of RAMP1-Flag on mock transfected and RAMP1-Flag *only* CHO-K1 cells saw no positive staining for Flag with negligible emission shift in Red 660/20-A (Figure 2.11A & B). CHO-K1 cells co-transfected with RAMP1-Flag and GPRC6A exhibited shift from unstained group with 28.1% of the total population positively expressing the RAMP1-Flag at the cell surface (Figure 2.11C).

No positive staining was observed when staining with isotype or secondary *only* control (Figure 2.11).

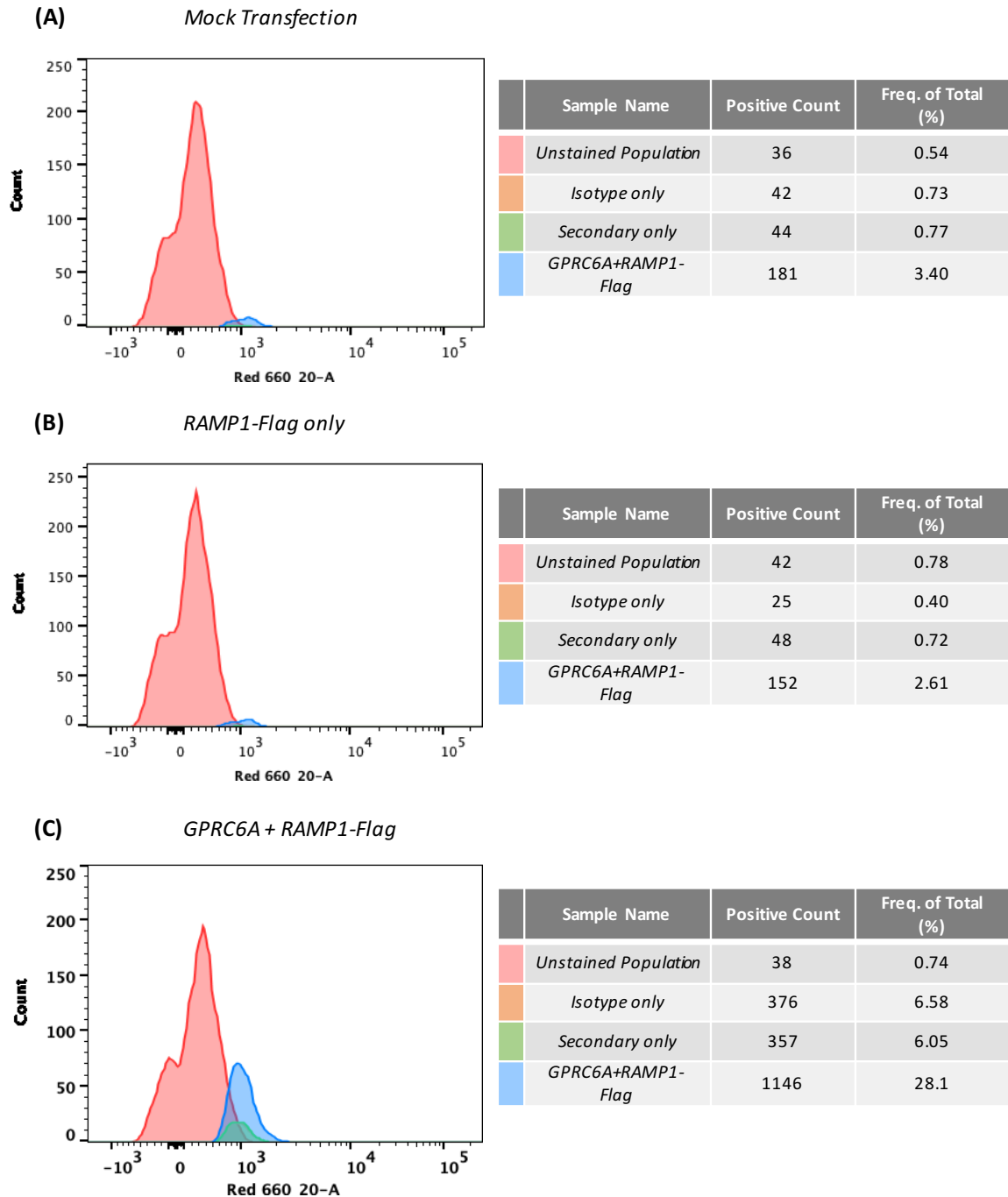
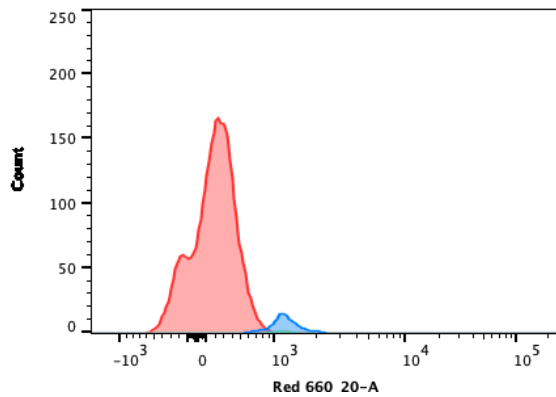


Figure 2.11 Flow Cytometry RAMP1-Flag Staining; Transiently transfected CHO-K1 cell surface RAMP1-Flag staining histogram plots. **(A)** **(B)** Negligible positive staining was observed from unstained group in mock and RAMP1-Flag *only* transfected control cells. **(C)** CHO-K1 cells co-transfected with RAMP1-Flag and hGPRC6A exhibited shift in Red 660/20 from unstained group with a larger number of cells positively expressing the RAMP1-Flag at the cell surface compared to the other control groups. Data collected is representative of 1 independent repeats. Negligible positive staining was observed for secondary *only* and isotype controls for all transfection groups.

2.3.5 *GPRC6A-myc Cell Surface Expression.*

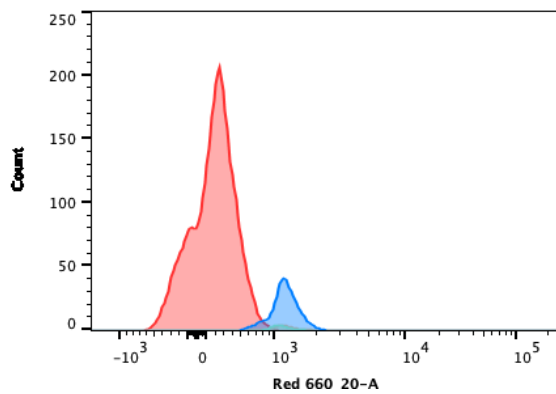
Staining of myc was used to revealed cell surface expression of GPRC6A-myc and to what degree RAMP1 affected the receptor's cell surface expression. Mock transfected CHO-K1 cells saw negligible positive Myc staining or shift in Red 660/20-A (Figure 2.12A). CHO-K1 cells transfected with GPRC6A-myc *only* exhibited a distinct shift in Red 660/20-A with small positive population of cell exhibiting GPRC6A-myc at the cell surface (7.28% of the total population) (Figure 2.12B). CHO-K1 cells co-transfected with both GPRC6A-myc and RAMP1 exhibit a distinct shift in Red 660/20-A from unstained group revealing 42.8% of the total population positively expressing the receptor at the cell surface compared to the other cell groups (Figure 2.12C). No positive staining was observed in isotype or secondary *only* staining (Figure 2.12).

(A) *Mock Transfection*



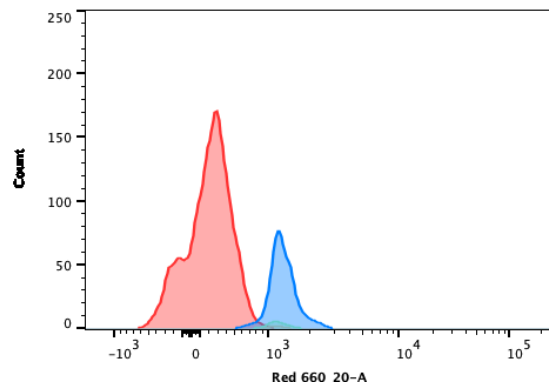
| | Sample Name | Positive Count | Freq. of Cell Population (%) |
|--|-----------------------------|----------------|------------------------------|
| | <i>Unstained Population</i> | 56 | 1.04 |
| | <i>Isotype only</i> | 49 | 0.94 |
| | <i>Secondary only</i> | 47 | 0.93 |
| | <i>GPRC6A-myc+RAMP1</i> | 268 | 6.87 |

(B) *GPRC6A-Myc only*



| | Sample Name | Positive Count | Freq. of Total (%) |
|--|-----------------------------|----------------|--------------------|
| | <i>Unstained Population</i> | 48 | 0.78 |
| | <i>Isotype only</i> | 111 | 1.96 |
| | <i>Secondary only</i> | 98 | 1.61 |
| | <i>GPRC6A-myc+RAMP1</i> | 383 | 7.28 |

(C) *GPRC6A-Myc + RAMP1*



| | Sample Name | Positive Count | Freq. of Total (%) |
|--|-----------------------------|----------------|--------------------|
| | <i>Unstained Population</i> | 68 | 1.04 |
| | <i>Isotype only</i> | 710 | 13.2 |
| | <i>Secondary only</i> | 424 | 6.69 |
| | <i>GPRC6A-myc+RAMP1</i> | 2448 | 42.8 |

Figure 2.12 Flow Cytometry GPRC6A-myc Staining; Transiently transfected CHO-K1 cell surface GPRC6A-Myc staining histogram plots. **(A)** Negligible positive staining was observed from unstained group in mock transfected control cells. **(B)** Small positive population seen in CHO-K1 cells transfected with GPRC6A-Myc construct *only* (7.28% of the total population). **(C)** CHO-K1 cells co-transfected with both GPRC6A-myc and RAMP1 exhibited distinct shift from unstained group in Red 660/20-A with 42.8% of the total population positively expressing the receptor at the cell surface compared to the other controls. Data collected is representative of 2 independent repeats. Negligible positive staining was observed for secondary *only* and isotype controls for all transfection groups.

2.3.6 Cell Surface Expression of GPRC6A-myc and RAMPs by ELISA.

Whole-cell cell surface ELISA was used to assess the influence of RAMPs on GPRC6A forward trafficking. Expression of GPRC6A was monitored by monoclonal antibodies against-Myc. Cell surface ELISA found that co-expression of GPRC6A-myc with RAMP1 significantly increased positive -myc staining compared to expression of GPRC6A-myc *only* ($p < 0.001$) (Figure 2.13). Furthermore, surface -myc positive staining was significantly higher when GPRC6A-myc was co-expression with RAMP1 compared to co-expression with GPRC6A-myc+RAMP2 ($p < 0.01$) and RAMP3 ($p < 0.0001$) combinations (Figure 2.13).

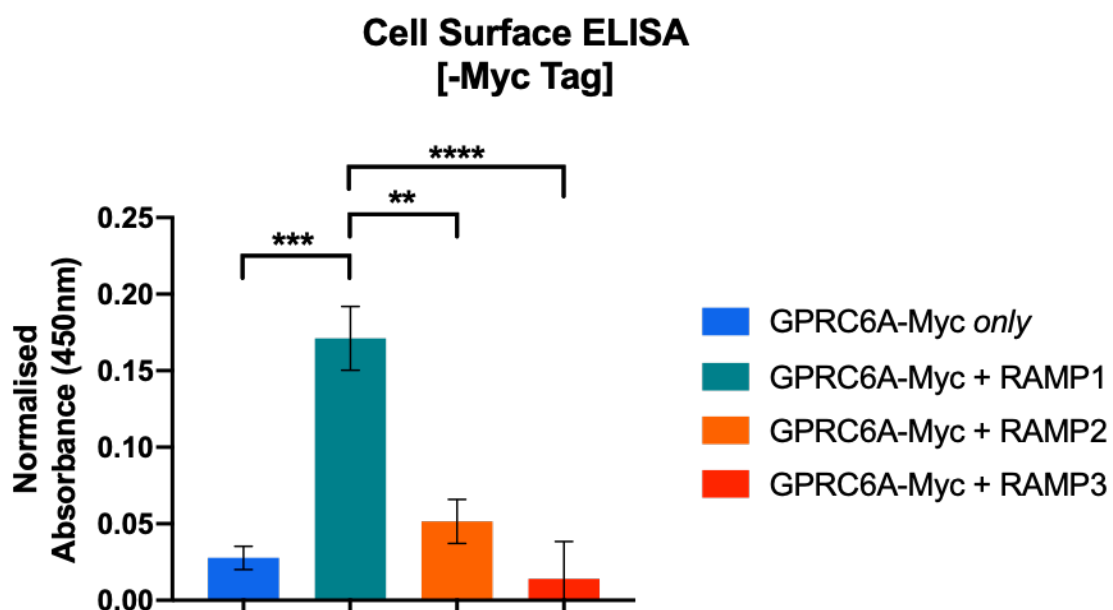


Figure 2.13 GPRC6A-myc Cell Surface Expression; anti-myc stain cell surface ELISA in GPRC6A-Myc/RAMP transiently co-expressing cells. All constructs were assayed in triplicate from 3 independent transfections. Each group of triplicates was corrected for background from ProLink II+pcDNA3.1 transfected cells and from cells treated with only secondary HRP-conjugated antibody for each transfected condition. significantly higher positive staining -Myc was observed when GPRC6A and RAMP1 are co-expressed, compared to GPRC6A *only* ($p < 0.001$); RAMP2 ($p < 0.01$); and RAMP3 ($p < 0.0001$). Data are from 3 independent experiments and are presented as mean \pm SEM.

2.3.7 Cell Surface Expression of GPRC6A and RAMPs-Flag by ELISA.

Whole-cell cell surface ELISA was additionally used to investigate which RAMP exhibited greater surface expression when co-expressed with hGPRC6A. Surface expression of RAMP1/2/3 was monitored by antibodies against Flag tag. Cell surface ELISA found that co-expression of GPRC6A with RAMP1-Flag significantly increased positive Flag staining compared to expression of GPRC6A *only* ($p < 0.05$). Furthermore, positive surface staining

for Flag was significantly increased when GPRC6A was co-expressed with RAMP1-Flag compared to co-expression with GPRC6A+RAMP2-Flag/3-Flag combinations ($p < 0.05$) (Figure 2.14). Both –Myc and –Flag ELISA experiment show comparable trend in hGPRC6A cell surface expression and mirrored data observed in the previous FRET-based experiments (see Figure 2.2).

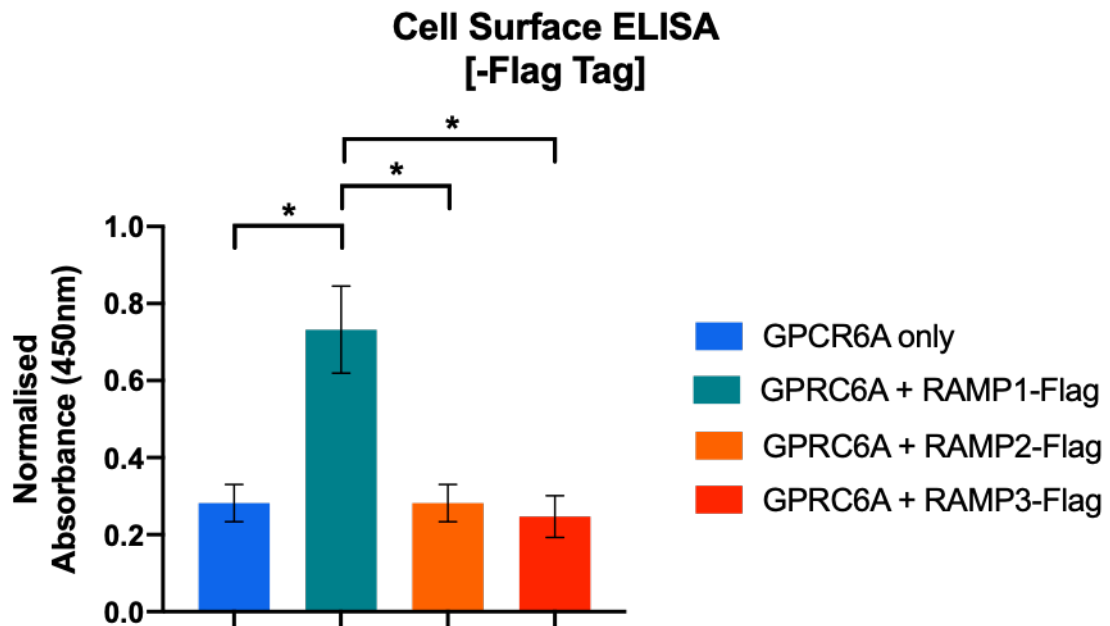


Figure 2.14 RAMP1-Flag Cell Surface Expression; anti-Flag stain cell surface ELISA in GPRC6A/RAMP-Flag transiently co-expressing cells. All constructs were assayed in triplicate from 4 independent transfections. Each group of triplicates was corrected for background from mock transfected cells and from cells treated with only secondary HRP-conjugated antibody for each transfected condition. Significantly higher positive staining –Flag ($p < 0.05$) was observed when GPRC6A and RAMP1-Flag are co-expressed, compared to GPRC6A *only* ($p < 0.05$); RAMP2-Flag ($p < 0.05$); and RAMP3-Flag ($p < 0.05$). Experiments were performed in triplicate and are from 4 independent experiments and are presented as mean \pm SEM.

2.4 Discussion.

The experiments detailed in this chapter sought to investigate the interactions between hGPCR6A and RAMPs. The work provided a fundamental basis to why the human variant of the receptor fails to be adequately expressed at the cell surface and further offers an explanation for the pharmacological discrepancies within the field. RAMP's tissue distribution is known to exceed that of their interacting partners, thus prompting the investigation of these unidentified proteins. Although it is known that predominantly class B GPCRs interact with RAMPs, recent discoveries have shown the concept of GPCR-RAMP hetero-dimerisation is transferrable across different GPCR classes. An increasing number of published reports show RAMPs to be fundamental components to class A & C GPCRs (Barbash et al., 2017; Bouschet et al., 2005, 2008, 2012; A. J. Desai et al., 2014; Lenhart et al., 2013).

A brief discussion of the data previously acquired from our group will be given here in order to provide context to the results obtained as part of this project. Preliminary experiments focussed towards providing supportive data for the previously obtained FRET data concerning hGPCR6A and RAMP1 interaction in COS-7 cells (A. Desai, 2012). Using the same constructs, we were able to produce CHO-K1 cell lines that stably expressed GPCR6A-Cit *only*, RAMP1-Cer *only* and a co-expressing GPCR6A-Cit + RAMP1-Cer, through combination of antibiotic selection and FACS.

2.4.1 FRET Analysis of GPCR6A and RAMP Interaction.

2.4.1.1 GPCR6A and RAMPs in COS-7 Cells.

GPCR6A and RAMP1 were tagged with the acceptor Cit and donor Cer fluorophores, respectively. These fluorophore mutants of YFP and CFP offer advantages over their derivatives. Being a long wavelength mutant; Cit provides greater peak separation from Cer, expressing easily with resistance to acidity quenching (Heikal *et al.*, 2000). Cer is known to be brighter than CFP with additional resistance to photo bleaching, improved fluorescence lifetime and signal to noise ratio (Rizzo *et al.*, 2004). Furthermore, C-terminal tagging the receptor and RAMPs reduces any forward trafficking which may be caused by

the inserted signal peptide of the fluorophore (Christopoulos *et al.*, 2003). Furthermore, it was important to select cell lines that didn't endogenously express either GPRC6A or RAMPs, as this might interfere with cell surface trafficking of the transfected hGPRC6A causing inaccurate FRET measurements. In previous work COS-7 showed no endogenous levels of GPRC6A or any of the RAMPs (Bouschet *et al.*, 2005; Christopoulos *et al.*, 2003; A. Desai, 2012; Harikumar *et al.*, 2010; Kelly *et al.*, 2008; Mclatchie *et al.*, 1998; Morfis *et al.*, 2008). The same was observed in our CHO-K1 cells (Figure 2.7Figure 2.8). Desai's PhD data demonstrated hGPRC6A to be intracellularly retained at the perinuclear region when GPRC6A is expressed by itself in COS-7 cells, supporting previous findings (Wellendorph, *et al.* 2005). However, distinct regions of co-localisation were observed when hGPRC6A was co-expressed with RAMP1 but not RAMP2/3 at sites commonly associated with GPCR forward trafficking (i.e. perinuclear region, ER, trafficking vesicles, Golgi, and plasma membrane (Figure 2.2) (Mclatchie *et al.*, 1998). Hence, it demonstrated for the first time that RAMP1 aided in the trafficking of hGPRC6A in COS-7 cells. Co-expression with RAMP2 did display regions of co-localisation; however, this was only seen around the perinuclear region which may be indicative of an GPRC6A/RAMP2 endo-cellular functional role, binding hydrophilic ligands (Figure 2.2). This idea of an endocellular function has previously been proposed by other groups, mirroring the functional characteristics of the classical oestrogen receptors and ARs (Pi *et al.*, 2008, 2011; Pi, Zhang, *et al.*, 2010). Further investigation is required here to delineate GPRC6A and RAMP2 role intracellularly.

2.4.1.2 GPRC6A and RAMPs in CHO-K1 Cells.

Characterisation of CHO-K1 cells for GPRC6A and RAMP1 revealed transcript endogenously present; albeit these bands are very faint (Figure 2.7). If repeated it would be recommended to run probes against a well-expressed housekeeping gene i.e. GAPDH in order to semi-quantify the relative expression levels. When probing for Although other groups have already reported negligible levels of endogenous RAMPs expression in CHO cells (Cegla *et al.*, 2017; Tilakaratne *et al.*, 2000; Wootten *et al.*, 2013); it would have been beneficial to probe endogenous RAMP2 and RAMP3 in our cells. As shown the previous FRET experiments in COS-7 cells RAMP2 also has the ability to complex with GPRC6A (A.

Desai, 2012). This promiscuous interaction could later interfere with trafficking and signalling experiments. Using the same constructs, we were able to produce CHO-K1 cell lines that stably expressed GPRC6A-Cit *only*, RAMP1-Cer *only* and a co-expressing GPRC6A-Cit / RAMP1-Cer, through combination of antibiotic selection and FACS. Antibiotic selection concentration was decided based upon G418 kill curve (Figure Ap.1); cell viability was assessed using the RealTime-Glo™ MT Cell Viability Kit (Promega, UK) (see section 4.2.3). CHO-K1 cells treated with 2.0 mg/mL G418 saw fastest decreases in cell viability. Interestingly, even at 0.0 mg/mL decreases were observed in cell viability in a bell-shaped curve. This is most likely due to the rapid growth rate of CHO-K1 cells (doubling time approx. 24 hours) outgrowing the well plate dish and beginning to die due to overcrowding. Subsequently, may wish to seed plates at lower densities to avoid this. Dual sorting strategy allowed for isolation of highly pure and viable cells (Kuka & Ashwell, 2013). Sorting transfected colonies based on both the Cit and Cer fluorescence yielded four distinct populations, the largest population of cells neither displayed high degrees of Cit or Cer fluorescence. Sorting based on fluorescence gave indication of successful co-transfection of both GPRC6A-Cit and RAMP1-Cer. However, both gift constructs were engineered to contain the G418 selection marker, thus it could be argued that populations collected were cell containing either construct in a heterogeneous population. Thus future work would benefit greatly from using constructs containing two distinct antibiotic selection markers. This would allow for dual selection, ensuring only cells containing both constructs would survive. Interestingly, in dual sorting the populations a large population of cells exhibiting neither Cit nor Cer fluorescence is observed, even following G418 antibiotic selection (Figure Ap.3). One possible explanation for this is the natural silencing of the gene cassette; allowing the cells to utilise the inserted antibiotic resistance but has silencing the pCMV promoter upstream from GPRC6A-Cit or RAMP1-Cer by methylation (Moritz et al., 2015). Other pCMV promoter mutants less prone to methylation could be used in future work to avoid this issue (Moritz et al., 2015). The low cell acquisition may, in part be due to loss of cells inside the instruments. Maximising throughput rates enables the rapid acquisition of cell populations; however, it can detrimentally affect the instruments ability to effectively identify exact populations within a sample (Cossarizza *et al.*, 2017). Lowering the throughput (<500 events/s) has been shown to provide data with fewer misidentified doublets and missed positive events (Baumgart *et al.*, 2017).

However, it is more plausible that the transfection method produced poor transfection efficiency (Figure Ap. 2). Clear distinct populations were observed displaying high levels of GPRC6A-Cit *only*, RAMP1-Cer *only*, and both GPRC6A-Cit + RAMP1-Cer co-expression. Imaging of these enriched populations revealed strong FRET signals only when both GPRC6A-Cit and RAMP1-Cer are co-expressed in CHO-K1 cells (Figure 2.2). Other transfection reagents are available and may provide greater efficiency when transfecting large constructs. A number of papers have reported using the FlpIn/FRT technology to achieve recombinant mGPRC6A expression in HEK-293T cells (Jacobsen *et al.*, 2013; Kuang *et al.*, 2005; Rueda *et al.*, 2016). The system relies upon the Flp recombinase facilitating the exchange of two FRT target sequences. A vector contains the gene of interest flanked by two regions homology to the host genome (Barnes *et al.*, 2003). This approach works very efficiently to delivery exogenous DNA to the target cells, and could be considered in future studies due to its ease in *in vivo* experiments (Goodrich, *et al.* 2018). However, when concerning the co-expression of multiple proteins, it can bring increased complexity and costings to experiments (Barnes *et al.*, 2003; Goodrich, *et al.* 2018). It is also important to note that overexpressing two proteins can have detrimental effects upon the cell. Overexpression systems can lead to resource overload, unnatural protein-protein interaction, stoichiometric imbalance and pathway modulation (reviewed by Moriya, 2015). Future work would benefit greatly from lowering the DNA concentrations used for transfection and see whether the subsequent FRET interactions are comparable. Furthermore, subsequent studies may use an expression system that natively expresses GPRC6A and RAMP1 may be provide greater insight in whether the interaction studied here is true. Comparison between a wild-type expressing system and a system that has had RAMP1 deleted would give a more accurate view of the interactions between GPRC6A and RAMP1 at physiologically relevant levels.

2.4.1.3 FRET System Limitations.

A major drawback of the FRET system pertains to the over-expression of large fluorophores proteins intracellularly. Areas of particularly high protein-protein co-localisation or fluorophore aggregation lead to non-linear fluorescence emission – this is

demonstrated as regions of saturated FRET intensity (regions of black in Figure 2.2), where protein-protein interactions are unable to be effaceable determined. This phenomenon can, in part be ameliorated with extensive mathematical normalisation taking the saturation into account to significantly reduce the dependence on the excitation intensity (Szendi-Szatmári *et al.*, 2019). It is also important to mention that in over-expressing conditions the interactions observed may not represent physiological interactions as the introduction of foreign proteins may detrimentally effect natural intracellular mechanisms within the cell. Larger fluorescent protein labels (above 30 kDa/4 nm) have a tendency to oligomerise into tetramers; however, the tags used here fall beneath this threshold (Citrine = 28 KDa and Cerulean = 26 KDa) (Baird *et al.*, 2000; Toseland, 2013).

The principal strength and weakness of the FRET system is it's highly sensitivity to protein-protein distance and orientation; chemical fluorophores – evenly covalently bonded are found to be highly mobile in physiological conditions (Hink *et al.*, 2000). For example, the binding of Ca²⁺-calmodulin has been shown to disrupt protein subunit interaction; binding fluorophores pairs and immobilise then in orientations unfavourable for efficient FRET exchange (Zheng *et al.* 2003). This could be partially accounted for by measuring the fluorophore anisotropy in the experimental environment allowing for better optimisation of the fluorophore pair. This methodology measures the light emitted by a fluorophore along different axes of polarisation (reviewed by Ojha *et al.*, 2020; Yengo & Berger, 2010). Accordingly, the results obtained from the preliminary FRET investigation represented initial observations and required further investigation to confirm this using alternative approaches.

2.4.2 Validation of GPRC6A-myc Subcloning.

The constructs generated by Desai *et al* (2012) enabled ample strategies for investigating GPRC6A receptor expression levels and co-localization. These constructs offered little insight into RAMPs effect on GPRC6A trafficking, and in the absence of validated hGPRC6A antibodies the generation of a construct containing GPR6CA with a recognizable epitope tag offered greater benefits for future experiments. The myc tag offers a great range of well-researched antibodies raised in a variety of animals hosts, optimized for flexibility in

many assays (Kolodziej & Young, 1991)(Terpe, 2003). Furthermore, although both provide high specificity to their desired target, anti-myc antibodies offer higher specificity when used in conjunction with enzyme-linked secondary detection antibody; a tactic that complimented future ELISA experiments when investigating cell surface expression (Kimple *et al.*, 2013).

Subcloning of the GPR6CA-myc construct saw successful re-ligation of the insertion into the pCMV ProLink II vector. Treatment with HindIII-HF and SacI-HF offered highly targeted DNA cleavage with the added reductions in star activity using high-fidelity forms of the restriction enzymes (Mayer, 1978; Roberts, 2005). Although the restriction digest observed two bands corresponding to the molecular weights of the vector and insert; the presence of a higher molecular weight band is indicative of improper restriction (Figure 2.10A). Restriction endonucleases - evolved as part of the prokaryote innate immunity - have notoriously low K_{max} and K_{cat} activity (Halford & Goodall, 1988). To combat this, it is common to maximise DNA concentrations in restriction reactions in an attempt to maximise the yields of products. However, endonucleases are essentially substrate inhibited as similar restriction sites act as inhibitors or alternate substrates (i.e. star activity) at sufficiently high concentrations (Robinson & Sligar, 1993). Future experiments hoping to clear up these reactions may adopt a few strategies. Preliminary tests may benefit from setting up reactions containing moderate concentrations of enzyme and DNA and allowing these reactions to incubate for an extended period; improving the product yields (Robinson & Sligar, 1993).

Attempts were made to run the gel for an extended period and decrease the agarose percentage; however, in doing so saw losses in band intensity and sample/ladder resolution. Based on the molecular weight equating to the sum of the vector and insert, this high molecular weight band was assumed to be an artefact from unrestricted vector (Figure 2.10A). This commonly is the results of inefficient endonuclease activity. If longer restriction times fail to ameliorate the issue, it may be possible that contaminants present in the reaction are inhibiting the enzymatic action (Yue & Labash, 1991). This can commonly be treated with dilution, using reactions of the same quantities of enzyme and

DNA in larger volumes of buffer (Matsumura, 2015; Zeng *et al.*, 1997). However, excision and sequencing of this band would provide better evidence in supporting this assumption.

Further validation of successful construct expression required measurement of GPRC6A-myc protein expression (Figure 2.10C). Western blotting found, following transfection into CHO-K1 cells, positive staining for GPRC6A-myc (~154.8 kDa) in comparison to CHO-K1 WT and mock transfected control groups. However, it must be stated that the repeatability of this experiment showed some degree in variation concerning the band intensity, repeatability and; in Western blotting, the antibody displayed non-specificity in binding to the unidentified proteins and the ladder itself. Thus we cannot definitively say GPRC6A-myc was expressed at the protein level. This may explain the low ELISA OD value readings close to the plate reader's linear limit 0.2-2.0. The introduction of higher concentration blocking buffer and/or increased incubation time might have ameliorated this issue.

It is important to note that although both constructs comprise a similar vector backbone and were engineered downstream of the same pCMV promoter, the introduction of two different vectors may cause alternative levels of expression on the cells. For the transient surface expression experiments, both vectors were transfected with the same amount of DNA and thus assumed to express at a comparable level. Furthermore, both pcDNA3.1 and Prolink II vectors again contained the same antibiotic G418 selection marker. Concerning the GPRC6A-Cit, successful transfection could be evaluated based on CHO-K1 Cit fluorescence; with GPRC6A-myc this was no longer possible. This could be evidenced by unsuccessful replication of flow cytometry staining and very low OD value readings close to the plate reader's linear limit 0.2-2.0. Future work would benefit greatly from utilising identical vector constructs combined with distinct antibiotic markers to ensure cells in all subsequent experiments are subject to identical metabolic load, protein production, toxicity etc. and selected populations co-expressed both vectors.

2.4.3 *GPRC6A Cell Surface Expression by Flow Cytometric Analysis.*

Flow cytometry of live transiently overexpressing CHO-K1 cells was used preliminarily to determine whether RAMP1 increased the cell surface expression of hGPRC6A. Flow

cytometric analysis of non-permeabilised cells allowed for targeting of proteins specifically localised to the plasma membrane. Literature has established that whilst the murine GPRC6A is successfully forward trafficked, human GPRC6A remains intracellularly retained; this suggests the requirement for a chaperone protein to allow adequate cell surface expression. This necessity for a chaperone may provide an explanation for the receptor's lack of surface expression when expressed recombinantly (Christiansen et al., 2007; Kuang et al., 2005; P Wellendorph et al., 2005). Here we have shown that in CHO-K1 cells overexpressing hGPRC6A and RAMP1, GPRC6A can be successfully detected at the cell membrane and that RAMP1 positively modulates hGPRC6A cell surface expression (Figure 2.11Figure 2.12). With our previous FRET data, the flow cytometric data provides supportive evidence of RAMP1 aiding in forward trafficking of hGPRC6A. Interestingly, with our knowledge that that RAMPs possess a promiscuous ability to complex with a variety of GPCRs (Hay & Pioszak, 2016); it may be expected to see some level of surface expression when staining for the Flag tag. Here, we see negligible surface when RAMP1-Flag is expressed alone (Figure 2.11). However, it's important to note that that RAMP1-Flag is overexpressed, any interaction that may occur with endogenous receptors will be significantly smaller as endogenous receptors may be expressed at a level that is undetectable at the cell surface. Furthermore, it is known that RAMPs, especially RAMP1 are unable to trafficking to the surface independently, and must undergo proper glycosylation in order to be forward trafficked (Christopoulos et al., 2002; Wootten et al., 2013). Thus, results from the anti-flag immunofluorescence staining can only provide the assumption of hGPRC6A/RAMP1 cell surface complexes. Hence, constitute insufficient proof to reliably confirm RAMP1 aiding in the receptors trafficking.

Using the GPRC6A-myc tagged construct gave us a more accurate insight into the receptors ability to forward traffic in the presence of RAMP1. Subsequent efforts to validate GPRC6A and RAMP1 interaction utilised GPRC6A-myc construct (Figure 2.4). This approach allowed for a wider range of well-validated antibodies to target the specific surface protein tags. Here we observed a comparable pattern in cell surface expression; expression of hGPRC6A *only* in myc experiments yielded negligible positive staining, comparable to mock transfection. Only co-expression of both GPRC6A-myc and RAMP1 produced a significant increase in cell surface positive staining (Figure 2.12). From these

findings, we can now start to draw more concrete conclusions from the data; showing RAMP1 to positively modulate hGPCR6A forward trafficking in CHO-K1 cells.

However, results of the anti-myc flow cytometry surface staining only represent n=2 as the repeatability of this experiment brought uncertainty to the validity of the methodology. Following considerable optimisation attempts, certain staining patterns would reveal no changes in shift between unstained and stained groups; whilst other attempts would display shift in isotype or secondary antibody control staining groups. Possible causes for the variability may be explained by the receptor's large size and the limited number of available receptors that can be expressed at the surface at one time. Furthermore, the methodology required numerous washing steps which may have been detrimental to the cells ability to expressed an adequate number of receptors at the plasma membrane. Due to the greater degree of variability; combined with the receptors low expression profile (Clemmensen, *et al.* 2014) and the promiscuous action of RAMPs (McLatchie *et al.*, 1998; Bouschet *et al.* 2008; 2012; Desai *et al.* 2014; Hay & Pioszak, *et al.* 2016), the flow cytometric approach required too much time in order to produce sufficient supporting data. Therefore, whole-cell cell surface ELISA was adopted to provide an additional methodology to illustrate RAMP-mediated GPCR6A cell surface expression.

2.4.4 GPCR6A Cell Surface Expression by Whole-Cell Surface ELISA.

One major advantage of using the whole-cell surface ELISA over flow cytometry was that it allowed for cells to be plated and grown overnight, without the need to be held in suspension when assayed. This method avoided the use potentially harmful detachment reagents; which may cleave surface proteins embedded within the plasma membrane. Similarly, in agreement with studies identifying retention motif present in the hGPCR6A (Jørgensen *et al.*, 2017; Kuang *et al.*, 2005; Wellendorph *et al.*, 2005), we observed that expression of hGPCR6A alone produced poor cell surface trafficking in CHO-K1 cells. However, levels of hGPCR6A surface expression were significantly increased when co-expressed with RAMP1 specifically in both –Flag and –myc staining experiments (Figure 2.13Figure 2.14). This pattern was seen in our FRET, ELISA and flow cytometry co-

localisation studies, observing high levels of GPRC6A/RAMP1 co-localisation at regions commonly associated with receptor assembly/processing and trafficking (i.e. ER, trafficking vesicles, plasma membrane) (Mclatchie *et al.*, 1998). Compared to flow cytometric analysis, whole-cell cell surface ELISA provided robust consistent data. Taken together, the data supports the notion that RAMP1 is an essential component in facilitating successful forward trafficking of the hGPRC6A receptor. Potential explanations for the lack of cell surface expression observed in previous pharmacological studies is that the cell lines used (i.e. commonly HEK293 & CHO-K1) lack the necessary scaffolding and/or accessory proteins (e.g. RAMPs) found in cells endogenously expressing GPRC6A.

2.4.5 Alternative Methodologies.

Cit and Cer possess extensive spectral overlap between the donor emission and the acceptor excitation. In an ideal system, there should be no overlap between in the excitation spectra and the emission spectra between the FRET pair; as this can result in the acceptor's direct excitation by the donor excitation wavelength (Ma *et al.*, 2014). Alternative strategies for validating cell surface expression may incorporate the use of bioluminescence resonance energy transfer technology; a relatively recent methodology, combining the protein-protein interaction of FRET with impermeable bioluminescent markers. This system uses an enzyme (i.e. luciferase) and substrate (i.e. luciferin) to generate the donor light and a fluorophore as the acceptor (Bacart *et al.*, 2008). This approach enables the donor to be excited chemically rather than optically and thus avoids issues concerning spectral overlap, bleed-through and crosstalk (Gandía *et al.*, 2008). The strategy has already been successfully employed to demonstrate the interaction of secretin receptor and RAMP3, identifying TM6 and TM7 as key interfaces for this molecular interaction (Harikumar *et al.*, 2010). The novel approach could provide data on specific domains (i.e. hGPRC6A ICL-3) involved in the hGPRC6A and RAMP1 interaction; tracking cell surface FRET intensity for successful cell surface trafficking. Additionally, this would negate the need to express a GPRC6A complex linked to a tagged protein that may well infer with normal receptor function (Prasad, Hollins and Lambert, 2010; Xie *et al.*, 2012; Namkung *et al.*, 2016).

Future studies might employ a more detailed approach for investigating the interaction between hGPCR6A and RAMP1; examining the specific interfaces involved in the complex. These include, affinity chromatography, co-immunoprecipitation, X-ray crystallography, and NMR spectroscopy (Rao *et al.*, 2014). Affinity chromatography offers a highly responsive methodology, detecting even the weak interactions between proteins. However, a major limitation when implementing this approach is its high degree of false positives arising from high specificity amongst proteins; incorrectly identifying protein-protein interaction when neither protein interact under physiological conditions. Because of this, protein-protein interactions studies cannot fully rely on this technology and is often required in combinations with other methods (e.g. SDS-PAGE or mass spectroscopy) to validate the findings (Rao *et al.*, 2014). One avenue may exploit X-ray crystallography enabling the visualisation of protein structures at the atomic level heightening our understanding of important structural motifs in binding. In particular, what conformational changes occur upon RAMP or ligand binding. This information would be especially crucial in designing novel small molecules targeting the hGPCR6A receptor. This approach could be broadened further utilising nuclear magnetic resonance spectroscopy to localise precise binding interfaces between the two proteins (Gao *et al.*, 2004; O'Connell *et al.*, 2009; Ortega-Roldan *et al.*, 2018; Tong *et al.*, 2001).

Chapter 3: GPRC6A Intracellular Signalling.

3.1 GPCR6A Signalling Introduction.

The current GPCR research field has undergone a large paradigm shift in terms of how these receptors are understood to operate. No longer does the “on” or “off” mechanism or the one-ligand one-receptor model apply. Mounting research have shown GPCRs to operate in a variety of receptor conformations exhibiting subtle differences in the receptors signalling and ligand-binding profile (Katritch *et al.*, 2013; Namkung *et al.*, 2016; P. S. H. Park *et al.*, 2008). GPCR6A has previously been demonstrated to activate multiple intracellular pathways through more than one G protein, characterising GPCR6A as a pleiotropic receptor (Jacobsen *et al.*, 2013; Pi *et al.*, 2005, 2016; Pi & Quarles, 2012b). Previous data has demonstrated RAMPs to play an integral role in the class C CaSR functionality, a human receptor that shares a significant homology with the GPCR6A (Bouschet *et al.*, 2005, 2012; A. J. Desai *et al.*, 2014; Rossol *et al.*, 2012; P Wellendorph *et al.*, 2005). Thus far, RAMPs have been shown to exhibit chaperone capabilities with GPCR6A (see chapter 2); however, studies have also reported RAMPs role in modulating GPCRs signalling functionality.

3.1.1 GPCR Signalling-Transduction Mechanism.

The putative model by which GPCRs transduce extracellular stimuli can be explained by the ternary complex model, accounting for the cooperative interactions between the receptor, G proteins and agonist. A combination of crystallography and biochemical data has proposed the concept that the majority of GPCRs exists in a dynamic equilibrium between an inactive state (R and R') and an active state (R'' and R*). The interaction of the heterotrimeric G protein complex can then convert this further to a signalling state (R*G) (Figure 3.1) (Katritch *et al.*, 2013). The G proteins will bind exclusively to the R* state, provoking a downstream cellular response. The binding of an agonist shifts the equilibrium in favour of the active states, demonstrated by large conformational changes within the GPCR. In the active states, the GPCR is capable of pre-coupling to a G protein and can therefore exist in a R*G state. Inverse agonists will shift the equilibrium towards the receptor's inactive states, while antagonists have no affect the equilibrium (Nygaard *et al.*, 2009). These five distinct receptor conformations have been well demonstrated in

the rhodopsin, β 1-andrenergic, β 2-andrenergic and A_{2A} adenosine receptors (find all the citations). Separate conformation active states are likely to exist for GPCRs coupling to G protein independent pathways, namely β -arrestin pathways (i.e. R^*A) and G protein receptor kinases (i.e. R^*GRK) (Katritch *et al.*, 2013).

Although the receptors studied possess stark architectural differences, comparisons of their inactive and active conformations revealed similar activation-dependant structural changes at the receptors intracellular side. The most distinct of these structural rearrangements occurs in helix VI, exhibiting an outward “swinging” in tandem with a movement in helix V. The size of this movement differs depending on the GPCR and the different active states. For example, helix VI is reported to move approximately 3.5 Å in the A_{2A} adenosine receptor in the R'' , 6 Å in the rhodopsin receptor in the R'' and R^* , and upto 11-14 Å in the β 2-andrenergic receptor-G protein complex (R^*G) (Rasmussen *et al.*, 2011). The rearrangements of helices V and VI in the R^*G state appear to be predominantly G protein-controlled and coincide with the release of GDP (Katritch *et al.*, 2013). Conformational changes in helices III and VII have also been demonstrated across these receptors. In the A_{2A} adenosine receptor, helix III is seen to move upwards along its axis and shift laterally. Helix VII is seen to move towards the interior of the 7TM domain, exhibiting a distortion in its helix backbone (Lebon *et al.*, 2011; F. Xu *et al.*, 2011). The data here suggest a crucial involvement of helices V and VI in G protein interaction and activation. While conformational changes helices III and VII are most likely to be receptor/ligand-dependent.

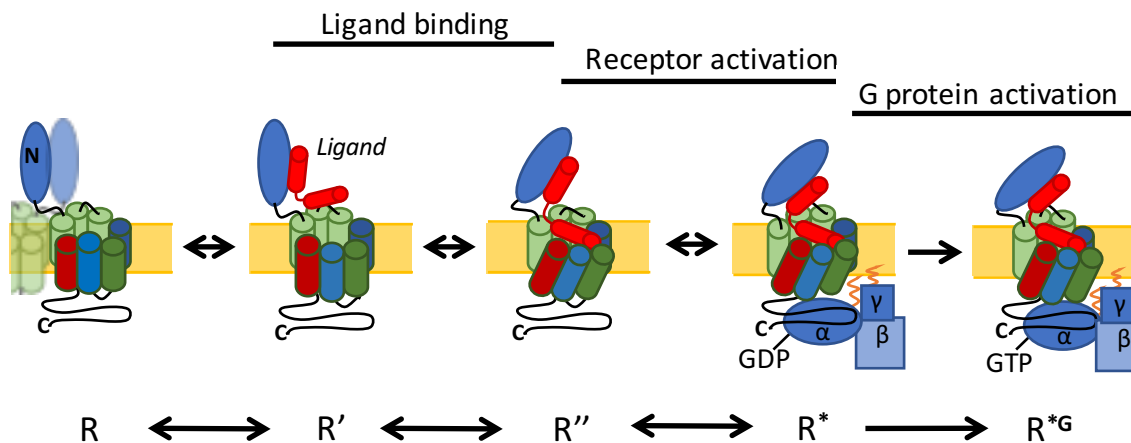


Figure 3.1 Mechanistic Model of GPCR Activation; In the lack of a bound agonist the receptor is in the inactive state (R). This conformation can be stabilised with the binding of an inverse agonist or an antagonist. Upon binding of an agonist, the receptor enters the inactive R' state, this state differs from R representing only small localised changes to the binding pocket. In the R'' state the receptor is said to be activated, represented by changes in conformation of the transmembrane helices exposing the G protein binding interface. In R* the activated receptor now begins to engage with the G proteins at the intracellular C-terminus. R*G represents the receptor-G protein signalling complex which is characterised by full activation of the receptor and Gαβγ subunits. The transition from R* to R*G occurs alongside the release of GDP therefore; the transition is unidirectional. Termination of the signal occurs upon dissociation of the protein complex and returns back to the inactive states when new Gαβγ-GDP binds to the receptor (adapted from Katritch, *et al.* 2013). Helices III (dark blue), V (red), VII (light blue), and VIII (dark green) are indicated.

In the unstimulated state, the Gα subunit directly binds a single GDP molecule in complex with the peripheral β and γ subunits. Guanosine nucleotides are thought to shift the equilibrium in favour of the low-affinity or uncoupled state (P. S. H. Park *et al.*, 2008). Ligand binding to the GPCR enables a conformation change within the GPCR structure allowing for transduction of the external stimuli to form a high affinity agonist-GPCR complex. Subsequent G protein activation allows for the displacement of the GDP molecule with a GTP molecule at the Gα subunit, followed by the dissociation of the βγ dimer (Namkung *et al.*, 2016; Prasad *et al.*, 2010; Xie *et al.*, 2012). Release of Gα subunit enables activation of membrane-associated effector proteins initiating downstream signalling cascade reactions. G proteins remain in the active state whilst GTP is bound; however, hydrolysis of GTP to GDP initiates the re-assembly of the α, β, and γ subunits into the inactive heterotrimer and re-association with the GPCR back to the basal state (Namkung *et al.*, 2016; Prasad *et al.*, 2010; Xie *et al.*, 2012). The mechanism by which GPCRs become activated exists in a dynamic conformation equilibrium between the inactive and active biophysical states.

3.1.2 *Promiscuous G-protein coupling.*

There is a growing consensus that GPCRs have the capability to couple to the different G signalling cascades to varying degrees. It is now clear that GPCRs can engage with multiple G proteins and the line between cognate and non-cognate signalling is increasingly blurred. Furthermore, the coupling of GPCRs to non-G-protein transducers, including β -arrestins or other scaffold proteins, to initiate additional signalling cascades has become an accepted property of GPCR signal transduction (Seyedabadi et al., 2019). Examples of this concept include the β -adrenergic receptors; with compounds metoprolol and bisoprolol activating $G\alpha_i$ proteins but not $G\alpha_s$; carvedilol displays partial agonism for β -arrestin signalling but antagonism for $G\alpha_s$ signalling; whereas, salmeterol acts in the reciprocal manner. The biases in G protein activation may explain the varied therapeutic profiles observed from different compounds. For example, salmeterol's full agonism on $G\alpha_s$ activation may explain its longer duration of action in chronic heart failure treatment in comparison to carvedilol (Carter & Hill, 2005; Malik et al., 2013; Onfroy et al., 2017; Rajagopal et al., 2011; Wisler et al., 2007).

3.1.2.1 *Promiscuous G Protein Signalling in Class C GPCRs.*

This concept has been thoroughly demonstrated in the well-researched GPCRs families and continues to hold true as novel studies are published. The class C CaSR, which possesses large sequence homology with the GPRC6A receptor has been reported to couple to multiple G-protein pathways (Gerbino et al., 2005; Mamillapalli et al., 2008; Okashah et al., 2019). Table 3.1 summarises the signalling pathways GPRC6A is reported to activate. The most studied and well-characterised mechanism is the $G\alpha_q$ -mediated PLC β pathway. This pathway initiates IP₃ cleavage, leading to the subsequent mobilisation of intracellular Ca²⁺ stores from the ER. PLC-mediated calcium release by the GPRC6A has been demonstrated in HEK-293 cells Wellendorph et al., (2005) and later supported by the by Pi et al., (2005) and Jacobsen et al., (2013). Using mGPRC6A-transfected HEK-293 cells and pathway selective inhibitors, the Quarles group observed that downstream serum-response element and ERK are activated by divalent cations ($G\alpha_q$ and $G\alpha_i$ pathways) (Pi et al., 2005; Pi, Zhang, et al., 2010; Pi & Quarles, 2012b), L-Arg (pathway not

investigated) (Pi et al., 2011), the steroid testosterone ($G\alpha_i$ pathway, $G\alpha_q$ not investigated) (Pi, Parrill, et al., 2010), and the peptide osteocalcin ($G\alpha_q$ pathway, $G\alpha_i$ not investigated) (Pi et al., 2011). In addition, this group has shown that all four agonist classes lead to cAMP accumulation in the mGPCR6A-HEK293 cell line and thus is likely also to be $G\alpha_s$ coupled (Dreaden et al., 2012; Pi et al., 2012). Finally, the Karsenty group has shown that osteocalcin leads to a bell-shaped, concentration-dependent increase in cAMP, indicating $G\alpha_s$ coupling, but no osteocalcin-mediated activation of the $G\alpha_q$ or ERK pathways in Leydig cells. These osteocalcin responses, however, were not shown specifically to be mediated by GPCR6A (Oury et al., 2011). Thus, conflicting findings regarding GPCR6A signalling have been reported, and physiologic relevant and signalling remain discrepant.

Table 3.1 Intracellular Signalling Pathways GPCR6A is reported to activate.

| GPCR6A Signalling Pathway | Ligand(s) | Species | References | Notes |
|---------------------------|--|--------------------------------------|---|--|
| $G\alpha_s$ | L-amino acids, Ocn, DJ-V-159, divalent cations | mGPCR6A | (Pi et al. 2012); (Pi, et al. 2016); (Pi, et al. 2018); (Oury, et al. 2014); (Pi, et al. 2005) | Oury, et al. 2014 could not show $G\alpha_q$ activation by Ocn |
| $G\alpha_q$ | L-amino acids, Ocn, divalent cations, | human/5.43 chimera, rGPCR6A, mGPCR6A | (Kuang, et al. 2005)(Wellendorph et al. 2005)(Wellendorph, et al. 2007)(Christiansen, et al. 2007)(Faure, et al. 2009)(Rueda, et al. 2016)(Jacobsen, et al. 2013) | Christiansen, et al. 2007 could not show $G\alpha_s$ nor $G\alpha_i$ activation. Rueda, et al. 2016 could not show ERK1/2, $G\alpha_s$ nor $G\alpha_i$ activation. Jacobsen, et al. 2013 could not show $G\alpha_s$ nor $G\alpha_i$ activation |
| $G\alpha_i$ | Ocn, divalent cations | mGPCR6A | (Pi, et al. 2005) | |
| ERK1/2 | L-amino acids, Ocn, DJ-V-159, Testosterone, divalent cations | mGPCR6A | (Pi et al. 2012)(Pi, et al. 2016) (Pi, et al. 2018)(Pi, et al. 2018)(Pi, et al. 2005)(Pi, et al. 2011)(Pi, et al. 2010)(Pi, et al. 2015) | |

3.1.3 GPCR6A & PLC/DAG/IP₂ Pathway Activation.

The cascade mechanisms for the PLC/DAG/IP₃ signalling pathway have been previously mentioned in chapter 1, section 1.2.1. Here we will focus on the literature published discerning GPCR6A's intracellularly signalling pathways. Preliminary studies of GPCR6A signalling came from Kuang *et al.* (2005), reporting a fish odorant-mouse chimeric receptor generated increases in intracellular calcium release and IP turnover when

stimulated with lysine. These data were later supported by Wellendorph *et al.* (2005) demonstrating the intracellular calcium responses mediated by the fish odorant-human chimeric receptor were ablated when pre-treated with the inhibitor BAPTA-AM. Moreover, the CaSR agonists, strontium, gadolinium, and magnesium were able to activate ERK downstream of the $G\alpha_q$ pathway through GPRC6A (Pi, *et al.* 2005). Subsequent studies, confirmed $G\alpha_q$ responses through the use of PLC and IP_3 receptor inhibitors (U-73122 and 2-aminoethoxydiphenyl borate (2-APB), respectively). Here, researchers found intracellular calcium responses were significantly suppressed when induced by L-Orn. Furthermore, co-treatment with the calcimimetic Calindol and calcilytic NPS-2143 ablated L-Orn calcium responses (Faure *et al.*, 2009). These results support the notion that the binding of extracellular L-Orn to GPRC6A increases intracellular calcium release via an $G\alpha_q$ /PLC/DAG/ IP_3 -mediated pathway (Christiansen *et al.*, 2007; Jacobsen *et al.*, 2013; Oya *et al.*, 2013b; Petrine Wellendorph *et al.*, 2007)

3.1.4 GPRC6A & $G\alpha_s$ /AC/cAMP Signalling Pathway.

In addition to the $G\alpha_q$ signalling cascade, GPCRs have been well-established to trigger AC activation and cAMP accumulation through activation of the $G\alpha_s$ signalling pathway (see chapter 1, section 1.2.2). Research into GPRC6A's proclivity to activate $G\alpha_s$ signalling has been more fraught with controversy with different groups generating discordant, unsupportive data (Jacobsen *et al.*, 2013; Pi *et al.*, 2012; Rueda *et al.*, 2016). Using the downstream serum-response element research by the Quarles group found L-Arg, osteocalcin, and Zn^{2+} resulted in significant increases in cAMP accumulation and ERK activation in HEK-293 cells expressing GPRC6A, but not in WT HEK-293 cells that do not endogenously express the receptor (Pi, *et al.* 2011; 2012). In addition, this group have reported the steroid testosterone and the peptide Ocn to stimulate $G\alpha_s$ signalling in GPRC6A-HEK-293 cells (Dreaden, 2012; Pi 2010; 2012). This was further supported by Oury, *et al.* (2013) reporting Ocn consistently stimulated cAMP production in GPRC6A expressing TM3 Leydig cells.

However, Jacobsen *et al.* (2013) were unable to confirm previously published data demonstrating $G\alpha_i$ - and $G\alpha_s$ -mediated signalling. Reporting L-Orn, Ca^{2+} , testosterone or Ocn did not induce cAMP production in mGPRC6A expressing CHO cell line. These findings were later echoed by Rueda *et al.* (2016), reporting no detectable modulation of cAMP accumulation or phosphorylation of ERK1/2 with L-Orn, or Ocn variant suggesting that the mouse receptor is primarily a $G\alpha_q$ -coupled receptor. Additionally, these same studies unable to confirm the reported $G\alpha_i$ -coupling of this receptor, demonstrating no $G\alpha_i$ -modulation was observed when stimulated with the aforementioned ligands.

One major limitation when testing the mGPRC6A receptor is the presence of L-amino acids and divalent cations in cell culture media; this may be responsible for activation and subsequent desensitisation of receptor; hence making it difficult to obtain robust responses of the recombinantly expressed receptor in mammalian cells. Furthermore, it is important to note that the vast majority of our pharmacological understanding of this receptor is based upon research conducted on the murine variant of the receptor. As previously mentioned in section 1.7, there is an emerging wealth of evidence that show the importance of tissue-type specific cofactor that are crucial to GPCR functionality (McLatchie, *et al.* 1998). Based on the disparity in data and different profiles between cell and receptor types, it could be hypothesised that GPRC6A and its interacting partners could be responsible for the activating several signalling cascades.

3.1.5 Role of RAMPs in GPCR Signalling.

RAMPs have been well reported to play a pivotal role in facilitating functional signalling of GPCRs. In addition to trafficking, the role of RAMPs in GPCR signalling has now become well documented over the last few decades; whereby RAMPs constitute an integral role in receptor functionality and/or intracellular signalling modulation (Christopoulos *et al.*, 2003; Gibbons *et al.*, 2007; Harikumar *et al.*, 2010; Hay & Pioszak, 2016; Wootten *et al.*, 2013; Zhongming Zhang *et al.*, 2011).

3.1.5.1 Class C GPCRs & RAMPs.

However, whether GPCR–RAMP interactions are a common and global feature in the human GPCR gene family is an open question and one with direct therapeutic implications (Namkung *et al.*, 2016; Prasad *et al.*, 2010; Xie *et al.*, 2012). The CaSR belongs to the class C GPCRs possessing significant homology with the human GPRC6A receptor (~34%) and its research has aided in preliminary studies of GPR6CA. The CaSR plays a predominant role in regulating systemic Ca²⁺ homeostasis through its sensing of small changes in extracellular Ca²⁺ and modulating calciotropic hormones (Neumann *et al.*, 2014). Barbash *et al.*, (2017) research sought to overview the molecular determinants controlling CaSR; reporting that in COS-7 cells CaSR fails to be effectively expressed at the cell surface due to negligible levels of native RAMP1 and RAMP3. However, HEK-293 have been characterised to express sufficient levels of RAMP1 saw successful forward trafficking of CaSR to the membrane. In addition, co-expression of RAMP1 or RAMP3 found restorative action on CaSR trafficking in COS-7 cells extended the concept of RAMP escorting intermediates of class C GPCRs (Bouschet *et al.*, 2012; A. J. Desai *et al.*, 2014). Research by Bouschet *et al.*, (2012) and Desai *et al.*, (2014) reported immunoglobulin inactivation of RAMP1 resulted in a dose dependent decline in CaSR-mediated signalling in response to Cinacalcet in Thyroid carcinoma TT cells, suggesting a novel functional role for RAMP1 in regulation of CaSR signalling in addition to its known role in receptor trafficking. The collective research suggests that RAMP1 is necessary for CaSR cell surface trafficking and, in conjunction with its homology to GPRC6A a comparative system can be hypothesised.

3.1.5.2 GPRC6A & RAMP1.

As previously described in section 2.1; a multitude of studies have shown the murine receptor to exhibit successful cell surface expression, whilst the human form fails to traffic to the surface, remaining intracellularly retained (Jacobsen *et al.*, 2017; S. Jørgensen *et al.*, 2017; Kuang *et al.*, 2005; Rueda *et al.*, 2016; Petrine Wellendorph & Bräuner-Osborne, 2004). The data provided from other GPCRs is evidence of the receptor-RAMP concept as transferrable across the families of GPCRs. Knowledge of RAMPs chaperone capabilities

and the mechanistic profiles of homologous GPCRs; the concept of a GPRC6A/RAMP heteromer may bridge the gap between discrepancies within the research field. As previously mentioned in chapter 2 we have already demonstrated hGPRC6A can interact with RAMP1, positively modulating the receptors forward trafficking. However, with the knowledge of RAMPs influence of GPCRs signalling capabilities, our subsequent experiments sought to elucidate whether the interaction influences downstream intracellular signalling capabilities.

3.1.6 GPRC6A Ligand Controversies.

As previously mentioned in section 2.1, preliminary pharmacological investigation of the GPRC6A receptor was conducted using a chimeric goldfish receptor, with studies reporting GPRC6A as a promiscuous L-type amino acids receptor (Kuang et al., 2005; Wellendorph et al., 2005). With subsequent studies primarily focussed towards the murine variant of the GPRC6A receptor (Jacobsen et al., 2013; Rueda et al., 2016). However, as the research has progressed discrepancies have begun to emerge from different *in vitro* and *in vivo* models. Although it is somewhat agreed upon that the GPRC6A is able to sense L-amino acids; some groups have also cited divalent cation Ca^{2+} and Mg^{2+} to enhance responses on mGPRC6A (Christiansen et al., 2007; Jacobsen et al., 2013). Furthermore, data collected from *in vivo* studies brought forth new ideas about GPRC6A's sensitivity to testosterone and Ocn, with certain groups firmly reporting testosterone and Ocn response whilst follow up studies failed to reproduce any activation (Pi, et al. 2005; 2011; 2016; Oury, et al. 2011; Mera, et al. 2016; Jacobsen et al., 2013; Rueda et al., 2016 Karsenty and Olson, 2017). GPRC6A affinity for physiologically important ligands has made it an intriguing target for therapeutic intervention. However, due to the promiscuous array of suggested agonist and the lack of supportive pharmacological data it has made clarification of the receptors physiological role increasingly complicated. Drawing on the evidence reporting the importance of RAMPs in certain GPCRs functionality, we hypothesised that RAMPs is a fundamental component in functional hGPRC6A signalling, explaining the discrepancies seen in the literature and offering a novel mechanism by which hGPRC6A initiates several signalling pathways.

3.1.7 *Research Aims.*

1. Provide supportive evidence of GPRC6A $G\alpha_q$ -activation via L-amino acids.
2. Investigate GPRC6A disputed sensitivity to hormones testosterone and osteocalcin.
3. Investigate GPRC6A activation of $G\alpha_s$ and $G\alpha_i$ pathway via L-amino acids and hormone ligands.

3.1.8 *Research Hypothesis.*

RAMP1 positively increases the level of intracellular G-protein signalling mediated by the hGPRC6A receptor.

3.2 Materials and Methods.

3.2.1 Intracellular $G\alpha_q$ /PLC/IP₃ Signalling.

3.2.1.1 Calcium 6 FLIPR Kit Assay protocol.

Intracellular calcium signalling was measured using the Calcium 6 FLIPR kit Assay (Molecular Devices); cells were grown in culture reagents and assayed in Loading buffer (1x HBSS buffer, 20mM HEPES, 10mM CaCl₂, and pH adjusted to 7.4) on 96 well black, clear bottom plates (Corning, USA).

The method was developed utilising CHO-K1 cells stably transfected with constructs 1b & 2b previously described in section 2.2.3 (Figure 2.4 & Figure 2.5). Cells were seeded at 10,000 cells/well in standard growth media, 48 h prior in 96-well black, clear-bottom plates (Corning, USA) at 37°C to give 80% confluency at time of assay. Media was replaced with 1% FBS media 24 h prior to stimulation. After thawing and equilibrating the Calcium 6 assay reagent to RT, it was dissolved (1:10 ratio) in 10 mL of loading buffer (1x HBSS buffer, 20 mM HEPES, 10 mM CaCl₂, and pH adjusted to 7.4). Mix by vortexing (~1-2 min) until contents of vial are completely dissolved. Probenecid was added to loading dye to give final in-well concentration of 2.5 mM. 100 µL of Calcium 6 loading dye was then added to all wells and incubated for 2 hours at 37°C, 5% CO₂. All compounds were diluted in 1X loading buffer to be 1X in-well concentration. Following incubation, plate was then transferred directly to the Flexstation3 assay plate carriage (Molecular Devices, California, US) and was allowed to equilibrate at 37°C for 10 minutes. Traces were collected for 300 seconds, including a 50 second baseline read prior to compound well addition (

Table **3.2**). Cell fluorescence (excitation at 485 nm; emission at 525 nm) was monitored following exposure to the compound. Protein tags Cit (Ex 516nm and Em 529nm) and Cer (Ex 433nm and Em 475nm) were outside excited by the calcium 6 dye and thus deemed to have minimal interference.

All intra-experimental traces were obtained in duplicate. Increases in intracellular calcium are reported as the maximum fluorescence value after exposure minus the basal fluorescence value before exposure.

Table 3.2 Flexstation 3 plate reader parameters; plate reader settings used to measure Calcium 6 FLIPR Kit assay.

| Fluorescence Parameters | 96-well plate |
|---|---------------|
| <i>Excitation Wavelength (nm)</i> | 485 |
| <i>Emission Wavelength (nm)</i> | 525 |
| <i>Automatic Emission Cut-Off (nm)</i> | 515 |
| <i>PMT Sensitivity</i> | 6 |
| <i>Pipette Height (μL)</i> | 230 |
| <i>Transfer Volume (μL)</i> | 50 |
| <i>Compound Concentration (Fold)</i> | 5X |
| <i>Addition Speed (Rate) Adherent Cells</i> | 3 |

3.2.1.2 UBO-QIC Treatment.

Cells were grown overnight in 100 μL of media in 96-well black plates at 37°C in 5% CO_2 . Cells were pretreated with 10 μM of UBO-QIC before the addition of agonists (Kukkonen, 2015). The calcium assay kit was used as described in the above section. 100 μL of the calcium 6 dye/probenecid mix was added to the plate was incubated with at 37°C for 120 minutes. The compound plate was prepared using dilutions of various compounds in Hank's Buffer (pH 7.4). Samples were run in duplicate using the Flexstation 3 as previously described above.

3.2.1.3 NPS-2143 Antagonism.

Cells were grown overnight in 100 μL of media in 96-well black plates at 37°C in 5% CO_2 . The calcium assay kit was used as described in the above section. Cells were incubated with 100 μL calcium 6 dye/probenecid at 37°C for 120 min. Cell were then pretreated with 25 μL of concentration range of NPS-2143 for 15 minutes prior to agonist addition. The compound plate was prepared using IC_{80} of varying agonists in Hank's Buffer (pH 7.4). Samples were run in duplicate using the Flexstation 3 as previously described.

3.2.2 Intracellular $G\alpha_s$ /AC/cAMP/PKA Signalling.

3.2.2.1 Cyclic AMP Accumulation assay.

To measure the extent of GPRC6A-induced $G\alpha_s$ activation, research adopted the LANCE cAMP Detection kit (Perkin Elmer) offering a time-resolved fluorescence energy transfer immunoassay capturing cAMP production upon modulation of the AC activity. The assay is based on the competition between sample cAMP and a Europium (Eu)-labelled cAMP tracer complex for binding sites on cAMP-specific antibodies conjugated to AlexaFluor-647. The Eu-labelled cAMP tracer complex comprises firmly bound biotin-cAMP and Eu-streptavidin. When the antibodies are bound to the Eu-streptavidin/biotin-cAMP tracer, excitation at 340 nm excites the Eu and the resultant energy is transferred to the AlexaFluor-labelled antibody. This concept is similar to the FRET principles discussed in section 2.1.2.4. The emitted fluorescence measured at 665 nm will decrease in the presence of sample cAMP, and resulting signals will be inversely proportional to the cAMP concentration of a sample (Figure 3.2).

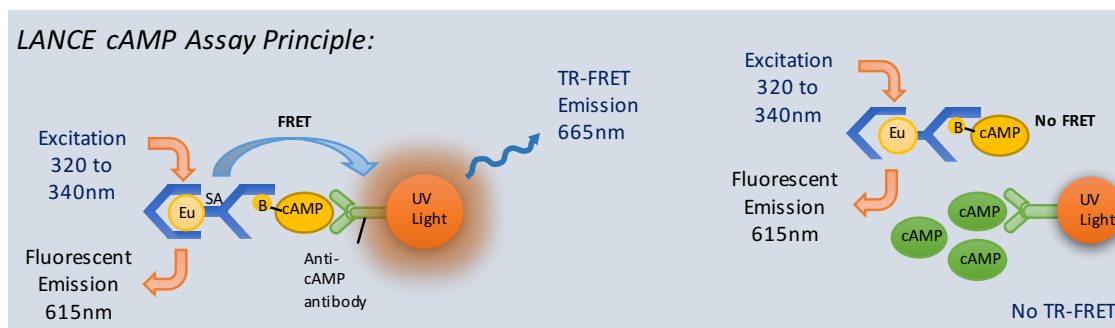


Figure 3.2 LANCE cAMP Assay Principle; Light pulse at 340 nm excites the Europium-chelate of the Eu-SA/bcAMP tracer. The energy emitted from the Eu-chelate is transferred to the Alexa Fluor® 647 labeled anti-cAMP antibodies bound to the tracer, generating a TR-FRET signal at 665 nm. Residual energy from the Eu-chelate will produce light at 615 nm. cAMP of a sample competes with the tracer for antibody binding sites and causes signal reduction.

CHO-K1 cells were seeded into 96-well plates to give 80% confluence after 24 hours (Figure Ap.4). Growth media was removed and replaced with stimulation buffer (HBSS 1X containing 1 mM $CaCl_2$, phenol red, 0.5 mM HEPES, 0.1% BSA, 0.5 mM 3-isobutyl-1-methylxanthine) and incubated at 37°C for 30 min before ligand stimulation to allow baseline equilibration in reduced serum. All ligands were diluted in stimulation buffer to twice the in-well concentration and added directly to the plate. Cells were incubated for

30 minutes at 37°C, and plates were placed on ice immediately thereafter to prevent further stimulation. Medium was quickly removed from all wells and cells were immediately lysed with 50 µL of ice-cold detection buffer (provided in the LANCE cAMP assay kit). Once the detection buffer was applied, cells were gently agitated for 15–30 minutes at 4°C to ensure full cell lysis.

G α_s activation was measured by cAMP accumulation using the LANCE cAMP assay kit (Perkin Elmer, Massachusetts, US). The proportion of sample to antibody was based on the suggested preparation of the standard curve. Thus, 6 µL of lysate sample was transferred to a white 384-well plate (Perkin Elmer, Massachusetts, US). Anti-cAMP antibody was diluted 1:100 in detection buffer was then added immediately to each well (6 µL of diluted anti-cAMP antibody/well). The lysate samples and antibody were mixed in the plate and incubated, protected from light, for 30 minutes prior to the addition of the detection mix with gentle agitation. The detection mix (europium-streptavidin and biotin-cAMP) was prepared as per LANCE kit instructions. First, intermediate dilutions of europium-streptavidin at 1:18, and biotin-cAMP at 1:6; then each intermediate dilution is further diluted 1:125 in detection buffer to give the detection mix); complexes were allowed to form for at least at room temperature 15 minutes. Following this, 12 µL of the detection mix was added per well. The plate was then left at room temperature for a further 60 minutes, before detection. Plates were read using the Enight TR-FRET-capable plate reader (Perkin Elmer, Massachusetts, US), with excitation at 340 nm and emissions at 615 nm and 665 nm.

3.2.2.2 *Pertussis Treatment.*

For investigation of G α_i modulation cells were pretreated 24 hours prior to assaying with growth media supplemented with 200 ng/µL (PTX) (Sigma-Aldrich, USA) (Weston *et al.* 2016). Following an overnight incubation, cells were stimulated with serial concentrations of agonists and the degree of G α_i activation was measured using the LANCE cAMP kit as previously described above.

3.2.3 Data & Statistical Analysis.

Concentration-response data were analysed using a three-parameter logistic function (Motulsky & Christopoulos, 2004) to generate estimates of agonist potency (LogEC_{50}). For intracellular calcium mobilisation, agonist responses were normalised to the peak response to 10 μM ATP as a positive activator of calcium response maximal response (Figure 3.3). For cAMP responses, data was normalised to 0.1 mM Forskolin (FSK) as a maximal response (Figure Ap.4). Data for all CHO-K1 assays represents the $\text{pEC}_{50} \pm \text{SEM}$ of three to ten independent experiments. Statistical analyses were performed using GraphPad Prism version 7.0 (GraphPad Software, San Diego, California, USA).

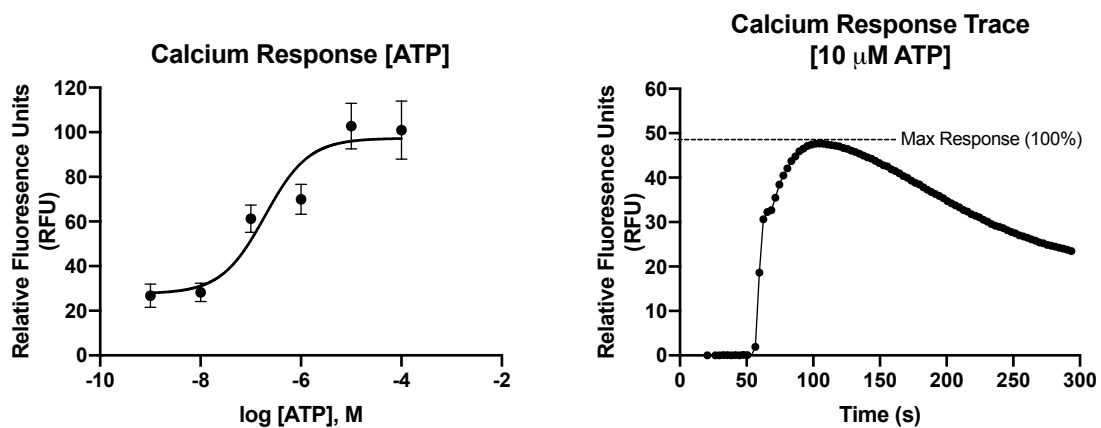


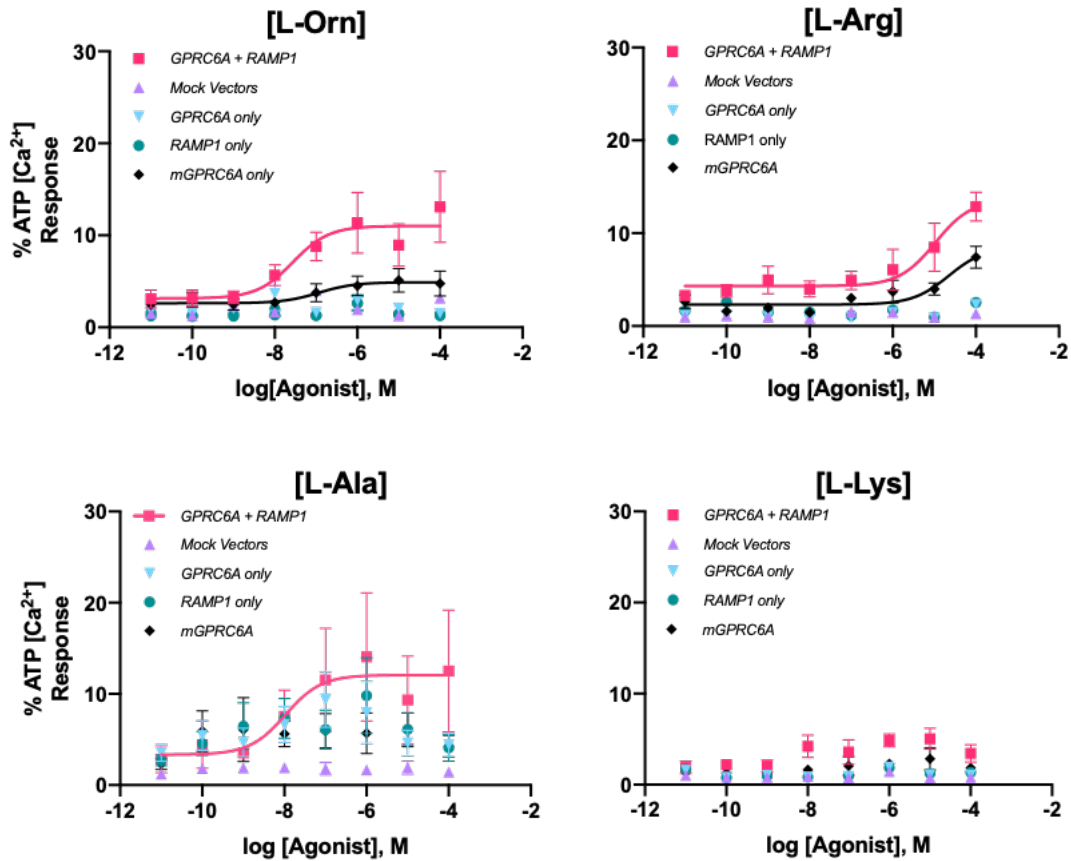
Figure 3.3 ATP Dose Response & Example ATP Traces of Intracellular Calcium Release; agonist responses were normalised to the peak response to 10 μM ATP.

3.3 Results.

3.3.1 *RAMP1 Influence on hGPCR6A-mediated Calcium Mobilisation.*

3.3.1.1 *L-amino acids.*

Since previous signalling studies suggest that GPCR6A preferentially couples to the $G\alpha_q$ pathway, we first assessed CHO-hGPCR6A cells in assays of calcium mobilisation. Negligible responses were observed from CHO-K1 cells expressing hGPCR6A *only*; however, when co-expressed with RAMP1 we observed dose-dependent responses to L-Orn [pEC_{50} 7.66 ± 0.53], L-Ala [pEC_{50} 7.34 ± 0.70] and L-Arg [pEC_{50} 4.98 ± 0.38]. No intracellular calcium responses were recorded when stimulated with L-Lys (Figure 3.4). Additionally, experiments were conducted against the mGPCR6A revealing small responses to L-Orn and L-Arg but not L-Ala or L-Lys.



| Agonist | pEC ₅₀ | SEM (±) |
|---------------------|-------------------|---------|
| <i>L</i> -Ornithine | 7.66 | 0.53 |
| <i>L</i> -Arginine | 4.98 | 0.38 |
| <i>L</i> -Lysine | - | - |
| <i>L</i> -Alanine | 7.34 | 0.70 |

Figure 3.4 Intracellular Calcium mobilisation induced by L-amino acids; Comparison of different transfection groups found only co-expression of the hGPRC6A with RAMP1 produced robust concentration-dependent increases in intracellular calcium release when stimulated with L-amino acids; L-Orn, L-Arg, L-Ala. Negligible responses were observed in GPRC6A *only* and RAMP1 *only* transfection groups. Responses displayed are expressed as a percentage of ATP-induced calcium release. Responses were observed with mGPRC6A *only* comparable to published literature. Data are from 3 independent experiments, grouped and are presented as mean ± SEM.

3.3.1.2 *Osteocalcin*.

To further address the pharmacological controversies of this receptor, we concomitantly sought to evaluate GPRC6A sensitivity to more pharmacologically intriguing ligands. Ocn is peptide hormone known to play key role in bone remodelling, existing in two forms dependant on the degree of carboxylation which is reported to be determinant for its signalling capabilities (Benton, ME *et al.* 1995). Here we found small responses uncarboxylated-Ocn variants [pEC₅₀ 7.20 ± 0.39] in the presence of both GPRC6A and RAMP1 (Figure 3.5) exhibiting similar partial agonism as L-amino acids. No responses were recorded to the carboxylated variant. Further experiments aimed to investigate whether Ocn indirectly activate hGPRC6A function; however, Ocn variants (IC₅₀ 0.40 μM) failed to elicit a response the potency or maximal response to L-Orn in assays of calcium mobilisation (*data not shown*).

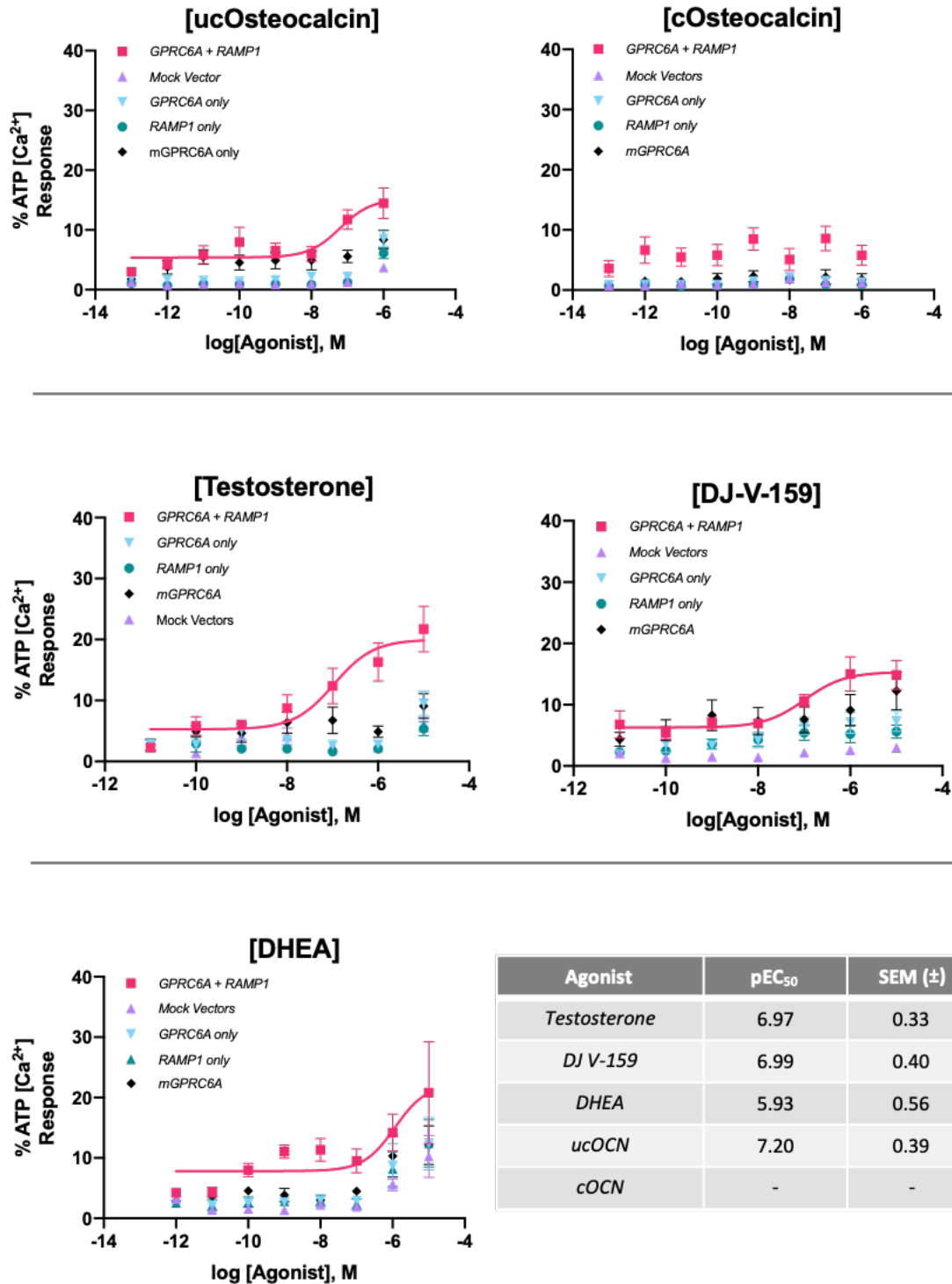
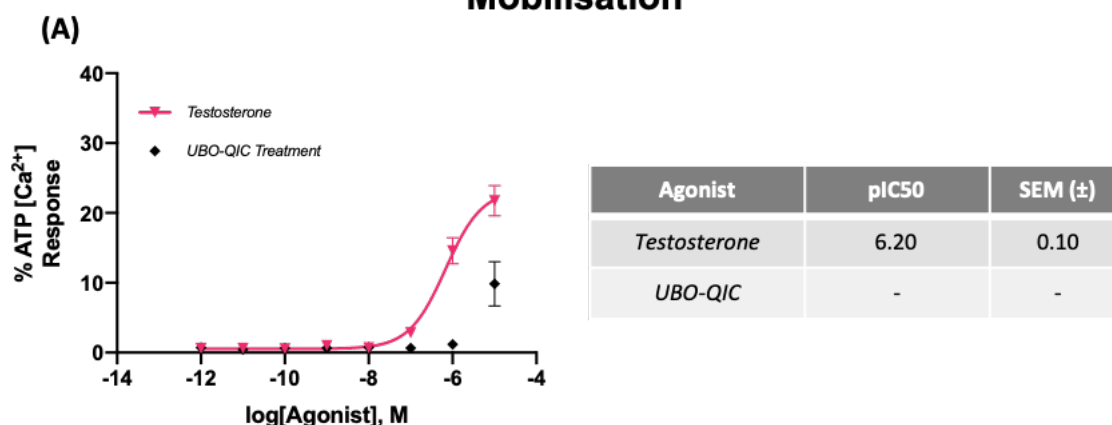


Figure 3.5 Calcium mobilisation induced by bone/hormone ligands on GPRC6A+RAMP1 expressing CHO-K1 cells; Dose-dependent responses were seen when stimulated with testosterone with the largest maximal responses observed at high doses of testosterone. Concentration dependent responses were also observed upon DHEA stimulation and the GPRC6A agonist DJ-V-159. Stimulation with osteocalcin variants produced partial or negligible responses in calcium mobilisation. Negligible responses were observed in mock vector, GPRC6A *only* and RAMP1 *only* transfection groups. Responses displayed are expressed as a percentage of ATP-induced calcium release. No responses were observed with mGPRC6A *only* comparable to published literature. Data are from 3 to 6 independent experiments, grouped and are presented as mean ± SEM.

3.3.1.3 Testosterone.

Subsequent studies aimed to elucidate hGPCR6A sensitivity to testosterone and related ligands. In calcium mobilisation assays we observed specific dose-dependent responses to testosterone when hGPCR6A is co-expressed with RAMP1 [pEC₅₀ 6.97 ± 0.33] with no responses seen in the mouse receptor, hGPCR6A *only*, RAMP1 *only* or mock vector control groups (Figure 3.5). No responses were observed with Testosterone metabolites; 5-DHT, 5-Androstenediol, or 4-Androstenedione (Figure Ap.5). Interestingly, DHEA a testosterone precursors elicited robust responses [pEC₅₀ 5.93 ± 0.56] in hGPCR6A when co-expressed with RAMP1 and smaller response with hGPCR6A *only* [pEC₅₀ 5.50 ± 0.31] and RAMP1 *only* [pEC₅₀ 5.06 ± 0.23] (Figure 3.5). Furthermore, we confirmed responses to the Quarles group (Pi, *et al.* 2018) GPCR6A synthesised tri-phenol agonist, DJ-V-159 [pEC₅₀ 6.99 ± 0.40]; with follow up experiments confirming hGPCR6A Gα_q-coupling through UBO-QIC treatment experiments (Figure 3.5 & Figure 3.6). Additionally, calcium mobilisation in response to a submaximal EC₈₀ dosing of testosterone was sensitive to application of the GPCR6A antagonist, NPS-2143 [pIC₅₀ 11.4 ± 0.60] this was similarly observed when stimulating with the GPCR6A agonist, DJ-V-150 [pIC₅₀ 11.3 ± 0.51] (Figure 3.6). The findings here, provide evidence that testosterone provokes intracellular calcium release partially via the hGPCR6A receptor in our CHO-K1 cells.

UBO-QIC treatment on Calcium Mobilisation



NPS-2143 treatment on Calcium Mobilisation

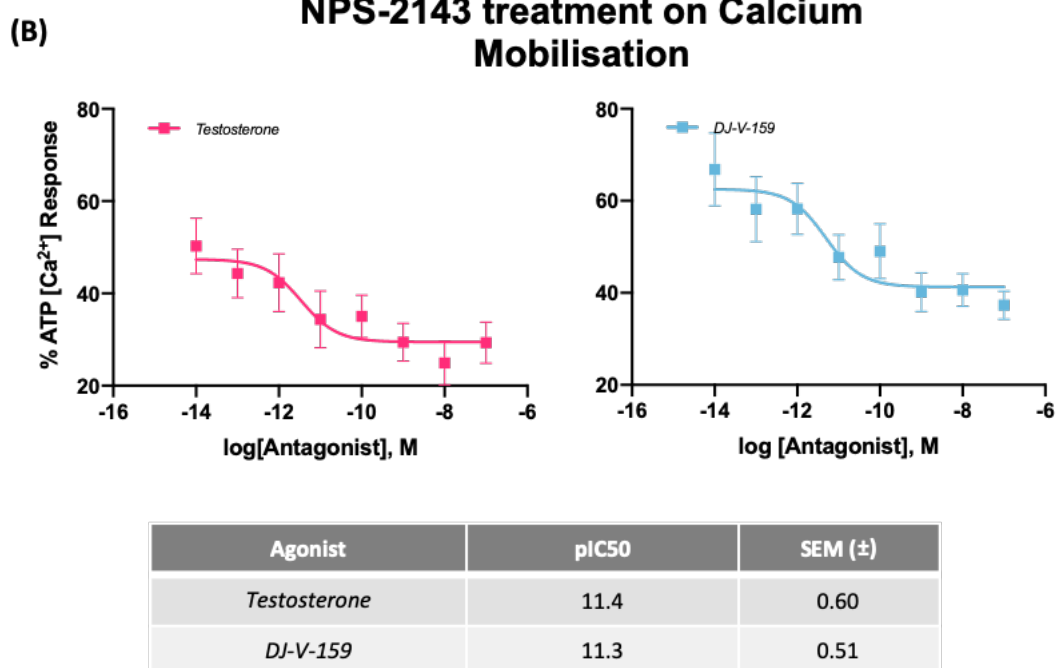


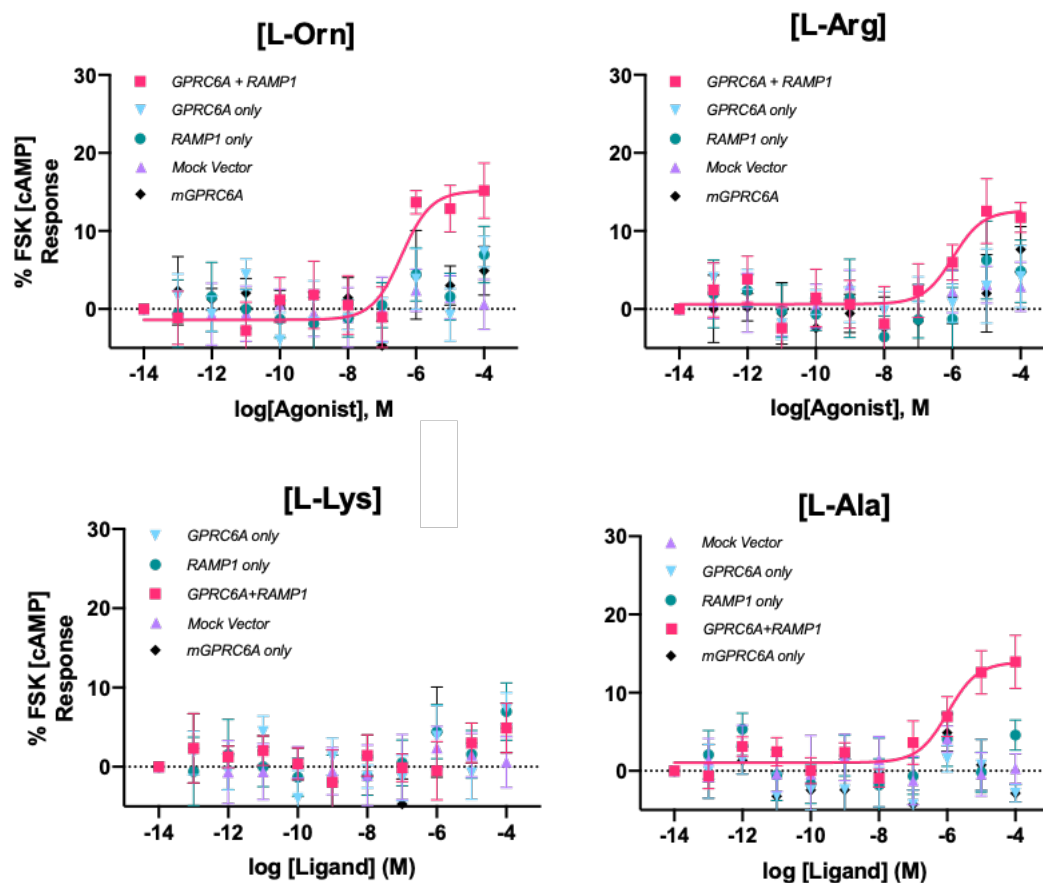
Figure 3.6; (A) Calcium mobilisation following UBO-QIC G_q inhibitor; GPRC6A/RAMP1 calcium mobilisation responses to testosterone are significantly attenuated following pretreatment with 10 μ M UBO-QIC $G\alpha_q$ inhibitor. Data are from 2 independent experiments and are presented as mean \pm SEM. (B) Treatment of NPS-2143 dose response; Stimulation of GPRC6A with EC_{80} doses of testosterone and DJ-V-159 following treatment with dose response of GPRC6A antagonist NPS-2143. Data are from 3-4 independent experiments, grouped and are presented as mean \pm SEM.

3.3.2 RAMP1 Influence on hGPRC6A-mediated cAMP Accumulation.

3.3.2.1 L-amino acids.

Published data has also reported GPRC6A to couple to the $G\alpha_s$ /cAMP/AC (Rueda *et al.* 2016; Oury *et al.* 2014; Pi, *et al.* 2012; 2011). Accordingly, experiments also endeavoured

to investigate hGPCR6A/RAMP1 involvement by quantifying cAMP accumulation assays. Preliminary experiments stimulated with putative L-amino acids showed small partial responses to L-Orn [pEC₅₀ 6.42 ± 0.40], L-Ala, [pEC₅₀ 5.77 ± 0.60] and L-Arg [pEC₅₀ 5.68 ± 0.30] (Figure 3.7) only when hGPCR6A was co-expressed with RAMP1. Negligible responses were observed in all control groups. No responses were recorded when stimulating with L-Lys.

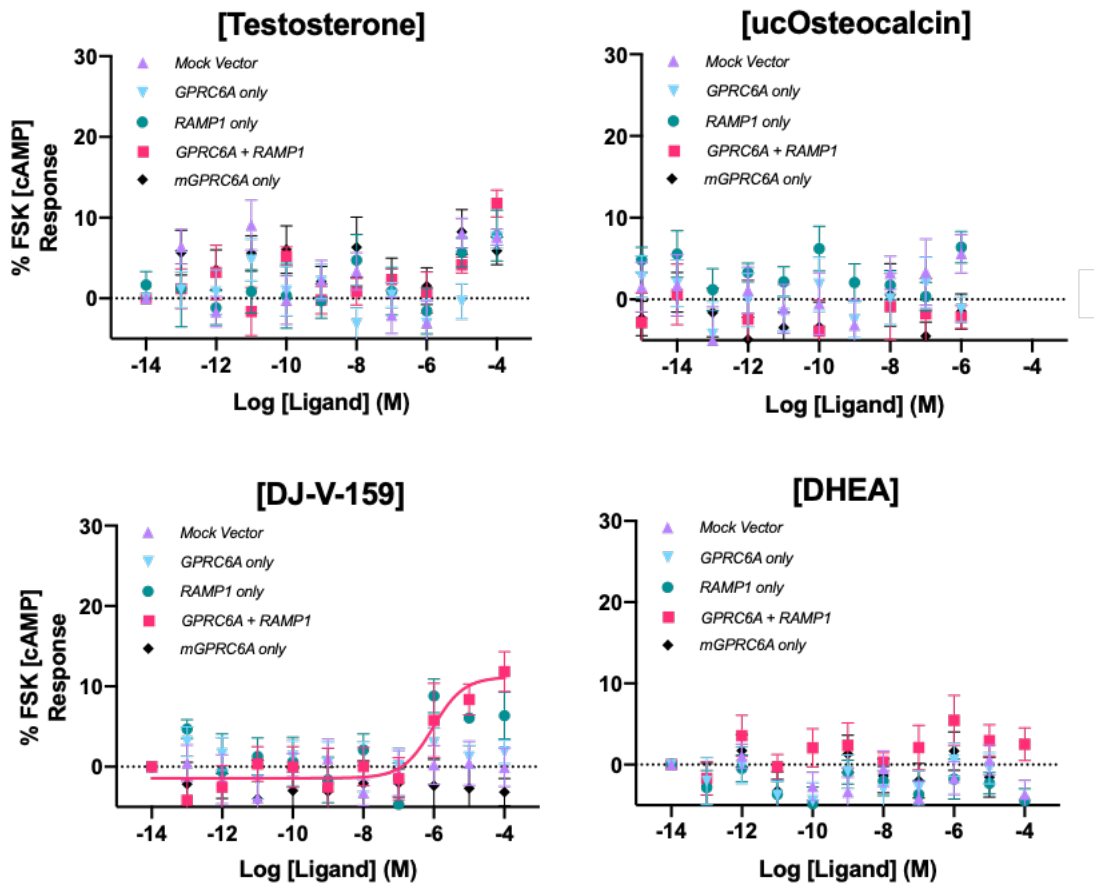


| Agonist | pEC ₅₀ | SEM (±) |
|-------------|-------------------|---------|
| L-Ornithine | 6.42 | 0.40 |
| L-Arginine | 5.68 | 0.60 |
| L-Alanine | 5.77 | 0.30 |
| L-Lysine | - | - |

Figure 3.7 Intracellular cAMP accumulation induced by L-amino acids; Comparison of different transfection groups found only co-expression of the hGPCR6A with RAMP1 produced robust concentration-dependent increases in intracellular cAMP accumulation when stimulated with L-amino acids; L-Orn, L-Arg, and L-Ala. Responses are similar to calcium release data however, degree of activation is seen of small magnitude. Negligible responses were observed in GPCR6A *only* and RAMP1 *only* transfection groups. Responses displayed are expressed as a percentage of FSK-induced cAMP accumulation. Data are from 3 independent experiments, grouped and are presented as mean ± SEM.

3.3.2.2 Bone & Hormone Ligands.

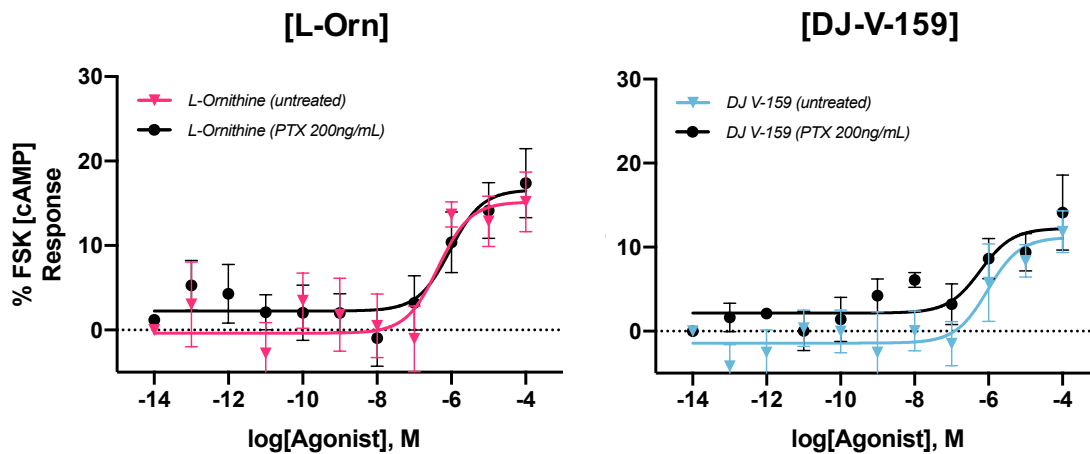
Experiments with ligands; testosterone, ucOcn, DHEA found negligible/none responses in cAMP accumulation (Figure 3.8). No responses were observed with testosterone metabolites; 5-DHT, 5-Androstenediol, or 4-Androstenedione (Figure Ap.5). Interestingly, DJ-V-159 compound provoked a small but robust response in cAMP accumulation [pEC_{50} 6.02 ± 0.43]; this was only observed in GPRC6A/RAMP1 co-expressing CHO-K1 cells.



| Agonist | pEC_{50} (μ M) | SEM (\pm) |
|--------------|-----------------------|---------------|
| DJ V-159 | 6.02 | 0.43 |
| Testosterone | - | - |
| DHEA | - | - |
| Osteocalcin | - | - |

Figure 3.8 Intracellular cAMP Accumulation induced by bone/hormone ligands; Negligible responses were observed in all CHO-K1 overexpressing cells when stimulating with testosterone, ucOcn and DHEA. Small dose-dependent response was observed when stimulated with DJ-V-159 [pEC_{50} 6.02 ± 0.43]. Data are from 3 independent experiments, grouped and are presented as mean \pm SEM.

From the previous finding, subsequent experiments sought to look at $G\alpha_i$ modulation mediated through the hGPCR6A. Two disparate ligands were selected, hGPCR6A L-Orn and DJ-V-159 cAMP accumulation responses showed no $G\alpha_i$ modulation when pre-treated with $G\alpha_i$ inhibitor, PTX toxin (200 ng/ μ L) (Figure 3.9).



| Agonist | pEC50 | SEM (\pm) |
|-----------------------------|-------|---------------|
| <i>L-Orn (untreated)</i> | 6.35 | 0.47 |
| <i>L-Orn (treated)</i> | 6.03 | 0.41 |
| <i>DJ-V-159 (untreated)</i> | 6.37 | 0.45 |
| <i>DJ V-159 (treated)</i> | 6.22 | 0.44 |

Figure 3.9 Adenylyl cyclase inhibition induced by L-Orn and DJ V-159; cells treatment with 200 ng/mL 24 hours prior to stimulation observed negligible G_i modulation when stimulated with L-Orn or DJ-V-159; with responses observing comparable dose response pIC₅₀ values to the untreated control groups. Data are from 3 independent experiments, grouped and are presented as mean \pm SEM.

3.4 Discussion.

Data from multiple groups concerning the signalling of GPRC6A has been considerably discrepant; thus, identifying physiologically relevant ligands of this receptor has remained elusive. Here we conducted a comprehensive study of the GPRC6A's intracellular G-protein signalling activation *in vitro*. Furthermore, we demonstrated a fundamental role RAMP1 plays in hGPRC6A signalling, expanding the range of diverse agonists it senses and differentiating it from the mouse receptor.

3.4.1 $G\alpha_q$ Signalling & Ca^{2+} Mobilisation.

In studying the downstream cellular signalling of recombinantly co-expressed hGPRC6A and hRAMP1 we have successfully confirmed $G\alpha_q$ coupled responses to basic L-amino acids, with L-Orn, L-Arg, and L-Ala as agonists (Figure 3.4). These findings support previously published data showing both human and murine GPRC6A to be a promiscuous L-amino acid-sensing receptor, without the need of co-expressing the mutated $G\alpha_{q(G66D)}$ protein as a prerequisite to elicit these responses (Kuang *et al.* 2005; Jacobsen *et al.* 2013; Rueda *et al.* 2016). However, L-Orn and L-Ala responses were observed to exhibit much higher potency in comparison to published pEC_{50} values (Christiansen *et al.*, 2007; Jacobsen *et al.*, 2013; Rueda *et al.*, 2016). This may in part be due to the species differences or difference in assay format. Stimulation with L-Arg showed much more comparable pEC_{50} to the aforementioned studies; however, future work may wish to stimulate at higher concentrations of L-amino acid to ensure max calcium mobilisation response is definitively recorded (Figure 3.4). However, responses observed were relatively small compared to ATP responses; this was somewhat expected as other papers using other methodologies have also shown GPRC6A to exhibit small responses to L-amino acids (Jacobsen *et al.*, 2013; Kuang *et al.*, 2005; Pi *et al.*, 2018; Rueda *et al.*, 2016). Furthermore, L-Ala exhibited large SEM values which questions the validity of the responses observed (Figure 3.4). Due to limited lab access and restrictions during the COVID-19 pandemic these data only represents $n=3$; further research would be needed to assess the validity and reproducibility of these results.

Signal traces observed for CHO-K1 cells overexpressing RAMP1 *only* may be the result of non-specific interaction of RAMP1 with endogenous hamster GPRC6A as observed at small levels in PCR analysis (Figure 2.7Figure 2.8).

In recent studies, GPRC6A's ability to sense ligands testosterone and Ocn, sparking intrigue into the receptors involvement in the bone-energy metabolism axis and the crosstalk between bone and the gonad (Pi, *et al.* 2015; 2016; 2018). Our calcium mobilisation studies only observed robust dose-dependent responses to testosterone when hGPRC6A was co-expressed with RAMP1 (Figure 3.5). It is important to note that these responses were only observable with the human GPRC6A, sensitivity to testosterone was not seen in the murine receptor (Figure 3.5). This distinction is pertinent as a large cause of the controversy surround this receptor's pharmacological profile stems from the majority of groups, excluding a few (S. Jørgensen *et al.*, 2017), reporting from inconsistent data concerning the human and mouse variants (reviewed by C. Clemmensen *et al.*, 2014). Moreover, use of the UBO-QIC $G\alpha_q$ inhibitor suggests that testosterone-induced calcium mobilisation is mediated through the $G\alpha_q$ signalling pathway in this system (Figure 3.6A). However, due to limited lab access and restrictions during the COVID-19 pandemic these data is only representative of 2 independent repeats; thus we cannot definitively confirm exclusive $G\alpha_q$ pathway activation. Furthermore, treatment with the GPRC6A antagonist, NPS-2143 partial inhibited these responses in a dose-dependent manner confirming the responses observed are receptor specific (Figure 3.6B). However, our treatments with NPS-2143 on CHO cells stimulated with testosterone and DJ-V-159 observed pIC_{50} values of 11.4 ± 0.60 and 11.3 ± 0.51 , respectively. These values are particular potent, especially in comparison to Faure *et al.*, (2009), reporting pIC_{50} values of 10 μ M. It may be beneficial to test whether NPS-2143 in the absence of testosterone or DJ-V-159 to determine any agonistic effects it may have on GPRC6A. This may explain the high potency exhibited here (Figure 3.6B). Interestingly, we also recorded small level calcium mobilisation when stimulated with uncarboxylated Ocn (Figure 3.5). Due to the magnitude of the responses Ocn cannot necessarily be classified as an agonist, as the calcium mobilisation experiments were conducted in a buffer containing Ca^{2+} and Mg^{2+} which have been previously reported as potential agonists (Pi, *et al.* 2012). It is plausible that the presence of divalent cations is needed to achieve robust GPRC6A

responses, and in that regard, Ocn may instead be classified as co-agonists (Kuang, *et al.* 2005; Pi, *et al.* 2005; Wellendorph, *et al.* 2005; Christiansen, *et al.* 2007; Jacobsen, *et al.* 2013).

Furthermore, investigation into the testosterone precursor DHEA saw robust responses in CHO-K1 cells co-expressing both hGPC6A and RAMP1 (Figure 3.5). DHEA metabolism may increase circulating levels of testosterone, posing a greater risk in prostate cancer patients. However, this stance is contested as current researcher publish disparaging reports unable to definitively confirm or deny the claim (Arnold *et al.*, 2005, 2008; Ciolino *et al.*, 2003; Green *et al.*, 2001). Interestingly, smaller responses were also observed in CHO-K1 cells expressing a hGPC6A *only* and RAMP1 *only*; which could be argued as evidence for RAMP1 coupling with an unknown endogenous DHEA receptor provoking an intracellular calcium release. This is an interesting area of research as a primary receptor for DHEA has long remained elusive. DHEA has been shown to bind class I and II nuclear receptors; AR, oestrogen receptors- α and β , pregnane X receptor/steroid, and xenobiotic receptor (R. M. Evans & Mangelsdorf, 2014; Prough *et al.*, 2016; Traish *et al.*, 2011; Webb *et al.*, 2006). From our findings, the likely explanation is that DHEA's lipophilic qualities enable its free diffusion across the membrane (Le *et al.*, 2012) and signal via one of the numerous endogenous nuclear receptors previously described (Hutchinson *et al.*, 2002). Further biochemical investigation is needed to discern whether hGPC6A is a viable receptor for DHEA.

In addition, the computationally identified compound; DJ-V-159 (Pi *et al.*, 2018) was also found to trigger intracellular calcium mobilisation (Figure 3.5). Again, these responses were only seen when hGPC6A was co-expressed with the RAMP1 protein and not in control groups – including the murine receptor (Figure 3.5). Similarly, to testosterone, NPS-2134 treatment saw dose-dependent inhibition of DJ-V-159-induced intracellular calcium response confirming them as GPC6A-mediated (Figure 3.6).

It is important to note that although certain deviations were observed in potencies and maximal responses when comparing previous reports; S. Jørgensen *et al.*, (2017) was able to show similar L-amino acid potency in both human and mouse GPC6A; however, the

vast majority of published pharmacological data on the GPRC6A receptor has characterised the murine GPRC6A not the human receptor (Clemmensen, *et al.* 2014; Jacobsen *et al.*, 2013; Rueda *et al.*, 2016). Therefore, the data may provide novel insight into the pharmacological differences between species specific receptors. Here our comparative study using the murine GPRC6A has elucidated species marked differences between the human and mouse receptor pharmacology. Recent mutational analysis studies examined ILC3 region of the GPRC6A; here the study reports that replacement of the human ICL-3-KGKKLY motif with the mouse ICL-3-KGKY variant resulted in restoration of successful cell surface trafficking in HEK293 cells (S. Jørgensen *et al.*, 2017). The study provides insight into the intracellular machinery of this receptor; reporting that many accessory proteins interact at the intracellular loops of GPCRs (Sexton *et al.*, 2009); Further supporting the concept that RAMPs may associated at this region of the GPCR in order to form a functional receptor.

3.4.2 FLIPR Calcium 6 Assay Format.

The data generated supports previous research using the Fluo-4 AM dye (*data not shown*); however FLIPR Calcium 6 dye was able to produce much greater signal as the previous Fluo-4 AM assay was only read using the EVOS FL II fluorescence microscope and was unable to be recorded using the Flexstation 3 plate reader. It must be noted that repetitions of the experiment led to small degree of variability between signal trace patterns as demonstrated by the SEM values. This variation may be the result of testing on different passaged populations of CHO-K1 cells expressing hGPRC6A and RAMP1; making resolution of subtle changes in Ca²⁺ mobilisation challenging. The generation of the stable expressing cell line may have combated this issue over transient systems; allowing for stringent antibiotic selection and FACS sorting favouring homogeneous expression and more consistent responses. However, further replicates are required to ensure the validity of these data. Furthermore, it could be argued that in using the receptor and ramps tagged to fluorescent proteins Cit and Cer may interfere with the fluorescence excitation and emission of the calcium dye. However, Protein tags Cit (Ex 516nm and Em 529nm) and Cer (Ex 433nm and Em 475nm) were outside the wavelengths required to excited the calcium 6 dye (Ex 485nm and Em 525nm) and thus deemed to

have minimal interference. Moreover, with the tags being around the similar range, this may have contributed to a dampening of the overall signal and interfered with the signal to noise ratio, evidenced by our low maximal responses (Figure 3.4 & Figure 3.5). To evaluate this extent of fluorophore interference, future work could replicate these experiments using untagged GPRC6A and RAMP and observe identical responses.

In comparison to previous work the FLIPR calcium 6 dye offered greater advantages of the Flou-4, Flou-4-AM, and Fluo-8 dyes (Pi, *et al.* 2010, 2011, 2012; Rueda, *et al.* 2016). The FLIPR Calcium 6 dye offers a much larger signal window; thus working with receptors with low expression profiles can produce lower overall responses. The calcium 6 dye larger signal window offers a robust assay for compound screening and optimised for challenging targets. In addition, the systems masking dye allows for a reduced reliance on anion transporter blockers (i.e. probenecid) which can be harmful to the target cells. Translating the assay to parallel system plate reader (i.e. Flexstation® 3, Molecular Devices Inc., Sunnyvale, California, US); the modified assay allows for high through-put screening of multiple compounds providing expanded biochemical information on dynamic range, pharmacokinetics, and compound potency (Heusinkveld & Westerink, 2011). Certain considerations were made when transferring to the plate reader format, ensuring novel data generated can be comparable and consistent. Although the sensitivity of single cell fluorescence microscopy is evidently superior when compared to the plate reader format; plate readers offer sufficient temporal resolution when measuring Ca²⁺ mobilisation (Heusinkveld & Westerink, 2011). Parallel systems reading multiple wells concurrently, provide real-time measurements whilst minimising delay between measurements of the first and last wells (Heusinkveld & Westerink, 2011).

3.4.3 *Gα_s Signalling & cAMP Accumulation.*

Here we have shown RAMP1 positively modulates GPRC6A ability to signals through Gα_s signalling when stimulated with L-amino acids. The findings display small doses-dependant responses when hGPRC6A is co-expressed with RAMP1. All L-amino acids tested here exhibited similar potencies and maximal cAMP responses. The small magnitude of these supports the idea that recombinant hGPRC6A is primarily a

Gα_q coupled receptor (Figure 3.7). These data are largely concordant with the findings of Jacobsen *et al.* (2013) and Rueda *et al.* (2016), who drew similar conclusions for the mGPRC6A recombinantly expressed in CHO-K1 and HEK293 cells, respectively. We were unable to support previous findings (Pi, *et al.* 2010) of the murine GPRC6A eliciting activation of the Gα_s pathway; however, this may be related to difference in assay format and sensitivity. Furthermore, testosterone, Ocn variants and DHEA stimulations, RAMP1 exhibited no agonistic activity on hGPRC6A (Figure 3.8). Interestingly, DJ-V-159 induced small dose-dependent increases in cAMP production comparable to L-amino acid responses observed in CHO-K1 cells co-expressing hGPRC6A and RAMP1 (Figure 3.8). This in part, may be explained by the modelling strategy used to identify DJ-V-159 as a potential agonist; cross-referencing putative L-amino acid binding sites residues within the ligand recognition VFT and 7TM domains of the GPRC6A receptor (Pi, *et al.* 2018).

The result suggests RAMP1 increases forward trafficking of the receptor, thus increasing the number of available GPRC6A receptors at the surface to transduce external stimuli. The dose responses curves observed indicate partial agonism which, in part may be explained by the receptor's low expression profile (Kuang *et al.*, 2005; Oury *et al.*, 2011; Pi & Quarles, 2012b; Smajilovic *et al.*, 2013; P Wellendorph *et al.*, 2005). Across all ligands, minimal responses were observed; future experiments, might benefit from using assay kits offering a greater level of sensitivity to detect more subtle fluctuations in intracellular cAMP accumulation (e.g. Perkin Elmer LANCE Ultra or the AlphaScreen cAMP kits).

However, the results may put forward the concept that this receptor may not signal through one distinct intracellular pathway but a combination, depending on the ligand stimuli. The co-expression of RAMP1 with GPRC6A may be the missing link between why certain groups report testosterone responsiveness whilst others fail to (S. Jørgensen *et al.*, 2017). Similar dose response curves were seen with L-amino acid stimulation (Figure 3.7). Partial activation is observed when GPRC6A is expressed alone; however, a much larger maximal response is seen when both the GPRC6A and RAMP1 are co-expressed, suggesting RAMP1 may escalate the degree of forward trafficking of the hGPRC6A. However, a comparable response is seen in cell expressing RAMP1 *only*, suggesting that L-Ala may be activating cAMP production via other endogenous receptors that may be

aided by the RAMP1 overexpression. The assay format allows for areas of optimisation including cell number, stimulation times and temperature which may open up the dynamic range of the assay allowing greater insight into the finer mechanisms of this receptors $G\alpha_s$ signalling. Taken together, the findings here support the claim that GPRC6A predominately couples to the $G\alpha_q$ /PLC/DAG pathways with minimal $G\alpha_s$ activation and negligible $G\alpha_i$ modulation.

3.4.4 G Protein Signalling & ERK1/2 activation.

As mentioned in section 1.2.5, GPRC6A has been reported to couple to the ERK1/2 signalling pathway. However, these findings have failed to be completely replicable, with different groups unable to produce concordant data. Research by Pi *et al.* (2011; 2016) showed in GPRC6A overexpressing HEK-293 dose dependant activation of ERK1/2 signalling when stimulated by Ocn. Moreover, these responses were significantly attenuated when treated with U73122 (PLC inhibitor) and Ro31-8220 (PKC inhibitor). In contrast, data reported by Jacobsen *et al.* (2013) and Rueda *et al.* (2016) failed to reproduce these findings, observing no activation in ERK activity upon Ocn stimulation. Here we demonstrated negligible activation of both the $G\alpha_q$ and $G\alpha_s$ pathways when stimulated with Ocn variants; in line with the latter studies. However, GPCRs have been shown to signal independently of G-proteins, through the recruitment of GRKs and arrestin proteins - known regulators of the ERK1/2 pathway (Gurevich & Gurevich, 2019; D. G. Tilley, 2011). Investigating into the role of RAMP1 in hGPRC6A-mediated ERK1/2 phosphorylation may clear up the current discrepancies over Ocn as a putative agonist for this receptor. Furthermore, ERK1/2 signalling has been shown to be crucial in regulating cell growth and apoptosis. Dysregulated activation of this pathway is commonly implicated in many common cancers (Guo *et al.*, 2020). As will be discussed in the following chapter, aberrant ERK signalling mediated by the GPRC6A/RAMP1 receptor heteromer may play a crucial role in the development and progression of castration resistant prostate cancer (Nickols *et al.*, 2019).

3.4.5 Further Biochemical Analysis.

To understand the pharmacological profile of GPRC6A further characterisation the mechanisms by which the receptor signals through $G\alpha_q$, $G\alpha_s$, and $G\alpha_i$ is required. The prospective studies may look at IP_3 accumulation, an intermediate of the $G\alpha_q$ signalling cascade as an alternate method for GPRC6A characterisation. Previous studies have utilised IP_3 as an effective method of measuring $G\alpha_q$ signalling (Kuang *et al.*, 2005; Pi & Quarles, 2012; Wellendorph & Bräuner-Osborne, 2009). By investigating several intermediates of the $G\alpha_q$ pathway, the combined data of intracellular Ca^{2+} mobilisation, IP_3 accumulation will offer a much clearer map of the GPRC6A signalling profile.

In addition to acting as a chaperone, several studies have also shown RAMPs ability to alter GPCR ligand affinity and signalling bias (Rueda *et al.*, 2016). We have already shown that GPRC6A has the potential to transduce through two distinct pathways; further investigation into which specific G-protein pathways may adopt scintillation proximity assays and DMR technology. Data here could confirm the concept of bias agonism opening up the research field to novel agonist/antagonist development as research tools or even pharmaceuticals. Knowledge of preferential signal activation and pathway specific compounds could allow for precise control over fundamental cell biology and the modulation of cellular activity.

Building on the functional data presented here, we intended to expand our current screening of potential GPRC6A orthologues to extend to pharmacological relevant DHEA derivatives. With ranging effects in breast and prostate cancer the discovery of a potentially novel DHEA receptor could shed new light on an area fraught with controversy (reviewed by Arnold 2009).

A large area of controversy includes the bone derived peptide hormone Ocn, shown to play an important physiological role along with testosterone in bone and gonadal development (Rueda *et al.*, 2016). Whilst some studies report Ocn and testosterone stimulate Ca^{2+} mobilisation, ERK1/2 phosphorylation, and cAMP accumulation (Barbash *et al.*, 2017; Weston *et al.*, 2016). Other groups fail to see Ocn and testosterone as viable

agonist of GPRC6A (Chamouni & Oury, 2014). In concordance with the latter studies our data is supportive of these conclusions observing no agonist activity on the mouse receptor nor the human receptor when expressed *alone*. Conversely, our data also shows when co-expressed with RAMP1, uncarboxylated-Ocn and testosterone induced $G\alpha_q$ signalling through the hGPRC6A. This data agrees with the findings by (Ferron et al., 2010; Oury et al., 2011, 2013; Pi et al., 2015, 2016) and Oury *et al.* (2011; 2013). Inclusion of RAMP1 in hGPRC6A mediated signalling could potentially begin to resolve current controversies concerning GPRC6A ligands transduction and physiological purpose.

The multiple positive reports logically should not be dismissed by the contrasting findings; the disparate results may be the result of differences in cell models and receptor species used. This dichotomy suggests the concept that cell-type specific co-factors (i.e. RAMPs) may be necessary to alter hGPRC6A function for certain stimuli. The findings comprehensively demonstrate a stark species delineation between the mouse and human receptor. This difference may be the consequence of previous evolutionary changes leading to disparate mechanistic differences between the two receptors; the higher order organism requiring trafficking aid in the form of RAMP1 to address the increase in complexity.

Chapter 4: GPRC6A & RAMP1 Role in Prostate Cancer.

4.1 GPRC6A & RAMP1 Role in Prostate Cancer Introduction.

In the previous chapters, we have comprehensively evaluated RAMP1's role in facilitating hGPRC6A's forward trafficking and intracellular signalling. We observed a marked difference in pharmacological profiles between the mouse and human forms of the GPRC6A receptor in *in vitro* overexpressing systems. The findings offer an explanation for the discrepancies seen in the literature when comparing mouse and human GPRC6A. With reports citing both GPRC6A and RAMP1 involvement in prostate cancer combined with our novel findings of testosterone sensitivity, we hypothesised a synergistic role in late stage androgen-insensitive carcinoma. This may also offer insight into why current anti-androgen therapies fail to impede the progression of anti-sensitive tumours to hormone refractory prostate tumours.

4.1.1 Prostate Cancer.

Prostate cancer is rapidly becoming the most common cancer in men in western countries, who have a 1 in 8 chance of being diagnosed with the disease in the UK (Lloyd *et al.*, 2015). Benign prostate tumours are often treated relatively successfully by prostatectomy and/or radiotherapy. However, recurrent prostate tumours are treated with hormonal therapies or androgen deprivation therapy (ADT). These treatments often work by blocking testosterone synthesis or preventing AR signalling. The AR is crucial for prostate development and normal function. Testosterone and its metabolite DHT exert their effects through the AR to initiate AR-mediated transcriptional factors. Approximately 80-90% of prostate cancer are dependent on androgen at initial diagnosis (Heinlein & Chang, 2004). These treatments are largely successful in androgen-sensitive tumours; however, the majority of patients will relapse with tumours resistant to anti-androgen therapies. This is commonly due to alternative mechanisms to canonical AR signalling, AR amplification or androgen production within the tumour; at this point the disease has progressed to castration-resistant or androgen-insensitive prostate cancer (Saraon, *et al.* 2019) (Knudsen & Kelly, 2011). Although there are treatment options available for early stage prostate cancer, for patients with advanced metastatic disease, options are much more limited with tumours often progressing to bone metastasis (Bubendorf *et al.*, 2000; Ziaee *et al.*, 2015). One consequence of this is that the

European Association of Urology estimates that all patients with anti-androgen therapy resistant prostate cancer are currently involved in clinical trials (Heidenreich *et al.* 2014). However, there is still a clear unmet clinical need to discover new pharmaceutical targets that are involved in advanced stages of prostate cancer and its metastasis.

Dynamic expression of AR is well-established and often can be managed during ADT. Recent interests have shifted from AR focussed interventions towards novel AR-independent pathways responsible for cell proliferation and survival in androgen-insensitive carcinomas. Tumours from patients with castration-resistant prostate cancers exhibit a down regulation of AR expression with one study reporting 41% of samples displaying >10% AR expression (R. B. Shah *et al.*, 2004). Similar observations were seen in a recent two-decade molecular study by Bluemn *et al.*, (2017), reporting a 'phenotypic shift' in metastatic castrate-resistant prostate cancer towards an AR-null phenotype. This data demonstrates the importance of alternate AR bypass mechanisms responsible for the disease progression. A number of studies have demonstrated multiple mechanisms that bypass the AR and potentiate tumorigenic signalling within these tumours (reviewed by Sahin *et al.*, 2018; Saraon *et al.*, 2014; Xu *et al.*, 2019). Examples of AR-independent signalling include the insulin-like growth factor (IGF) and epidermal growth factor (EGF) receptors. Research has reported IGF-1 and EGF receptors can initiate signalling cascades resulting in the activation of AR-regulated gene transcription under low androgen conditions (Culig *et al.*, 1994). These receptors are known to initiate the downstream activation of pathways; Akt, MAPK, and STAT, aberrantly expressed pathways in prostate tumours (Edwards & Bartlett, 2005). Growth factor receptors have been shown to activate important cell-cycle regulatory and proliferative transcription factors AP1, c-MYC and NF- κ B through the MAPK/Ras/Raf/PKC pathway (Edwards & Bartlett, 2005; Weber & Gioeli, 2004).

Although significant advances have afforded vast benefits to patients with androgen-insensitive prostate cancer; no current treatments provide a cure for the disease. The majority of patients will undergo a regime of palliative therapy, aimed at improving quality of life and pain reduction. Currently approved therapies used in the management of androgen-insensitive carcinomas either act by inhibiting androgen signalling, inhibiting

depolymerisation of microtubules, promoting polymerisation, radioactive calcium mimetics targeting bone metastasis or immunotherapies. At present, abiraterone, enzalutamide, apalutamide, darolutamide and cabazitaxel are the frontline treatments for androgen-insensitive disease

Table 4.1) (M. A. Rice et al., 2019; Swami et al., 2020; L. Xu et al., 2019). The recent trials from these drugs have demonstrated marked improvements in overall survival, progression-free survival, and metastasis-free survival

Table 4.1); however, all have shown to possess a high percentage chance of cardiovascular/clotting events, nausea and vomiting, neurological events and metabolic disturbances (De Bono *et al.*, 2011; Fizazi *et al.*, 2012; Graff *et al.*, 2015; Hussain *et al.*, 2018; M. A. Rice *et al.*, 2019; Scher *et al.*, 2012; E. J. Small *et al.*, 2019; Eric J. Small *et al.*, 2006; Smith *et al.*, 2018a). Numerous novel therapeutics are currently in trials and has been reviewed extensively by (M. A. Rice *et al.*, 2019; Swami *et al.*, 2020).

Table 4.1 Current Anti-Androgen Therapies; Pharmacological and clinical properties of anti-androgen therapies approved for treatment of castration resistant prostate cancer. Abiraterone (De Bono *et al.*, 2011; Ryan *et al.*, 2010, 2015); Enzalutamide (Beer *et al.*, 2014; C. P. Evans *et al.*, 2016; Graff *et al.*, 2015; Hussain *et al.*, 2018; Scher *et al.*, 2012) Apalutamide (Rathkopf *et al.*, 2017; E. J. Small *et al.*, 2019; Smith *et al.*, 2016, 2018b) Darolutamide (Fizazi *et al.*, 2019; Massard *et al.*, 2016). Not reported (NR), Androgen receptor (AR), castration resistant prostate cancer (CRPC), castration-sensitive prostate cancer (CSPC). *survival at 24 months; **median survival.

| Compound | Classification | Target | Primary endpoint (intervention vs control) | | | Adverse effects | Applications | References |
|--------------|---------------------------|---------------------------|--|---------------------------|---------------------------------|--|--|---|
| | | | Overall Survival at 3 years | Progression-free survival | Median Metastasis-free survival | | | |
| Abiraterone | Biosynthesis Inhibitor | Cytochrome p450 enzyme 17 | 75% vs 45% | 33 months vs 14.8 months | NR | <ul style="list-style-type: none"> hypertension hypokalemia edema hepatotoxicity adrenocortical insufficiency | metastatic CRPC, metastatic high-risk CSPC | (Fizazi, <i>et al.</i> 2017; de Bono, <i>et al.</i> 2011; Ryan <i>et al.</i> 2010; 2015) |
| Enzalutamide | Androgen Receptor Blocker | AR antagonist | 80% vs 72% | NR | 36.5 months vs 14.7 months | <ul style="list-style-type: none"> fatigue hypertension dizziness nausea and falls risk of seizure | non-metastatic CRPC, metastatic CSPC | (Davis, <i>et al.</i> 2019; Hussain, <i>et al.</i> 2018; Beer, <i>et al.</i> 2014; Evans, <i>et al.</i> 2016; Graff, <i>et al.</i> 2015; Scher, <i>et al.</i> 2012) |
| Apalutamide | Androgen Receptor Blocker | Competitive AR inhibitor | 82.4% vs 14.7%* | 68.2% vs 47.5%* | 40.4 months vs 18.4 months | <ul style="list-style-type: none"> fatigue hypertension rash diarrhea nausea arthralgia peripheral edema | non-metastatic CRPC | (Chi, <i>et al.</i> 2019; Smith, <i>et al.</i> 2018; Rathkopf, <i>et al.</i> 2017; EJ Small, <i>et al.</i> 2019; Small, <i>et al.</i> 2016; 2018) |
| Darolutamide | Androgen Receptor Blocker | AR antagonist | NR | NR | 40.4 months vs 18.4 months | <ul style="list-style-type: none"> fatigue nausea pain in extremities rashes ischemia heart failure | non-metastatic CRPC | (Fizazi, <i>et al.</i> 2019; Massard, <i>et al.</i> 2016) |
| Cabazitaxel | Androgen Receptor Blocker | Microtubule inhibitor | 13.4 months vs 14.5 months** | 8 months vs 3.7 months** | NR | <ul style="list-style-type: none"> fatigue nausea pain in extremities hair loss shortness of breath Abdominal pain | metastatic CRPC | (Eisenberger, <i>et al.</i> 2017; de Wit, <i>et al.</i> 2019) |

4.1.2 GPRC6A & RAMP1 in Prostate Cancer.

4.1.2.1 Evidence of GPRC6A/RAMP1 & Prostate Cancer In Vivo.

The majority of our understanding GPRC6A's role in prostate cancer has stemmed from phenotypic mouse studies. GPRC6A^{-/-} mice are observed to exhibit feminisation measured by the reductions in testicular and seminal vesicle size and weight in both global and Leydig cell KO models (De Toni, *et al.* 2016; Oury, F. *et al.* 2011; Pi *et al.* 2010). In subsequent studies *Gprc6a* transcript were reported to be significantly elevated in prostate cancer cell types; 22Rv-1, LNCap, and PC-3 when compared to healthy prostate cells (Pi, *et al.* 2012). In addition, researchers here crossbred *Gprc6a*^{-/-} mice with TRAMP (TRansgenic Adenocarcinoma Mouse Prostate) prostate cancer mice and found significant reductions in prostate cancer progression and improvements in survival. In a more recent study, treatment of PC-3 cells with GPRC6A siRNA drastically attenuated PC-3's migratory and invasive capabilities. (Liu, *et al.*, 2016). Moreover, the report noted the increase in matrix metalloprotease-2 and -9 activity often responsible for metastatic progression, were reduced when subjected to GPRC6A siRNA treatment. Generation of a novel GPRC6A exon III KO using the CRIPSR/Cas technology, reported the attenuation of tumorigenesis in human prostate cancer xenograph mice; with reductions in proliferation, migration, and expression of genes involved for regulating testosterone biosynthesis (Pi, *et al.* 2012; Ye *et al.*, 2017). Similar trends have been reported with RAMP1's involvement in prostate cancer progression. We, and other groups have observed RAMP1 expression to be significantly upregulated in prostate cancer cell lines; and knock down of RAMP1 drastically reduced tumour size, proliferative capabilities and tumourigenicity *in vitro* and *in vivo* (Logan *et al.*, 2013; Romanuik *et al.*, 2009; Warrington 2018). Taken together, we hypothesise that GPRC6A and RAMP1 could play a combined role in prostate cancer and may provide a novel therapeutic target where current androgen-insensitive interventions fail.

4.1.2.2 Clinical Evidence of GPRC6A & Prostate Cancer

In a GWAS, *GPRC6A* has been identified as one of five prostate cancer susceptibility loci in both the Asian and European population (Takata, S. *et al.* 2010; Wang, W. *et al.* 2012; Long, *et al.* 2012; Lindstrom S. 2012; Sullivan 2015). In a seminal GWAS study found in a Japanese cohort of 4,584 participants with prostate cancer, *GPRC6A* SNP rs339331 showed significantly association with prostate cancer risk ($p = 1.6 \times 10^{-7}$) (Takata *et al.*, 2010). Subsequent studies in the Chinese cohorts, replicated these findings reporting the same rs339331 SNP led to increased prostate cancer risk ($p = 1.43 \times 10^{-5}$) (Long *et al.*, 2012). Furthermore, research conducted by Wang *et al.*, (2012) reported individuals with multiple copies of the risk alleles saw cumulative effect with an increased prostate cancer risk in a dose-dependent manner. The rs339331 TT allele was observed to be significantly associated with higher *GPRC6A* mRNA expression compared to the C allele. However, none of the variants were seen to be associated with clinical stage or Gleason score. These combined reports coincide with multiple studies reporting a rapidly increasing incidence of prostate cancer in the East Asian population (Ha Chung *et al.*, 2019; Kimura & Egawa, 2018; Matsuda & Saika, 2009). In multiple European cohorts totalling 265,000 Caucasian participants, research found a significant association between the *GPRC6A* rs339331 SNP and prostate cancer risk ($p = 1.9 \times 10^{-3}$) (Lindström *et al.*, 2012). This trend was also found in a subsequent American cohort, observing a significant increase in prostate specific antigen after radical prostatectomy ($p = 0.02$). However, no associations were observed in risk of developing castrate-resistant metastasis (Sullivan *et al.*, 2015).

4.1.3 Prostate Cancer Cell lines.

To investigate *GPRC6A*'s disputed involvement in prostate cancer, relevant cell lines are needed in order to accurately model prostate cancer signalling. Many cell lines have been characterised, based on the different stages of prostate cancer progression. Cell lines are often chosen based tumorigenic properties and their ability to accurately imitate increasing stages of prostate cancer progression. This also includes sites commonly associated with tumour metastasis. The first cell lines used were Du-145, PC-3, and LNCap, considered to be the standard cell lines widely used in prostate cancer research.

4.1.3.1 DU-145 Prostate Cancer Cell Line.

The DU-145 cell line are epithelial cells derived from a central nervous system metastasis from a 69 year old Caucasian male with prostate adenocarcinoma (Stone *et al.*, 1978). DU-145 are androgen insensitive, are negative for prostate-specific antigen, and androgen receptor expression (Pulukuri *et al.*, 2005). The ability to sense androgens is a marker of early prostate cancer; with patients often being treated with anti-androgen therapies to inhibit further growth. However, patients can enter remission whereby tumours non longer respond to these treatments; this is term hormone-refractory or androgen insensitive (Leone *et al.*, 2018). DU-145 cells have been characterised to exhibit moderate metastatic potential in comparison to other prostate cancer cell lines (Paul & Breul, 2000). This cell line is commonly used when investigating the later stages of prostate cancer development and metastasis.

4.1.3.2 LNCaP Prostate Cancer Cell Line.

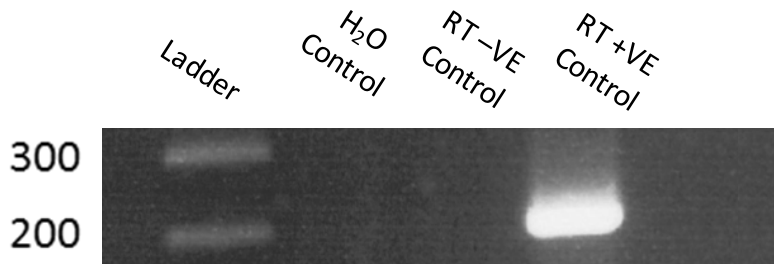
LNCaP cells are prostate adenocarcinoma cells isolated from metastasised lymph node biopsy from a 50 year old Caucasian male (Horoszewicz *et al.*, 1980). LNCaP cells were characterised to be androgen sensitive, exhibiting AR-mediated signalling and demonstrating poor tumorigenesis *in vivo* in the absence of co-cultured mesenchymal and/or stromal cells (Gleave *et al.*, 1992; Lim *et al.*, 1993). This demonstrated the significance of extracellular matrix in prostate cancer progression and the secreted paracrine factors that surround tumours. Sub cell line C4-2 and C4-2B, cultured from LNCaP cells are often used to study lymph and bone metastasis of primary prostate cancers (Thalmann *et al.*, 2000).

4.1.3.3 PC-3 Prostate Cancer Cell Line.

The PC-3 cell line was first derived in 1979, from a 62-year-old white man from a lumbar vertebral metastasis (Kaighn *et al.*, 1979). The PC-3 cell line is characterised as highly metastatic, reported to establish lymph node and bone metastases with osteolytic responses in mice (Pettaway *et al.*, 1996; Shevrin *et al.*, 1988; Stephenson *et al.*, 1992).

PC-3 cells are thought to be androgen insensitive as they do not express the androgen receptor, representing an appropriate model for late-stage androgen-insensitive carcinoma (Dozmorov *et al.*, 2009). Transcriptome from the PC-3 cell line, have previously been characterised for endogenous expression RAMP1 and hGPC6A transcripts (Figure 4.1) (Warrington, 2018; Ye *et al.*, 2017, 2019) . It is important to note that these studies also found PC-3 cells to be negative for the expression of the nuclear AR (Figure 4.1). Furthermore, to investigate the involvement of hGPC6A and RAMP1 in PC-3 intracellular signalling, we had generated a RAMP1^{-/-} PC-3 cell line. This was carried out using CRISPR/Cas9 (Clustered Regularly Interspaced Short Palindromic Repeats) methodology to successfully KO the endogenous *RAMP1* gene in PC-3 cells.

(A) PC-3 RAMP1; (~193bp)



(B) Human RAMP1;

| Score | Expect | Identities | Gaps | Strand | Frame |
|--------------|---------|--|-----------|-----------|-------|
| 167 bits(90) | 1e-38() | 96/100(96%) | 1/100(1%) | Plus/Plus | |
| Features: | | | | | |
| Query | 96 | GCCCATCACCTCTTCATGACCACTGCCTGCCAGGAGGCTAACTACGGTGCCCTCCTCCGG | | | 155 |
| Sbjct | 184 | GCCCATCACCTCTTCATGACCACTGCCTGCCAGGAGGCTAACTACGGTGCCCTCCTCCGG | | | 243 |
| Query | 156 | GAGCTCTGCCTCACCCAGTTCCAGGTANN-ATGNAGGCCG | | | 194 |
| Sbjct | 244 | GAGCTCTGCCTCACCCAGTTCCAGGTAGACATGGAGGCCG | | | 283 |

(C) Prostate Carcinoma cell lines hGPC6A;

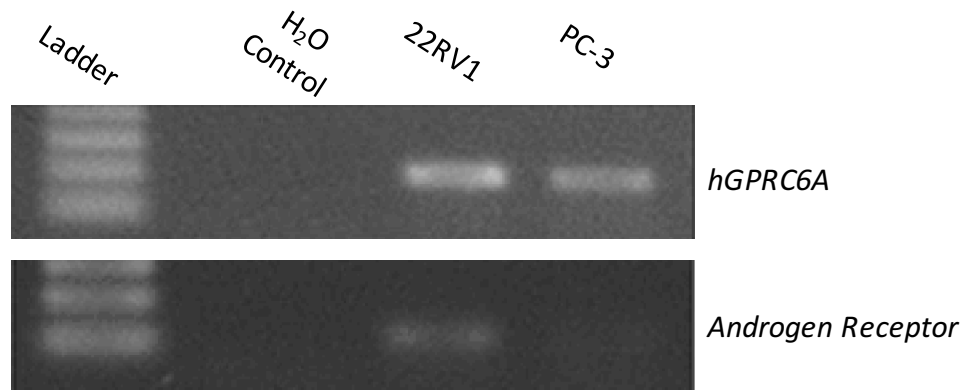


Figure 4.1; (A) Amplified PC-3 DNA samples by endpoint PCR targeting RAMP1 (193bp). (B) Sanger sequencing and nBLAST for RAMP1 aligned with NCBI NM_005855.3 RAMP1 mRNA sequence with a 96% match (Warrington, 2018). (C) Multiple papers have shown WT PC-3 cells to be negative for the androgen receptor expression whilst endogenously express hGPC6A; as well as other androgen-insensitive prostate cancer cell lines DU145, PC-3, LNCaP, & 22Rv1 (Lui, *et al.* 2016; Ye *et al.* 2017; 2019).

4.1.4 Generation of RAMP1^{-/-} PC-3 Cell line.

A prostate cancer RAMP1 KO cell has yet to be reported in the literature bar a PC-3 RAMP1 knock *down* cell line (Logan *et al.*, 2013). However, with increasing evidence of a link between RAMP1 and GPRC6A involvement in prostate cancer progression, the need for a RAMP1 KO cell line would be an essential tool to study GPRC6A and RAMP1 in prostate cancer. The Clustered Regularly Interspaced Palindromic Repeat (CRISPR)/Cas9 HDR

system was adopted here by previous PhD student Dr. Warrington to successfully generate a PC-3 RAMP1 KO cell line in order to investigate GPRC6A and its subcomponents in prostate cancer.

4.1.4.1 *Clustered Regularly Interspaced Short Palindromic Repeats (CRISPR) Technology.*

Gene KO technologies often exploit intrinsic cellular processes involved in DNA repair. Non-homologous end joining (NHEJ) is the most simplistic of these mechanisms, occurring in the absence of template DNA. This process involves the insertion of indiscriminate nucleotides into the region of DNA to reconnect the damaged sequence; however, this method is non-specific and often results in inactivation mutations (Rodgers & Mcvey, 2016). Homology-directed repair (HDR) utilises native template DNA to enable targeted repair of genetic material. It is understood that in mammalian cells, HDR accounts for 30-50% of repair events following endonuclease double-strand DNA breaks (DSBs) (F. Liang *et al.*, 1998). Exploiting these cellular repair mechanisms in tandem with specific endonucleases has enabled precise genomic editing by point mutations at any given gene locus. Initial users of these methods led to the development of gene KO technologies such as the zinc finger nucleases (ZFN) and the transcription activator-like effector protein system (TALENs) (Bogdanove & Voytas, 2011; Cermak *et al.*, 2011; Klug, 2010; Mak *et al.*, 2013).

CRISPR/Cas9 technology differs from these aforementioned systems by its use of Cas9 endonucleases. In prokaryotes, Cas9 endonucleases offer an immunological defence mechanism against viral invasion. Complexing with guide RNA (gRNA), homologous with the target locus in the protospacer adjacent motif site. Active Cas9 induces DSB in DNA sequences recognized as foreign to the host. The excised fragments can then become incorporated in the CRISPR sequence. In subsequent infections the Cas proteins can then express the CRISPR loci to enable recruitment of CRISPR RNAs to guide the Cas endonuclease to target, cleave and destroy invasive DNA. (Barrangou *et al.*, 2007). Preliminary studies saw CRISPR/Cas9 induced DSB *in vitro* which were subsequently repaired by NHEJ, producing insertion/deletion mutations in the sequence (Jinek *et al.*,

2012). Subsequent studies combined the technology with donor DNA sequences complementary to sites of interest. Here, researchers found donor DNA was inserted in the sites at which Cas9 DSB had been induced by HDR (Cong *et al.*, 2013; Mali *et al.*, 2013). CRISPR/Cas9, ZFNs and TALENs technologies all exploit intrinsic cellular repair mechanisms; however, the use of gRNA provides efficient, targeted genomic editing.

4.1.4.2 *RAMP1*^{-/-} Influence on PC-3 cells *In Vitro* & *In Vivo*.

With both proteins have been reported to be upregulated in prostate cancer cell lines it is unsurprising that GPRC6A and RAMP1 have emerged as interesting therapeutic targets due to their putative role in mediating multiple *in vivo* effects (Logan *et al.*, 2013; Pi, Parrill, *et al.*, 2010; Pi & Quarles, 2012a; Ye *et al.*, 2017, 2019). Using a range of techniques, previous PhD student Dr. Warrington demonstrated that RAMP1 deletion in PC-3 cells leads to reductions in pro-tumorigenic capabilities *in vitro* and *in vivo*. A brief summary of Dr. Warrington's PhD findings will be made as a background to the subsequent signalling data performed as part of this study. Specifically, RAMP1 deletion in PC-3 cells led to reduced viability and increased basal levels of apoptosis-associated caspases (Figure 4.2). Furthermore, key markers of invasion mechanisms such as colony formation and invasion were also significantly inhibited *in vitro* following RAMP1 deletion (Figure 4.2) (Warrington, 2018). Analysis of downstream pathways led to significant reductions in expression of phosphorylated Akt and STAT3 proteins in RAMP1^{-/-} cells. Akt is a key factor for cell survival and has been previously linked with prostate cancer cell growth. Whilst STAT3 proteins are key regulators in transduction pathways responsible for numerous growth factors and control of apoptosis (Warrington, 2018). Furthermore Dr. Warrington's PhD work demonstrated for the importance of RAMP1 specifically in prostate cancer growth is further supported by data we obtained from *in vivo* cancer models in mice. Subcutaneous injection of PC-3 cells in immunocompromised balb/c nude mice was associated with a dramatic inhibition of tumour growth in mice injected with RAMP1^{-/-} cells compared with WT controls. In many cases RAMP1^{-/-} tumours failed to establish as tumours; of those that did, shown negligible increases in size (Figure 4.3) (Warrington, 2018). It is important to note the RAMPs propensity to complex with the

other GPCRs; particularly the CLR. It may therefore be argued that these phenotypic changes observed may be the result of the loss of action from CGRP receptors (CLR+RAMP1) (see chapter 1, section 1.7.1). To determine this, PC-3 WT cells were treated with either CGRP agonist or Telcagepant (a CGRP antagonist). In cAMP accumulation experiments negligible effects were seen from either CGRP or Telcagepant, indicating that neither the CGRP nor its receptor is involved in inhibiting tumour growth observed in the RAMP1^{-/-} cells (data not shown) (Warrington, 2018).

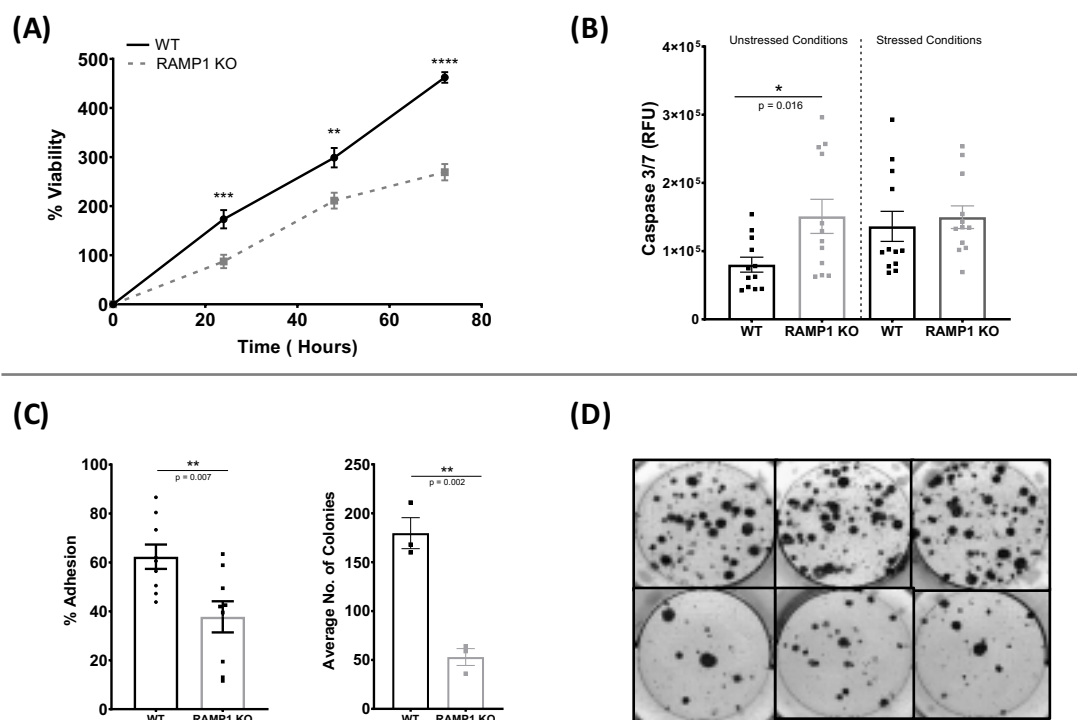


Figure 4.2 Dr. Warrington's data demonstrating deletion of RAMP1 reduces the tumorigenic capability of PC3 cells in vitro; (A) Viability assay plot showing the number of viable cells on days 1-3, calculated as a percentage from cell counts at day zero. (B) Quantification of caspase 3/7 levels in normal cell culture conditions and after 48 hours of serum starvation. (C) Percentage of cells (compared to number seeded) adhering to fibronectin-coated culture plates after washing with PBS. (D) Number of colonies formed in culture after seeding of 100 WT or RAMP1 KO cells. Unpaired Student's t-test (Mean \pm SEM). * $p < 0.05$; ** $p < 0.01$; *** $p < 0.001$; **** $p < 0.0001$ (Warrington, 2018).

Histological analysis of the tumours revealed major differences in the tissue architecture. Haematoxylin and eosin staining of tumours from mice injected with WT PC-3 cells had a high frequency of necrotic centres and were densely packed with tumour cells, a common consequence of outgrowing of the blood supply (Figure 4.3). In contrast, tumours from mice injected with RAMP1^{-/-} cells were smaller, less dense, more homogenous and lacked central necrotic lesions (Warrington, 2018). Necrotic centres are common architectural

changes observed in subcutaneous tumours, where they become too large for an adequate blood supply to reach the inner core limiting the supply of nutrients (Lee *et al.*, 2018). Immunostaining of PC-3 WT cells for GPRC6A revealed an organized staining pattern with clear distribution of positive staining localized to the plasma membranes (*data not shown*). Conversely, in RAMP1^{-/-} PC-3 cells GPRC6A staining appeared prominently cytosolic and disorganised (*data not shown*). Naturally without further confirmation, those inferences might appear less than fully justified. However, our results should be considered against the background of other work linking GPRC6A and RAMP1 to cancer and specifically prostate cancer.

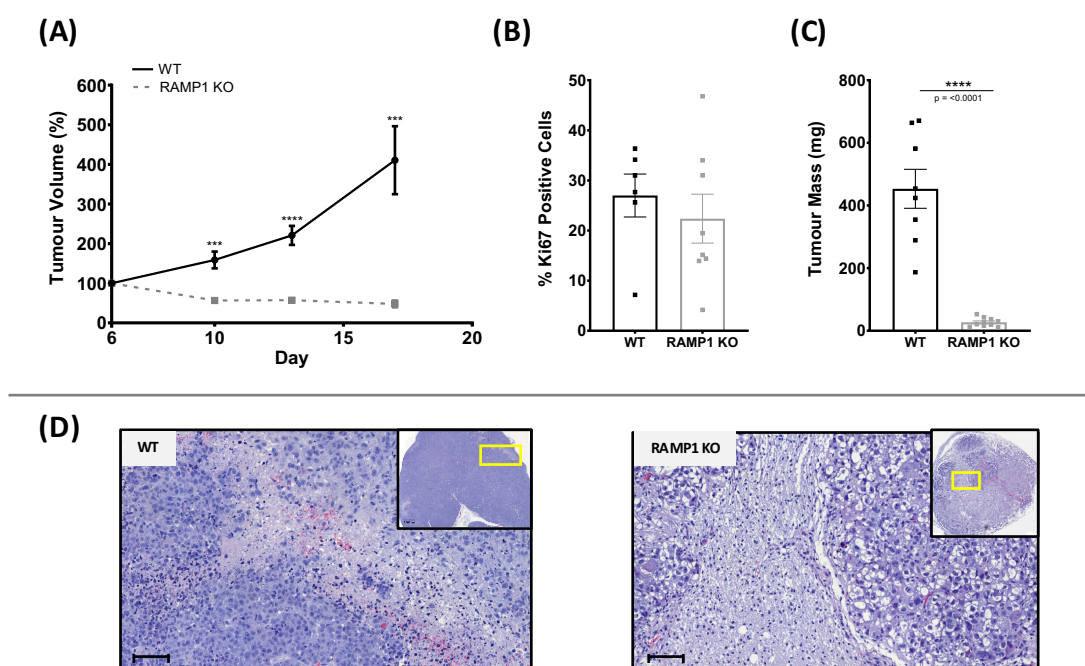


Figure 4.3 Dr. Warrington data demonstrating the deletion of RAMP1 leads to reduction of subcutaneous xenograft tumour growth; **(A)** Tumour volume measurements as a percentage increase from first measurement after tumour establishment at Day 6. **(B)** Tumour mass measured at Day 17. **(C)** Quantitative measurements of Ki67 (a marker of cell proliferation) in equivalent tumour sections. **(D)** Haematoxylin and eosin staining of tumour sections was used to disclose morphological differences. Scale bar = 100 μM. Unpaired Student's t-test (Mean ± SEM). * $p < 0.05$; ** $p < 0.01$; *** $p < 0.001$; **** $p < 0.0001$. (Warrington, 2018)

Following metastasis, prostate cancer frequently becomes a terminal disease. 80% of prostate tumour metastases are found in the bone (Bubendorf *et al.*, 2000) and therefore identifying key factors responsible for the engraftment and tumorigenesis in the bone environment reflects an important clinical need. Intracardiac injection of PC-3 cells into immunocompromised balb/c nude mice recapitulates the process of prostate cancer cells metastasizing from the bloodstream and colonizing bone (N. Wang *et al.*, 2015). MicroCT

scanning of the tibiae of the mice revealed significant differences in the level of bone destruction after skeletal metastasis. Although Dr. Warrington could not confirm a change in the number of osteolytic lesions, the reduced bone tumour burden may be caused by a slower growth rate of RAMP1^{-/-} cells within the bone environment.

Taken together Dr. Warrington's previous findings alongside a number of papers begin to suggest GPRC6A may play an integral role in prostate cancer development and progression with a clear reliance on RAMP1. Therefore, establishing the link between GPRC6A and RAMP1 within the context of prostate cancer is crucial factor for the development of potentially novel treatment. For this, strong pharmacological data is necessary for target identification.

4.1.5 *Research Aims.*

1. *Investigate the involvement of GPRC6A/RAMP1 in PC-3 cell downstream signalling*
2. *Investigate hGPRC6A involvement in PC-3 cell viability.*

4.1.6 *Research Hypothesis.*

RAMP1 facilitate hGPRC6A intracellular signalling in PC-3 cells.

4.2 Materials & Methods.

4.2.1 *PC-3 Cell Culturing.*

PC-3 cells were cultured in T-75 cm² flasks (Nunclon, Thermo Scientific) in RPMI 1640 medium containing Glutamax™ (Gibco), 10% fetal calf serum (Sigma-Aldrich), 10 mg/mL Streptomycin, and 1% penicillin (Sigma-Aldrich, St Louis, Missouri, US) at 37°C in a 5% CO₂ incubator. Passaging and subculturing of PC-3 cells was carried as described in sections 2.2.1.1 & 2.2.1.2.

4.2.2 *Calcium 6 FLIPR Kit Assay.*

Intracellular calcium signalling was measured using the Calcium 6 FLIPR Kit Assay (Molecular Devices); all procedures were carried out as previously described in chapter 3, sections 3.2.1.1 & 3.2.1.3.

4.2.3 *PC-3 Cell Viability Assay.*

Cell viability was measured using the RealTime-Glo™ MT Cell Viability Kit (Promega, UK). The kit measures real time cell viability by a non-lytic bioluminescent method. Cell viability is determined in culture by measuring the metabolic activity and reducing potential of the cells. Cells were seeded at 1000 cells/well into clear-bottomed white 96 well plates and incubated overnight at 37°C in 5% CO₂. PC-3 WT seeding densities had been optimised previously (Warrington, 2018). 2 µL of 1000X NanoLuc cell-permeable substrate along with 2 µL 1000X NanoLuc enzyme luciferase was added to PC-3 WT cells to give a 1X in-well concentration. Viable cells will reduce the synthesized substrate into luciferin; this second substrate can then go on to be hydrolysed by the NanoLuc luciferase emitting a luminescent signal detected using the Ensign plate reader (Perkin Elmer). Cell viability was monitored over 5 days. Cell viability can then be read in real-time, due to the format enabling the signal to be read continually over an extended time period. Cells were treated daily with the GPRC6A antagonist NPS-2134; 2 µL dilutions of NPS-2143 were diluted in PBS to give a 1X in-well final concentration.

4.2.4 *Statistical Analysis.*

All data are expressed as mean \pm SD with the statistical significance being tested for using a 2way ANOVA with Dunnett's multiple comparisons with Prism 7 software (GraphPad). P < 0.05 was considered significant.

4.3 Results.

4.3.1 Calcium Signalling in PC-3 Cell line.

Following the fundamental pharmacological data, we then sought to investigate hGPC6A in a pathophysiological role. Testosterone is a well-established pro-oncogenic facilitator of prostate cancer progression and in conjunction with our novel data showing hGPC6A testosterone sensitivity, experiments were designed to investigate the potential hGPC6A and RAMP1 involvement in androgen-insensitive carcinoma.

As previously stated CRISPR generated RAMP1 KO PC-3 cells endogenously expressed hGPC6A and RAMP1, but not the AR (Figure 4.1). Calcium mobilisation assays revealed AR negative PC-3 WT cells were responsive to high doses of testosterone [pEC_{50} 6.23 ± 0.18] whilst RAMP1 KO PC-3 cells exhibited no sensitivity (Figure 4.4). In addition, the GPCR6A agonist DJ-V-159 provoked intracellular calcium mobilisation in PC-3 WT cells [pEC_{50} 6.01 ± 0.26]; however, this response was not seen in RAMP1 KO PC-3 cells. Responses for both testosterone and DJ-V-159 exhibited comparable pEC_{50} values to the overexpressing hGPC6A+RAMP1 CHO-K1 cells and to previous data (Figure 3.5). Negligible calcium mobilisations were observed in mock vector controls, hGPC6A *only* and RAMP1 *only* transfection groups when stimulating with either agonist (Figure 4.4).

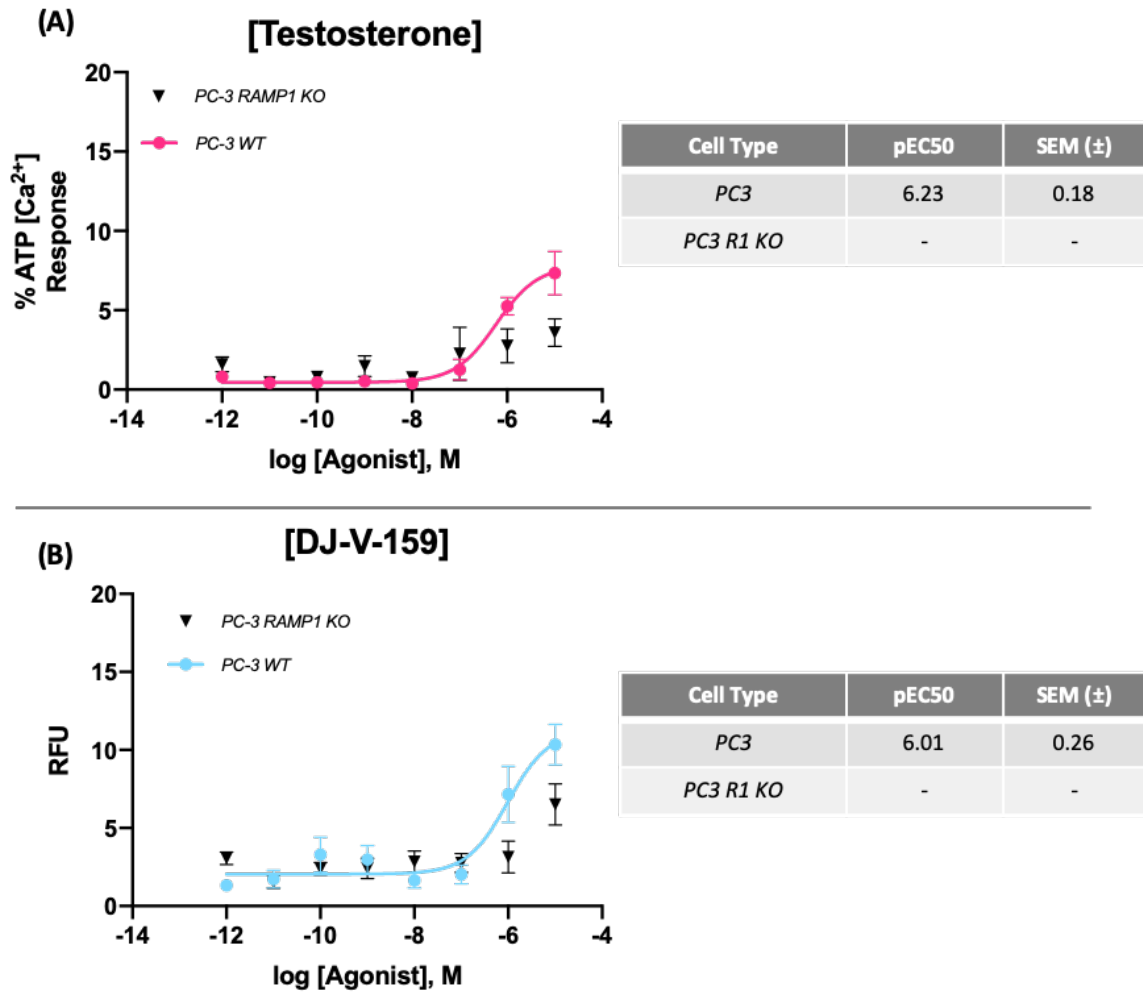


Figure 4.4 Calcium mobilisation stimulation on PC3 RAMP1 KO cells; **(A)** Testosterone stimulation on PC3 R1 KO cells; Dose-dependent responses were similarly seen with testosterone stimulation with the largest maximal responses observed at high doses of testosterone. Androgen receptor negative WT PC3 cells display smaller degree of calcium mobilisation, whilst this response is ablated in the R1 KO cells. **(B)** DJ-V-159 stimulation on PC3 R1 KO cells; Dose-dependent responses were similarly seen with DJ-V-159 stimulation with the largest maximal responses observed at high doses of DJ-V-159. Androgen receptor negative WT PC3 cells display smaller degree of calcium mobilisation, whilst this response is ablated in the R1 KO cells. Negligible calcium mobilisation was observed in mock vector controls, hGPC6A *only* and RAMP1 *only* transfection groups. Data are from 3 independent experiments and are presented as mean \pm SEM.

Moreover, in WT PC-3 cells treatment with the GPRC6A antagonist, NPS-2143 displayed dose dependant inhibitions of submaximal EC₈₀ dosing of testosterone [pIC₅₀ 11.5 \pm 0.54] attenuating the previously observed PC-3 WT responses (Figure 4.5). However, treatment with NPS-2143 failed to inhibit WT PC-3 calcium in a dose dependant manner when stimulated with EC₈₀ dosing of DJ-V-159.

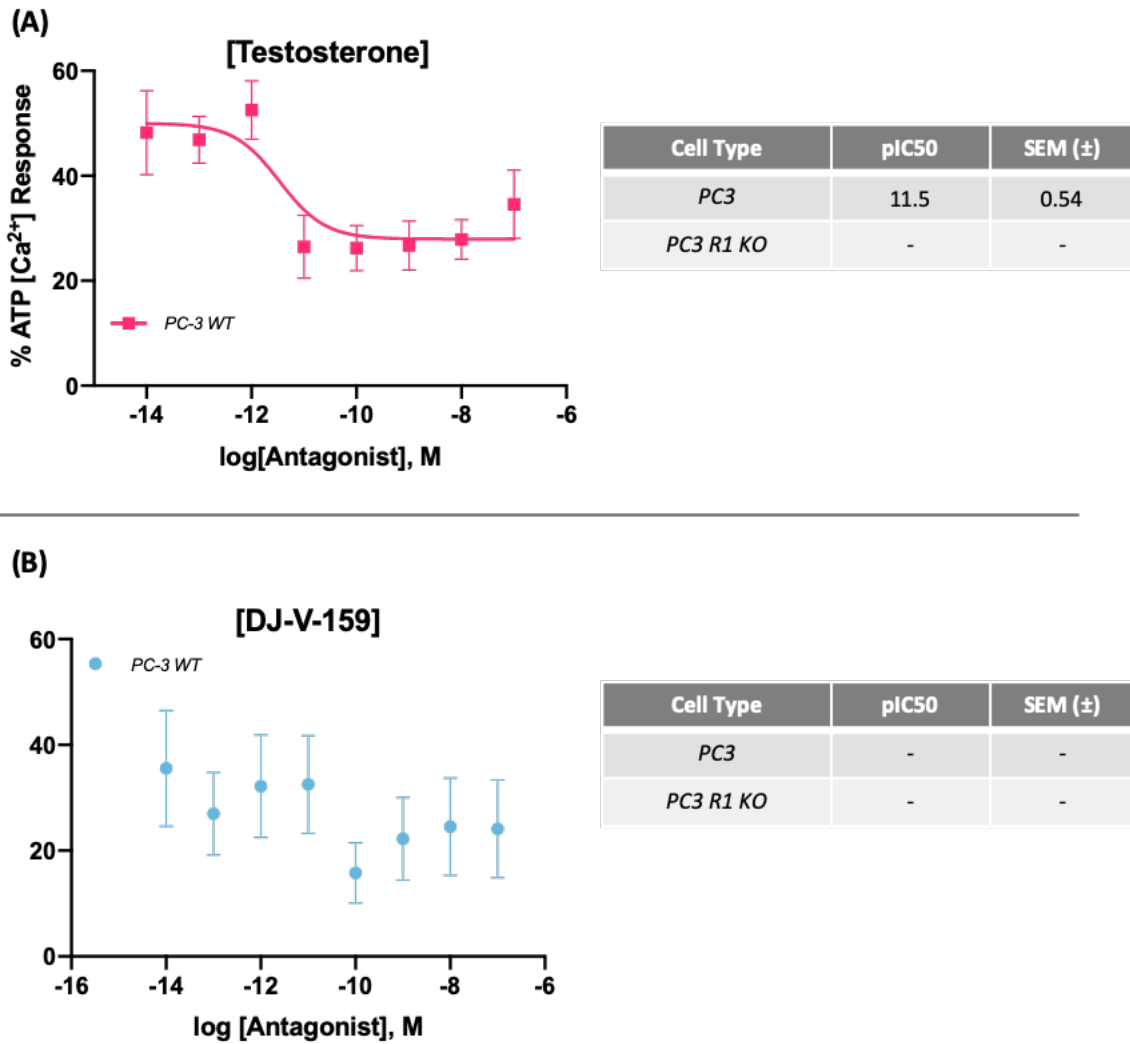


Figure 4.5 Treatment of NPS-2143 dose response on PC-3 cell line; Stimulation of PC-3 cells with EC₈₀ doses of testosterone and DJ-V-159 following treatment with dose response of GPRC6A antagonist NPS-2143. **(A)** NPS-2143 exhibits partial dose dependant inhibition of PC-3 calcium mobilisation when stimulated with testosterone; with curves display comparable pIC₅₀ for NPS-2143 to that of the hGPRC6A+RAMP1 overexpressing CHO-K1 cell line. **(B)** PC-3 calcium mobilisation induced by DJ-V-159 failed to be inhibited by NPS-2143 in a dose dependant manner. Data are from 3-4 independent experiments and are presented as mean \pm SEM.

4.3.2 NPS-2143 Effect on PC-3 Cells Viability.

PC-3 WT cells were treated with the GPRC6A antagonist NPS-2143 to investigate its effect on cell viability. Luminescent signal was recorded every 24 hours over the course of 5 days. When treated with increasing concentrations of NPS-2143, WT PC-3 cells exhibited dose-dependent decreases in cell viability. Vehicle control showed no effect on cell viability. After 3 experimental repeats it was found that treatment with NPS-2143 at doses greater than 1 μ M over 5 days showed significant decreases in WT PC-3 cell viability compared to vehicle controls groups. 5 μ M and 3 μ M showed a 100% decrease after 72

hours, whilst 1 μM displayed a 51.4% decrease after 72 hours; increasing to a 76.1% reduction at 120 hours. Treatment at 0.1 μM NPS-2143 only began to show slight reductions in cell viability after 120 hours with a 10.1%; however, these reductions were not statistically significant (Figure 4.6).

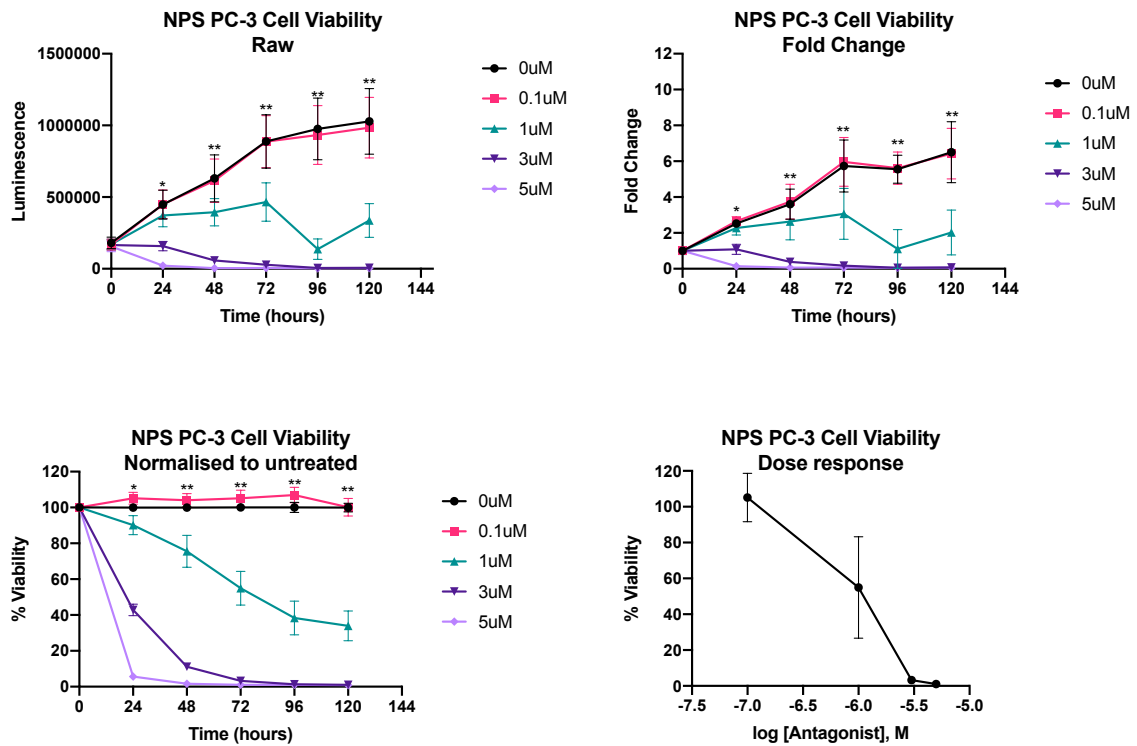


Figure 4.6 NPS-2143 Treatment PC-3 Cell Viability Assay; Dose-dependent decreases in PC-3 cell viability when treated with the GPRC6A antagonist NPS-2143 [pIC_{50} 6.0 ± 0.14]. Data represents mean \pm SD from 3 independent repeats.

4.4 Discussion.

GPRC6A has previously been identified as a prostate cancer susceptibility loci, with subsequent research strengthening the link between this receptor and prostate cancer progression (Lindström *et al.*, 2012; Long *et al.*, 2012; Takata *et al.*, 2010). With our new understanding of the hGPRC6A's requirement of the RAMP1 accessory protein, and its novel sensitivity to testosterone our efforts sought to investigate their combined role in prostate cancer development/progression.

4.4.1 *hGPRC6A-mediated Testosterone Signalling in Wild Type PC-3 Cells.*

The major findings from this study reveal that PC-3 WT cells still displayed the ability to sense testosterone, even in the absence of traditional ARs. Moreover, deletion of the RAMP1 protein reduced these responses for both testosterone and DJ-V-159-induced calcium mobilisation (Figure 4.5). Both our PC-3 WT and RAMP1^{-/-} PC-3 cells were characterised for endogenous RAMP1; not GPRC6A expression. PC-3 WT cells have been shown to express endogenous GPRC6A (Ye *et al.*, 2017, 2019); however, characterising our cells for endogenous GPRC6A would ensure the lack of GPRC6A-mediated response to due to the deletion of RAMP1 and not absence of both. he may explain the small calcium mobilisation response seen in the RAMP1^{-/-} PC-3 cells. Calcium signalling has been well described to be a major contributing pathway towards prostate cancer apoptotic evasion, angiogenesis, migration and invasion, and metastatic homing of tumour cells to bone (reviewed by Ardura *et al.*, 2020). GPRC6A has previously been reported to mediate testosterone signalling in prostate cell lines. Reports by Ye *et al.*, (2017, 2019), showed dose-dependent activation of the ERK1/2, protein kinases B, and mTORC1 pathways in PC-3 WT cells. It will be beneficial to investigate RAMP1 role in GPRC6A's ability to activate ERK1/2 signalling PC-3 cells, supporting this Ye *et al.* (2017; 2019) findings. Interestingly, in the aforementioned study PC-3 cells endogenously expressed the short ICL-3 variant of the GPRC6A that is known to be functional but poorly expressed at the cell surface (S. Jørgensen *et al.*, 2017). Findings from this study demonstrate the necessity for RAMP1 in order to facilitate functional cell surface signalling of the hGPRC6A. Data gathered here may suggest an alternate signalling pathway for testosterone to "bypass" conventional AR-mediated signalling and initiate cell growth and proliferation. Numerous reports have

implicated GPRC6A as a novel receptor that may enable continued androgen signalling in prostate tumours (M. Liu *et al.*, 2016; Long *et al.*, 2012; Pi, Parrill, *et al.*, 2010; Pi & Quarles, 2012a; Takata *et al.*, 2010; Meilin Wang *et al.*, 2012; Ye *et al.*, 2017, 2019). To our knowledge, this is the first study to link both GPRC6A and RAMP1 in prostate cancer signalling and may provide a novel explanation for the associations between the hormonal factors and prostate cancer risks; specifically, when regarding the molecular mechanisms for androgen-insensitive carcinoma progression.

Testosterone-induced calcium mobilisation in WT PC-3 was observed to be partially inhibited by NPS-2143 in a dose dependant manner comparable to CHO-K1 overexpressing cells (Figure 3.6B). However, although DJ-V-159 responses continued to exhibit dose-dependent inhibition by NPS-2143 treatment in overexpressing CHO-K1 cells; in PC-3 WT cells calcium mobilisation failed to be antagonised (Figure 4.5). Thus, the results cannot definitively confirm the responses were explicitly mediated through the hGPRC6A receptor, and may suggest the presence of alternate GPCRs endogenous to the PC-3 cells responsible for the observed response. For example, papers have shown PC-3 cells do possess a narrow range of AR expression and activity, that can be modulated with varying levels of numerous factors (Alimirah *et al.*, 2006; Sampson *et al.*, 2013; Tararova *et al.*, 2007) and thus could explain the partial antagonism of testosterone-induced calcium mobilisation. Research carried out by Alimirah *et al.* (2006), found DU-145 and PC-3 cells to endogenously express AR at both the mRNA and protein level but at lower levels to that of AR-positive LNCaP cells. Treatment with DHT saw no increases in the AR signalling but reported increases in AR expression and nuclear accumulation. Knockdown of AR in PC-3 cells resulted in decreases in the cyclin-dependent kinase inhibitor, p21^{CIP1}; a phenotype common in aggressive prostate cancer (Roy *et al.*, 2008). Future investigations would benefit greatly from the inclusion of other prostate cancer cell lines – i.e. androgen-sensitive DU145, LNCaP and -insensitive C4-2, CWRR22R, DU145, 22Rv1 – to broaden our understanding of GPRC6A in prostate cancer. In addition, the addition of generating a GPRC6A KO cell line would further cement these observed responses are hGPRC6A mediated gain a wider scope of GPRC6A/RAMP1 combined effect on hormone refractory carcinoma and their involvement in the process of androgen resistance.

4.4.2 GPRC6A on PC-3 Cell Viability.

When looking at cell viability; treatment with the GPRC6A antagonist NPS-2143 saw significant dose-dependent decreases in PC-3 cell viability (Figure 4.6). These findings are supportive of previous reports demonstrating the importance of GPRC6A in prostate cancer cell proliferation and survival. However, future work should replicate this data on PC-3 RAMP1 KO cells as a control, as no change in viability would be expected.

Proliferative capability of GPRC6A^{-/-} PC-3 cells exhibited significant decreases in cell number and survival compared to WT controls (Ye *et al.*, 2017). Researchers also reported decreases in the proliferative markers Ki-67 and PCNA expression as a consequent of GPRC6A KO (Ye *et al.*, 2019). It may be interesting to evaluate the specificity of the NPS-2143 antagonist. NPS-2143 was preliminary designed to act as a CaSR antagonist (Nemeth *et al.*, 2001) and its specificity to antagonise GPRC6A was reported later (Faure *et al.*, 2009). Recent reports have previously shown NPS-2143 treatment to inhibit PC-3 proliferation and migration, as well as downregulation of CaSR (Yamamura *et al.*, 2019). Treatment of PC-3 in combination with other CaSR calcilytic antagonists such as the SB423557 (Kumar *et al.* 2010) may provide a greater insight into the specificity of NPS-2143 action on GPRC6A. The preliminary findings here begin to draw together the link between the importance of GPRC6A and RAMP1 in prostate cancer progression. Future experiments would benefit greatly from investigating GPRC6A action in prostate cancer mouse models. Previous work has demonstrated that loss of RAMP1 in PC-3 cells leads to the failure of tumour establishment *in vivo* (Warrington, 2018). RAMP1 is well-known to couple to a variety of GPCRs, most notably the CLR forming the CGRP receptor (see chapter 1, section 1.7.1) (Mclatchie *et al.*, 1998). However, treatment of these tumours with CGRP antagonists olcagepant and telcagepant saw no changes to tumour development; thus, suggest an alternative receptor may facilitate tumorigenesis. Tracking the effects of NPS-2143 treatment in PC-3 cell tumours *in vivo* would further support the receptors involvement; measuring whether the reductions in viability were conserved *in vivo* and whether these decreases were of a similar magnitude to those seen in the RAMP1^{-/-} PC-3 tumours (Figure 4.3).

Findings from previous chapters have shown RAMP1 to be integral role in facilitating hGPCR6A signalling; potentially explaining current controversies over its signalling profile. The data proposes the GPCR6A/RAMP1 receptor may play an important role in prostate cancer tumorigenesis and metastasis. Deletion of RAMP1 leads to a downregulation of GPCR6A-mediated signalling in PC-3 cells, as well as decreases in cell growth *in vitro* with increased markers of apoptosis and inhibition of markers of metastasis as well as potent effects *in vivo*. Furthermore, blocking of the GPCR6A receptor in PC-3 leads to the inhibition of PC-3 testosterone signalling, cell viability and growth capabilities.

Chapter 5: General Discussion.

5.1 General Discussion.

The GPRC6A receptor has now been studied in depth for nearly two decades and although the field has been challenged by controversy; different groups have been able to agree upon GPRC6A to be a promiscuous L-amino acid receptor in mouse and humans (Christiansen et al., 2007; Jacobsen et al., 2013; Pi et al., 2005, 2012; Rueda et al., 2016; P. Wellendorph & Bräuner-Osborne, 2009; P Wellendorph et al., 2005). However, there is a lack of certainty over the receptor's ability to respond to other ligands; such as testosterone, and osteocalcin, where species differences are concerned making defining the receptors overall physiological role challenging (sections GPRC6A Ligand Controversies. & Role of GPRC6A in Physiology & Pathophysiology.). The major issued faced in prior hGPRC6A research is the receptor's inability to effectively transport the surface to allow comprehensive biochemical analysis. Here we have presented a comprehensive evaluation of the hGPRC6A receptor, demonstrating RAMP1 as an intrinsic requirement to facilitate receptor functionality. Through generating a CHO-K1 cell line that stably co-express hGPRC6A and RAMP1, we systematically tested different putative agonists (L-amino acids, testosterone, Ocn) to elucidate the receptor pharmacological profile and begin to delineate differences seen between the mouse and human forms of the receptor Figure 3.4 -Figure 3.9.

Numerous studies have delineated the receptor's mRNA at the tissue level; demonstrating GPRC6A is widely expressed in a multitude of tissues at low levels, with functionality only observed in specific tissues (C. Clemmensen *et al.*, 2014). Most notably researchers have reported GPRC6A-mediated action in pancreatic tissues, testes, bone and adipose tissue (De Toni *et al.*, 2017; Otani *et al.*, 2015; Oury *et al.*, 2011; Pi *et al.*, 2008, 2012, 2016). However, the absence of well-established commercially available antibodies has made mapping of the receptor protein at the sub-tissue level difficult. In addition, due to the lack of receptor-specific pharmacological tool compounds, the physiological function of the receptor has so far mainly been addressed by phenotype assessment of KO mice. However, comparisons between different exon KO's models has brought further inconsistencies, with different groups unable to agree upon phenotypic changes.

From the multitude of research, it is clear that RAMPs possess the ability to engender altered GPCR phenotypes; ligand binding affinities, and signalling patterns. This concept has been demonstrated most prolifically through class B GPCRs (McLatchie, *et al.* 1998; Muff *et al.* 1999; Christopoulos, *et al.* 2003; Harikumar, *et al.* 2006); however, as the research field has progressed this phenomenon has been exhibited in multiple GPCR classes. Most pertinent of these is the class C GPCR, CaSR receptor with multiple papers identifying RAMP1 and RAMP3 as crucial components of the functional CaSR machinery (Bouschet *et al.*, 2008, 2012; Desai *et al.*, 2014). The mechanisms by which the GPRC6A binds multiple ligands, and activates multiple signalling pathways have remained elusive. This is in-part due to the receptors poor cell surface trafficking, especially when expressed recombinantly – a characteristic it shares with other class C GPCRs (i.e. CaSR) (Clemmensen, *et al.* 2014). Accordingly, the project aimed to fundamentally characterise the hGPRC6A's pharmacological profile and whether RAMPs subcellular interaction influenced the trafficking and intracellular signalling capabilities of the human receptor.

The project was subdivided into three main objectives:

- To gain a greater understanding of the interactions between the GPRC6A receptor and RAMPs.
- To identify whether RAMPs possess a functional role in GPRC6A-mediated signalling and elucidate similarities/difference between the mouse and human forms.
- To begin to investigate the synergistic role of GPRC6A and RAMPs in prostate physiology and hormone refractory carcinomas.

5.1.1 GPRC6A Cell Surface Trafficking.

The starting point of the present study was that recombinantly expressed hGPRC6A is retained intracellularly in contrast to mouse, rat and goldfish analogs. In agreement with studies identifying the retention motif present in the hGPRC6A (Kuang, *et al.* 2005; Wellendorph, *et al.* 2005; Jorgensen, *et al.* 2017), we observed that expression of hGPRC6A alone produced poor cell surface trafficking in CHO-K1 cells. hGPRC6A's wide spread expression but inefficient forward trafficking may suggest the necessity for a tissue-specific accessory protein for effective chaperoning. However, levels of hGPRC6A

surface expression were significantly increased when co-expressed with RAMP1 specifically. This was seen in our ELISA experiments and confirmed findings from previous FRET co-localisation PhD studies by Desai; observing high levels of GPRC6A/RAMP1 co-localisation at regions commonly associated with receptor assembly/processing and trafficking (i.e. ER, trafficking vesicles, plasma membrane) (Figure 2.2, Figure 2.13 & Figure 2.14). This demonstrated that in CHO-K1 cells hGPRC6A is capable of forming higher-order oligomer complexes with RAMP1; subsequently increasing the trafficking and signalling properties of the hGPRC6A receptor.

Similar to the human CaSR the hGPRC6A is proposed to possess a ER retention motif preventing the receptor from dimerization and subsequently trafficking (Bouschet et al., 2005; Cavanaugh et al., 2010; C. Clemmensen et al., 2014; Stepanchick et al., 2010). With the identification of the importance of the ICL-3 situated within the human receptor, it may be plausible to hypothesise that this region represents a core binding site for RAMP1 to interact and aide in trafficking the hGPRC6A. With the evidence presented here it could be argued that the interactions between RAMP1 at the receptor's ICL-3 region enable the efficient transportation of the hGPRC6A from the ER to the Golgi. Here it can undergo N-terminal glycosylation and then be delivered to the cell surface (Fan, *et al.* 1997) as observed by our FRET and ELISA experiments. Future studies discerning crucial amino acid residues within both proteins would be greatly beneficial further supporting this concept. Taken together, the data supports the notion that RAMP1 is an essential component in facilitating successful forward trafficking of the hGPRC6A receptor (Figure 2.11, Figure 2.14). Potential explanations for the lack of cell surface expression observed in previous pharmacological studies is that the cell lines used lack the necessary scaffolding and/or signalling proteins found in cells endogenously expressing GPRC6A.

Interestingly, our FRET experiments also demonstrated hGPRC6A was able to complex with RAMP2 to a lesser extent (Figure 2.2). Unlike RAMP1, hGPRC6A exhibited co-localisation with RAMP2 at the perinuclear region, and remained intracellularly retained. This may be evidence for a possible endo-cellular nuclear receptor function, offering a novel mechanism for compartmentalised signalling. The classical dogma of GPCR signalling dictates that GPCRs localise to the plasma membrane in order to initiate a

cascade of effector proteins to permit intracellular signalling. However, there is now mounting evidence that suggests GPCRs localise to a multitude of intracellular membranes; particularly the nucleus (Cheng *et al.*, 2011; Pupo *et al.*, 2013; Revankar *et al.*, 2007; Zimmerman *et al.*, 2016).

The recent development of FRET biosensors and super-resolution microscopy has revealed the importance of temporal and spatial organisation of internal GPCRs in endocellular signalling (Halls & Canals, 2018). The recent advancements in genetically encoded biosensors has shown that compartmentalised GPCR signalling is often reliant upon the formation of higher-order oligomers to enable the efficient organisation and activation of signalling proteins (Conti *et al.*, 2014; Ellisdon & Halls, 2016; Halls, 2012; D. D. Jensen *et al.*, 2017; Willoughby & Cooper, 2007). The findings of a RAMP1 or RAMP2-dependent signalling mechanism for compartmentalised hGPCR6A signalling may bring a novel multimodal function, elucidating its subcellular signalling localisation.

Furthermore, with prevailing evidence demonstrating RAMPs ability to engender bias agonism; it would be noteworthy to consider receptor location as an important factor in GPCR signalling mechanisms. Future research investigating GPCR6A ability to signal from several intracellular locations could provide novel strategies that may improve the effectiveness of future drug development. The concept of selective intracellular endosomal targeting with GPCR antagonists has already been demonstrated by Jensen, *et al.* (2017); and serves as evidence of not only targeting the receptor but also at the right location.

One major challenge faced in the research field is due to the receptor's poor cell surface expression when recombinantly expressed. This had made thorough investigation of the receptor's pharmacological profile, and ultimately its physiological role increasingly challenging. The findings presented here, have given a comprehensive evaluation of the hGPCR6A trafficking mechanisms, demonstrating RAMP1 as a fundamental component for successful cell surface expression of the hGPCR6A (Figure 5.1).

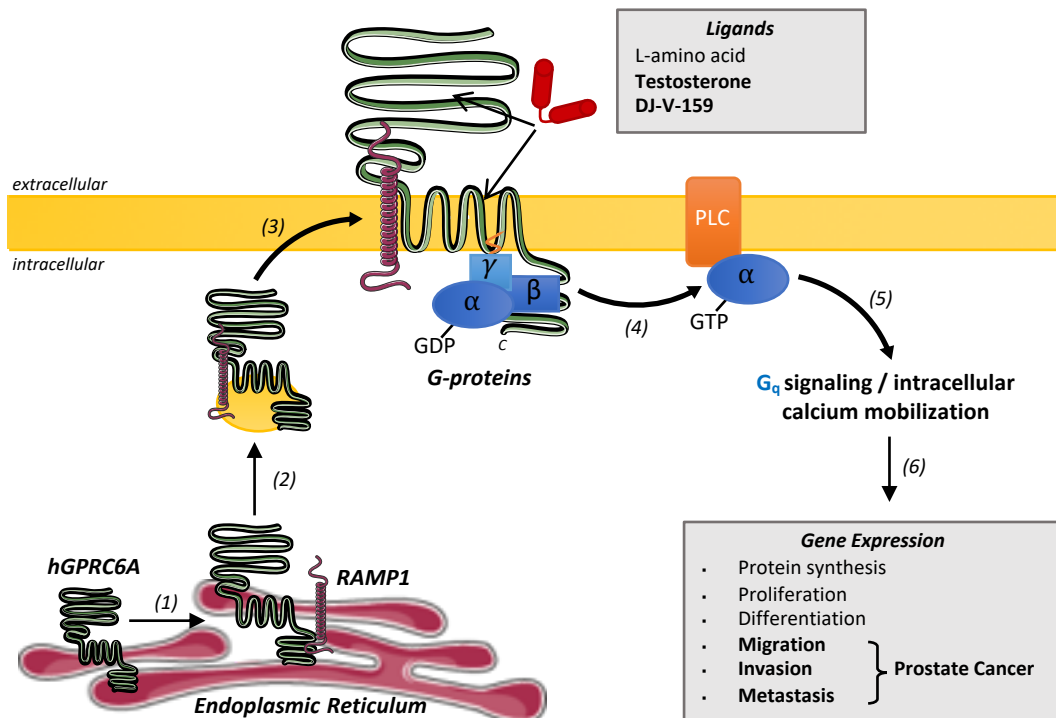


Figure 5.1 Proposed model for human GPRC6A and RAMP1 trafficking and signalling; starting from the bottom left (clockwise) **(1)** Translated GPRC6A polypeptide chains are localised to the endoplasmic reticulum (ER) for assembly. Diffusion enables GPRC6A to complex with RAMP1 proteins present at the ER. **(2)** GPRC6A/RAMP1 heterodimers are then packaged into budding trafficking vesicles and sent through the ER and Golgi to allow further post-translational modification (i.e N-glycosylation). **(3)** Mature GPRC6A now reaches the plasma membrane, where it can freely diffuse until homo-dimerization with a pool of GPRC6A. **(4)** Upon extracellular ligand binding (e.g. testosterone), signal transduction allows G protein activation and subsequent activation of membrane-bound effector proteins (i.e. PLC). **(5)** Activation of signalling cascade secondary messengers result in the activation of transcription factors and gene regulation. **(6)** Resultant gene expression initiates cellular proliferation and differentiation, etc. Aberrant expression of these processes can lead to tumorigenesis and ultimately metastasis.

5.1.2 CHO-K1 GPRC6A/RAMP1 Overexpression System.

It's important to note the study designed using a CHO-K1 GPRC6A and RAMP1 overexpression system. Given the receptor's famously low expression (Wellendorph *et al.*, 2005), this approach enabled successful identification of receptor/RAMP complexes at the surface and permitted measurable signal in our biochemical assays. Overexpression experiments are most useful for identifying novel protein and studying their function in a qualitative manner (Andréll & Tate, 2013). Four primary mechanisms of cellular defects as a result of protein overexpression; resource overload, stoichiometric imbalance, promiscuous interactions, and pathway modulation (Moriya, 2015). Protein overexpression has been shown to burden cellular machinery involved in protein assembly (P. Shah *et al.*, 2013). Overexertion of this apparatus could impair or impede its function to synthesize other important proteins. Furthermore, other energy-dependent

components of successful protein production may become hampered such as gene 'reading', protein maturation, transportation and recycling (Bolognesi & Lehner, 2018; A. M. Rice & McLysaght, 2017). These changes in cell growth can largely be explained by resource overload and toxicity (Tomala *et al.*, 2014). Protein overexpression creates an abnormal cellular environment through enhanced metabolic activity and/or turnover. Moreover, the introduction of an exogenous protein in abundance can often lead to a stoichiometric imbalance resulting in toxicity through promiscuous interactions and/or pathway modulation (Moriya, 2015).

Therefore, future studies would benefit greatly from the inclusion of hGPCR6A native systems to investigate the role of RAMP1 in hGPCR6A-mediated signalling under more physiological conditions. In both COS-7 and CHO-K1 GPCR6A and RAMP1 were overexpressed; this approach allowed for rapid identification of GPCR6A and RAMP1 co-localisation, surface expression and signalling. However, for the reasons stated above; protein aggregation, mis-localisation and pathway modulation could be participating factors in the data collected here. Due to this the inclusion of native endogenously expressing systems in combination with the KO strategy (i.e. PC3 RAMP1^{-/-}) would provide a more physiologically relevant insight into RAMP1 role in GPCR6A-mediated signalling. Nonetheless, no approach is without its caveats and concerns of using an overexpressing system are seen as negligibly different from those associated with an alternate mutant background; be it, gene KO or a gain-of-function mutations (Prelich, 2012).

5.1.3 *GPCR6A Downstream Signalling Profile.*

Here we have comprehensively demonstrated that both the mouse and human receptor are able to initiate downstream $G\alpha_q$ coupled responses to L-amino acids, with L-Orn, L-Arg, L-Ala and L-Lys as agonists. The data here suggests that RAMP1 is a fundamental requirement to facilitate successful hGPCR6A signalling. These findings are in concordance with previously published data showing GPCR6A to be a promiscuous L-amino acid-sensing receptor, without the need of co-expressing the permutated $G\alpha_{q(G66D)}$ protein as a requisite to elicit these responses (Jacobsen *et al.*, 2013; S. Jørgensen *et al.*, 2017; Rueda *et al.*, 2016; Petrine Wellendorph *et al.*, 2007). GPCR6A has emerged in

recent years as an interesting target due to its reported sensitivity to ligands; testosterone and Ocn (Pi *et al.*, 2011, 2015, 2016; Pi, Parrill, *et al.*, 2010). The vast majority of data has focussed towards the murine variant of the receptor; with groups reporting distinct GPRC6A-dependent differences in physiology (Ko *et al.*, 2014; Oury *et al.*, 2011; Pi, Parrill, *et al.*, 2010; Pi & Quarles, 2012a; Ye *et al.*, 2017). However, when attempting to replicate these findings *in vitro*, discrepancies begin to emerge with groups reporting no agonist activity (Jacobsen *et al.*, 2013). From our investigations, we were not able to confirm the reported $G\alpha_q$ responses mediated by the mouse receptor in response to testosterone or Ocn stimulation (Figure 3.5). This was also true of the human receptor when expressed alone. In our study, only when the human receptor was co-expressed with RAMP1 did we see robust dose-dependent response to testosterone (Figure 3.5). Moreover, by further biochemical investigation we demonstrate these responses to be specifically mediated through the hGPRC6A receptor via $G\alpha_q$ coupling (Figure 3.6). Thus, our data in part agrees with the groups Christiansen *et al.*, (2007); Jacobsen *et al.*, (2013); P. Wellendorph & Bräuner-Osborne, (2009); P Wellendorph *et al.*, (2005; 2007) and Rueda *et al.*, (2016), failing to show testosterone or Ocn sensitivity in the mouse or human receptor. The findings here show marked differences between the mouse and human receptor when concerning GPRC6A's testosterone sensitivity; demonstrating RAMP1 to be an essential component for functional hGPRC6A signalling. The necessity for sufficient RAMP1 tissue expression may be a fundamental explanation for the discrepancies seen in the literature.

It is also important to note we recorded small responses in intracellular calcium mobilisation when stimulating with uncarboxylated-Ocn. As mentioned in chapter 4, the magnitude of these responses provides insufficient evidence of targeted hGPRC6A-mediated calcium mobilisation, and thus from this data set it is unsuitable to classify Ocn as a putative agonist of this receptor. This is largely concordant with data published concerning the mouse receptor, agreeing with the Christiansen *et al.*, (2007); Jacobsen *et al.*, (2013); P Wellendorph *et al.*, (2005) and Rueda *et al.*, (2016); reporting negligible responses in calcium mobilisation or IP_3 accumulation. Further investigation is required using a variety of signalling assay to accurately classify Ocn as an hGPRC6A agonist.

The major findings here suggest the mouse and human GPRC6A possess distinctly different pharmacological profiles; with the latter requiring the presence of RAMP1 in order to form a functional receptor. This disparity between the two species variants may explain some of the differences seen in the literature. A large portion of our knowledge concerning the GPRC6A has stemmed from phenotypic *in vivo* KO studies in an attempt to assess the receptor's physiological role. This approach has produced large discrepancies through the generation of different KO models and focused subsequent investigations towards the murine variant (C. V. Jørgensen et al., 2019; Pi et al., 2008; Petrine Wellendorph et al., 2009; Ye et al., 2017). Here, our data suggests mouse and human receptors behave fundamentally differently and make cross-species comparison increasingly difficult.

Further investigation shows responses to DHEA and the computationally identified GPRC6A agonist; DJ-V-159 (Pi, *et al.* 2018). Again, responses in both $G\alpha_q$ and $G\alpha_s$ were only seen when hGPRC6A was co-expressed with the RAMP1 protein (Figure 3.5, Figure 3.6, Figure 3.8 & Figure 3.9). Minimal modulation of the $G\alpha_s$ or $G\alpha_i$ pathways was observed with L-amino acids, testosterone or Ocn (Figure 3.7 & Figure 3.9) supporting the idea that recombinant hGPRC6A is primarily a $G\alpha_q$ coupled receptor. These data are largely concordant with the findings of Jacobsen *et al.* (2013) and Rueda *et al.* (2016), who drew similar conclusions for the mGPRC6A recombinantly expressed in CHO-K1 and HEK293 cells, respectively. Data produced has revealed complexing with RAMP1 infers additional functionality; extending the range of ligands capable of activating this receptor.

Since the receptors cloning, a multitude of studies have contributed knowledge towards GPRC6A expression pattern, distribution and pharmacological profile. Reports have shown the rat GPRC6A forms disulphide-linked homodimers and is constitutively internalised (Norskov-Lauritsen, *et al.* 2015; Jacobsen, *et al.* 2017). Phenotypic *in vivo* data has failed to elucidate the physiological function of GPRC6A as the different exon KO have produced different phenotypic responses of which remained unconfirmed by independent research groups. Recently published data using the full locus mGPRC6A KO model have demonstrated similar phenotypic changes to that of the exon VI KO model with respect to bone and metabolism (Clemmensen, *et al.* 2017; Jorgensen, *et al.* 2019).

Other studies indicate a role of GPRC6A in male reproduction and prostate cancer, and will be important to validate in other groups/mouse models before firm conclusions can be drawn. However, it is important to note these studies were conducted using the murine receptor and considerations must be made concerning the translational value to the human receptor.

Interestingly, on top of the recent publications by the Bräuner-Osborne group (2019) revealing a indel in the ICL-3 causing the intracellular retention of the hGPRC6A; hundreds of additional SNPs have been reported in the hGPRC6A gene (Lek et al., 2016). This data provides an ideal foundation for working with large human cohorts to reveal the associations of GPRC6A and various phenotypes. The major advantage here being much greater population sizes in comparison to previous mouse studies and directly addressing human relevance. With this grounding, resultant phenotypes can be assessed in mice to discern mechanisms and evaluate if the murine models hold real translational value. Furthermore, with the emergence of novel SNP screening, future studies would benefit greatly from cross referencing notable mutant variants with the mechanistic GPRC6A characteristics – i.e. cell surface expression and degree of intracellular signalling. This would enable honing in on specific SNPs, identifying their physiological and clinical relevance. As stated in chapter 4, section 4.1.2.2, cross referencing of GPRC6A SNP rs339331 in particular with GPRC6A responsiveness to testosterone may strengthen the association with prostate cancer.

5.1.4 *GPRC6A & RAMP1 in Prostate Cancer*

Prostate cancer is now rapidly becoming ever more prevalent worldwide, with a fifth of those fatal diagnosed (Rawla, 2019). Over the past decade, huge advances have been made in identifying the molecular mechanisms behind prostate cancer and its associated risk factors; this has led to vast improvements in diagnosis, treatment and overall survival rates (Gatta *et al.*, 2014; Lloyd *et al.*, 2015). However, despite it still remains the second leading cause of death in the US (Rawla, 2019). A subset of this group that has failed to yield any major clinical improvements, are that of hormone-refractory prostate cancers, with patients often presenting with relapsing tumours that are resistant to current anti-

androgen therapies and develop metastases leading to a median survival time of 9-12 months (Cattrini *et al.*, 2019; Tamada *et al.*, 2018). Research has shown that late-stage androgen-resistance carcinomas still pose as an unmet clinical need requiring alternative novel treatment modalities, estimating all patients with anti-androgen therapy resistant prostate cancer are currently enrolled in clinical trials (Heidenreich *et al.*, 2014a, 2014b). Published data in tandem with GWAS has implicated GPRC6A and RAMP1 as the link between hormonal factors and prostate cancer risk (Logan *et al.*, 2013; Long *et al.*, 2012; Pi & Quarles, 2012a; Takata *et al.*, 2010; Ye *et al.*, 2017). As previously stated in section 4.1.2.2, the association with GPRC6A and prostate cancer has been shown across Japanese, Chinese, African and European cohorts; all demonstrating the increased risk of prostate cancer development. providing an alternate molecular mechanism by which androgen-insensitive carcinoma continue to progress under current therapies.

In addition to our novel findings demonstrating RAMP1's necessity in hGPRC6A forward trafficking and signalling capabilities; we have also shown PC-3 cell testosterone sensitivity partially mediated through the hGPRC6A receptor (Figure 4.4Figure 4.5). These results may provide an explanation for late-stage hormone refractory prostate cancer progression, offering a novel mechanism by which these tumours can utilise androgen growth factors without the expression of the classical ARs. With the increasing number of reports showing the involvement of GPRC6A in prostate along with our groups previous findings of RAMP1 necessity for its progression *in vitro* and *in vivo* (Figure 4.2Figure 4.3), it can be argued that both play a synergistic role in late-stage androgen insensitive prostate cancer.

5.1.5 Conclusions.

In summary, we have conducted a fundamental pharmacological evaluation of the hGPRC6A and shown RAMP1 to be an integral part of the receptor molecular machinery. Our cells' responses to testosterone are robust and consistent with KO mouse phenotypes. The finding of an important role for RAMP1 in GPRC6A signalling could potentially bridge the gap between current controversies the field faces. Furthermore, we propose, the GPRC6A/RAMP1 receptor may play an important role in prostate cancer

tumorigenesis and metastasis. Deletion of RAMP1 leads to a downregulation of GPRC6A ability to mediated downstream PC-3 signalling, as well as attenuate tumorigenic characteristics *in vitro* and *in vivo*. Our data, taken together with other findings linking GPRC6A and RAMP1 with progression of other cancers, opens up this receptor for future therapeutic exploitation and implies value for agents that can modulate function of the heteromeric receptor complex.

References.

- Adan, A., Alizada, G., Kiraz, Y., Baran, Y., & Nalbant, A. (2017). Flow cytometry: basic principles and applications. In *Critical Reviews in Biotechnology* (Vol. 37, Issue 2, pp. 163–176). Taylor and Francis Ltd. <https://doi.org/10.3109/07388551.2015.1128876>
- Ahn, S., Shenoy, S. K., Wei, H., & Lefkowitz, R. J. (2004). Differential kinetic and spatial patterns of β -arrestin and G protein-mediated ERK activation by the angiotensin II receptor. *Journal of Biological Chemistry*, 279(34), 35518–35525. <https://doi.org/10.1074/jbc.M405878200>
- Aittaleb, M., Boguth, C. A., & Tesmer, J. J. G. (2010). Structure and function of heterotrimeric G protein-regulated Rho guanine nucleotide exchange factors. In *Molecular Pharmacology* (Vol. 77, Issue 2, pp. 111–125). American Society for Pharmacology and Experimental Therapeutics. <https://doi.org/10.1124/mol.109.061234>
- Alamshah, A., MCGavigan, A. K., Spreckley, E., Kinsey-Jones, J. S., Amin, A., Tough, I. R., O'hara, H. C., Moolla, A., Banks, K., France, R., Hyberg, G., Norton, M., Cheong, W., Lehmann, A., Bloom, S. R., Cox, H. M., & Murphy, K. G. (n.d.). *L-Arginine promotes gut hormone release and reduces food intake in rodents. Running title: L-arginine on food intake in rodents.*
- Alexander, S. P. H., Benson, H. E., Faccenda, E., Pawson, A. J., Sharman, J. L., Spedding, M., Peters, J. A., & Harmar, A. J. (2013). The concise guide to PHARMACOLOGY 2013/14: G protein-coupled receptors. *British Journal of Pharmacology*, 170(8), 1459–1581. <https://doi.org/10.1111/bph.12445>
- Ali, E. S., Hua, J., Wilson, C. H., Tallis, G. A., Zhou, F. H., Rychkov, G. Y., & Barritt, G. J. (2008). Biochimica et Biophysica Acta The glucagon-like peptide-1 analogue exendin-4 reverses impaired intracellular Ca²⁺ signalling in steatotic hepatocytes. *BBA - Molecular Cell Research*, 1863(9), 2135–2146. <https://doi.org/10.1016/j.bbamcr.2016.05.006>
- Alimirah, F., Chen, J., Basrawala, Z., Xin, H., & Choubey, D. (2006). DU-145 and PC-3 human prostate cancer cell lines express androgen receptor: Implications for the androgen receptor functions and regulation. *FEBS Letters*, 580(9), 2294–2300. <https://doi.org/10.1016/j.febslet.2006.03.041>
- Andréll, J., & Tate, C. G. (2013). Overexpression of membrane proteins in mammalian cells for structural studies. *Molecular Membrane Biology*, 30(1), 52–63.

<https://doi.org/10.3109/09687688.2012.703703>

- Anselmo, A., Mazzon, C., Borroni, E. M., Bonecchi, R., Graham, G. J., & Locati, M. (2014). Flow cytometry applications for the analysis of chemokine receptor expression and function. *Cytometry Part A*, *85*(4), 292–301. <https://doi.org/10.1002/cyto.a.22439>
- Ardura, J. A., Álvarez-Carrión, L., Gutiérrez-Rojas, I., & Alonso, V. (2020). Role of calcium signaling in prostate cancer progression: Effects on cancer hallmarks and bone metastatic mechanisms. In *Cancers* (Vol. 12, Issue 5). MDPI AG. <https://doi.org/10.3390/cancers12051071>
- Armstrong, J. F., Faccenda, E., Harding, S. D., Pawson, A. J., Southan, C., Sharman, J. L., Campo, B., Cavanagh, D. R., Alexander, S. P. H., Davenport, A. P., Spedding, M., & Davies, J. A. (2020). The IUPHAR/BPS Guide to PHARMACOLOGY in 2020: Extending immunopharmacology content and introducing the IUPHAR/MMV Guide to MALARIA PHARMACOLOGY. *Nucleic Acids Research*, *48*(D1), D1006–D1021. <https://doi.org/10.1093/nar/gkz951>
- Arnold, J. T., Gray, N. E., Jacobowitz, K., Viswanathan, L., Cheung, P. W., McFann, K. K., Le, H., & Blackman, M. R. (2008). Human prostate stromal cells stimulate increased PSA production in DHEA-treated prostate cancer epithelial cells. *Journal of Steroid Biochemistry and Molecular Biology*, *111*(3–5), 240–246. <https://doi.org/10.1016/j.jsbmb.2008.06.008>
- Arnold, J. T., Le, H., McFann, K. K., & Blackman, M. R. (2005). Comparative effects of DHEA vs. testosterone, dihydrotestosterone, and estradiol on proliferation and gene expression in human LNCaP prostate cancer cells. *American Journal of Physiology - Endocrinology and Metabolism*, *288*(3 51-3). <https://doi.org/10.1152/ajpendo.00454.2004>
- Asuthkar, S., Velpula, K. K., Elustondo, P. A., Demirkhanyan, L., & Zakharian, E. (2015). TRPM8 channel as a novel molecular target in androgen-regulated prostate cancer cells. *Oncotarget*, *6*(19), 17221–17236. <https://doi.org/10.18632/oncotarget.3948>
- Bacart, J., Corbel, C., Jockers, R., Bach, S., & Couturier, C. (2008). The BRET technology and its application to screening assays. In *Biotechnology Journal* (Vol. 3, Issue 3, pp. 311–324). Biotechnol J. <https://doi.org/10.1002/biot.200700222>
- Bai, M., Trivedi, S., & Brown, E. M. (1998). Dimerization of the extracellular calcium-sensing receptor (CaR) on the cell surface of CaR-transfected HEK293 cells. *Journal*

- of Biological Chemistry*, 273(36), 23605–23610.
<https://doi.org/10.1074/jbc.273.36.23605>
- Bailey, R. J., & Hay, D. L. (2007). Agonist-dependent consequences of proline to alanine substitution in the transmembrane helices of the calcitonin receptor. *British Journal of Pharmacology*, 151(5), 678–687. <https://doi.org/10.1038/sj.bjp.0707246>
- Baird, G. S., Zacharias, D. A., & Tsien, R. Y. (2000). Biochemistry, mutagenesis, and oligomerization of DsRed, a red fluorescent protein from coral. *Proceedings of the National Academy of Sciences of the United States of America*, 97(22), 11984–11989. <https://doi.org/10.1073/pnas.97.22.11984>
- Barbash, S., Lorenzen, E., Persson, T., Huber, T., & Sakmar, T. P. (2017). *GPCRs globally coevolved with receptor activity-modifying proteins, RAMPs*. 114(45), 12015–12020. <https://doi.org/10.1073/pnas.1713074114>
- Barnes, L. M., Bentley, C. M., & Dickson, A. J. (2003). Stability of protein production from recombinant mammalian cells. In *Biotechnology and Bioengineering* (Vol. 81, Issue 6, pp. 631–639). <https://doi.org/10.1002/bit.10517>
- Barrangou, R., Fremaux, C., Deveau, H., Richards, M., Boyaval, P., Moineau, S., Romero, D. A., & Horvath, P. (2007). CRISPR provides acquired resistance against viruses in prokaryotes. *Science*, 315(5819), 1709–1712.
<https://doi.org/10.1126/science.1138140>
- Basith, S., Cui, M., Macalino, S. J. Y., Park, J., Clavio, N. A. B., Kang, S., & Choi, S. (2018). Exploring G protein-coupled receptors (GPCRs) ligand space via cheminformatics approaches: Impact on rational drug design. In *Frontiers in Pharmacology* (Vol. 9, Issue MAR, p. 128). Frontiers Media S.A. <https://doi.org/10.3389/fphar.2018.00128>
- Baumgart, S., Schulz, A. R., Peddinghaus, A., Stanislawiak, S., Gillert, S., Hirseland, H., Krauthäuser, S., Dose, C., Mei, H. E., & Grützkau, A. (2017). Dual-labelled antibodies for flow and mass cytometry: A new tool for cross-platform comparison and enrichment of target cells for mass cytometry. *European Journal of Immunology*, 47(8), 1377–1385. <https://doi.org/10.1002/eji.201747031>
- Beer, T. M., Armstrong, A. J., Rathkopf, D. E., Lorient, Y., Sternberg, C. N., Higano, C. S., Iversen, P., Bhattacharya, S., Carles, J., Chowdhury, S., Davis, I. D., De Bono, J. S., Evans, C. P., Fizazi, K., Joshua, A. M., Kim, C. S., Kimura, G., Mainwaring, P., Mansbach, H., ... Tombal, B. (2014). Enzalutamide in metastatic prostate cancer

- before chemotherapy. *New England Journal of Medicine*, 371(5), 424–433.
<https://doi.org/10.1056/NEJMoa1405095>
- Beerepoot, P., Lam, V. M., & Salahpour, A. (2013). Measurement of G protein-coupled receptor surface expression. *Journal of Receptors and Signal Transduction*, 33(3), 162–165. <https://doi.org/10.3109/10799893.2013.781625>
- Bhasin, S., & Jasuja, R. (2009). Selective androgen receptor modulators as function promoting therapies. In *Current Opinion in Clinical Nutrition and Metabolic Care* (Vol. 12, Issue 3, pp. 232–240). Curr Opin Clin Nutr Metab Care.
<https://doi.org/10.1097/MCO.0b013e32832a3d79>
- Bluemn, E. G., Coleman, I. M., Lucas, J. M., Coleman, R. T., Hernandez-Lopez, S., Tharakan, R., Bianchi-Frias, D., Dumpit, R. F., Kaipainen, A., Corella, A. N., Yang, Y. C., Nyquist, M. D., Mostaghel, E., Hsieh, A. C., Zhang, X., Corey, E., Brown, L. G., Nguyen, H. M., Pienta, K., ... Nelson, P. S. (2017). Androgen Receptor Pathway-Independent Prostate Cancer Is Sustained through FGF Signaling. *Cancer Cell*, 32(4), 474–489.e6. <https://doi.org/10.1016/j.ccell.2017.09.003>
- Bogdanove, A. J., & Voytas, D. F. (2011). TAL effectors: Customizable proteins for DNA targeting. In *Science* (Vol. 333, Issue 6051, pp. 1843–1846). American Association for the Advancement of Science. <https://doi.org/10.1126/science.1204094>
- Bolognesi, B., & Lehner, B. (2018). Reaching the limit. In *eLife* (Vol. 7).
<https://doi.org/10.7554/eLife.39804>
- Bouschet, T., Martin, S., & Henley, J. M. (2005). Receptor-activity-modifying proteins are required for forward trafficking of the calcium-sensing receptor to the plasma membrane. *Journal of Cell Science*, 118(20), 4709–4720.
<https://doi.org/10.1242/jcs.02598>
- Bouschet, T., Martin, S., & Henley, J. M. (2008). *Regulation of calcium-sensing-receptor trafficking and cell- surface expression by GPCRs and RAMPs*. 29(12), 633–639.
<https://doi.org/10.1016/j.tips.2008.09.002>.Regulation
- Bouschet, T., Martin, S., & Henley, J. M. (2012). Regulation of Calcium Sensing Receptor Trafficking by RAMPs. In W. S. Spielman & N. Parameswaran (Eds.), *RAMPs* (pp. 39–48). Springer US. https://doi.org/10.1007/978-1-4614-2364-5_4
- Brauner-Osborne, H., Wellendorph, P., & Jensen, A. (2007). Structure, Pharmacology and Therapeutic Prospects of Family C G-Protein Coupled Receptors. *Current Drug*

- Targets*. <https://doi.org/10.2174/138945007779315614>
- Bubendorf, L., Schöpfer, A., Wagner, U., Sauter, G., Moch, H., Willi, N., Gasser, T. C., & Mihatsch, M. J. (2000). Metastatic patterns of prostate cancer: An autopsy study of 1,589 patients. *Human Pathology*, *31*(5), 578–583.
<https://doi.org/10.1053/hp.2000.6698>
- Burns, D. L. (1988). Subunit structure and enzymic activity of pertussis toxin. *Microbiological Sciences*, *5*(9), 285–287.
<http://www.ncbi.nlm.nih.gov/pubmed/2908558>
- Bystrova, M. F., Romanov, R. A., Rogachevskaja, O. A., Churbanov, G. D., & Kolesnikov, S. S. (2010). Functional expression of the extracellular-Ca²⁺-sensing receptor in mouse taste cells. *Journal of Cell Science*, *123*(6), 972–982.
<https://doi.org/10.1242/jcs.061879>
- Cabrera-vera, T. M., Vanhauwe, J., Thomas, T. O., Medkova, M., Preininger, A., Mazzone, M. R., Hamm, H. E., Pharmacology, M., & C, B. C. T. M. (2018). *Insights into G Protein Structure, Function, and Regulation*. *24*(July), 765–781.
<https://doi.org/10.1210/er.2000-0026>
- Campbell, A. P., & Smrcka, A. V. (2018). Targeting G protein-coupled receptor signalling by blocking G proteins. In *Nature Reviews Drug Discovery* (Vol. 17, Issue 11, pp. 789–803). Nature Publishing Group. <https://doi.org/10.1038/nrd.2018.135>
- Carpenter, B., Nehmé, R., Warne, T., Leslie, A. G. W., & Tate, C. G. (2016). Structure of the adenosine A2A receptor bound to an engineered G protein. *Nature*, *536*(7614), 104–107. <https://doi.org/10.1038/nature18966>
- Carter, A. A., & Hill, S. J. (2005). Characterization of isoprenaline- and salmeterol-stimulated interactions between β 2-adrenoceptors and β -arrestin 2 using β -galactosidase complementation in C2C12 cells. *Journal of Pharmacology and Experimental Therapeutics*, *315*(2), 839–848.
<https://doi.org/10.1124/jpet.105.088914>
- Cattrini, C., Castro, E., Lozano, R., Zanardi, E., Rubagotti, A., Boccardo, F., & Olmos, D. (2019). Current treatment options for metastatic hormone-sensitive prostate cancer. In *Cancers* (Vol. 11, Issue 9). MDPI AG.
<https://doi.org/10.3390/cancers11091355>
- Cavanaugh, A., McKenna, J., Stepanchick, A., & Breitwieser, G. E. (2010). Calcium-sensing

- receptor biosynthesis includes a cotranslational conformational checkpoint and endoplasmic reticulum retention. *Journal of Biological Chemistry*, 285(26), 19854–19864. <https://doi.org/10.1074/jbc.M110.124792>
- Cegla, J., Jones, B. J., Gardiner, J. V., Hodson, D. J., Marjot, T., McGlone, E. R., Tan, T. M., & Bloom, S. R. (2017). RAMP2 influences glucagon receptor pharmacology via trafficking and signaling. *Endocrinology*, 158(8), 2680–2693. <https://doi.org/10.1210/en.2016-1755>
- Cermak, T., Doyle, E. L., Christian, M., Wang, L., Zhang, Y., Schmidt, C., Baller, J. A., Somia, N. V., Bogdanove, A. J., & Voytas, D. F. (2011). Efficient design and assembly of custom TALEN and other TAL effector-based constructs for DNA targeting. *Nucleic Acids Research*, 39(12). <https://doi.org/10.1093/nar/gkr218>
- Chamouni, A., & Oury, F. (2014). Reciprocal interaction between bone and gonads. *Archives of Biochemistry and Biophysics*, 561, 147–153. <https://doi.org/10.1016/j.abb.2014.06.016>
- Charpentier, T. H., Waldo, G. L., Lowery-Gionta, E. G., Krajewski, K., Strahl, B. D., Kash, T. L., Harden, T. K., & Sondek, J. (2016). Potent and selective peptide-based inhibition of the G protein Gαq. *Journal of Biological Chemistry*, 291(49), 25608–25616. <https://doi.org/10.1074/jbc.M116.740407>
- Cheng, S. Bin, Graeber, C. T., Quinn, J. A., & Filardo, E. J. (2011). Retrograde transport of the transmembrane estrogen receptor, G-protein-coupled-receptor-30 (GPR30/GPER) from the plasma membrane towards the nucleus. *Steroids*, 76(9), 892–896. <https://doi.org/10.1016/j.steroids.2011.02.018>
- Christiansen, B., Hansen, K., Wellendorph, P., & Bräuner-Osborne, H. (2007). Pharmacological characterization of mouse GPRC6A, an L-a-amino-acid receptor modulated by divalent cations. *British Journal of Pharmacology*, 150, 798–807. <https://doi.org/10.1038/sj.bjp.0707121>
- Christopoulos, A., Christopoulos, G., Morfis, M., Udawela, M., Laburthe, M., Couvineau, A., Kuwasako, K., Tilakaratne, N., & Sexton, P. M. (2002). *Novel Receptor Partners and Function of Receptor Activity-modifying Proteins**. <https://doi.org/10.1074/jbc.C200629200>
- Christopoulos, A., Christopoulos, G., Morfis, M., Udawela, M., Laburthe, M., Couvineau, A., Kuwasako, K., Tilakaratne, N., & Sexton, P. M. (2003). Novel receptor partners

- and function of receptor activity-modifying proteins. *Journal of Biological Chemistry*, 278(5), 3293–3297. <https://doi.org/10.1074/jbc.C200629200>
- Chun, L., Zhang, W. H., & Liu, J. F. (2012). Structure and ligand recognition of class C GPCRs. In *Acta Pharmacologica Sinica* (Vol. 33, Issue 3, pp. 312–323). Nature Publishing Group. <https://doi.org/10.1038/aps.2011.186>
- Ciolino, H., MacDonald, C., Memon, O., Dankwah, M., & Yeh, G. C. (2003). Dehydroepiandrosterone inhibits the expression of carcinogen-activating enzymes in vivo. *International Journal of Cancer*, 105(3), 321–325. <https://doi.org/10.1002/ijc.11075>
- Clemmensen, C., Smajilovic, S., Wellendorph, P., & Bräuner-Osborne, H. (2014). The GPCR, class C, group 6, subtype A (GPC6A) receptor: From cloning to physiological function. In *British Journal of Pharmacology*. <https://doi.org/10.1111/bph.12365>
- Clemmensen, Christoffer, Smajilovic, S., Madsen, A. N., Klein, A. B., Holst, B., & Bräuner-Osborne, H. (2013). Increased susceptibility to diet-induced obesity in GPCR6A receptor knockout mice. *Journal of Endocrinology*, 217, 151–160. <https://doi.org/10.1530/JOE-12-0550>
- Cong, L., Ran, F. A., Cox, D., Lin, S., Barretto, R., Habib, N., Hsu, P. D., Wu, X., Jiang, W., Marraffini, L. A., & Zhang, F. (2013). Multiplex genome engineering using CRISPR/Cas systems. *Science*, 339(6121), 819–823. <https://doi.org/10.1126/science.1231143>
- Conti, M., Mika, D., & Richter, W. (2014). Cyclic AMP compartments and signaling specificity: Role of cyclic nucleotide phosphodiesterases. In *Journal of General Physiology* (Vol. 143, Issue 1, pp. 29–38). The Rockefeller University Press. <https://doi.org/10.1085/jgp.201311083>
- Cossarizza, A., Chang, H. D., Radbruch, A., Akdis, M., Andrä, I., Annunziato, F., Bacher, P., Barnaba, V., Battistini, L., Bauer, W. M., Baumgart, S., Becher, B., Beisker, W., Berek, C., Blanco, A., Borsellino, G., Boulais, P. E., Brinkman, R. R., Büscher, M., ... Zimmermann, J. (2017). Guidelines for the use of flow cytometry and cell sorting in immunological studies. *European Journal of Immunology*, 47(10), 1584–1797. <https://doi.org/10.1002/eji.201646632>
- Culig, Z., Hobisch, A., Cronauer, M. V., Radmayr, C., Trapman, J., Hittmair, A., Bartsch, G., & Klocker, H. (1994). Androgen Receptor Activation in Prostatic Tumor Cell Lines by

Insulin-like Growth Factor-I, Keratinocyte Growth Factor, and Epidermal Growth Factor. *Cancer Research*, 54(20).

De Bono, J. S., Logothetis, C. J., Molina, A., Fizazi, K., North, S., Chu, L., Chi, K. N., Jones, R. J., Goodman, O. B., Saad, F., Staffurth, J. N., Mainwaring, P., Harland, S., Flaig, T. W., Hutson, T. E., Cheng, T., Patterson, H., Hainsworth, J. D., Ryan, C. J., ... Scher, H. I. (2011). Abiraterone and increased survival in metastatic prostate cancer. *New England Journal of Medicine*, 364(21), 1995–2005.

<https://doi.org/10.1056/NEJMoa1014618>

De Toni, L., Di Nisio, A., Rocca, M. S., De Rocco Ponce, M., Ferlin, A., & Foresta, C. (2017). Osteocalcin, a bone-derived hormone with important andrological implications. In *Andrology*. <https://doi.org/10.1111/andr.12359>

Derouazi, M., Girard, P., Van Tilborgh, F., Iglesias, K., Muller, N., Bertschinger, M., & Wurm, F. M. (2004). Serum-free large-scale transient transfection of CHO cells. *Biotechnology and Bioengineering*, 87(4), 537–545.

<https://doi.org/10.1002/bit.20161>

Desai, A. (2012). *Novel insights into the interaction of the Calcium Sensing Receptor with the Receptor Activity Modifying Proteins PhD, [submitted as part of PhD thesis] University of Sheffield.*

Desai, A. J., Roberts, D. J., Richards, G. O., & Skerry, T. M. (2014). Role of Receptor Activity Modifying Protein 1 in Function of the Calcium Sensing Receptor in the Human TT Thyroid Carcinoma Cell Line. *PLoS ONE*, 9(1).

<https://doi.org/10.1371/journal.pone.0085237>

Deupi, X., Edwards, P., Singhal, A., Nickle, B., Oprian, D., & Schertler, G. (2011). Stabilized G protein binding site in the structure of constitutively active metarhodopsin-II. *Proceedings of the National Academy of Sciences of the United States of America*, 109(1), 119–124. <https://doi.org/10.1073/pnas.1114089108>

Di Nisio, A., Rocca, M. S., Fadini, G. P., De Toni, L., Marcuzzo, G., Marescotti, M. C., Sanna, M., Plebani, M., Vettor, R., Avogaro, A., & Foresta, C. (2017). The rs2274911 polymorphism in *GPRC6A* gene is associated with insulin resistance in normal weight and obese subjects. *Clinical Endocrinology*, 86(2), 185–191.

<https://doi.org/10.1111/cen.13248>

Doumazane, E., Scholler, P., Zwier, J. M., Trinquet, E., Rondard, P., & Pin, J. (2011). A new

- approach to analyze cell surface protein complexes reveals specific heterodimeric metabotropic glutamate receptors. *The FASEB Journal*, 25(1), 66–77.
<https://doi.org/10.1096/fj.10-163147>
- Dozmorov, M. G., Hurst, R. E., Culkin, D. J., Kropp, B. P., Frank, M. B., Osban, J., Penning, T. M., & Lin, H. K. (2009). Unique patterns of molecular profiling between human prostate cancer LNCaP and PC-3 cells. *Prostate*, 69(10), 1077–1090.
<https://doi.org/10.1002/pros.20960>
- Dreaden, E. C., Gryder, B. E., Austin, L. A., Tene Defo, B. A., Hayden, S. C., Pi, M., Quarles, L. D., Oyelere, A. K., & El-Sayed, M. A. (2012). Antiandrogen gold nanoparticles dual-target and overcome treatment resistance in hormone-insensitive prostate cancer cells. *Bioconjugate Chemistry*, 23(8), 1507–1512.
<https://doi.org/10.1021/bc300158k>
- Dror, R. O., Mildorf, T. J., Hilger, D., Manglik, A., Borhani, D. W., Arlow, D. H., Philippsen, A., Villanueva, N., Yang, Z., Lerch, M. T., Hubbell, W. L., Kobilka, B. K., Sunahara, R. K., & Shaw, D. E. (2015). Structural basis for nucleotide exchange in heterotrimeric G proteins. *Science*, 348(6241), 1361–1365.
<https://doi.org/10.1126/science.aaa5264>
- Du, Y., Duc, N., Rasmussen, S., Hilger, D., Kubiak, X., Wang, L., Bohon, J., Kim, H., Wegrecki, M., Asuru, A., Jeong, K., Lee, J., Chance, M., Lodowski, D., Kobilka, B., & Chung, K. (2019). Assembly of a GPCR-G Protein Complex. *Cell*, 177(5), 1232–1242.e11. <https://doi.org/10.1016/J.CELL.2019.04.022>
- Ducy, P., Desbois, C., Boyce, B., Pinero, G., Story, B., Dunstan, C., Smith, E., Bonadio, J., Goldstein, S., Gundberg, C., Bradley, A., & Karsenty, G. (1996). Increased bone formation in osteocalcin-deficient mice. *Nature*, 382(6590), 448–452.
<https://doi.org/10.1038/382448a0>
- Dupré, D. J., Robitaille, M., Rebois, R. V., & Hébert, T. E. (2009). The role of Gβγ subunits in the organization, assembly, and function of GPCR signaling complexes. In *Annual Review of Pharmacology and Toxicology* (Vol. 49, pp. 31–56). NIH Public Access.
<https://doi.org/10.1146/annurev-pharmtox-061008-103038>
- Edwards, J., & Bartlett, J. M. S. (2005). The androgen receptor and signal-transduction pathways in hormone-refractory prostate cancer. Part 2: Androgen-receptor cofactors and bypass pathways. In *BJU International* (Vol. 95, Issue 9, pp. 1327–

- 1335). *BJU Int.* <https://doi.org/10.1111/j.1464-410X.2005.05527.x>
- Eishingdrelo, H. (2013). Minireview: Targeting GPCR Activated ERK Pathways for Drug Discovery. *Current Chemical Genomics and Translational Medicine*, 7, 9–15. <https://doi.org/10.2174/2213988501307010009>
- Ellisdon, A. M., & Halls, M. L. (2016). Compartmentalization of GPCR signalling controls unique cellular responses. *Biochemical Society Transactions*, 44(2), 562–567. <https://doi.org/10.1042/BST20150236>
- Engvall, E. (1980). [28] Enzyme Immunoassay ELISA and EMIT. *Methods in Enzymology*, 70(C), 419–439. [https://doi.org/10.1016/S0076-6879\(80\)70067-8](https://doi.org/10.1016/S0076-6879(80)70067-8)
- Evans, C. P., Higano, C. S., Keane, T., Andriole, G., Saad, F., Iversen, P., Miller, K., Kim, C. S., Kimura, G., Armstrong, A. J., Sternberg, C. N., Loriot, Y., de Bono, J., Noonberg, S. B., Mansbach, H., Bhattacharya, S., Perabo, F., Beer, T. M., & Tombal, B. (2016). The PREVAIL Study: Primary Outcomes by Site and Extent of Baseline Disease for Enzalutamide-treated Men with Chemotherapy-naïve Metastatic Castration-resistant Prostate Cancer. *European Urology*, 70(4), 675–683. <https://doi.org/10.1016/j.eururo.2016.03.017>
- Evans, R. M., & Mangelsdorf, D. J. (2014). Nuclear receptors, RXR, and the big bang. In *Cell* (Vol. 157, Issue 1, pp. 255–266). Cell Press. <https://doi.org/10.1016/j.cell.2014.03.012>
- Faure, H., Gorojankina, T., Rice, N., Dauban, P., Dodd, R. H., Bräuner-Osborne, H., Rognan, D., & Ruat, M. (2009). Molecular determinants of non-competitive antagonist binding to the mouse GPRC6A receptor. *Cell Calcium*, 46(5–6), 323–332. <https://doi.org/10.1016/j.ceca.2009.09.004>
- Ferguson, S. (2001). Evolving concepts in G protein-coupled receptor endocytosis: the role in receptor desensitization and signaling. *Pharmacological Reviews*, 53(1), 1–24.
- Ferron, M., Wei, J., Yoshizawa, T., Fattore, A. Del, Ronald, A., Teti, A., Ducy, P., & Karsenty, G. (2010). Insulin signaling in osteoblasts integrates bone remodeling and energy metabolism. *Cell*, 142(2), 296–308. <https://doi.org/10.1016/j.cell.2010.06.003>
- Filardo, E., Quinn, J., Pang, Y., Graeber, C., Shaw, S., Dong, J., & Thomas, P. (2007). Activation of the novel estrogen receptor G protein-coupled receptor 30 (GPR30) at

- the plasma membrane. *Endocrinology*. <https://doi.org/10.1210/en.2006-1605>
- Fizazi, K., Scher, H. I., Molina, A., Logothetis, C. J., Chi, K. N., Jones, R. J., Staffurth, J. N., North, S., Vogelzang, N. J., Saad, F., Mainwaring, P., Harland, S., Goodman, O. B., Sternberg, C. N., Li, J. H., Kheoh, T., Haqq, C. M., & de Bono, J. S. (2012). Abiraterone acetate for treatment of metastatic castration-resistant prostate cancer: Final overall survival analysis of the COU-AA-301 randomised, double-blind, placebo-controlled phase 3 study. *The Lancet Oncology*, *13*(10), 983–992. [https://doi.org/10.1016/S1470-2045\(12\)70379-0](https://doi.org/10.1016/S1470-2045(12)70379-0)
- Fizazi, K., Shore, N., Tammela, T. L., Ulys, A., Vjaters, E., Polyakov, S., Jievaltas, M., Luz, M., Alekseev, B., Kuss, I., Kappeler, C., Snapir, A., Sarapohja, T., & Smith, M. R. (2019). Darolutamide in Nonmetastatic, Castration-Resistant Prostate Cancer. *New England Journal of Medicine*, *380*(13), 1235–1246. <https://doi.org/10.1056/NEJMoa1815671>
- Flock, T., Hauser, A. S., Lund, N., Gloriam, D. E., Balaji, S., & Babu, M. M. (2017). Selectivity determinants of GPCR–G-protein binding. *Nature* *2017* *545*:7654, *545*(7654), 317–322. <https://doi.org/10.1038/nature22070>
- Gandía, J., Lluís, C., Ferré, S., Franco, R., & Ciruela, F. (2008). Light resonance energy transfer-based methods in the study of G protein-coupled receptor oligomerization. In *BioEssays* (Vol. 30, Issue 1, pp. 82–89). Bioessays. <https://doi.org/10.1002/bies.20682>
- Gao, G., Williams, J. G., & Campbell, S. L. (2004). Protein-protein interaction analysis by nuclear magnetic resonance spectroscopy. In *Methods in molecular biology (Clifton, N.J.)* (Vol. 261, pp. 79–92). Humana Press. <https://doi.org/10.1385/1-59259-762-9:079>
- Gardella, T. J., & Vilardaga, J.-P. (2015). International Union of Basic and Clinical Pharmacology. XCIII. The Parathyroid Hormone Receptors--Family B G Protein-Coupled Receptors. *Pharmacological Reviews*, *67*(2), 310–337. <https://doi.org/10.1124/pr.114.009464>
- Gatta, G., Mallone, S., van der Zwan, J. M., Trama, A., Siesling, S., Capocaccia, R., Hackl, M., Eycken, E. Van, Henau, K., Hedelin, G., Velten, M., Launoy, G., Guizard, A. V., Bouvier, A. M., Maynadié, M., Woronoff, A. S., Buemi, A., Colonna, M., Ganry, O., ... Steward, J. A. (2014). Cancer survival in Europe 1999-2007 by country and age:

- Results of EURO CARE-5 - A population-based study. *The Lancet Oncology*, 15(1), 23–34. [https://doi.org/10.1016/S1470-2045\(13\)70546-1](https://doi.org/10.1016/S1470-2045(13)70546-1)
- Geib, S., Sandoz, G., Mabrouk, K., Matavel, A., Marchot, P., Hoshi, T., Villaz, M., Ronjat, M., Miquelis, R., Lévêque, C., & De Waard, M. (2002). Use of a purified and functional recombinant calcium-channel $\beta 4$ subunit in surface-plasmon resonance studies. *Biochemical Journal*, 364(1), 285–292. <https://doi.org/10.1042/bj3640285>
- Geng, Y., Mosyak, L., Kurinov, I., Zuo, H., Sturchler, E., Cheng, T. C., Subramanyam, P., Brown, A. P., Brennan, S. C., Mun, H. C., Bush, M., Chen, Y., Nguyen, T. X., Cao, B., Chang, D. D., Quick, M., Conigrave, A. D., Colecraft, H. M., McDonald, P., & Fan, Q. R. (2016). Structural mechanism of ligand activation in human calcium-sensing receptor. *ELife*, 5(JULY), 1–25. <https://doi.org/10.7554/eLife.13662>
- Gerbino, A., Ruder, W. C., Curci, S., Pozzan, T., Zaccolo, M., & Hofer, A. M. (2005). Termination of cAMP signals by Ca^{2+} and Gai via extracellular Ca^{2+} sensors: A link to intracellular Ca^{2+} oscillations. *Journal of Cell Biology*, 171(2), 303–312. <https://doi.org/10.1083/jcb.200507054>
- Gesty-Palmer, D., Chen, M., Reiter, E., Ahn, S., Nelson, C. D., Wang, S., Eckhardt, A. E., Cowan, C. L., Spurney, R. F., Luttrell, L. M., & Lefkowitz, R. J. (2006). Distinct β -arrestin- and G protein-dependent pathways for parathyroid hormone receptor-stimulated ERK1/2 activation. *Journal of Biological Chemistry*, 281(16), 10856–10864. <https://doi.org/10.1074/jbc.M513380200>
- Ghosh, J. G., Nguyen, A. A., Bigelow, C. E., Poor, S., Qiu, Y., Rangaswamy, N., Ornberg, R., Jackson, B., Mak, H., Ezell, T., Kenanova, V., De La Cruz, E., Carrion, A., Etemad-Gilbertson, B., Caro, R. G., Zhu, K., George, V., Bai, J., Sharma-Nahar, R., ... Roguska, M. (2017). Long-acting protein drugs for the treatment of ocular diseases. *Nature Communications*, 8(1), 1–10. <https://doi.org/10.1038/ncomms14837>
- Gibbons, C., Dackor, R., Dunworth, W., Fritz-Six, K., & Caron, K. M. (2007). Receptor activity-modifying proteins: RAMPing up adrenomedullin signaling. In *Molecular Endocrinology* (Vol. 21, Issue 4, pp. 783–796). Oxford Academic. <https://doi.org/10.1210/me.2006-0156>
- Gingell, J. J., Simms, J., Barwell, J., Poyner, D. R., Watkins, H. A., Pioszak, A. A., Sexton, P. M., & Hay, D. L. (2016). An allosteric role for receptor activity-modifying proteins in defining GPCR pharmacology. *Nature Publishing Group*.

- <https://doi.org/10.1038/celldisc.2016.12>
- Givan, A. L. (2011). *Flow Cytometry: An Introduction* (pp. 1–29).
https://doi.org/10.1007/978-1-61737-950-5_1
- Gleave, M. E., Hsieh, J. T., von Eschenbach, A. C., & Chung, L. W. (1992). Prostate and bone fibroblasts induce human prostate cancer growth in vivo: implications for bidirectional tumor-stromal cell interaction in prostate carcinoma growth and metastasis. *The Journal of Urology*, *147*(4), 1151–1159.
[https://doi.org/10.1016/S0022-5347\(17\)37506-7](https://doi.org/10.1016/S0022-5347(17)37506-7)
- Goodman, J., Krupnick, J. G., Santini, F., Gurevich, V. V., Penn, R. B., Gagnon, A. W., Keen, J. H., & Benovic, J. L. (1996). β -Arrestin acts as a clathrin adaptor in endocytosis of the β 2- adrenergic receptor. *Nature*, *383*(6599), 447–450.
<https://doi.org/10.1038/383447a0>
- Graff, J. N., Gordon, M. J., & Beer, T. M. (2015). Safety and effectiveness of enzalutamide in men with metastatic, castration-resistant prostate cancer. In *Expert Opinion on Pharmacotherapy* (Vol. 16, Issue 5, pp. 749–754). Informa Healthcare.
<https://doi.org/10.1517/14656566.2015.1016911>
- Gray, A. C., Raingo, J., & Lipscombe, D. (2007). Neuronal calcium channels: Splicing for optimal performance. *Cell Calcium*, *42*(4–5), 409–417.
<https://doi.org/10.1016/j.ceca.2007.04.003>
- Green, J. E., Shibata, M.-A., Shibata, E., Moon, R. C., Anver, M. R., Kelloff, G., & Lubet, R. (2001). 2-Difluoromethylornithine and Dehydroepiandrosterone Inhibit Mammary Tumor Progression but not Mammary or Prostate Tumor Initiation in C3(1)/SV40 T/t-antigen Transgenic Mice 1. In *CANCER RESEARCH* (Vol. 61).
- Greenberg, N. M., Demayo, F., Finegold, M. J., Medina, D., Tilley, W. D., Aspinall, J. O., Cunha, G. R., Donjacour, A. A., Matusik, R. J., & Rosen, J. M. (1995). Prostate cancer in a transgenic mouse. *Proceedings of the National Academy of Sciences of the United States of America*, *92*(8), 3439–3443.
<https://doi.org/10.1073/pnas.92.8.3439>
- Guo, Y., Pan, W., Liu, S., Shen, Z., Xu, Y., & Hu, L. (2020). ERK/MAPK signalling pathway and tumorigenesis (Review). *Experimental and Therapeutic Medicine*, *19*(3), 1997–2007. <https://doi.org/10.3892/etm.2020.8454>
- Gurevich, V. V., & Gurevich, E. V. (2019). GPCR signaling regulation: The role of GRKs and

- arrestins. *Frontiers in Pharmacology*, 10(FEB), 125.
<https://doi.org/10.3389/fphar.2019.00125>
- Ha Chung, B., Horie, S., & Chiong, E. (2019). The incidence, mortality, and risk factors of prostate cancer in Asian men. In *Prostate International* (Vol. 7, Issue 1, pp. 1–8). Elsevier B.V. <https://doi.org/10.1016/j.pnil.2018.11.001>
- Haid, D. C., Jordan-Biegger, C., Widmayer, P., & Breer, H. (2012). Receptors responsive to protein breakdown products in G-cells and D-cells of mouse, swine and human. *Frontiers in Physiology*, 3 APR(April), 1–15.
<https://doi.org/10.3389/fphys.2012.00065>
- Haid, D., Widmayer, P., & Breer, H. (2011). Nutrient sensing receptors in gastric endocrine cells. *Journal of Molecular Histology*, 42(4), 355–364.
<https://doi.org/10.1007/s10735-011-9339-1>
- Halford, S. E., & Goodall, A. J. (1988). Modes of DNA Cleavage by the EcoRV Restriction Endonuclease. *Biochemistry*, 27(5), 1771–1777.
<https://doi.org/10.1021/bi00405a058>
- Halls, M. L. (2012). Constitutive formation of an RXFP1-signalosome: a novel paradigm in GPCR function and regulation. *British Journal of Pharmacology*, 165(6), 1644–1658.
<https://doi.org/10.1111/j.1476-5381.2011.01470.x>
- Halls, M. L., & Canals, M. (2018). Genetically Encoded FRET Biosensors to Illuminate Compartmentalised GPCR Signalling. In *Trends in Pharmacological Sciences* (Vol. 39, Issue 2, pp. 148–157). Elsevier Ltd. <https://doi.org/10.1016/j.tips.2017.09.005>
- Harikumar, K. G., Simms, J., Christopoulos, G., Sexton, P. M., & Miller, L. J. (2010). THE MOLECULAR BASIS OF ASSOCIATION OF RECEPTOR ACTIVITY-MODIFYING PROTEIN 3 WITH THE FAMILY B G PROTEIN-COUPLED SECRETIN RECEPTOR. *Biochemistry*, 48(49), 11773–11785. <https://doi.org/10.1021/bi901326k>
- Hauschka, P. V., & Carr, S. A. (1982). Calcium-Dependent α -Helical Structure in Osteocalcin. *Biochemistry*, 21(10), 2538–2547.
<https://doi.org/10.1021/bi00539a038>
- Hauser, A. S., Attwood, M. M., Rask-andersen, M., Schiöth, H. B., & Gloriam, D. E. (2017). Trends in GPCR drug discovery : new agents , targets and indications. *Nature Publishing Group*, 16(12), 829–842. <https://doi.org/10.1038/nrd.2017.178>
- Hay, D. L., & Pioszak, A. A. (2016). Receptor Activity-Modifying Proteins (RAMPs): New

- Insights and Roles. *Annual Review of Pharmacology and Toxicology*.
<https://doi.org/10.1146/annurev-pharmtox-010715-103120>
- Heidenreich, A., Bastian, P. J., Bellmunt, J., Bolla, M., Joniau, S., Van Der Kwast, T., Mason, M., Matveev, V., Wiegel, T., Zattoni, F., & Mottet, N. (2014a). EAU Guidelines on Prostate Cancer. Part 1: Screening, Diagnosis, and Local Treatment with Curative Intent-Update 2013. *European Urology*, *65*, 124–137.
<https://doi.org/10.1016/j.eururo.2013.09.046>
- Heidenreich, A., Bastian, P. J., Bellmunt, J., Bolla, M., Joniau, S., Van Der Kwast, T., Mason, M., Matveev, V., Wiegel, T., Zattoni, F., & Mottet, N. (2014b). EAU guidelines on prostate cancer. Part II: Treatment of advanced, relapsing, and castration-resistant prostate cancer. *European Urology*, *65*(2), 467–479.
<https://doi.org/10.1016/j.eururo.2013.11.002>
- Heikal, A. A., Hess, S. T., Baird, G. S., Tsien, R. Y., & Webb, W. W. (2000). Molecular spectroscopy and dynamics of intrinsically fluorescent proteins: Coral red (dsRed) and yellow (Citrine). *Proceedings of the National Academy of Sciences of the United States of America*, *97*(22), 11996–12001.
<https://doi.org/10.1073/pnas.97.22.11996>
- Heinlein, C. A., & Chang, C. (2004). Androgen receptor in prostate cancer. In *Endocrine Reviews* (Vol. 25, Issue 2, pp. 276–308). Oxford Academic.
<https://doi.org/10.1210/er.2002-0032>
- Hepler, J. R., & Gilman, A. G. (1992). G proteins. *Trends in Biochemical Sciences*, *17*(10), 383–387. [https://doi.org/10.1016/0968-0004\(92\)90005-T](https://doi.org/10.1016/0968-0004(92)90005-T)
- Heusinkveld, H. J., & Westerink, R. H. S. (2011). Caveats and limitations of plate reader-based high-throughput kinetic measurements of intracellular calcium levels. *Toxicology and Applied Pharmacology*, *255*(1), 1–8.
<https://doi.org/10.1016/j.taap.2011.05.020>
- Hink, M. A., Griep, R. A., Borst, J. W., Van Hoek, A., Eppink, M. H. M., Schots, A., & Visser, A. J. W. G. (2000). Structural dynamics of green fluorescent protein alone and fused with a single chain Fv protein. *Journal of Biological Chemistry*, *275*(23), 17556–17560. <https://doi.org/10.1074/jbc.M001348200>
- Hislop, J. N., & Von Zastrow, M. (2011). Analysis of GPCR localization and trafficking. *Methods in Molecular Biology*, *746*, 425–440. <https://doi.org/10.1007/978-1->

- Hoang, Q. Q., Sicheri, F., Howard, A. J., & Yang, D. S. C. (2003). Bone recognition mechanism of porcine osteocalcin from crystal structure. *Nature*, *425*(6961), 977–980. <https://doi.org/10.1038/nature02079>
- Hohenegger, M., Waldhoer, M., Beindl, W., Böing, B., Kreimeyer, A., Nickel, P., Nanoff, C., & Freissmuth, M. (1998). G α -selective G protein antagonists. *Proceedings of the National Academy of Sciences of the United States of America*, *95*(1), 346–351. <https://doi.org/10.1073/pnas.95.1.346>
- Hoppe, A., Christensen, K., & Swanson, J. A. (2002). Fluorescence resonance energy transfer-based stoichiometry in living cells. *Biophysical Journal*, *83*(6), 3652–3664. [https://doi.org/10.1016/S0006-3495\(02\)75365-4](https://doi.org/10.1016/S0006-3495(02)75365-4)
- Horoszewicz, J. S., Leong, S. S., Chu, T. M., Wajzman, Z. L., Friedman, M., Papsidero, L., Kim, U., Chai, L. S., Kakati, S., Arya, S. K., & Sandberg, A. A. (1980). The LNCaP cell line—a new model for studies on human prostatic carcinoma. *Progress in Clinical and Biological Research*, *37*, 115–132. <https://europepmc.org/article/med/7384082>
- Hu, G. M., Mai, T. L., & Chen, C. M. (2017). Visualizing the GPCR Network: Classification and Evolution. *Scientific Reports*, *7*(1), 1–15. <https://doi.org/10.1038/s41598-017-15707-9>
- Hu, J., Hauache, O., & Spiegel, A. M. (2000). Human Ca²⁺ receptor cysteine-rich domain: Analysis of function of mutant and chimeric receptors. *Journal of Biological Chemistry*, *275*(21), 16382–16389. <https://doi.org/10.1074/jbc.M000277200>
- Hurwitz, A. A., Foster, B. A., Allison, J. P., Greenberg, N. M., & Kwon, E. D. (2001). The TRAMP mouse as a model for prostate cancer. *Current Protocols in Immunology / Edited by John E. Coligan ... [et Al.], Chapter 20*(1). <https://doi.org/10.1002/0471142735.im2005s45>
- Hussain, M., Fizazi, K., Saad, F., Rathenborg, P., Shore, N., Ferreira, U., Ivashchenko, P., Demirhan, E., Modelska, K., Phung, D., Krivoshik, A., & Sternberg, C. N. (2018). Enzalutamide in Men with Nonmetastatic, Castration-Resistant Prostate Cancer. *New England Journal of Medicine*, *378*(26), 2465–2474. <https://doi.org/10.1056/NEJMoa1800536>
- Hutchinson, D. S., Bengtsson, T., Evans, B. A., & Summers, R. J. (2002). Mouse β 3a and β 3b-adrenoceptors expressed in Chinese hamster ovary cells display identical

- pharmacology but utilize distinct signalling pathways. *British Journal of Pharmacology*, 135(8), 1903–1914. <https://doi.org/10.1038/sj.bjp.0704654>
- Inoue, A., Raimondi, F., Marie, F., Kadji, N., Gutkind, J. S., Aoki, J., & Russell, R. B. (2019). *Illuminating G-Protein-Coupling Selectivity of GPCRs Graphical Abstract Highlights d Large datasets of quantitative coupling between 148 human GPCRs and 11 G proteins d Identification of GPCR sequence-encoded features underlying G-protein selectivity d A powerful predictor for scoring G-protein coupling from a given GPCR sequence d Data-driven engineering of G12-selective designer GPCRs In Brief*. <https://doi.org/10.1016/j.cell.2019.04.044>
- Jacobsen, S. E., Ammendrup-Johnsen, I., Jansen, A. M., Gether, U., Madsen, K. L., & Bräuner-Osborne, H. (2017). The GPRC6A receptor displays constitutive internalization and sorting to the slow recycling pathway. *Journal of Biological Chemistry*. <https://doi.org/10.1074/jbc.M116.762385>
- Jacobsen, S. E., Nørskov-Lauritsen, L., Thomsen, A. R. B., Smajilovic, S., Wellendorph, P., Larsson, N. H. P., Lehmann, A., Bhatia, V. K., & Bräuner-Osborne, H. (2013). Delineation of the GPRC6A receptor signaling pathways using a mammalian cell line stably expressing the receptor. *Journal of Pharmacology and Experimental Therapeutics*, 347(2), 298–309. <https://doi.org/10.1124/jpet.113.206276>
- Jensen, A. A., & Spalding, T. A. (2004). Allosteric modulation of G-protein coupled receptors. *European Journal of Pharmaceutical Sciences*, 21(4), 407–420. <https://doi.org/10.1016/j.ejps.2003.11.007>
- Jensen, D. D., Lieu, T. M., Halls, M. L., Veldhuis, N. A., Imlach, W. L., Mai, Q. N., Poole, D. P., Quach, T., Aurelio, L., Conner, J., Herenbrink, C. K., Barlow, N., Simpson, J. S., Scanlon, M. J., Graham, B., McCluskey, A., Robinson, P. J., Escriou, V., Nassini, R., ... Bunnett, N. W. (2017). Neurokinin 1 receptor signaling in endosomes mediates sustained nociception and is a viable therapeutic target for prolonged pain relief. *Science Translational Medicine*, 9(392). <https://doi.org/10.1126/scitranslmed.aal3447>
- Jiang, M., & Bajpayee, N. S. (2009). *Molecular Mechanisms of Go Signaling*. 23–41. <https://doi.org/10.1159/000186688>
- Jiang, P., Ji, Q., Liu, Z., Snyder, L. A., Benard, L. M. J., Margolskee, R. F., & Max, M. (2004). The cysteine-rich region of T1R3 determines responses to intensely sweet proteins.

Journal of Biological Chemistry, 279(43), 45068–45075.

<https://doi.org/10.1074/jbc.M406779200>

Jinek, M., Chylinski, K., Fonfara, I., Hauer, M., Doudna, J. A., & Charpentier, E. (2012). A programmable dual-RNA-guided DNA endonuclease in adaptive bacterial immunity. *Science*, 337(6096), 816–821. <https://doi.org/10.1126/science.1225829>

Jørgensen, S., Have, C. T., Underwood, C. R., Johansen, L. D., Wellendorph, P., Gjesing, A. P., Jørgensen, C. V., Quan, S., Rui, G., Inoue, A., Linneberg, A., Grarup, N., Jun, W., Pedersen, O., Hansen, T., & Bräuner-Osborne, H. (2017). Genetic variations in the human G protein-coupled receptor class C, group 6, member A (GPCR6A) control cell surface expression and function. *Journal of Biological Chemistry*. <https://doi.org/10.1074/jbc.M116.756577>

Jørgensen, C. V., & Bräuner-Osborne, H. (2020). Pharmacology and physiological function of the orphan GPCR6A receptor. *Basic & Clinical Pharmacology & Toxicology*, 126(S6), 77–87. <https://doi.org/10.1111/bcpt.13397>

Jørgensen, C. V., Gasparini, S. J., Tu, J., Zhou, H., Seibel, M. J., & Bräuner-Osborne, H. (2019). Metabolic and skeletal homeostasis are maintained in full locus GPCR6A knockout mice. *Scientific Reports*, 9(1). <https://doi.org/10.1038/s41598-019-41921-8>

Kaighn, M. E., Narayan, K. S., Ohnuki, Y., Lechner, J. F., & Jones, L. W. (1979). Establishment and characterization of a human prostatic carcinoma cell line (PC-3). *Invest Urol*, 17(1), 16–23.

Katada, T., & Ui, M. (1982). Direct modification of the membrane adenylate cyclase system by islet-activating protein due to ADP-ribosylation of a membrane protein. *Proceedings of the National Academy of Sciences of the United States of America*, 79(10), 3129–3133. <https://doi.org/10.1073/pnas.79.10.3129>

Katritch, V., Cherezov, V., & Stevens, R. C. (2013). Structure-function of the G protein-coupled receptor superfamily. In *Annual Review of Pharmacology and Toxicology* (Vol. 53, pp. 531–556). NIH Public Access. <https://doi.org/10.1146/annurev-pharmtox-032112-135923>

Kaupmann, K., Huggel, K., Heid, J., Flor, P. J., Bischoff, S., Mickel, S. J., McMaster, G., Angst, C., Bittiger, H., Froestl, W., & Bettler, B. (1997). Expression cloning of GABA(B) receptors uncovers similarity to metabotropic glutamate receptors.

- Nature*, 386(6622), 239–246. <https://doi.org/10.1038/386239a0>
- Kelly, E., Bailey, C. P., & Henderson, G. (2008). Agonist-selective mechanisms of GPCR desensitization. 379–388. <https://doi.org/10.1038/sj.bjp.0707604>
- Khan, S. M., Sleno, R., Gora, S., Zylbergold, P., Laverdure, J. P., Labbé, J. C., Miller, G. J., & Hébert, T. E. (2013). The expanding roles of Gβγ subunits in G protein-coupled receptor signaling and drug action. *Pharmacological Reviews*, 65(2), 545–577. <https://doi.org/10.1124/pr.111.005603>
- Kimple, M. E., Brill, A. L., & Pasker, R. L. (2013). Overview of affinity tags for protein purification. *Current Protocols in Protein Science*, 73(SUPPL.73). <https://doi.org/10.1002/0471140864.ps0909s73>
- Kimura, T., & Egawa, S. (2018). Epidemiology of prostate cancer in Asian countries. *International Journal of Urology*, 25(6), 524–531. <https://doi.org/10.1111/iju.13593>
- Kinsey-Jones, J. S., Alamshah, A., McGavigan, A. K., Spreckley, E., Banks, K., Cereceda Monteoliva, N., Norton, M., Bewick, G. A., & Murphy, K. G. (2015). GPRC6a is not required for the effects of a high-protein diet on body weight in mice. *Obesity*, 23(6), 1194–1200. <https://doi.org/10.1002/oby.21083>
- Klein, K. R., Matson, B. C., Caron, K. M., & Carolina, N. (2017). *HHS Public Access*. 51(1), 65–71. <https://doi.org/10.3109/10409238.2015.1128875>.The
- Klug, A. (2010). The Discovery of Zinc Fingers and Their Applications in Gene Regulation and Genome Manipulation. *Annual Review of Biochemistry*, 79(1), 213–231. <https://doi.org/10.1146/annurev-biochem-010909-095056>
- Knudsen, K. E., & Kelly, W. K. (2011). Outsmarting androgen receptor: Creative approaches for targeting aberrant androgen signaling in advanced prostate cancer. In *Expert Review of Endocrinology and Metabolism* (Vol. 6, Issue 3, pp. 483–493). NIH Public Access. <https://doi.org/10.1586/eem.11.33>
- Ko, E., Choi, H., Kim, B., Kim, M., Park, K. N., Bae, I. H., Sung, Y. K., Lee, T. R., Shin, D. W., & Bae, Y. S. (2014). Testosterone stimulates Duox1 activity through GPRC6A in skin keratinocytes. *Journal of Biological Chemistry*, 289(42), 28835–28845. <https://doi.org/10.1074/jbc.M114.583450>
- Koehl, A., Hu, H., Feng, D., Sun, B., Zhang, Y., Robertson, M. J., Chu, M., Kobilka, S., Steyaert, J., Tarrasch, J., Dutta, S., Fonseca, R., Weis, W. I., Mathiesen, J. M., Skiniotis, G., & Kobilka, B. K. (2019). Structural insights into the activation of

- metabotropic glutamate receptors. *Nature*. <https://doi.org/10.1038/s41586-019-0881-4>
- Kolodziej, P. A., & Young, R. A. (1991). Epitope tagging and protein surveillance. *Methods in Enzymology*, *194*(C), 508–519. [https://doi.org/10.1016/0076-6879\(91\)94038-E](https://doi.org/10.1016/0076-6879(91)94038-E)
- Kotecha, S. A., Oak, J. N., Jackson, M. F., Perez, Y., Orser, B. A., Van Tol, H. H. M., & MacDonald, J. F. (2002). A D2 class dopamine receptor transactivates a receptor tyrosine kinase to inhibit NMDA receptor transmission. *Neuron*, *35*(6), 1111–1122. [https://doi.org/10.1016/S0896-6273\(02\)00859-0](https://doi.org/10.1016/S0896-6273(02)00859-0)
- Kuang, D., Yao, Y., Lam, J., Tsushima, R. G., & Hampson, D. R. (2005). Cloning and characterization of a Family C orphan G-protein coupled receptor. *Journal of Neurochemistry*, *93*(2), 383–391. <https://doi.org/10.1111/j.1471-4159.2005.03025.x>
- Kuka, M., & Ashwell, J. D. (2013). A method for high purity sorting of rare cell subsets applied to TDC. *Journal of Immunological Methods*, *400–401*(1), 111–116. <https://doi.org/10.1016/j.jim.2013.10.002>
- Kumari, P., Srivastava, A., Banerjee, R., Ghosh, E., Gupta, P., Ranjan, R., Chen, X., Gupta, B., Gupta, C., Jaiman, D., & Shukla, A. K. (2016). Functional competence of a partially engaged GPCR- β -arrestin complex. *Nature Communications*, *7*. <https://doi.org/10.1038/ncomms13416>
- Kunishima, N., Shimada, Y., Tsuji, Y., Sato, T., Yamamoto, M., Kumasaka, T., Nakanishi, S., Jingami, H., & Morikawa, K. (2000). Structural basis of glutamate recognition by a dimeric metabotropic glutamate receptor. *Nature*, *407*(6807), 971–977. <https://doi.org/10.1038/35039564>
- Lacombe, J., & Ferron, M. (2015). Gamma-carboxylation regulates osteocalcin function. In *Oncotarget* (Vol. 6, Issue 24, pp. 19924–19925). Impact Journals LLC. <https://doi.org/10.18632/oncotarget.5126>
- Lai, T., Yang, Y., & Ng, S. K. (2013). Advances in mammalian cell line development technologies for recombinant protein production. In *Pharmaceuticals* (Vol. 6, Issue 5, pp. 579–603). Multidisciplinary Digital Publishing Institute (MDPI). <https://doi.org/10.3390/ph6050579>
- Lambert, L. J., Challa, A. K., Niu, A., Zhou, L., Tucholski, J., Johnson, M. S., Nagy, T. R., Eberhardt, A. W., Estep, P. N., Kesterson, R. A., & Grams, J. M. (2016). Increased

- trabecular bone and improved biomechanics in an osteocalcin-null rat model created by CRISPR/Cas9 technology. *DMM Disease Models and Mechanisms*, 9(10), 1169–1179. <https://doi.org/10.1242/dmm.025247>
- Laporte, S. A., Oakley, R. H., Zhang, J., Holt, J. A., Ferguson, S. S. G., Caron, M. G., & Barak, L. S. (1999). The β 2-adrenergic receptor/ β arrestin complex recruits the clathrin adaptor AP-2 during endocytosis. *Proceedings of the National Academy of Sciences of the United States of America*, 96(7), 3712–3717. <https://doi.org/10.1073/pnas.96.7.3712>
- Law, N. C., White, M. F., Hunzicker-dunn, M. E., & Medical, H. (2016). *G protein-coupled receptors (GPCRs) that signal via protein kinase A (PKA) cross-talk at insulin receptor substrate 1 (IRS1) to activate the PI3K/AKT pathway* Nathan C. Law. 1. <https://doi.org/10.1074/jbc.M116.763235>
- Le, T. N., Nestler, J. E., Strauss, J. F., & Wickham, E. P. (2012). Sex hormone-binding globulin and type 2 diabetes mellitus. In *Trends in Endocrinology and Metabolism* (Vol. 23, Issue 1, pp. 32–40). Elsevier. <https://doi.org/10.1016/j.tem.2011.09.005>
- Leach, K., & Gregory, K. J. (2017). Molecular insights into allosteric modulation of Class C G protein-coupled receptors. In *Pharmacological Research*. <https://doi.org/10.1016/j.phrs.2016.12.006>
- Lebon, G., Warne, T., Edwards, P. C., Bennett, K., Langmead, C. J., Leslie, A. G. W., & Tate, C. G. (2011). Agonist-bound adenosine A2A receptor structures reveal common features of GPCR activation. *Nature*, 474(7352), 521–525. <https://doi.org/10.1038/nature10136>
- Lee, S. Y., Ju, M. K., Jeon, H. M., Jeong, E. K., Lee, Y. J., Kim, C. H., Park, H. G., Han, S. I., & Kang, H. S. (2018). Regulation of Tumor Progression by Programmed Necrosis. In *Oxidative Medicine and Cellular Longevity* (Vol. 2018). Hindawi Limited. <https://doi.org/10.1155/2018/3537471>
- Lefkowitz, R. J. (2007). Seven transmembrane receptors: Something old, something new. *Acta Physiologica*, 190(1), 9–19. <https://doi.org/10.1111/j.1365-201X.2007.01693.x>
- Lek, M., Karczewski, K. J., Minikel, E. V., Samocha, K. E., Banks, E., Fennell, T., O'Donnell-Luria, A. H., Ware, J. S., Hill, A. J., Cummings, B. B., Tukiainen, T., Birnbaum, D. P., Kosmicki, J. A., Duncan, L. E., Estrada, K., Zhao, F., Zou, J., Pierce-Hoffman, E., Berghout, J., ... Williams, A. L. (2016). Analysis of protein-coding genetic variation in

- 60,706 humans. *Nature*, 536(7616), 285–291. <https://doi.org/10.1038/nature19057>
- Lenhart, P. M., Broselid, S., Barrick, C. J., Fredrik Leeb-Lundberg, L. M., & Caron, K. M. (2013). G-protein-coupled receptor 30 interacts with receptor activity-modifying protein 3 and confers sex-dependent cardioprotection. *Journal of Molecular Endocrinology*, 51(1), 191–202. <https://doi.org/10.1530/JME-13-0021>
- Leone, G., Tucci, M., Buttigliero, C., Zichi, C., Pignataro, D., Bironzo, P., Vignani, F., Scagliotti, G. V., & Di Maio, M. (2018). Antiandrogen withdrawal syndrome (AAWS) in the treatment of patients with prostate cancer. In *Endocrine-Related Cancer* (Vol. 25, Issue 1, pp. R1–R9). BioScientifica Ltd. <https://doi.org/10.1530/ERC-17-0355>
- Leroy, D., Missotten, M., Waltzinger, C., Martin, T., & Scheer, A. (2007). G protein-coupled receptor-mediated ERK1/2 phosphorylation: Towards a generic sensor of GPCR activation. *Journal of Receptors and Signal Transduction*, 27(1), 83–97. <https://doi.org/10.1080/10799890601112244>
- Liang, F., Han, M., Romanienko, P. J., & Jasin, M. (1998). Homology-directed repair is a major double-strand break repair pathway in mammalian cells. *Proceedings of the National Academy of Sciences of the United States of America*, 95(9), 5172–5177. <https://doi.org/10.1073/pnas.95.9.5172>
- Liang, Y. L., Khoshouei, M., Radjainia, M., Zhang, Y., Glukhova, A., Tarrasch, J., Thal, D. M., Furness, S. G. B., Christopoulos, G., Coudrat, T., Danev, R., Baumeister, W., Miller, L. J., Christopoulos, A., Kobilka, B. K., Wootten, D., Skiniotis, G., & Sexton, P. M. (2017). Phase-plate cryo-EM structure of a class B GPCR-G-protein complex. *Nature*, 546(7656), 118–123. <https://doi.org/10.1038/nature22327>
- Lim, D. J., Liu, X. -L, Sutkowski, D. M., Braun, E. J., Lee, C., & Kozlowski, J. M. (1993). Growth of an androgen-sensitive human prostate cancer cell line, LNCaP, in nude mice. *The Prostate*, 22(2), 109–118. <https://doi.org/10.1002/pros.2990220203>
- Lindström, S., Schumacher, F. R., Campa, D., Albanes, D., Andriole, G., Berndt, S. I., Bueno-de-Mesquita, H. B., Chanock, S. J., Diver, W. R., Ganziano, J. M., Gapstur, S. M., Giovannucci, E., Haiman, C. A., Henderson, B., Hunter, D. J., Johansson, M., Kolonel, L. N., Le Marchand, L., Ma, J., ... Kraft, P. (2012). Replication of five prostate cancer loci identified in an Asian population - Results from the NCI Breast and Prostate Cancer Cohort Consortium (BPC3). *Cancer Epidemiology Biomarkers and Prevention*, 21(1), 212–216. <https://doi.org/10.1158/1055-9965.EPI-11-0870-T>

- Liu, J., Maurel, D., Etzol, S., Brabet, I., Ansanay, H., Pin, J. P., & Rondard, P. (2004). Molecular Determinants Involved in the Allosteric Control of Agonist Affinity in the GABAB Receptor by the GABAB2 Subunit. *Journal of Biological Chemistry*, *279*(16), 15824–15830. <https://doi.org/10.1074/jbc.M313639200>
- Liu, M., Zhao, Y., Yang, F., Wang, J., Shi, X., Zhu, X., Xu, Y., Wei, D., Sun, L., Zhang, Y., Yang, K., Qu, Y., Wang, X., Liang, S., Chen, X., Zhao, C., Zhu, L., Tang, L., Zheng, C., & Yang, G. (2016). 2235-2248-Evidence-for-a-role-of-GPRC6A-in-prostate-cancer-metastasis-based-on-case-control-and-in-vitro-analyses-1. *European Review for Medical and Pharmacological Sciences*.
- Liu, S., Gao, F., Wen, L., Ouyang, M., Wang, Y., Wang, Q., Luo, L., & Jian, Z. (2017). Cellular Physiology and Biochemistry Cellular Physiology and Biochemistry Liu et al.: Osteocalcin Induces Proliferation and Promotes Differentiation in C2C12 Myoblast Cells Osteocalcin Induces Proliferation via Positive Activation of the PI3K/Akt, P38 MAP. *Cell Physiol Biochem*, *43*, 1100–1112. <https://doi.org/10.1159/000481752>
- Liu, X., Xu, X., Hilger, D., Aschauer, P., Tiemann, J., Du, Y., Liu, H., Hirata, K., Sun, X., Guixà-González, R., Mathiesen, J., Hildebrand, P., & Kobilka, B. (2019). Structural Insights into the Process of GPCR-G Protein Complex Formation. *Cell*, *177*(5), 1243-1251.e12. <https://doi.org/10.1016/J.CELL.2019.04.021>
- Lloyd, T., Hounsome, L., Mehay, A., Mee, S., Verne, J., & Cooper, A. (2015). Lifetime risk of being diagnosed with, or dying from, prostate cancer by major ethnic group in England 2008-2010. *BMC Medicine*, *13*(1), 171. <https://doi.org/10.1186/s12916-015-0405-5>
- Logan, M., Anderson, P. D., Saab, S. T., Hameed, O., & Abdulkadir, S. A. (2013). RAMP1 Is a Direct NKX3 . 1 Target Gene Up-Regulated in Prostate Cancer that Promotes Tumorigenesis. *The American Journal of Pathology*, *183*(3), 951–963. <https://doi.org/10.1016/j.ajpath.2013.05.021>
- Logothetis, D. E., Kurachi, Y., Galper, J., Neer, E. J., & Clapham, D. E. (1987). The $\beta\gamma$ subunits of GTP-Binding proteins activate the muscarinic K⁺ channel in heart. *Nature*, *325*(6102), 321–326. <https://doi.org/10.1038/325321a0>
- Long, Q. Z., Du, Y. F., Ding, X. Y., Li, X., Song, W. Bin, Yang, Y., Zhang, P., Zhou, J. P., & Liu, X. G. (2012). Replication and fine mapping for association of the C2orf43, FOXP4, GPRC6A and RFX6 genes with prostate cancer in the Chinese population. *PLoS ONE*,

- 7(5). <https://doi.org/10.1371/journal.pone.0037866>
- Luo, J., Liu, Z., Liu, J., & Eugene, C. Y. (2010). Distribution pattern of GPRC6A mRNA in mouse tissue by in situ hybridization. *Journal of Central South University (Medical Sciences)*. <https://doi.org/10.3969/j.issn.1672-7347.2010.01.001>
- Luttrell, L. M., Ferguson, S. S. G., Daaka, Y., Miller, W. E., Maudsley, S., Della Rocca, G. J., Lin, F. T., Kawakatsu, H., Owada, K., Luttrell, D. K., Caron, M. G., & Lefkowitz, R. J. (1999). β -arrestin-dependent formation of β 2 adrenergic receptor-src protein kinase complexes. *Science*, *283*(5402), 655–661. <https://doi.org/10.1126/science.283.5402.655>
- Luttrell, Louis M., Roudabush, F. L., Choy, E. W., Miller, W. E., Field, M. E., Pierce, K. L., & Lefkowitz, R. J. (2001). Activation and targeting of extracellular signal-regulated kinases by β -arrestin scaffolds. *Proceedings of the National Academy of Sciences of the United States of America*, *98*(5), 2449–2454. <https://doi.org/10.1073/pnas.041604898>
- Ma, L., Yang, F., & Zheng, J. (2014). Application of fluorescence resonance energy transfer in protein studies. *Journal of Molecular Structure*, *1077*, 87–100. <https://doi.org/10.1016/j.molstruc.2013.12.071>
- Magalhaes, A. C., Dunn, H., & Ferguson, S. S. G. (2012). Regulation of GPCR activity, trafficking and localization by GPCR-interacting proteins. *British Journal of Pharmacology*, *165*(6), 1717–1736. <https://doi.org/10.1111/j.1476-5381.2011.01552.x>
- Mahoney, J. P., & Sunahara, R. K. (2016). Mechanistic insights into GPCR–G protein interactions. In *Current Opinion in Structural Biology* (Vol. 41, pp. 247–254). Elsevier Ltd. <https://doi.org/10.1016/j.sbi.2016.11.005>
- Mak, A. N. S., Bradley, P., Bogdanove, A. J., & Stoddard, B. L. (2013). TAL effectors: Function, structure, engineering and applications. In *Current Opinion in Structural Biology* (Vol. 23, Issue 1, pp. 93–99). NIH Public Access. <https://doi.org/10.1016/j.sbi.2012.11.001>
- Mali, P., Yang, L., Esvelt, K. M., Aach, J., Guell, M., DiCarlo, J. E., Norville, J. E., & Church, G. M. (2013). RNA-guided human genome engineering via Cas9. *Science*, *339*(6121), 823–826. <https://doi.org/10.1126/science.1232033>
- Malik, R. U., Ritt, M., DeVree, B. T., Neubig, R. R., Sunahara, R. K., & Sivaramakrishnan, S.

- (2013). Detection of G protein-selective G protein-coupled receptor (GPCR) conformations in live cells. *Journal of Biological Chemistry*, 288(24), 17167–17178. <https://doi.org/10.1074/jbc.M113.464065>
- Mamillapalli, R., VanHouten, J., Zawalich, W., & Wysolmerski, J. (2008). Switching of G-protein usage by the calcium-sensing receptor reverses its effect on parathyroid hormone-related protein secretion in normal versus malignant breast cells. *Journal of Biological Chemistry*, 283(36), 24435–24447. <https://doi.org/10.1074/jbc.M801738200>
- Mangmool, S., & Kurose, H. (2011). Gi/o protein-dependent and -independent actions of pertussis toxin (ptx). *Toxins*, 3(7), 884–899. <https://doi.org/10.3390/toxins3070884>
- Markwardt, M. L., Kremers, G. J., Kraft, C. A., Ray, K., Cranfill, P. J. C., Wilson, K. A., Day, R. N., Wachter, R. M., Davidson, M. W., & Rizzo, M. A. (2011). An improved cerulean fluorescent protein with enhanced brightness and reduced reversible photoswitching. *PLoS ONE*, 6(3), 17896. <https://doi.org/10.1371/journal.pone.0017896>
- Massard, C., Penttinen, H. M., Vjaters, E., Bono, P., Lietuvietis, V., Tammela, T. L., Vuorela, A., Nykänen, P., Pohjanjousi, P., Snapir, A., & Fizazi, K. (2016). Pharmacokinetics, Antitumor Activity, and Safety of ODM-201 in Patients with Chemotherapy-naive Metastatic Castration-resistant Prostate Cancer: An Open-label Phase 1 Study. *European Urology*, 69(5), 834–840. <https://doi.org/10.1016/j.eururo.2015.09.046>
- Matsuda, T., & Saika, K. (2009). Comparison of time trends in prostate cancer incidence (1973-2002) in Asia, from cancer incidence in five continents, vols IV-IX. *Japanese Journal of Clinical Oncology*, 39(7), 468–469. <https://doi.org/10.1093/jjco/hyp077>
- Matsumura, I. (2015). Why Johnny can't clone: Common pitfalls and not so common solutions. *BioTechniques*, 59(3), 4–13. <https://doi.org/10.2144/000114324>
- Mayer, H. (1978). Optimization of the EcoRI*-activity of EcoRI endonuclease. *FEBS Letters*, 90(2), 341–344. [https://doi.org/10.1016/0014-5793\(78\)80400-1](https://doi.org/10.1016/0014-5793(78)80400-1)
- Mclatchie, L. M., Fraser, N. J., Main, M. J., Wise, A., Brown, J., Thompson, N., Solari, R., Lee, M. G., & Foord, S. M. (1998). RAMPs regulate the transport and ligand specificity of the calcitonin-receptor-like receptor. *393*(May), 333–339.
- Mera, P., Laue, K., Wei, J., Berger, J. M., & Karsenty, G. (2016). Osteocalcin is necessary

- and sufficient to maintain muscle mass in older mice. *Molecular Metabolism*, 5(10), 1042–1047. <https://doi.org/10.1016/j.molmet.2016.07.002>
- Mochizuki, N., Ohba, Y., Kiyokawa, E., Kurata, T., Murakami, T., Ozaki, T., Kitabatake, A., Nagashima, K., & Matsuda, M. (1999). Activation of the ERK/MAPK pathway by an isoform of rap1 GAP associated with Gα(i). *Nature*, 400(6747), 891–894. <https://doi.org/10.1038/23738>
- Morfis, M., Tilakaratne, N., Furness, S. G. B., Christopoulos, G., Werry, T. D., Christopoulos, A., & Sexton, P. M. (2008). Receptor activity-modifying proteins differentially modulate the G protein-coupling efficiency of amylin receptors. *Endocrinology*, 149(11), 5423–5431. <https://doi.org/10.1210/en.2007-1735>
- Moritz, B., Becker, P. B., & Göpfert, U. (2015). CMV promoter mutants with a reduced propensity to productivity loss in CHO cells. *Scientific Reports*, 5(1), 1–8. <https://doi.org/10.1038/srep16952>
- Moriya, H. (2015). Quantitative nature of overexpression experiments. In *Molecular Biology of the Cell* (Vol. 26, Issue 22, pp. 3932–3939). American Society for Cell Biology. <https://doi.org/10.1091/mbc.E15-07-0512>
- Muto, T., Tsuchiya, D., Morikawa, K., & Jingami, H. (2007). Structures of the extracellular regions of the group II/III metabotropic glutamate receptors. *Proceedings of the National Academy of Sciences*, 104(10), 3759–3764. <https://doi.org/10.1073/pnas.0611577104>
- Namkung, Y., Le Gouill, C., Lukashova, V., Kobayashi, H., Hogue, M., Khoury, E., Song, M., Bouvier, M., & Laporte, S. (2016). Monitoring G protein-coupled receptor and b - arrestin trafficking in live cells using enhanced bystander BRET. *Nature Communications*, 7(12178), 1–12. <https://doi.org/10.1038/ncomms12178>
- Nango, E., Akiyama, S., Maki-Yonekura, S., Ashikawa, Y., Kusakabe, Y., Krayukhina, E., Maruno, T., Uchiyama, S., Nuemket, N., Yonekura, K., Shimizu, M., Atsumi, N., Yasui, N., Hikima, T., Yamamoto, M., Kobayashi, Y., & Yamashita, A. (2016). Taste substance binding elicits conformational change of taste receptor T1r heterodimer extracellular domains. *Scientific Reports*, 6(April), 1–8. <https://doi.org/10.1038/srep25745>
- Nelson, G., Hoon, M. A., Chandrashekar, J., Zhang, Y., Ryba, N. J. P., & Zuker, C. S. (2001). Mammalian sweet taste receptors. *Cell*, 106(3), 381–390.

[https://doi.org/10.1016/S0092-8674\(01\)00451-2](https://doi.org/10.1016/S0092-8674(01)00451-2)

- Nemeth, E. F., Delmar, E. G., Heaton, W. L., Miller, M. A., Lambert, L. D., Conklin, R. L., Gowen, M., Gleason, J. G., Bhatnagar, P. K., & Fox, J. (2001). Calcilytic compounds: Potent and selective Ca²⁺ receptor antagonists that stimulate secretion of parathyroid hormone. *Journal of Pharmacology and Experimental Therapeutics*, *299*(1), 323–331.
- Neumann, E., Khawaja, K., & Müller-ladner, U. (2014). REVIEWS G protein-coupled receptors in rheumatology. *Nature Publishing Group*, *10*(7), 429–436.
<https://doi.org/10.1038/nrrheum.2014.62>
- Nevins, A. M., & Marchese, A. (2018). Detecting cell surface expression of the g protein-coupled receptor CXCR4. In *Methods in Molecular Biology* (Vol. 1722, pp. 151–164). Humana Press Inc. https://doi.org/10.1007/978-1-4939-7553-2_10
- Newsholme, P., & Krause, M. (2012). Nutritional Regulation of Insulin Secretion: Implications for Diabetes. In *Clinical Biochemist Reviews* (Vol. 33, Issue 2, pp. 35–47). The Australian Association of Clinical Biochemists. </pmc/articles/PMC3387883/>
- Nickols, N. G., Nazarian, R., Zhao, S. G., Tan, V., Uzunangelov, V., Xia, Z., Baertsch, R., Neeman, E., Gao, A. C., Thomas, G. V., Howard, L., De Hoedt, A. M., Stuart, J., Goldstein, T., Chi, K., Gleave, M. E., Graff, J. N., Beer, T. M., Drake, J. M., ... Rettig, M. B. (2019). MEK-ERK signaling is a therapeutic target in metastatic castration resistant prostate cancer. *Prostate Cancer and Prostatic Diseases*, *22*(4), 531–538.
<https://doi.org/10.1038/s41391-019-0134-5>
- Nolan, J. P., & Condello, D. (2013). Spectral flow cytometry. *Current Protocols in Cytometry*, CHAPTER(SUPPL.63), Unit1.27.
<https://doi.org/10.1002/0471142956.cy0127s63>
- Nørskov-Lauritsen, L., Jørgensen, S., & Bräuner-Osborne, H. (2015). N-glycosylation and disulfide bonding affects GPRC6A receptor expression, function, and dimerization. *FEBS Letters*. <https://doi.org/10.1016/j.febslet.2015.01.019>
- Nygaard, R., Frimurer, T. M., Holst, B., Rosenkilde, M. M., & Schwartz, T. W. (2009). Ligand binding and micro-switches in 7TM receptor structures. In *Trends in Pharmacological Sciences* (Vol. 30, Issue 5, pp. 249–259). Elsevier Current Trends.
<https://doi.org/10.1016/j.tips.2009.02.006>
- O’Connell, M. R., Gamsjaeger, R., & Mackay, J. P. (2009). The structural analysis of

- protein-protein interactions by NMR spectroscopy. In *Proteomics* (Vol. 9, Issue 23, pp. 5224–5232). Proteomics. <https://doi.org/10.1002/pmic.200900303>
- Ojha, N., Rainey, K. H., & Patterson, G. H. (2020). Imaging of fluorescence anisotropy during photoswitching provides a simple readout for protein self-association. *Nature Communications*, *11*(1), 1–11. <https://doi.org/10.1038/s41467-019-13843-6>
- Okashah, N., Wan, Q., Ghosh, S., Sandhu, M., Inoue, A., Vaidehi, N., & Lambert, N. A. (2019). Variable G protein determinants of GPCR coupling selectivity. *PNAS*, *116*(24), 12054–12059.
- Onfroy, L., Galandrin, S., Pontier, S. M., Seguelas, M. H., N'Guyen, D., Sénard, J. M., & Galés, C. (2017). G protein stoichiometry dictates biased agonism through distinct receptor-G protein partitioning. *Scientific Reports*, *7*(1), 1–14. <https://doi.org/10.1038/s41598-017-07392-5>
- Ortega-Roldan, J. L., Blackledge, M., & Jensen, M. R. (2018). Characterizing protein-protein interactions using solution NMR spectroscopy. In *Methods in Molecular Biology* (Vol. 1764, pp. 73–85). Humana Press Inc. https://doi.org/10.1007/978-1-4939-7759-8_5
- Otani, T., Mizokami, A., Hayashi, Y., Gao, J., Mori, Y., Nakamura, S., Takeuchi, H., & Hirata, M. (2015). Signaling pathway for adiponectin expression in adipocytes by osteocalcin. *Cellular Signalling*, *27*(3), 532–544. <https://doi.org/10.1016/j.cellsig.2014.12.018>
- Otto, C., Rohde-Schulz, B., Schwarz, G., Fuchs, I., Klewer, M., Brittain, D., Langer, G., Bader, B., Prella, K., Nubbemeyer, R., & Fritzscheier, K. H. (2008). G protein-coupled receptor 30 localizes to the endoplasmic reticulum and is not activated by estradiol. *Endocrinology*, *149*(10), 4846–4856. <https://doi.org/10.1210/en.2008-0269>
- Oury, F., Ferron, M., Huizhen, W., Confavreux, C., Xu, L., Lacombe, J., Srinivas, P., Chamouni, A., Lugani, F., Lejeune, H., Kumar, T. R., Plotton, I., & Karsenty, G. (2013). Osteocalcin regulates murine and human fertility through a pancreas-bone-testis axis. *Journal of Clinical Investigation*. <https://doi.org/10.1172/JCI65952>
- Oury, F., Sumara, G., Sumara, O., Ferron, M., Chang, H., Smith, C. E., Hermo, L., Suarez, S., Roth, B. L., Ducy, P., & Karsenty, G. (2011). Endocrine regulation of male fertility by the skeleton. *Cell*. <https://doi.org/10.1016/j.cell.2011.02.004>
- Oya, M., Kitaguchi, T., Pais, R., Reimann, F., Gribble, F., & Tsuboi, T. (2013a). The G

- protein-coupled receptor family C group 6 subtype a (GPC6A) receptor is involved in amino acid-induced glucagon-like peptide-1 secretion from GLUTag cells. *Journal of Biological Chemistry*. <https://doi.org/10.1074/jbc.M112.402677>
- Oya, M., Kitaguchi, T., Pais, R., Reimann, F., Gribble, F., & Tsuboi, T. (2013b). The G protein-coupled receptor family C group 6 subtype a (GPC6A) receptor is involved in amino acid-induced glucagon-like peptide-1 secretion from GLUTag cells. *Journal of Biological Chemistry*, 288(7), 4513–4521. <https://doi.org/10.1074/jbc.M112.402677>
- Pagano, A., Rovelli, G., Mosbacher, J., Lohmann, T., Duthey, B., Stauffer, D., Ristig, D., Schuler, V., Meigel, I., Lampert, C., Stein, T., Prézeau, L., Blahos, J., Pin, J. P., Froestl, W., Kuhn, R., Heid, J., Kaupmann, K., & Bettler, B. (2001). C-terminal interaction is essential for surface trafficking but not for heteromeric assembly of GABAB receptors. *Journal of Neuroscience*, 21(4), 1189–1202. <https://doi.org/10.1523/jneurosci.21-04-01189.2001>
- Pandey, S., Roy, D., & Shukla, A. K. (2019). Measuring surface expression and endocytosis of GPCRs using whole-cell ELISA. In *Methods in Cell Biology* (Vol. 149, pp. 131–140). Academic Press Inc. <https://doi.org/10.1016/bs.mcb.2018.09.014>
- Park, J., Selvam, B., Sanematsu, K., Shigemura, N., Shukla, D., & Procko, E. (2019). Structural architecture of a dimeric class C GPCR based on co-trafficking of sweet taste receptor subunits. *Journal of Biological Chemistry*, 294(13), 4759–4774. <https://doi.org/10.1074/jbc.RA118.006173>
- Park, P. S. H., Lodowski, D. T., & Palczewski, K. (2008). Activation of G protein-coupled receptors: Beyond two-state models and tertiary conformational changes. In *Annual Review of Pharmacology and Toxicology* (Vol. 48, pp. 107–141). NIH Public Access. <https://doi.org/10.1146/annurev.pharmtox.48.113006.094630>
- Paul, R., & Breul, J. (2000). Antiandrogen withdrawal syndrome associated with prostate cancer therapies: Incidence and clinical significance. In *Drug Safety* (Vol. 23, Issue 5, pp. 381–390). Adis International Ltd. <https://doi.org/10.2165/00002018-200023050-00003>
- Peterson, Y. K., & Luttrell, L. M. (2017). The diverse roles of arrestin scaffolds in G protein-coupled receptor signaling. *Pharmacological Reviews*, 69(3), 256–297. <https://doi.org/10.1124/pr.116.013367>

- Pettaway, C. A., Pathak, S., Greene, G., Ramirez, E., Wilson, M. R., Killion, J. J., & Fidler, I. J. (1996). Selection of highly metastatic variants of different human prostatic carcinomas using orthotopic implantation in nude mice. *Clinical Cancer Research*, 2(9).
- Philip, F., Kadamur, G., Silos, R. G., Woodson, J., & Ross, E. M. (2010). Synergistic activation of phospholipase C- β 3 by G α q and G β y describes a simple two-state coincidence detector. *Current Biology*, 20(15), 1327–1335.
<https://doi.org/10.1016/j.cub.2010.06.013>
- Pi, M., Chen, L., Huang, M. Z., Zhu, W., Ringhofer, B., Luo, J., Christenson, L., Li, B., Zhang, J., Jackson, P. D., Faber, P., Brunden, K. R., Harrington, J. J., & Quarles, L. D. (2008). GPRC6A null mice exhibit osteopenia, feminization and metabolic syndrome. *PLoS ONE*. <https://doi.org/10.1371/journal.pone.0003858>
- Pi, M., Faber, P., Ekema, G., Jackson, P. D., Ting, A., Wang, N., Fontilla-Poole, M., Mays, R. W., Brunden, K. R., Harrington, J. J., & Quarles, L. D. (2005). Identification of a novel extracellular cation-sensing G-protein-coupled receptor. *Journal of Biological Chemistry*, 280(48), 40201–40209. <https://doi.org/10.1074/jbc.M505186200>
- Pi, M., Kapoor, K., Wu, Y., Ye, R., Senogles, S. E., Nishimoto, S. K., Hwang, D.-J., Miller, D. D., Narayanan, R., Smith, J. C., Baudry, J., & Quarles, L. D. (2015). Structural and Functional Evidence for Testosterone Activation of GPRC6A in Peripheral Tissues. *Molecular Endocrinology*. <https://doi.org/10.1210/me.2015-1161>
- Pi, M., Kapoor, K., Ye, R., Hwang, D. J., Miller, D. D., Smith, J. C., Baudry, J., & Quarles, L. D. (2018). Computationally identified novel agonists for GPRC6A. *PLoS ONE*, 13(4). <https://doi.org/10.1371/journal.pone.0195980>
- Pi, M., Kapoor, K., Ye, R., Nishimoto, S. K., Smith, J. C., Baudry, J., & Quarles, L. D. (2016). Evidence for osteocalcin binding and activation of GPRC6A in β -cells. *Endocrinology*. <https://doi.org/10.1210/en.2015-2010>
- Pi, M., Nishimoto, S. K., & Quarles, L. D. (2017). GPRC6A: Jack of all metabolism (or master of none). In *Molecular Metabolism*. <https://doi.org/10.1016/j.molmet.2016.12.006>
- Pi, M., Parrill, A. L., & Quarles, L. D. (2010). GPRC6A mediates the non-genomic effects of steroids. *Journal of Biological Chemistry*, 285(51), 39953–39964. <https://doi.org/10.1074/jbc.M110.158063>

- Pi, M., & Quarles, L. D. (2012a). GPRC6A regulates prostate cancer progression. *Prostate*.
<https://doi.org/10.1002/pros.21442>
- Pi, M., & Quarles, L. D. (2012b). Multiligand specificity and wide tissue expression of GPRC6A reveals new endocrine networks. In *Endocrinology* (Vol. 153, Issue 5).
<https://doi.org/10.1210/en.2011-2117>
- Pi, M., Wu, Y., Lenchik, N. I., Gerling, I., & Quarles, L. D. (2012). GPRC6A Mediates the Effects of l-Arginine on Insulin Secretion in Mouse Pancreatic Islets. *Endocrinology*, 153(10), 4608–4615. <https://doi.org/10.1210/en.2012-1301>
- Pi, M., Wu, Y., & Quarles, L. D. (2011). GPRC6A mediates responses to osteocalcin in β -cells in vitro and pancreas in vivo. *Journal of Bone and Mineral Research*.
<https://doi.org/10.1002/jbmr.390>
- Pi, M., Zhang, L., Lei, S. F., Huang, M. Z., Zhu, W., Zhang, J., Shen, H., Deng, H. W., & Quarles, L. D. (2010). Impaired osteoblast function in GPRC6A null mice. *Journal of Bone and Mineral Research*, 25(5), 1092–1102.
<https://doi.org/10.1359/jbmr.091037>
- Pin, J. P., Galvez, T., & Prézeau, L. (2003). Evolution, structure, and activation mechanism of family 3/C G-protein-coupled receptors. In *Pharmacology and Therapeutics* (Vol. 98, Issue 3, pp. 325–354). Elsevier Inc. [https://doi.org/10.1016/S0163-7258\(03\)00038-X](https://doi.org/10.1016/S0163-7258(03)00038-X)
- Piston, D. W., & Kremers, G. J. (2007). Fluorescent protein FRET: the good, the bad and the ugly. In *Trends in Biochemical Sciences* (Vol. 32, Issue 9, pp. 407–414). Trends Biochem Sci. <https://doi.org/10.1016/j.tibs.2007.08.003>
- Pittman, M. (1979). Pertussis toxin: The cause of the harmful effects and prolonged immunity of whooping cough. a hypothesis. *Reviews of Infectious Diseases*, 1(3), 401–412. <https://doi.org/10.1093/clinids/1.3.401>
- Poon, L. S. W., Chan, A. S. L., & Wong, Y. H. (2009). G β 3 forms distinct dimers with specific G γ subunits and preferentially activates the β 3 isoform of phospholipase C. *Cellular Signalling*, 21(5), 737–744. <https://doi.org/10.1016/j.cellsig.2009.01.018>
- Prasad, B., Hollins, B., & Lambert, N. A. (2010). *Methods to detect cell surface expression and constitutive activity of GPR6*. 6(706), 179–195. <https://doi.org/10.1016/B978-0-12-381298-8.00010-1.Methods>
- Prelich, G. (2012). Gene overexpression: Uses, mechanisms, and interpretation. In

- Genetics* (Vol. 190, Issue 3, pp. 841–854). Genetics Society of America.
<https://doi.org/10.1534/genetics.111.136911>
- Prossnitz, E. R., & Maggiolini, M. (2009). Mechanisms of estrogen signaling and gene expression via GPR30. In *Molecular and Cellular Endocrinology*.
<https://doi.org/10.1016/j.mce.2009.03.026>
- Prough, R. A., Clark, B. J., & Klinge, C. M. (2016). Novel mechanisms for DHEA action. In *Journal of Molecular Endocrinology* (Vol. 56, Issue 3, pp. R139–R155). BioScientifica Ltd. <https://doi.org/10.1530/JME-16-0013>
- Puck, T. (1985). Development of the Chinese hamster ovary (CHO) cell for use in somatic cell genetics. *Molecular Cell Genetics*, 37–64.
- Pulukuri, S. M. K., Gondi, C. S., Lakka, S. S., Jutla, A., Estes, N., Gujrati, M., & Rao, J. S. (2005). RNA interference-directed knockdown of urokinase plasminogen activator and urokinase plasminogen activator receptor inhibits prostate cancer cell invasion, survival, and tumorigenicity in vivo. *Journal of Biological Chemistry*, 280(43), 36529–36540. <https://doi.org/10.1074/jbc.M503111200>
- Pupo, M., Vivacqua, A., Perrotta, I., Pisano, A., Aquila, S., Abonante, S., Gasperi-Campani, A., Pezzi, V., & Maggiolini, M. (2013). The nuclear localization signal is required for nuclear GPER translocation and function in breast Cancer-Associated Fibroblasts (CAFs). *Molecular and Cellular Endocrinology*, 376(1–2), 23–32.
<https://doi.org/10.1016/j.mce.2013.05.023>
- Putney, J., & Tomita, T. (2013). *NIH Public Access*. 52(1), 152–164.
<https://doi.org/10.1016/j.advenzreg.2011.09.005>. Phospholipase
- Quandt, D., Rothe, K., Baerwald, C., & Rossol, M. (2015). GPRC6A mediates Alum-induced Nlrp3 inflammasome activation but limits Th2 type antibody responses. *Scientific Reports*. <https://doi.org/10.1038/srep16719>
- Rajagopal, S., Ahn, S., Rominger, D. H., Gowen-MacDonald, W., Lam, C. M., DeWire, S. M., Violin, J. D., & Lefkowitz, R. J. (2011). Quantifying ligand bias at seven-transmembrane receptors. *Molecular Pharmacology*, 80(3), 367–377.
<https://doi.org/10.1124/mol.111.072801>
- Rao, V. S., Srinivas, K., Sujini, G. N., & Kumar, G. N. S. (2014). Protein-Protein Interaction Detection: Methods and Analysis. *International Journal of Proteomics*, 2014, 1–12.
<https://doi.org/10.1155/2014/147648>

- Rask-andersen, M., Masuram, S., & Schi, H. B. (2014). *The Druggable Genome : Evaluation of Drug Targets in Clinical Trials Suggests Major Shifts in Molecular Class and Indication*. <https://doi.org/10.1146/annurev-pharmtox-011613-135943>
- Rasmussen, S. G. F., Devree, B. T., Zou, Y., Kruse, A. C., Chung, K. Y., Kobilka, T. S., Thian, F. S., Chae, P. S., Pardon, E., Calinski, D., Mathiesen, J. M., Shah, S. T. A., Lyons, J. A., Caffrey, M., Gellman, S. H., Steyaert, J., Skiniotis, G., Weis, W. I., Sunahara, R. K., & Kobilka, B. K. (2011). Crystal structure of the β 2 adrenergic receptor-Gs protein complex. *Nature*, *477*(7366), 549–557. <https://doi.org/10.1038/nature10361>
- Rathkopf, D. E., Antonarakis, E. S., Shore, N. D., Tutrone, R. F., Alumkal, J. J., Ryan, C. J., Saleh, M., Hauke, R. J., Bandekar, R., Maneval, E. C., De Boer, C. J., Yu, M. K., & Scher, H. I. (2017). Safety and antitumor activity of apalutamide (ARN-509) in metastatic castration-resistant prostate cancer with and without prior abiraterone acetate and prednisone. *Clinical Cancer Research*, *23*(14), 3544–3551. <https://doi.org/10.1158/1078-0432.CCR-16-2509>
- Rawla, P. (2019). Epidemiology of Prostate Cancer. *Review World J Oncol*, *10*(2), 63–89. <https://doi.org/10.14740/wjon1191>
- Ray, K., & Hauschild, B. C. (2000). Cys-140 is critical for metabotropic glutamate receptor-1 dimerization. *Journal of Biological Chemistry*, *275*(44), 34245–34251. <https://doi.org/10.1074/jbc.M005581200>
- Ray, K., Hauschild, B. C., Steinbach, P. J., Goldsmith, P. K., Hauache, O., & Spiegel, A. M. (1999). Identification of the cysteine residues in the amino-terminal extracellular domain of the human Ca²⁺ receptor critical for dimerization. Implications for function of monomeric Ca²⁺ receptor. *Journal of Biological Chemistry*, *274*(39), 27642–27650. <https://doi.org/10.1074/jbc.274.39.27642>
- Regard, J. B., Kataoka, H., Cano, D. a, Camerer, E., Yin, L., Zheng, Y., Scanlan, T. S., Hebrok, M., & Coughlin, S. R. (2007). *1SPCJOH DFMM UZQFmTQFDJGJD GVODUJJPOT PG (J JO WJWP JEFUJGJFT (1 \$ 3 SFHVMBUPST PG JOTVMJO TFDSFUJPO*. *117*(12). <https://doi.org/10.1172/JCI32994DS1>
- Reiter. (2013). *NIH Public Access*. *2*, 179–197. <https://doi.org/10.1146/annurev.pharmtox.010909.105800.Molecular>
- Revankar, C. M., Mitchell, H. D., Field, A. S., Burai, R., Corona, C., Ramesh, C., Sklar, L. A., Arterburn, J. B., & Prossnitz, E. R. (2007). Synthetic estrogen derivatives

- demonstrate the functionality of intracellular GPR30. *ACS Chemical Biology*, 2(8), 536–544. <https://doi.org/10.1021/cb700072n>
- Rice, A. M., & McLysaght, A. (2017). Dosage-sensitive genes in evolution and disease. In *BMC Biology* (Vol. 15, Issue 1, pp. 1–10). BioMed Central Ltd. <https://doi.org/10.1186/s12915-017-0418-y>
- Rice, M. A., Malhotra, S. V., & Stoyanova, T. (2019). Second-generation antiandrogens: From discovery to standard of care in castration resistant prostate cancer. In *Frontiers in Neurology* (Vol. 10, Issue AUG, p. 801). Frontiers Media S.A. <https://doi.org/10.3389/fonc.2019.00801>
- Rizzo, M. A., Springer, G. H., Granada, B., & Piston, D. W. (2004). An improved cyan fluorescent protein variant useful for FRET. *Nature Biotechnology*, 22(4), 445–449. <https://doi.org/10.1038/nbt945>
- Roberts, R. J. (2005). How restriction enzymes became the workhorses of molecular biology. In *Proceedings of the National Academy of Sciences of the United States of America* (Vol. 102, Issue 17, pp. 5905–5908). National Academy of Sciences. <https://doi.org/10.1073/pnas.0500923102>
- Robinson, C. R., & Sligar, S. G. (1993). Molecular recognition mediated by bound water: A mechanism for star activity of the restriction endonuclease EcoRI. In *Journal of Molecular Biology* (Vol. 234, Issue 2, pp. 302–306). Academic Press. <https://doi.org/10.1006/jmbi.1993.1586>
- Rodgers, K., & Mcvey, M. (2016). Error-Prone Repair of DNA Double-Strand Breaks. In *Journal of Cellular Physiology* (Vol. 231, Issue 1, pp. 15–24). Wiley-Liss Inc. <https://doi.org/10.1002/jcp.25053>
- Rojas Bie Thomsen, A., Smajilovic, S., & Brauner-Osborne, H. (2012). Novel Strategies in Drug Discovery of the Calcium-Sensing Receptor Based on Biased Signaling. *Current Drug Targets*, 13(10), 1324–1335. <https://doi.org/10.2174/138945012802429642>
- Romano, C., Miller, J. K., Hyrc, K., Dikranian, S., Mennerick, S., Takeuchi, Y., Goldberg, M. P., & O'Malley, K. L. (2001). Covalent and noncovalent interactions mediate metabotropic glutamate receptor mGlu5 dimerization. *Molecular Pharmacology*, 59(1), 46–53. <https://doi.org/10.1124/mol.59.1.46>
- Romanuik, T. L., Ueda, T., Le, N., Haile, S., Yong, T. M. K., Thomson, T., Vessella, R. L., & Sadar, M. D. (2009). *Novel Biomarkers for Prostate Cancer Including Noncoding*

- Transcripts*. 175(6), 2264–2276. <https://doi.org/10.2353/ajpath.2009.080868>
- Rondard, P., Goudet, C., Kniazeff, J., Pin, J. P., & Prézeau, L. (2011a). The complexity of their activation mechanism opens new possibilities for the modulation of mGlu and GABABclass C G protein-coupled receptors. *Neuropharmacology*, 60(1), 82–92. <https://doi.org/10.1016/j.neuropharm.2010.08.009>
- Rondard, P., Goudet, C., Kniazeff, J., Pin, J. P., & Prézeau, L. (2011b). The complexity of their activation mechanism opens new possibilities for the modulation of mGlu and GABABclass C G protein-coupled receptors. *Neuropharmacology*, 60(1), 82–92. <https://doi.org/10.1016/j.neuropharm.2010.08.009>
- Rondard, P., Huang, S., Monnier, C., Tu, H., Blanchard, B., Oueslati, N., Malhaire, F., Li, Y., Trinquet, E., Labesse, G., Pin, J. P., & Liu, J. (2008). Functioning of the dimeric GABAB receptor extracellular domain revealed by glycan wedge scanning. *EMBO Journal*, 27(9), 1321–1332. <https://doi.org/10.1038/emboj.2008.64>
- Rondard, P., Liu, J., Huang, S., Malhaire, F., Vol, C., Pinault, A., Labesse, G., & Pin, J. P. (2006). Coupling of agonist binding to effector domain activation in metabotropic glutamate-like receptors. *Journal of Biological Chemistry*, 281(34), 24653–24661. <https://doi.org/10.1074/jbc.M602277200>
- Rossol, M., Pierer, M., Raulien, N., Quandt, D., Meusch, U., Rothe, K., Schubert, K., Schöneberg, T., Schaefer, M., Krügel, U., Smajilovic, S., Bräuner-Osborne, H., Baerwald, C., & Wagner, U. (2012). Extracellular Ca²⁺ is a danger signal activating the NLRP3 inflammasome through G protein-coupled calcium sensing receptors. *Nature Communications*. <https://doi.org/10.1038/ncomms2339>
- Routledge, S. J., Ladds, G., & Poyner, D. R. (2017). Molecular and Cellular Endocrinology The effects of RAMPs upon cell signalling. *Molecular and Cellular Endocrinology*, 449, 12–20. <https://doi.org/10.1016/j.mce.2017.03.033>
- Roy, S., Singh, R. P., Agarwal, C., Siriwardana, S., Sclafani, R., & Agarwal, R. (2008). Downregulation of both p21/Cip1 and p27/Kip1 produces a more aggressive prostate cancer phenotype. *Cell Cycle*, 7(12), 1828–1835. <https://doi.org/10.4161/cc.7.12.6024>
- Rueda, P., Harley, E., Lu, Y., Stewart, G. D., Fabb, S., Diepenhorst, N., Cremers, B., Rouillon, M. H., Wehrle, I., Geant, A., Lamarche, G., Leach, K., Charman, W. N., Christopoulos, A., Summers, R. J., Sexton, P. M., & Langmead, C. J. (2016). Murine

GPRC6A mediates cellular responses to L-amino acids, but not osteocalcin variants.

PLoS ONE. <https://doi.org/10.1371/journal.pone.0146846>

- Ryan, C. J., Smith, M. R., Fizazi, K., Saad, F., Mulders, P. F. A., Sternberg, C. N., Miller, K., Logothetis, C. J., Shore, N. D., Small, E. J., Carles, J., Flaig, T. W., Taplin, M. E., Higano, C. S., de Souza, P., de Bono, J. S., Griffin, T. W., De Porre, P., Yu, M. K., ... Rathkopf, D. E. (2015). Abiraterone acetate plus prednisone versus placebo plus prednisone in chemotherapy-naive men with metastatic castration-resistant prostate cancer (COU-AA-302): Final overall survival analysis of a randomised, double-blind, placebo-controlled phase 3 study. *The Lancet Oncology*, *16*(2), 152–160. [https://doi.org/10.1016/S1470-2045\(14\)71205-7](https://doi.org/10.1016/S1470-2045(14)71205-7)
- Ryan, C. J., Smith, M. R., Fong, L., Rosenberg, J. E., Kantoff, P., Raynaud, F., Martins, V., Lee, G., Kheoh, T., Kim, J., Molina, A., & Small, E. J. (2010). Phase I clinical trial of the CYP17 inhibitor abiraterone acetate demonstrating clinical activity in patients with castration-resistant prostate cancer who received prior ketoconazole therapy. *Journal of Clinical Oncology*, *28*(9), 1481–1488. <https://doi.org/10.1200/JCO.2009.24.1281>
- Sahin, I., Mega, A. E., & Carneiro, B. A. (2018). Androgen receptor-independent prostate cancer: an emerging clinical entity. *Cancer Biology and Therapy*, *19*(5), 347–348. <https://doi.org/10.1080/15384047.2018.1423926>
- Sampson, N., Neuwirt, H., Puhr, M., Klocker, H., & Eder, I. E. (2013). In vitro model systems to study androgen receptor signaling in prostate cancer. In *Endocrine-Related Cancer* (Vol. 20, Issue 2, pp. R49–R64). Society for Endocrinology. <https://doi.org/10.1530/ERC-12-0401>
- Santos, R., Ursu, O., Gaulton, A., Bento, A. P., Donadi, R. S., Bologa, C. G., Karlsson, A., Al-lazikani, B., Hersey, A., Oprea, T. I., & Overington, J. P. (2016). A comprehensive map of molecular drug targets. *Nature Publishing Group*, *16*(1), 19–34. <https://doi.org/10.1038/nrd.2016.230>
- Saraon, P., Drabovich, A. P., Jarvi, K. A., & Diamandis, E. P. (2014). Mechanisms of Androgen-Independent Prostate Cancer. *EJIFCC*, *25*(1), 42–54. <http://www.ncbi.nlm.nih.gov/pubmed/27683456>
- Scher, H. I., Fizazi, K., Saad, F., Taplin, M.-E., Sternberg, C. N., Miller, K., de Wit, R., Mulders, P., Chi, K. N., Shore, N. D., Armstrong, A. J., Flaig, T. W., Fléchon, A.,

- Mainwaring, P., Fleming, M., Hainsworth, J. D., Hirmand, M., Selby, B., Seely, L., & de Bono, J. S. (2012). Increased Survival with Enzalutamide in Prostate Cancer after Chemotherapy. *New England Journal of Medicine*, *367*(13), 1187–1197.
<https://doi.org/10.1056/NEJMoa1207506>
- Schrage, R., Schmitz, A. L., Gaffal, E., Annala, S., Kehraus, S., Wenzel, D., Büllsbach, K. M., Bald, T., Inoue, A., Shinjo, Y., Galandrin, S., Shridhar, N., Hesse, M., Grundmann, M., Merten, N., Charpentier, T. H., Martz, M., Butcher, A. J., Slodczyk, T., ... Kostenis, E. (2015). The experimental power of FR900359 to study Gq-regulated biological processes. *Nature Communications*, *6*.
<https://doi.org/10.1038/ncomms10156>
- Seachrist, J. L., & Ferguson, S. S. G. (2003). Regulation of G protein-coupled receptor endocytosis and trafficking by Rab GTPases. *Life Sciences*, *74*(2–3), 225–235.
<https://doi.org/10.1016/j.lfs.2003.09.009>
- Seo, M. J., Heo, J., Kim, K., Chung, K. Y., & Yu, W. (2021). Coevolution underlies GPCR-G protein selectivity and functionality. *Scientific Reports 2021 11:1*, *11*(1), 1–11.
<https://doi.org/10.1038/s41598-021-87251-6>
- Sexton, P. M., Poyner, D. R., Simms, J., Christopoulos, A., & Hay, D. L. (2009). *Modulating receptor function through RAMPs : can they represent drug targets in themselves ?* *14*(April), 413–419. <https://doi.org/10.1016/j.drudis.2008.12.009>
- Seyedabadi, M., Ghahremani, M. H., & Albert, P. R. (2019). Biased signaling of G protein coupled receptors (GPCRs): Molecular determinants of GPCR/transducer selectivity and therapeutic potential. In *Pharmacology and Therapeutics* (Vol. 200, pp. 148–178). Elsevier Inc. <https://doi.org/10.1016/j.pharmthera.2019.05.006>
- Shah, P., Ding, Y., Niemczyk, M., Kudla, G., & Plotkin, J. B. (2013). Rate-limiting steps in yeast protein translation. *Cell*, *153*(7), 1589.
<https://doi.org/10.1016/j.cell.2013.05.049>
- Shah, R. B., Mehra, R., Chinnaiyan, A. M., Shen, R., Ghosh, D., Zhou, M., MacVicar, G. R., Varambally, S., Harwood, J., Bismar, T. A., Kim, R., Rubin, M. A., & Pienta, K. J. (2004). Androgen-independent prostate cancer is a heterogeneous group of diseases: Lessons from a rapid autopsy program. *Cancer Research*, *64*(24), 9209–9216. <https://doi.org/10.1158/0008-5472.CAN-04-2442>
- Shaner, N. C., Steinbach, P. A., & Tsien, R. Y. (2005). A guide to choosing fluorescent

- proteins. *Nature Methods*, 2(12), 905–909. <https://doi.org/10.1038/nmeth819>
- Shevrin, D. H., Kukreja, S. C., Ghosh, L., & Lad, T. E. (1988). Development of skeletal metastasis by human prostate cancer in athymic nude mice. *Clinical & Experimental Metastasis*, 6(5), 401–409. <https://doi.org/10.1007/BF01760575>
- Shukla, A. K., Singh, G., & Ghosh, E. (2014). Emerging structural insights into biased GPCR signaling. *Trends in Biochemical Sciences*, 39(12), 594–602. <https://doi.org/10.1016/j.tibs.2014.10.001>
- Simms, J., Hay, D. L., Bailey, R. J., Konycheva, G., Bailey, G., Wheatley, M., & Poyner, D. R. (2009). *Structure - Function Analysis of RAMP1 by Alanine Mutagenesis †*. 198–205.
- Smajilovic, S., Clemmensen, C., Johansen, L. D., Wellendorph, P., Holst, J. J., Thams, P. G., Ogo, E., & Bräuner-Osborne, H. (2013). The I- α -amino acid receptor GPRC6A is expressed in the islets of Langerhans but is not involved in I-arginine-induced insulin release. *Amino Acids*. <https://doi.org/10.1007/s00726-012-1341-8>
- Small, E. J., Saad, F., Chowdhury, S., Oudard, S., Hadaschik, B. A., Graff, J. N., Olmos, D., Mainwaring, P. N., Lee, J. Y., Uemura, H., De Porre, P., Smith, A. A., Zhang, K., Lopez-Gitlitz, A., & Smith, M. R. (2019). Apalutamide and overall survival in non-metastatic castration-resistant prostate cancer. *Annals of Oncology*, 30(11), 1813–1820. <https://doi.org/10.1093/annonc/mdz397>
- Small, Eric J., Schellhammer, P. F., Higano, C. S., Redfern, C. H., Nemunaitis, J. J., Valone, F. H., Verjee, S. S., Jones, L. A., & Hershberg, R. M. (2006). Placebo-controlled phase III trial of immunologic therapy with Sipuleucel-T (APC8015) in patients with metastatic, asymptomatic hormone refractory prostate cancer. *Journal of Clinical Oncology*, 24(19), 3089–3094. <https://doi.org/10.1200/JCO.2005.04.5252>
- Smith, M. R., Antonarakis, E. S., Ryan, C. J., Berry, W. R., Shore, N. D., Liu, G., Alumkal, J. J., Higano, C. S., Chow Maneval, E., Bandekar, R., de Boer, C. J., Yu, M. K., & Rathkopf, D. E. (2016). Phase 2 Study of the Safety and Antitumor Activity of Apalutamide (ARN-509), a Potent Androgen Receptor Antagonist, in the High-risk Nonmetastatic Castration-resistant Prostate Cancer Cohort. *European Urology*, 70(6), 963–970. <https://doi.org/10.1016/j.eururo.2016.04.023>
- Smith, M. R., Saad, F., Chowdhury, S., Oudard, S., Hadaschik, B. A., Graff, J. N., Olmos, D., Mainwaring, P. N., Lee, J. Y., Uemura, H., Lopez-Gitlitz, A., Trudel, G. C., Espina, B. M., Shu, Y., Park, Y. C., Rackoff, W. R., Yu, M. K., & Small, E. J. (2018a). Apalutamide

- Treatment and Metastasis-free Survival in Prostate Cancer. *New England Journal of Medicine*, 378(15), 1408–1418. <https://doi.org/10.1056/NEJMoa1715546>
- Smith, M. R., Saad, F., Chowdhury, S., Oudard, S., Hadaschik, B. A., Graff, J. N., Olmos, D., Mainwaring, P. N., Lee, J. Y., Uemura, H., Lopez-Gitlitz, A., Trudel, G. C., Espina, B. M., Shu, Y., Park, Y. C., Rackoff, W. R., Yu, M. K., & Small, E. J. (2018b). Apalutamide Treatment and Metastasis-free Survival in Prostate Cancer. *New England Journal of Medicine*, 378(15), 1408–1418. <https://doi.org/10.1056/NEJMoa1715546>
- Smrcka, A. V. (2008). G protein β subunits: Central mediators of G protein-coupled receptor signaling. In *Cellular and Molecular Life Sciences* (Vol. 65, Issue 14, pp. 2191–2214). NIH Public Access. <https://doi.org/10.1007/s00018-008-8006-5>
- Sriram, K., & Insel, P. A. (2018). G protein-coupled receptors as targets for approved drugs: How many targets and how many drugs? *Molecular Pharmacology*, 93(4), 251–258. <https://doi.org/10.1124/mol.117.111062>
- Stepanchick, A., McKenna, J., McGovern, O., Huang, Y., & Breitwieser, G. E. (2010). Calcium sensing receptor mutations implicated in pancreatitis and idiopathic epilepsy syndrome disrupt an arginine-rich retention motif. *Cellular Physiology and Biochemistry*, 26(3), 363–374. <https://doi.org/10.1159/000320560>
- Stephenson, R. A., Dinney, C. P. N., Gohji, K., Ordonez, N. G., Killion, J. J., & Fidler, I. J. (1992). Metastatic model for human prostate cancer using orthotopic implantation in nude mice. *Journal of the National Cancer Institute*, 84(12), 951–957. <https://doi.org/10.1093/jnci/84.12.951>
- Stone, K. R., Mickey, D. D., Wunderli, H., Mickey, G. H., & Paulson, D. F. (1978). Isolation of a human prostate carcinoma cell line (DU 145). *International Journal of Cancer*, 21(3), 274–281. <https://doi.org/10.1002/ijc.2910210305>
- Sullivan, J., Kopp, R., Stratton, K., Manschreck, C., Corines, M., Rau-Murthy, R., Hayes, J., Lincon, A., Ashraf, A., Thomas, T., Schrader, K., Gallagher, D., Hamilton, R., Scher, H., Lilja, H., Scardino, P., Eastham, J., Offit, K., Vijai, J., & Klein, R. J. (2015). An analysis of the association between prostate cancer risk loci, PSA levels, disease aggressiveness and disease-specific mortality. *British Journal of Cancer*, 113(1), 166–172. <https://doi.org/10.1038/bjc.2015.199>
- Sunahara, R. K., Dessauer, C. W., & Gilman, A. G. (1996). Complexity and diversity of mammalian adenylyl cyclases. In *Annual Review of Pharmacology and Toxicology*

- (Vol. 36, Issue 1, pp. 461–480). Annual Reviews Inc.
<https://doi.org/10.1146/annurev.pa.36.040196.002333>
- Sunahara, R. K., & Taussig, R. (2002). Isoforms of mammalian adenylyl cyclase: multiplicities of signaling. In *Molecular interventions* (Vol. 2, Issue 3, pp. 168–184). Mol Interv. <https://doi.org/10.1124/mi.2.3.168>
- Swami, U., McFarland, T. R., Nussenzveig, R., & Agarwal, N. (2020). Advanced Prostate Cancer: Treatment Advances and Future Directions. In *Trends in Cancer* (Vol. 6, Issue 8, pp. 702–715). Cell Press. <https://doi.org/10.1016/j.trecan.2020.04.010>
- Swedlow, J. R., Hu, K., Andrews, P. D., Roos, D. S., & Murray, J. M. (2002). Measuring tubulin content in *Toxoplasma gondii*: A comparison of laser-scanning confocal and wide-field fluorescence microscopy. *Proceedings of the National Academy of Sciences of the United States of America*, *99*(4), 2014–2019.
<https://doi.org/10.1073/pnas.022554999>
- Syrovatkina, V., Alegre, K. O., Dey, R., & Huang, X. Y. (2016). Regulation, Signaling, and Physiological Functions of G-Proteins. In *Journal of Molecular Biology* (Vol. 428, Issue 19, pp. 3850–3868). Academic Press.
<https://doi.org/10.1016/j.jmb.2016.08.002>
- Szendi-Szatmári, T., Szabó, Á., Szöllösi, J., & Nagy, P. (2019). Reducing the Detrimental Effects of Saturation Phenomena in FRET Microscopy. *Analytical Chemistry*, *91*(9), 6378–6382. <https://doi.org/10.1021/acs.analchem.9b01504>
- Takasaki, J., Saito, T., Taniguchi, M., Kawasaki, T., Moritani, Y., Hayashi, K., & Kobori, M. (2004). A novel Gαq/11-selective inhibitor. *Journal of Biological Chemistry*, *279*(46), 47438–47445. <https://doi.org/10.1074/jbc.M408846200>
- Takata, R., Akamatsu, S., Kubo, M., Takahashi, A., Hosono, N., Kawaguchi, T., Tsunoda, T., Inazawa, J., Kamatani, N., Ogawa, O., Fujioka, T., Nakamura, Y., & Nakagawa, H. (2010). Genome-wide association study identifies five new susceptibility loci for prostate cancer in the Japanese population. In *Nature Genetics*.
<https://doi.org/10.1038/ng.635>
- Tamada, S., Iguchi, T., Kato, M., Asakawa, J., Kita, K., Yasuda, S., Yamasaki, T., Matsuoka, Y., Yamaguchi, K., Matsumura, K., Go, I., Ohmachi, T., & Nakatani, T. (2018). Time to progression to castration-resistant prostate cancer after commencing combined androgen blockade for advanced hormone-sensitive prostate cancer. *Oncotarget*,

- 9(97), 36966–36974. <https://doi.org/10.18632/oncotarget.26426>
- Tamura, M., Nogimori, K., Murai, S., Yajima, M., Ito, K., Katada, T., Ui, M., & Ishii, S. (1982). Subunit Structure of Islet-Activating Protein, Pertussis Toxin, in Conformity with the A-B Model. *Biochemistry*, *21*(22), 5516–5522. <https://doi.org/10.1021/bi00265a021>
- Tararova, N. D., Narizhneva, N., Krivokrisenko, V., Gudkov, A. V., & Gurova, K. V. (2007). Prostate cancer cells tolerate a narrow range of androgen receptor expression and activity. *Prostate*, *67*(16), 1801–1815. <https://doi.org/10.1002/pros.20662>
- Taussig, R., Tang, W.-J., Hepler, J. R., & Gilman, A. G. (1994). *THE JOURNAL OF BIOLOGICAL CHEMISTRY Distinct Patterns of Bidirectional Regulation of Mammalian Adenylyl Cyclases** (Vol. 269, Issue 8).
- Terpe, K. (2003). Overview of tag protein fusions: From molecular and biochemical fundamentals to commercial systems. In *Applied Microbiology and Biotechnology* (Vol. 60, Issue 5, pp. 523–533). Springer Verlag. <https://doi.org/10.1007/s00253-002-1158-6>
- Thalmann, G. N., Sikes, R. A., Wu, T. T., Degeorges, A., Chang, S. M., Ozen, M., Pathak, S., & Chung, L. W. K. (2000). LNCaP progression model of human prostate cancer: Androgen-independence and osseous metastasis. *Prostate*, *44*(2), 91–103. [https://doi.org/10.1002/1097-0045\(20000701\)44:2<91::AID-PROS1>3.0.CO;2-L](https://doi.org/10.1002/1097-0045(20000701)44:2<91::AID-PROS1>3.0.CO;2-L)
- The complexity of their activation mechanism opens new possibilities for the modulation of mGlu and GABAB class C G protein-coupled receptors. (2011). *Neuropharmacology*, *60*(1), 82–92. <https://doi.org/10.1016/J.NEUROPHARM.2010.08.009>
- Tilakaratne, N., Christopoulos, G., Zumpe, E. T., Foord, S. M., & Sexton, P. M. (2000). Amylin Receptor Phenotypes Derived from Human Calcitonin Receptor/RAMP Coexpression Exhibit Pharmacological Differences Dependent on Receptor Isoform and Host Cell Environment. *Journal of Pharmacology and Experimental Therapeutics*, *294*(1).
- Tilley, D. G. (2011). G protein-dependent and G protein-independent signaling pathways and their impact on cardiac function. In *Circulation Research* (Vol. 109, Issue 2, pp. 217–230). NIH Public Access. <https://doi.org/10.1161/CIRCRESAHA.110.231225>
- Tilley, W. D., Wilson, C. M., Marcelli, M., & McPhaul, M. J. (1990). Androgen Receptor

- Gene Expression in Human Prostate Carcinoma Cell Lines. *Cancer Research*, 50(17).
- Tomala, K., Pogoda, E., Jakubowska, A., & Korona, R. (2014). Fitness costs of minimal sequence alterations causing protein instability and toxicity. *Molecular Biology and Evolution*, 31(3), 703–707. <https://doi.org/10.1093/molbev/mst264>
- Tong, A. H. Y., Evangelista, M., Parsons, A. B., Xu, H., Bader, G. D., Pagé, N., Robinson, M., Raghizadeh, S., Hogue, C. W. V., Bussey, H., Andrews, B., Tyers, M., & Boone, C. (2001). Systematic genetic analysis with ordered arrays of yeast deletion mutants. *Science*, 294(5550), 2364–2368. <https://doi.org/10.1126/science.1065810>
- Toseland, C. P. (2013). Fluorescent labeling and modification of proteins. In *Journal of Chemical Biology* (Vol. 6, Issue 3, pp. 85–95). Springer. <https://doi.org/10.1007/s12154-013-0094-5>
- Traish, A. M., Kang, H. P., Saad, F., & Guay, A. T. (2011). Dehydroepiandrosterone (DHEA)-A precursor steroid or an active hormone in human physiology (CME). In *Journal of Sexual Medicine* (Vol. 8, Issue 11, pp. 2960–2982). Blackwell Publishing Ltd. <https://doi.org/10.1111/j.1743-6109.2011.02523.x>
- Tsuchiya, D., Kunishima, N., Kamiya, N., Jingami, H., & Morikawa, K. (2002). Structural views of the ligand-binding cores of a metabotropic glutamate receptor complexed with an antagonist and both glutamate and Gd³⁺. *Proceedings of the National Academy of Sciences of the United States of America*, 99(5), 2660–2665. <https://doi.org/10.1073/pnas.052708599>
- Tsuji, Y., Shimada, Y., Takeshita, T., Kajimura, N., Nomura, S., Sekiyama, N., Otomo, J., Usukura, J., Nakanishi, S., & Jingami, H. (2000). Cryptic dimer interface and domain organization of the extracellular region of metabotropic glutamate receptor subtype 1. *Journal of Biological Chemistry*, 275(36), 28144–28151. <https://doi.org/10.1074/jbc.M003226200>
- Van Rheenen, J., Langeslag, M., & Jalink, K. (2004). Correcting Confocal Acquisition to Optimize Imaging of Fluorescence Resonance Energy Transfer by Sensitized Emission. *Biophysical Journal*, 86(4), 2517–2529. [https://doi.org/10.1016/S0006-3495\(04\)74307-6](https://doi.org/10.1016/S0006-3495(04)74307-6)
- Wall, M. A., Coleman, D. E., Lee, E., IAiguez-Lluhi, J. A., Posner, B. A., Gilman, A. G., & Ft Sprang, S. (1995). The Structure of the G Protein Heterotrimer GialPlyz. In *Cell* (Vol. 83).

- Wang, J., Hua, T., & Liu, Z. (2020). Structural features of activated GPCR signaling complexes. *Current Opinion in Structural Biology*, 63, 82–89.
<https://doi.org/10.1016/J.SBI.2020.04.008>
- Wang, Meilin, Liu, F., Hsing, A. W., Wang, X., Shao, Q., Qi, J., Ye, Y., Wang, Z., Chen, H., Gao, X., Wang, G., Chu, L. W., Ding, Q., Ouyang, J., Gao, X., Huang, Y., Chen, Y., Gao, Y. T., Zhang, Z. F., ... Xu, J. (2012). Replication and cumulative effects of GWAS-identified genetic variations for prostate cancer in Asians: A case-control study in the ChinaPCa consortium. *Carcinogenesis*, 33(2), 356–360.
<https://doi.org/10.1093/carcin/bgr279>
- Wang, Minghua, Yao, Y., Kuang, D., & Hampson, D. R. (2006). Activation of Family C G-protein-coupled receptors by the tripeptide glutathione. *Journal of Biological Chemistry*, 281(13), 8864–8870. <https://doi.org/10.1074/jbc.M512865200>
- Wang, N., Reeves, K. J., Brown, H. K., Fowles, A. C. M., Docherty, F. E., Ottewill, P. D., Croucher, P. I., Holen, I., & Eaton, C. L. (2015). The frequency of osteolytic bone metastasis is determined by conditions of the soil, not the number of seeds; evidence from in vivo models of breast and prostate cancer. *Journal of Experimental and Clinical Cancer Research*, 34(1). <https://doi.org/10.1186/s13046-015-0240-8>
- Wang, T., Larcher, L. M., Ma, L., & Veedu, R. N. (2018). Systematic screening of commonly used commercial transfection reagents towards efficient transfection of single-stranded oligonucleotides. *Molecules*, 23(10).
<https://doi.org/10.3390/molecules23102564>
- Ward, D. T., Brown, E. M., & Harris, H. W. (1998). Disulfide bonds in the extracellular calcium-polyvalent cation-sensing receptor correlate with dimer formation and its response to divalent cations in vitro. *Journal of Biological Chemistry*, 273(23), 14476–14483. <https://doi.org/10.1074/jbc.273.23.14476>
- Warrington, J. I. (2018). *The Role of Receptor Activity Modifying Protein 1 in Prostate Cancer [submitted as part of PhD thesis] University of Sheffield.*
- Wauson, E. M., Lorente-Rodríguez, A., & Cobb, M. H. (2013). Minireview: Nutrient sensing by G protein-coupled receptors. In *Molecular Endocrinology* (Vol. 27, Issue 8, pp. 1188–1197). The Endocrine Society. <https://doi.org/10.1210/me.2013-1100>
- Webb, S. J., Geoghegan, T. E., Prough, R. A., & Miller, K. K. M. (2006). The biological

- actions of dehydroepiandrosterone involves multiple receptors. In *Drug Metabolism Reviews* (Vol. 38, Issues 1–2, pp. 89–116). Taylor & Francis.
<https://doi.org/10.1080/03602530600569877>
- Weber, M. J., & Gioeli, D. (2004). Ras signaling in prostate cancer progression. In *Journal of Cellular Biochemistry* (Vol. 91, Issue 1, pp. 13–25). J Cell Biochem.
<https://doi.org/10.1002/jcb.10683>
- Wei, H., Ahn, S., Shenoy, S. K., Karnik, S. S., Hunyady, L., Luttrell, L. M., & Lefkowitz, R. J. (2003). Independent β -arrestin 2 and G protein-mediated pathways for angiotensin II activation of extracellular signal-regulated kinases 1 and 2. *Proceedings of the National Academy of Sciences of the United States of America*, *100*(19), 10782–10787. <https://doi.org/10.1073/pnas.1834556100>
- Wei, J., Hanna, T., Suda, N., Karsenty, G., & Ducy, P. (2014). Osteocalcin promotes β -cell proliferation during development and adulthood through Gprc6a. *Diabetes*, *63*(3), 1021–1031. <https://doi.org/10.2337/db13-0887>
- Weis, W. I., & Kobilka, B. K. (2018). The Molecular Basis of G Protein-Coupled Receptor Activation. In *Annual Review of Biochemistry* (Vol. 87, pp. 897–919). Annual Reviews Inc. <https://doi.org/10.1146/annurev-biochem-060614-033910>
- Wellendorph, P., & Bräuner-Osborne, H. (2009). Molecular basis for amino acid sensing by family C G-protein-coupled receptors. In *British Journal of Pharmacology* (Vol. 156, Issue 6, pp. 869–884). Wiley-Blackwell. <https://doi.org/10.1111/j.1476-5381.2008.00078.x>
- Wellendorph, P., Hansen, K. B., Balsgaard, A., Greenwood, J. R., Egebjerg, J., & Bräuner-Osborne, H. (2005). Deorphanization of GPRC6A: A Promiscuous L- α -Amino Acid Receptor with Preference for Basic Amino Acids. *Mol. Pharmacol.*, *67*, 589–597.
<https://doi.org/10.1124/mol.104.007559.difficult>
- Wellendorph, Petrine, & Bräuner-Osborne, H. (2004). Molecular cloning, expression, and sequence analysis of GPRC6A, a novel family C G-protein-coupled receptor. *Gene*.
<https://doi.org/10.1016/j.gene.2004.03.003>
- Wellendorph, Petrine, Burhenne, N., Christiansen, B., Walter, B., Schmale, H., & Bräuner-Osborne, H. (2007). The rat GPRC6A: Cloning and characterization. *Gene*, *396*(2), 257–267. <https://doi.org/10.1016/j.gene.2007.03.008>
- Wellendorph, Petrine, Johansen, L. D., Jensen, A. A., Casanova, E., Gassmann, M.,

- Deprez, P., Clément-Lacroix, P., Bettler, B., & Bräuner-Osborne, H. (2009). No evidence for a bone phenotype in GPRC6A knockout mice under normal physiological conditions. *Journal of Molecular Endocrinology*.
<https://doi.org/10.1677/JME-08-0149>
- Weston, C., Winfield, I., Harris, M., Hodgson, R., Shah, A., Dowell, S. J., Carlos, J., Woodlock, D. A., Reynolds, C. A., Poyner, D. R., Watkins, H. A., & Ladds, G. (2016). *Receptor Activity-modifying Protein-directed G Protein Signaling Specificity for the Calcitonin Gene-related Peptide Family of Receptors* * □. *291(42)*, 21925–21944.
<https://doi.org/10.1074/jbc.M116.751362>
- Wilden, U., Hall, S. W., & Kuhn, H. (1986). Phosphodiesterase activation by photoexcited rhodopsin is quenched when rhodopsin is phosphorylated and binds the intrinsic 48-kDa protein of rod outer segments. *Proceedings of the National Academy of Sciences of the United States of America*, *83(5)*, 1174–1178.
<https://doi.org/10.1073/pnas.83.5.1174>
- Willoughby, D., & Cooper, D. M. F. (2007). Organization and Ca²⁺ regulation of adenylyl cyclases in cAMP microdomains. In *Physiological Reviews* (Vol. 87, Issue 3, pp. 965–1010). American Physiological Society.
<https://doi.org/10.1152/physrev.00049.2006>
- Wisler, J. W., DeWire, S. M., Whalen, E. J., Violin, J. D., Drake, M. T., Ahn, S., Shenoy, S. K., & Lefkowitz, R. J. (2007). A unique mechanism of β -blocker action: Carvedilol stimulates β -arrestin signaling. *Proceedings of the National Academy of Sciences of the United States of America*, *104(42)*, 16657–16662.
<https://doi.org/10.1073/pnas.0707936104>
- Wooten, D., Lindmark, H., Kadmiel, M., Willcockson, H., Caron, K. M., Barwell, J., Drmota, T., & Poyner, D. R. (2013). Receptor activity modifying proteins (RAMPs) interact with the VPAC 2 receptor and CRF1 receptors and modulate their function. *British Journal of Pharmacology*, *168(4)*, 822–834. <https://doi.org/10.1111/j.1476-5381.2012.02202.x>
- Wu, H., Wang, C., Gregory, K. J., Han, G. W., Cho, H. P., Xia, Y., Niswender, C. M., Katritch, V., Meiler, J., Cherezov, V., Conn, P. J., & Stevens, R. C. (2014). Structure of a class C GPCR metabotropic glutamate receptor 1 bound to an allosteric modulator. *Science*, *344(6179)*, 58–64. <https://doi.org/10.1126/science.1249489>

- Wurm, F. M. (2004). Production of recombinant protein therapeutics in cultivated mammalian cells. In *Nature Biotechnology* (Vol. 22, Issue 11, pp. 1393–1398). Nat Biotechnol. <https://doi.org/10.1038/nbt1026>
- Wurm, F. M., & Hacker, D. (2011). First CHO genome. *Nature Biotechnology*, 29(8), 718–720. <https://doi.org/10.1038/nbt.1943>
- Xie, Q., Soutto, M., Xu, X., Zhang, Y., & Johnson, C. H. (2012). *Bioluminescence Resonance Energy Transfer (BRET) Imaging in Plant Seedlings and Mammalian Cells*. 1–22. <https://doi.org/10.1007/978-1-60761-901-7>
- Xu, F., Wu, H., Katritch, V., Han, G. W., Jacobson, K. A., Gao, Z.-G., Cherezov, V., & Stevens, R. C. (2011). Structure of an Agonist-Bound Human A2A Adenosine Receptor. *Science*, 332(6027), 322–327. <https://doi.org/10.1126/science.1202793>
- Xu, L., Chen, J., Liu, W., Liang, C., Hu, H., & Huang, J. (2019). Targeting androgen receptor-independent pathways in therapy-resistant prostate cancer. In *Asian Journal of Urology* (Vol. 6, Issue 1, pp. 91–98). Editorial Office of Asian Journal of Urology. <https://doi.org/10.1016/j.ajur.2018.11.002>
- Yamamura, A., Nayeem, M. J., & Sato, M. (2019). Calcilytics inhibit the proliferation and migration of human prostate cancer PC-3 cells. *Journal of Pharmacological Sciences*, 139(3), 254–257. <https://doi.org/10.1016/j.jphs.2019.01.008>
- Ye, R., Pi, M., Cox, J. V., Nishimoto, S. K., & Quarles, L. D. (2017). CRISPR/Cas9 targeting of GPRC6A suppresses prostate cancer tumorigenesis in a human xenograft model. *Journal of Experimental & Clinical Cancer Research*. <https://doi.org/10.1186/s13046-017-0561-x>
- Ye, R., Pi, M., Nooh, M. M., Bahout, S. W., & Quarles, L. D. (2019). Human GPRC6A mediates testosterone-induced mitogen-activated protein kinases and mTORC1 signaling in prostate cancer cells. *Molecular Pharmacology*, 95(5), 563–572. <https://doi.org/10.1124/mol.118.115014>
- Yengo, C. M., & Berger, C. L. (2010). Fluorescence anisotropy and resonance energy transfer: Powerful tools for measuring real time protein dynamics in a physiological environment. In *Current Opinion in Pharmacology* (Vol. 10, Issue 6, pp. 731–737). NIH Public Access. <https://doi.org/10.1016/j.coph.2010.09.013>
- Yue, C. C., & Labash, J. D. (1991). Resistance to restriction digestion by plasmids prepared with a lithium-containing lysis buffer. *BioTechniques*, 11(3), 331.

- Zamponi, G. W., Bourinet, E., Nelson, D., Nargeot, J., & Snutch, T. P. (1997). Crosstalk between G proteins and protein kinase C mediated by the calcium channel $\alpha 1$ subunit. *Nature*, *385*(6615), 442–446. <https://doi.org/10.1038/385442a0>
- Zeng, Q., Eidsness, M. K., & Summer, A. O. (1997). Near-Zero Background Cloning of PCR Products. *BioTechniques*, *23*, 412–418.
- Zhang, F., Klebansky, B., Fine, R. M., Xu, H., Pronin, A., Liu, H., Tachdjian, C., & Li, X. (2008). Molecular mechanism for the umami taste synergism. *Proceedings of the National Academy of Sciences of the United States of America*, *105*(52), 20930–20934. <https://doi.org/10.1073/pnas.0810174106>
- Zhang, Jin, Campbell, R. E., Ting, A. Y., & Tsien, R. Y. (2002). Creating new fluorescent probes for cell biology. In *Nature Reviews Molecular Cell Biology* (Vol. 3, Issue 12, pp. 906–918). Nature Publishing Group. <https://doi.org/10.1038/nrm976>
- Zhang, Jing, Loew, L. M., & Davidson, R. M. (1996). Faster voltage-dependent activation of Na⁺ channels in growth cones versus somata of neuroblastoma N1E-115 cells. *Biophysical Journal*, *71*(5), 2501–2508. [https://doi.org/10.1016/S0006-3495\(96\)79443-2](https://doi.org/10.1016/S0006-3495(96)79443-2)
- Zhang, Y., Sun, B., Feng, D., Hu, H., Chu, M., Qu, Q., Tarrasch, J. T., Li, S., Sun Kobilka, T., Kobilka, B. K., & Skiniotis, G. (2017). Cryo-EM structure of the activated GLP-1 receptor in complex with a G protein. *Nature*, *546*(7657), 248–253. <https://doi.org/10.1038/nature22394>
- Zhang, Zaixiang, Sun, S., Quinn, S. J., Brown, E. M., & Bai, M. (2001). The Extracellular Calcium-sensing Receptor Dimerizes through Multiple Types of Intermolecular Interactions. *Journal of Biological Chemistry*, *276*(7), 5316–5322. <https://doi.org/10.1074/jbc.M005958200>
- Zhang, Zhongming, Liu, X., Morgan, D. A., Kuburas, A., Thedens, D. R., Russo, A. F., & Rahmouni, K. (2011). Neuronal receptor activity - Modifying protein 1 promotes energy expenditure in mice. *Diabetes*, *60*(4), 1063–1071. <https://doi.org/10.2337/db10-0692>
- Zhao, G. Q., Zhang, Y., Hoon, M. A., Chandrashekar, J., Erlenbach, I., Ryba, N. J. P., & Zuker, C. S. (2003). The receptors for mammalian sweet and umami taste. *Cell*, *115*(3), 255–266. [https://doi.org/10.1016/S0092-8674\(03\)00844-4](https://doi.org/10.1016/S0092-8674(03)00844-4)
- Zhou, X. E., He, Y., de Waal, P. W., Gao, X., Kang, Y., Van Eps, N., Yin, Y., Pal, K., Goswami,

D., White, T. A., Barty, A., Latorraca, N. R., Chapman, H. N., Hubbell, W. L., Dror, R. O., Stevens, R. C., Cherezov, V., Gurevich, V. V., Griffin, P. R., ... Xu, H. E. (2017). Identification of Phosphorylation Codes for Arrestin Recruitment by G Protein-Coupled Receptors. *Cell*, 170(3), 457-469.e13.

<https://doi.org/10.1016/j.cell.2017.07.002>

Ziaee, S., Chu, G. C. Y., Huang, J. M., Sieh, S., & Chung, L. W. K. (2015). Prostate cancer metastasis: Roles of recruitment and reprogramming, cell signal network and three-dimensional growth characteristics. In *Translational Andrology and Urology* (Vol. 4, Issue 4, pp. 438–454). AME Publishing Company.

<https://doi.org/10.3978/j.issn.2223-4683.2015.04.10>

Zimmerman, M. A., Budish, R. A., Kashyap, S., & Lindsey, S. H. (2016). GPER - Novel membrane oestrogen receptor. In *Clinical Science* (Vol. 130, Issue 12, pp. 1005–1016). Portland Press Ltd. <https://doi.org/10.1042/CS20160114>

Appendix.

CHO-K1 G418 Kill Curve

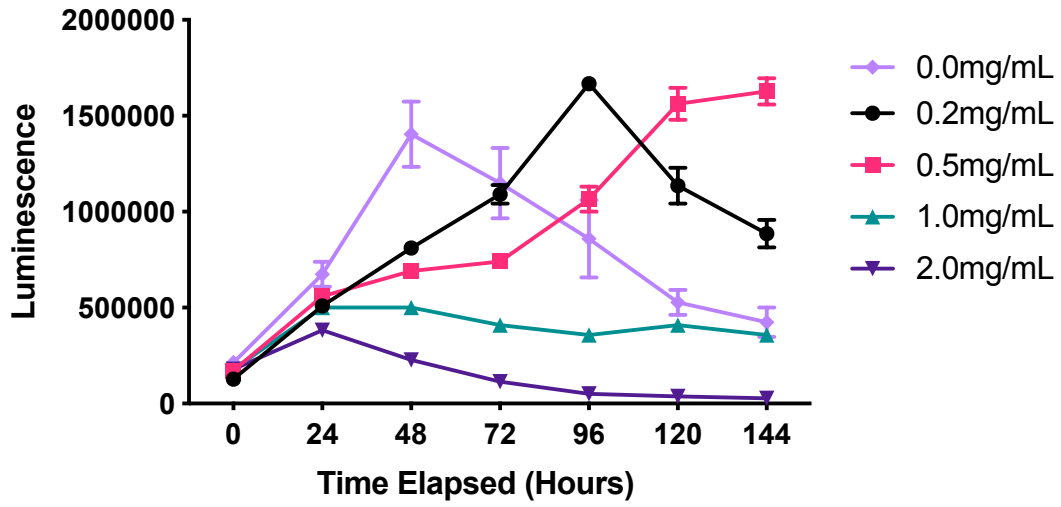


Figure Ap.1 G418 antibiotic concentration kill curve; CHO-K1 cell viability following daily G418 treatment. Dose-dependent decreases in CHO-K1 cell viability when treated with the G418 antibiotic.

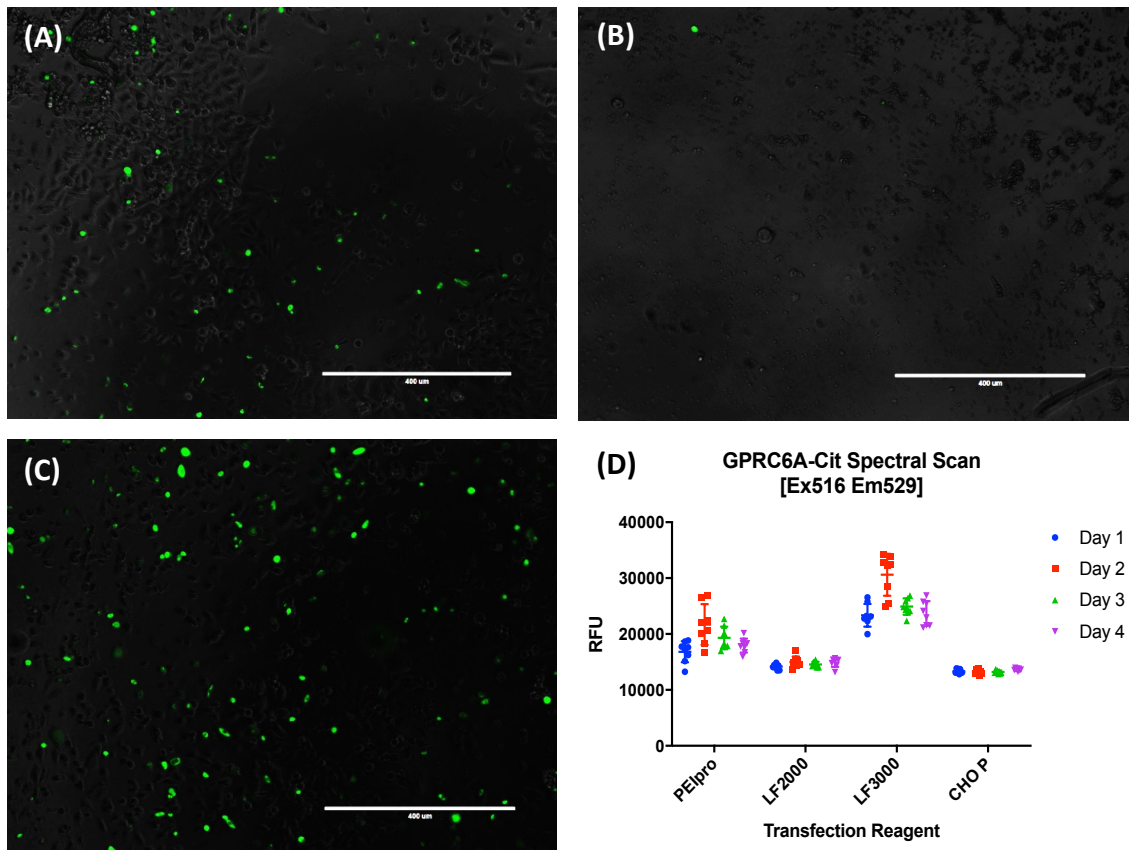
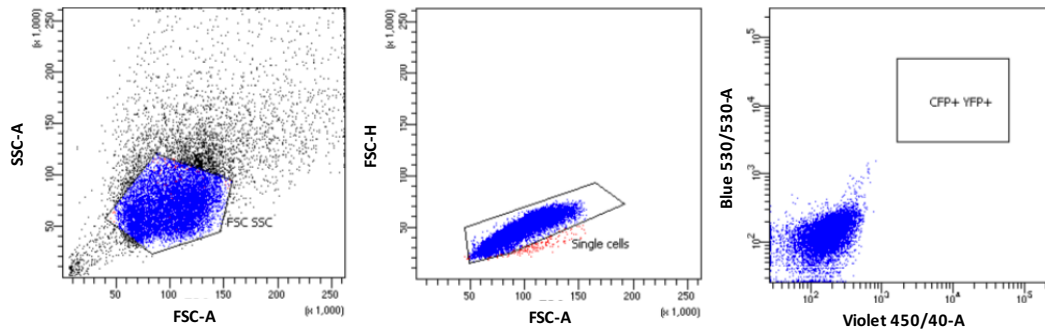


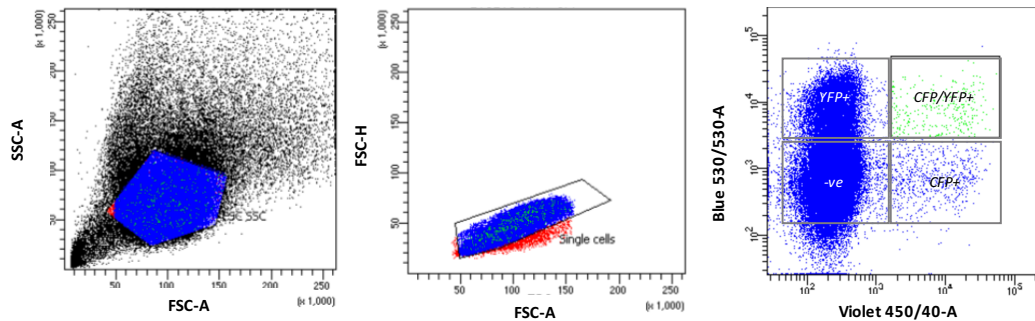
Figure Ap. 2 Optimisation of GPRC6A-Cit transfection method; (A) PEIpro Transfection reagent day 2 (B) Lipofectamine 2000 reagent day 2 (C) Lipofectamine 3000 reagent day 2 (D) Spectral Scan (Ex 516 nm and Em 529 nm) comparison of different transfection reagents used over the time course of 4 days.

(A) Mock Transfected CHO-K1 YFP / CFP Dual Sort



| Population | No of Events | Of the Parent (%) | Of Total (%) |
|--------------|--------------|-------------------|--------------|
| All Events | 13,761 | - | 100.0 |
| FSC vs. SSC | 10,244 | 74.4 | 74.4 |
| Single cells | 10,065 | 98.3 | 73.1 |
| CFP+ | 0 | 0 | 0 |
| YFP+ | 0 | 0 | 0 |
| CFP/YFP+ | 0 | 0.0 | 0.0 |

(B) GPRC6A-Cit + RAMP1-Cer CHO-K1 YFP / CFP Dual Sort



| Population | No of Events | Of the Parent (%) | Of Total (%) |
|--------------|--------------|-------------------|--------------|
| All Events | 85,821 | - | 100.0 |
| FSC vs. SSC | 61,781 | 72.0 | 72.0 |
| Single cells | 60,363 | 97.7 | 70.3 |
| CFP+ | 408 | 4.8 | 3.0 |
| YFP+ | 4,160 | 44.4 | 29.1 |
| CFP/YFP+ | 297 | 0.5 | 0.3 |

Figure Ap.3 Fluorescence-assisted cell sort of GPRC6A-Cit and RAMP1-Cer populations; Flow cytometry gating; FSC-A/SSC-A gating of live cells, FSC-A/FSC-H gating of doublets; Violet 450/40-A/ Blue 530/30-A of Cit and Cer positive populations. **(A)** Mock transfected CHO-K1 control cells **(B)** hGPRC6A-Cit + RAMP1-Cer CHO-K1 cell line.

Cell Number Optimisation cAMP Accumulation

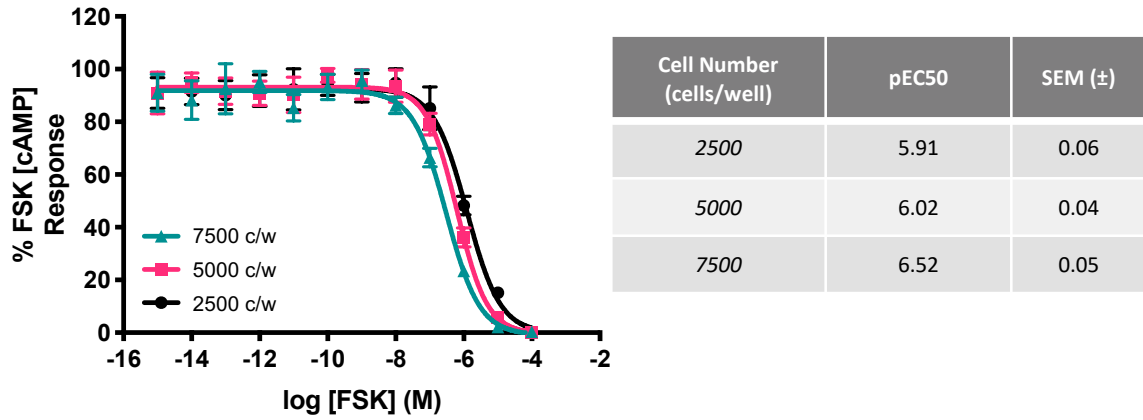


Figure Ap.4 CHO-K1 LANCE cAMP kit assay cell number optimisation; forskolin dose response cAMP standard curves used to obtain the dynamic range and sensitivity of the assay and to determine the optimal cell densities. Curves represent 3 independent repeats and are presented as mean \pm SEM. forskolin, (FSK); cells/well (c/w).

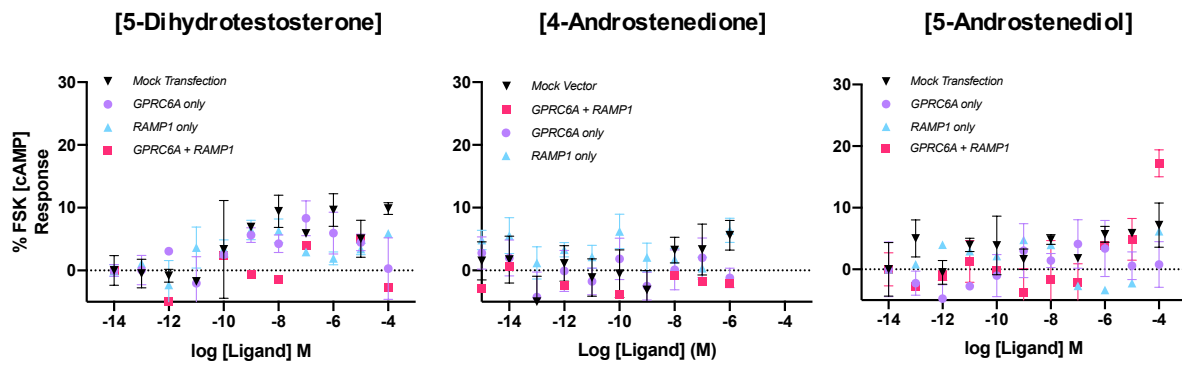


Figure Ap.5 Intracellular cAMP accumulation induced by testosterone metabolic derivatives; Negligible responses were observed in all CHO-K1 overexpressing cells when stimulating with all metabolites. Data are from 3 independent experiments and are presented as mean \pm SEM.